

**FORMATION AND STABILITY OF AEROBIC GRANULAR
SLUDGE IN SEWAGE TREATMENT UNDER LOW LOADING
CONDITIONS**

NIK AZIMATOLAKMA BINTI AWANG

**THESIS SUBMITTED IN FULFILMENT OF THE
REQUIREMENTS FOR THE DEGREE OF DOCTOR OF
PHILOSOPHY**

**FACULTY OF ENGINEERING
UNIVERSITY OF MALAYA
KUALA LUMPUR**

2016

ABSTRACT

The increasing pollution loads and types of pollutants constituents in sewage treatment plant (STPs) as compared to the original design requirement urge for a demand in upgrading of the old STPs. Land acquisition will become a major issue in upgrading the new STPs since conventional biological STPs requires a large footprint for the installation of reactors that accommodate different conversions and sludge stabilisation process. Aerobic granular sludge (AGS) technology offers a possibility in designing a compact STPs based on simultaneous organics and nutrient removal and settling process in a sequencing batch reactor (SBR). The research trend on AGS has been integrated from factors affecting the formation process and chemical characteristic towards the stability for a long term operation. Thus, this study is aimed to determine the formation and stability of AGS system in achieving stable conditions and after being tested with a series of constrained conditions will be a critical factor to highlight the environmental biotechnology novelty of AGS. In this research, a series of AGS Batches were developed in SBRs with different height/diameter (H/D) ratios at a similar working volume of 4.5 L and an aeration rate of 4 L/min. The performance of each Batch was assessed based on the biomass production, effluent quality and AGS characteristics, with the determination to correlate the operational conditions with AGS formation and stability. The results are divided into 5 major sections: 1) the effects of low organic loading rate (OLR), 2) the effects of differences in reactor H/D ratio, 3) the increase of formation and stability of AGS developed in a low reactor H/D ratio by adding divided draft tubes, 4) the reformation process of long term stored AGS and 5) the biokinetics parameters. First, AGS (Control Batch) was successfully attained after 55 days of a formation period although the applied OLR was exceptionally low, which were in range of 0.2 and 0.48 kg COD/m³ d. Second, although the periods to attain AGS

(Batch1) in high H/D ratio reactor was shorter, AGS (Batch2) produced in a low H/D ratio reactor appeared to be more resistant towards fluctuated and low OLR by providing a short settling distance for biomass in facing the unfavorable circumstances. Third, the uses of divided draft tubes proved to be beneficial in shortening the time period setup for AGS (Batch3) development. Fourth, the result proved that the stability and ability of AGS (Batch4) were to be reformed after long term storing and under a fluctuated OLR and a low COD/N ratio. Fifth, the biokinetics parameters attained during the steady state further proved the result and the conclusion given from the first result until the fourth result. Thus, the present thesis is enlightened and being overcome with a much promising new insight in AGS formation and stability by preparing the development medium of AGS similar to real site. Research results also help to enlighten the limitations experienced by AGS technology and further endorsed for the full-scale application.

ABSTRAK

Peningkatan beban pencemaran dan jenis bahan pencemar dalam loji rawatan kumbahan (STP) berbanding dengan keperluan reka bentuk asal menyebabkan STP lama perlu dinaik taraf. Penggunaan tanah akan menjadi isu utama dalam menaik taraf STP baru kerana konvensional biologi STP memerlukan kawasan yang luas bagi pemasangan reaktor-reaktor yang menampung pelbagai proses penukaran dan penstabilan enapcemar. Teknologi enapcemar berbutir aerobik (AGS) menawarkan kemungkinan untuk mereka bentuk kompleks STP berdasarkan pada kebolehan penyingkiran serentak organik dan nutrient dan proses enapan di dalam satu reaktor penjujukan berkumpulan (SBR). Trend penyelidikan mengenai AGS telah berubah dari faktor yang mempengaruhi proses pembentukan dan ciri-ciri kimia ke arah kestabilan untuk operasi jangka panjang. Oleh itu, kajian ini bertujuan untuk melihat perubahan dalam pembentukan dan kestabilan sistem AGS bagi mencapai keadaan stabil selepas diuji dalam keadaan dikekang yang berlanjutan, di mana ia akan menjadi faktor kritikal untuk menengahkan pembaharuan bioteknologi alam sekitar oleh AGS. Dalam kajian ini, satu siri kelompok AGS telah dibangunkan di dalam SBRs yang berbeza nisbah ketinggian /diameter (H/D) dan pada jumlah isipadu kerja yang sama iaitu 4.5 L dan kadar pengudaraan 4 L/min. Prestasi setiap kelompok telah dinilai berdasarkan pada pengeluaran biomass, kualiti efluen dan ciri-ciri AGS, dengan keazaman untuk mengaitkan keadaan operasi dengan pembentukan dan kestabilan AGS. Keputusan dibahagikan kepada 5 bahagian utama: 1) kesan kadar pembebanan organik (OLR) yang rendah, 2) kesan perbezaan dalam nisbah reaktor H/D , 3) meningkatkan proses pembentukan dan kestabilan AGS yang terhasil di dalam reaktor nisbah H/D rendah dengan penambah draf tiub dibahagikan, 4) proses pembentukan semula AGS yang disimpan dalam jangka masa lama, dan 5) parameter biokinetik. Pertama, AGS (Control

Batch) berjaya diperolehi selepas 55 hari tempoh pembentukan walaupun OLR digunakan adalah sangat rendah, dan berada dalam julat 0.2 hingga 0.48 kg COD/m³ d. Kedua, walaupun tempoh untuk mencapai AGS (Batch1) dalam reaktor nisbah H/D tinggi adalah lebih singkat, AGS (Batch2) yang dihasilkan dalam reaktor nisbah H/D rendah kelihatan lebih tahan terhadap OLR yang turun naik dan rendah dengan menyediakan jarak penganapan yang pendek bagi biomass dalam menghadapi keadaan yang tidak terduga. Ketiga, penggunaan draf tiub dibahagikan terbukti bermanfaat dalam memendekkan tempoh persediaan masa untuk AGS (Batch3) terbentuk. Keempat, keputusan membuktikan kestabilan dan keupayaan AGS (Batch4) untuk pembentukan semula selepas disimpan dalam jangka masa yang lama dan dalam keadaan OLR turun naik dan nisbah COD/N rendah. Kelima, parameter biokinetic yang dicapai dalam keadaan mantap membuktikan keputusan dan kesimpulan yang diberikan dalam perkara pertama hingga keempat. Oleh itu, secara keseluruhannya tesis ini mengentegahkan dan mengatasi keterbatasan dalam pembentukan dan kestabilan AGS dalam bentuk yang berbeza, iaitu dengan menyediakan medium pembangunan AGS sama seperti di tapak sebenar. Hasil penyelidikan membantu mengatasi keterbatasan yang dialami oleh teknologi AGS dan seterusnya membantu untuk pengguna pada skala penuh

ACKNOWLEDGEMENT

The first person I would like to express my deepest gratitude is my supervisor, Prof. Dr. Ghazaly Shaaban for being so responsible to guide and give me a lot of assistance throughout my research project. He is a great mentor who gave me lots of freedom in designing my research work and fully committed whenever I need his guidance. I would like to express my gratitude towards University of Malaya and Department of Higher Education Malaysia for the awarding research grants (RG160-12SUS, PV038-2012, FP041-2013B). I wish to express my appreciation towards Ministry of Education Malaysia and Universiti Sains Malaysia which had financially support my PhD fellowship. I am thankful to Associate Prof. Dr. Lee Choon Weng from Institute of Biological Sciences which had advised me regarding microbial identification. Special acknowledgments go to Madam Kalai, Puan Rozita and Cik Alliah for their kind technical and administrative supports. Thanks to my fellow lab friends especially Mohd. Izziuddin for his advised and opinion during my preliminary research work. Lastly, I would like to convey my gratitude to my husband, Abdul Hafiz Bin Abdullah, my parents; Awang Bin Hamzah and Nik Aminah Binti Nik Mahmood, and my siblings for their unconditional support and love.

TABLE OF CONTENTS

<i>ORIGINAL LITERARY WORK DECLARATION FORM</i>	<i>ii</i>
<i>ABSTRACT</i>	<i>iii</i>
<i>ABSTRAK</i>	<i>v</i>
<i>ACKNOWLEDGEMENT</i>	<i>vii</i>
<i>TABLE OF CONTENTS</i>	<i>viii</i>
<i>LIST OF FIGURES</i>	<i>xii</i>
<i>LIST OF TABLES</i>	<i>xvi</i>
<i>LIST OF SYMBOLS AND ABBREVIATIONS</i>	<i>xvii</i>
CHAPTER 1	1
INTRODUCTION	1
1.1 Background of the Study	1
1.2 Objective of the Study	5
1.3 Research Scope	6
1.4 Thesis overview	7
CHAPTER 2	9
LITERATURE REVIEW	9
2.1 AGS Background	9
2.2 Factors Effecting Formation of AGS	10
2.2.1 Substrate Composition and Concentration	13
2.2.2 Operating Conditions.....	16
2.2.2.1 Hydrodynamic Shear Force	18
2.2.2.2 Organic Loading Rate (ORL)	18
2.2.2.3 Settling Time.....	19
2.3 Stability of AGS.....	20

2.3.1	Mechanism of Aerobic Granules Formation and Stability	22
2.3.2	Stability Loss	27
2.4	Research Gaps on AGS formation and stability	28
CHAPTER 3.....		41
METHODOLOGY		41
3.1	Study Outline	41
3.2	Experiments Set-Up	43
3.2.1	Sewage and Activated Sludge Collection Site	43
3.2.2	Reactor Design	44
3.3	Experimental Phases and Operational Conditions	45
3.4	Analytical Procedures	50
3.5	Physical Characterization of AGS	51
3.5.1	Evaluation of AGS Size.....	51
3.5.2	Morphology of AGS.....	51
3.6	Chemical Characterization of AGS	52
3.6.1	Extraction of Extracellular Polymeric Substances (EPS).....	52
3.6.2	Elements Composition in AGS	53
3.6.3	Distribution of Active Cells, Protein and β -polysaccharides in AGS ...	53
3.7	Biological Characterization of AGS	54
3.7.1	DNA Extraction.....	55
3.7.2	Quality Control of Extracted DNA.....	55
3.7.3	Bioinformatics Analysis and Taxonomic Classification	56
CHAPTER 4.....		57
RESULTS AND DISCUSSION.....		57
4.1	Sewage Characterization.....	57
4.2	Impact of Low OLR on AGS Formation (Control)	59

4.2.1	Profile of Biomass Concentration and Settling Properties	59
4.2.2	Ammonium Removal Efficiencies	63
4.2.3	Morphology Observation of Control	65
4.2.4	Chemical Composition of Control.....	66
4.2.5	Summary on Result Analysis	67
4.3	Impact of Reactor H/D Ratio on AGS Formation (Batch1 and Batch2)	69
4.3.1	Effect of Reactor H/D Ratio on Period to Achieved Mature Granules .	70
4.3.2	Effect of Reactor H/D Ratio on Settling Properties of Biomass	73
4.3.2.1	Formation of Batch1 in reactor with high H/D ratio (SBR1)	73
4.3.2.2	Formation of Batch2 in reactor with low H/D ratio (SBR2)	76
4.3.3	Effect of Reactor H/D Ratio on Efficiencies of Ammonium Removal .	79
4.3.4	Morphology observation of Batch1 and Batch2.....	82
4.3.5	Chemical Composition of Batch1 and Batch2	85
4.3.6	Advantages and Disadvantages of Reactor with Low H/D Ratio	88
4.4	Formation of AGS in Airlift Reactor with Divided Draft Tubes (Batch3)...	89
4.4.1	Flow Pattern of Liquid in SBR3.....	90
4.4.2	Size and Morphology Evolution of Aerobic Granules	92
4.4.3	Effect of low COD/N Ratio on Reactor Performance	100
4.4.4	Composition and Distribution of EPS	104
4.4.5	The Diversity in Microbial Community	110
4.4.6	Advantage of Airlift Reactor	116
4.5	Reformation and Stability of Long Term Storage AGS (Batch4)	118
4.5.1	The Reformation Indices for Batch4	119
4.5.2	Reactor Performance	125
4.5.3	Characteristic of AGS at Different Phase of Reformation Indices.....	127
4.5.3.1	Composition and Distribution of EPS in Batch4	128

4.5.3.2	Role of Microbial Community and Morphology Change.....	133
4.5.4	Summary on Result Analysis	141
4.6	Bioactivity of Aerobic Granules	141
4.6.1	Development of Kinetic Equation for Biokinetic Parameters	142
4.6.2	Determination of Process Kinetic Coefficients	144
4.6.3	Effect of OLR and Reactor H/D ratio on Kinetic Coefficients	146
4.6.4	Significance of biokinetic parameters	152
CHAPTER 5	158
CONCLUSIONS AND RECOMMENDATIONS	158
5.1	Conclusions.....	158
5.2	Recommendations for further work.....	160
REFERENCES	162
LIST OF PUBLICATIONS AND PAPERS PRESENTED	173
APPENDIX A1	174
APPENDIX A2	175
APPENDIX A3	176
APPENDIX A4	177
APPENDIX A5	178

LIST OF FIGURES

Figure 2.1	Schematic of SBR operating during 1 cycle (de Kreuk, 2006)	10
Figure 2.2	Schematic view of multi-layer structural of aerobic granules in biological wastewater treatment	12
Figure 2.3	Microscopic images of aerobic granules develop in (a) acetate and (b) domestic wastewater (Peyong et al., 2012)	15
Figure 2.4	Multi-layer structural model of AGS in terms of stability (Sheng et al., 2010)	21
Figure 2.5	Illustration of EPS distribution around cell wall (Mittelman, 1985) and proposed structure of repeat unit of exopolysaccharides from AGS (Seviour et al. 2011)	23
Figure 2.6	Physicochemical interaction and entanglement of EPS components from different cells that dominate the stability of EPS matrix (Flemming and Wingender, 2010)	25
Figure 2.7	A conceptual of granule formation and breakage	26
Figure 3.1	Flowchart of study outline	42
Figure 3.2	Schematic diagram of SBR operation	44
Figure 3.3	Schemes of SBRs with 3 different configurations	46
Figure 4.1	Relationship between total COD and CODs with SS increment. Data obtained between June 2013 and November 2013.	58
Figure 4.2	Profile of biomass concentration and CODs influent for Control	60
Figure 4.3	Removal of CODs and SS by Control	60
Figure 4.4	Profile of SVI at 5 min intervals of settling time for Control	61
Figure 4.5	Profile of pH, ammonium, nitrite and nitrate effluent for Control	64
Figure 4.6	FESEM images of mature granules from Control at day 80 (a, b, c, d, e) and activated sludge (f).	66
Figure 4.7	Elemental mapping images (a, b, c, d) and localized elementals spectra (e) from EDX analysis for Figure 4.6b surface area.	68
Figure 4.8	Profile of MLSS and CODs influent for Batch1 and Batch2	70

Figure 4.9	CODs removal and SS effluent for Batch1 and Batch2	71
Figure 4.10	Profile of F/M ratio and SRT for Batch1 and Batch2	72
Figure 4.11	Profile of SVI at 5 min intervals of settling time for Batch1	73
Figure 4.12	Profile of OLR, MLVSS, OUR and SOUR for Batch1	75
Figure 4.13	Profile of SVI at 5 min intervals of settling time for Batch2	76
Figure 4.14	Profile of OLR, MLVSS, OUR and SOUR for Batch2	78
Figure 4.15	Profile of pH, ammonium, nitrite and nitrate effluent for Batch1	80
Figure 4.16	Profile of pH, ammonium, nitrite and nitrate effluent for Batch2	81
Figure 4.17	FESEM images for Batch1 on day 38 (a, c) and day 60 (b, d)	82
Figure 4.18	FESEM images for Batch2 on day 38 (a, c) and day 93 (b, d)	84
Figure 4.19	Presence of protozoa in Batch2 on day 93	84
Figure 4.20	Elemental mapping images (a: carbon, b: oxygen, c: silicon, d: aluminium) and localized elementals spectra (f) from EDX analysis for (e) surface area of Batch1 on day 60	86
Figure 4.21	Elemental mapping images (a: carbon, b: oxygen, c: iron, d: sodium, e: calcium, f: copper) and map elementals spectra (g) from EDX analysis for Figure 4.18(d) surface area of Batch2 on day 93	87
Figure 4.22	The flow pattern of liquid in bubble column and airlift type reactor based on report by Liu and Tay (2002; 2007), Jin et al. (2008) and Chan et al. (2009)	91
Figure 4.23	Evolution of aerobic granules in SBR3. Bar = 500 μ m	92
Figure 4.24	Deviation in aerobic granules size for SBR3	93
Figure 4.25	Profile of SVI at 5 min intervals of settling time for Batch3	94
Figure 4.26	Morphological development of aerobic granules during the experimental run	95
Figure 4.27	Profile of biomass (MLSS and MLVSS), OLR and CODs influent for Batch3	97
Figure 4.28	Profile of F/M ratio and SRT for Batch3	98
Figure 4.29	VSS effluent, SS and CODs removal for Batch3	101

Figure 4.30	Profile of pH, ammonium, nitrite and nitrate effluent for Batch3	101
Figure 4.31	FTIR spectrum of freezing EPS from seed to day 105 for Batch3	105
Figure 4.32	Localized elementals spectra from EDX analysis for Batch3 on day 32, 50, 77 and 105	106
Figure 4.33	CLSM images of Batch3 on day 77 and 105; a. contrast images, b. β -D-glucopyranose polysaccharides (calcofluor white), c. protein (FITC), d. nuclei acid (SYTO 63), e. overlap images of b-d, f. Z-sectioning on whole aerobic granules on day 50, 77 and 105	108
Figure 4.34	Cluster analysis for the first 15 taxonomic classifications from bacterial community of seed, day 8, 50, 77 and 105 at the class level for Batch3	112
Figure 4.35	Taxonomic classification of pyrosequences from bacterial community of seed, day 8, 50, 77 and 105 at the genus level for Batch3	113
Figure 4.36	Evolution of aerobic granules in SBR4. Bar = 1 mm for day 0, 1, 67, 77, 91, and 105. Bar = 500 μ m for day 18, 32 and 46 for Batch4	120
Figure 4.37	Deviation in aerobic granules size for Batch4	120
Figure 4.38	Profile of biomass (MLSS and MLVSS), OLR and CODs influent for Batch4	121
Figure 4.39	Profile of SVI at 5 min intervals of settling time for Batch4	122
Figure 4.40	Profile of F/M ratio and SRT for Batch4	124
Figure 4.41	VSS effluent, SS and CODs removal for Batch4	126
Figure 4.42	Profile of pH, ammonium, nitrite and nitrate effluent for Batch4	126
Figure 4.43	FTIR spectrum of freezing EPS from day 0 (seed) to 105 for Batch4	129
Figure 4.44	CLSM images of Batch4 on day 0 (seed), 50 and 105; a. contrast images, b. β -D-glucopyranose polysaccharides (calcofluor white), c. protein (FITC), d. nuclei acid (SYTO 63), e. overlap images of b-d.	131
Figure 4.45	Z-sectioning on whole aerobic granules on day 0 (seed), 8, 50, 77 and 105 for Batch4	132
Figure 4.46	Cluster analysis for the first 15 taxonomic classifications from bacterial community of seed, day 8, 50, 77 and 105 at the class	134

	level for Batch4	
Figure 4.47	Taxonomic classification of pyrosequences from bacterial community of seed, day 8, 50, 77 and 105 at the genus level for Batch4	136
Figure 4.48	FESEM images of aerobic granules for Batch4	140
Figure 4.49	Linear plot of substrate utilization for determination of k and K_s coefficients during steady state.	145
Figure 4.50	Linear plot of microbial growth for determination of Y and K_d coefficients during steady state	145
Figure 4.51	Relationship between maximum specific microbial growth rate (μ_{max}) and half saturation coefficient (K_s); Control = ▲, Batch1 = ●, Batch2 = *, Batch3 = +, Batch4 = ■	147
Figure 4.52	Relationship between OLR and synthesis yield coefficient (Y); Control = ▲, Batch1 = ●, Batch2 = *, Batch3 = +, Batch4 = ■	148
Figure 4.53	Relationship between steady state period and endogenous coefficient (K_d); Control = ▲, Batch1 = ●, Batch2 = *, Batch3 = +, Batch4 = ■	151

LIST OF TABLES

Table 2.1	Accumulation of SBR configurations and operating conditions for mature aerobic granules	17
Table 2.2	Accumulation of experimental design on aerobic granules for sewage treatment	32-37
Table 2.3	Strategies controls to serve the stability of concern from AGS formation.	39-40
Table 3.1	Operating conditions applied for formation of AGS	48
Table 3.2	Excitation and emission wavelengths of fluorophores (Chen et al., 2007b)	53
Table 4.1	Characteristics of raw sewage	57
Table 4.2	Effect of COD/NH ₄ ⁺ ratio on COD and ammonium removal	103
Table 4.3	Corresponding kinetic coefficient of substrate utilization and microbial growth for this study	146
Table 4.4	Corresponding kinetic coefficients of substrate utilization and microbial growth from others study based on Monod equation	149
Table 4.5	Group Statistic for reactor with different H/D ratio	153
Table 4.6	Descriptive statistic associated for kinetic coefficients	153
Table 4.7	Independent Sample Test for reactor with different H/D ratio	154
Table 4.8	Group Statistic for Organic Loading Rate	155
Table 4.9	Independent Sample Test for Effect of OLR	157

LIST OF SYMBOLS AND ABBREVIATIONS

Symbols

τ	Hydraulic retention time (hour)
μ_{max}	Maximum specific microbial growth rate

Abbreviations

AGS	Aerobic granular sludge
AOB	Ammonium-oxidising bacteria
A/V	Surface area to volume ratio
BOD	Biochemical oxygen demand
BOD ₅	Biochemical oxygen demand after 5 days
CLSM	Confocal laser scanning microscope
COD	Chemical oxygen demand (mg/L)
COD _s	Soluble COD (mg/L)
COD/N	COD to Nitrogen ratio
D	Diameter
DGGE	Denaturing gradient gel electrophoresis
DO	Dissolved oxygen (mg/L)
DNA	Deoxyribonucleic acid
GAO	Glycogen-accumulating organisms
EDX	Energy dispersive X-ray spectrometer
EPS	Extracellular polymeric substance
FA	Free ammonia
FESEM	Field emission scanning electron microscope
F/M ratio	Food to microorganism ratio (g COD/g MLVSS d)
FNA	Free nitrous acid
FTIR	Fourier transform infrared
H	Height

H/D ratio	Reactor height/diameter ratio
HRT or τ	Hydraulic retention time (hour)
ISO	International organization for standardization
IWK	Indah Water Konsortium
MLSS	Mixed liquor suspended solids (mg/L)
MLVSS	Mixed liquor volatile suspended solids (mg/L)
NGS	Next generation sequencing
NOB	Nitrite-oxidising bacteria
NOB	Nitrite oxidation bacteria
OLR	Organic loading rate (kg COD/m ³ d)
PAO	Phosphate-accumulating organisms
OUR	Oxygen utilization rate
PHB	Polyhydroxybutyrate
PCR	Polymerase chain reaction
PE	Population equivalent
SBR	Sequencing batch reactor
SOUR	Specific oxygen uptake rate ((mg/L)/min)
SRT	Sludge retention time (day)
SS	Suspended solids (mg/L)
SND	Simultaneous nitrification and denitrification
STP	Sewage treatment plant
SUAV	Superficial air velocity (cm/s)
SVI	Sludge Volume index (mL/g)
SVI ₅	Sludge Volume index after 5 min
SVI ₃₀	Sludge Volume index after 30 min
UAASB	Single up-flow aerobic/anoxic sludge bed
V _{ER}	Volumetric exchange rate (%)
VSS	Volatile suspended solid (mg/L)

Variables

k	Maximum specific substrate utilization rate (mg CODs/mg VSS d)
K_d	Endogenous decay coefficient (1/d)
K_s	Half saturation coefficient (mg CODs/L)
Q	Influent flow rate (m ³ /d)
r_g	Microbial growth rate (mg VSS/L d)
R^2	Fit line of trendline
r_{su}	Substrate utilization rate (mg CODs/L d)
S	Concentration of substrate in reactor (mg CODs/L)
S_o	Influent substrate concentration (mg CODs/L)
S_e	Effluent substrate concentration (mg CODs/L)
U	Specific substrate utilization rate (mg CODs/mg VSS d).
V	Reactor working volume (L)
X	Biomass concentration in reactor (mg MLVSS/L)
X_e	Effluent biomass concentration (mg VSS/L)
X_o	Influent biomass concentration (mg VSS/L)
Y	Synthesis yield coefficient (mg VSS/mg CODs)

Chemical formula

C=O	Carboxyl
C-O	Methoxyl
O=C-N	Cyanate bond
O-H	Hydrogen bonding
N-H	Amines
NH ₄ ⁺	Ammonium
NO ₂ ⁻	Nitrite
NO ₃ ⁻	Nitrate
OsO ₄	Osmium
PO ₂ ⁻ stretch	phosphodiester asymmetric

CHAPTER 1

INTRODUCTION

1.1 Background of the Study

From the early 1950s there has been a steady evolution of sewage treatments in Malaysia into today's modern sewage treatment plants, which produce a high quality effluent to be discharged to the environment. Before the invention of septic tanks in the 1960s, Malaysian wastes were disposed directly into rivers, where water sources were being contaminated. Nevertheless, the problem remained unsolved since the septic tanks only provide basic primary treatment via sedimentation and digestion in which the discharged effluent was largely left untreated and still rich with organic materials. This has potential in creating public health and environmental problems, particularly in urban areas.

As the urban areas continued to develop and the population densities arose, the need to improve the environmental condition led to the enactment of the Environmental Quality Act in 1974. Hence, the technological advancement was shifted from an improved version of a primary treatment, Imhoff tank to a partial secondary treatment system such as oxidation pond and aerated lagoons. The need to improve the sewerage system became more stringent when the Environmental Quality Act in 1979 was enacted. A full secondary treatment via mechanical sewage treatment such as conventional activated sludge and biological filters has gradually replaced the old treatment systems. As of 2013, 38% of the public sewage treatment plants in Malaysia are mechanical plants (DOE, 2014).

Prior to 1994, most of the sewage treatment plants (STPs) (PE less than 5, 000) in Malaysia had been built by housing developers to serve for their own development schemes. However, inefficient system design had occurred and this resulted in an ad-hoc and chaotic collection of networks and treatment efficiency. Even after the privatization of the national sewerage system to the Indah Water Konsortium (IWK) in the early 1994, via the enactment and the gazettelement of a new act, namely as Sewerage Services Act, 1993, the problems are still remained persistent until today (Hamid et al. 2009). As of December 2008, the average of STPs/year annual growth by developers reached 300.

Apart from that, the existing conventional STPs which are mostly oxidation ponds or extended aeration have failed to operate according to the original design's requirements and further to comply with the prescribed effluent discharge standards by the Department of Environment (DOE). This was attributed by increasing the pollutions loads and pollutants composition of raw sewage in conjunction with the changing socio economics and life style, especially in highly populated areas. Malaysia Environmental Quality Report in 2014 (DOE, 2014) indicated that sewage has remained as the largest contributor to river pollution. An analysis of three main parameters that have significantly affected the quality of river water showed that the pollutants were consisted of 36% BOD₅, 30% SS and 77% ammoniacal nitrogen which were contributed by sewage. A report also showed that 86% of river pollution sources came from small SPTs with a population equivalent (PE) of less than 5000. Unstandardized designs, operation and scattered development of small STPs, and the use of obsolete technology had led to problems in managing sewage treatment. At present, a total of 3285 extended aeration type of STPs which are under the IWK maintenance are serving 6.6 million PE in Malaysia (IWK, 2012). Thus, this has urged on the demand in

upgrading the old STPs especially in highly populated area, where land acquisition will become a major issue in selecting or upgrading the new STPs

In Malaysia, a secondary treatment is directed to the removal of biodegradable organic and suspended solids, mainly by using biological treatments. Biological wastewater treatment is often associated with the problems of a high amount of sludge production due to the treatment of highly concentrated wastewater (industrial wastewater), relatively low volumetric conversion capacity caused by the treatment of low concentrated wastewater (sewage) and a low flexibility with respect to fluctuating loading rates (Beun et al., 2002; Di Iaconi et al., 2007; Mulder et al., 2001). In addition, de Kreuk (2006) stated that wastewater treatments have to deal with different numbers of conversion processes (the chemical oxidation of carbon and ammonium, and the reduction of nitrate and phosphate) and the sludge stabilisation process (the gravity and mechanical thickener, and dewatering). On top of that, large area requirements are also needed to accommodate the different conversion and the sludge stabilisation process.

Thus, a great effort has been made around the world to tackle these problems, with the aim to have innovative technologies that can provide better compactness, better operational flexibility and lower sludge production system. One of the technologies is an anaerobic granulation system. Anaerobic granulation is a biofilms system in which many full-scale anaerobic granular sludge units have been operated worldwide to treat the highly concentrated wastewater (Liu & Tay, 2004). However, due to the flaws of anaerobic technology for instance, the long start-up period (from 2 to 8 months), the high operation temperature, the inapplicability for low concentrated wastewater and the unsuitability for nutrients removal, have limits on its applications (Liu & Tay, 2004; Qin et al., 2004a).

In order to overcome those weaknesses of the anaerobic granulation process, research efforts have been shifted towards the aerobic granular sludge (AGS) technology. Unlike the conventional activated sludge system, AGS technology has a regular, dense and strong microbial structure, good settling ability, a high biomass retention, and the ability to withstand shock and toxic loadings (Wang et al., 2007a). Moreover, de Kreuk (2006) showed that AGS technology offers a possibility of designing a much compact wastewater treatment plant based on the simultaneous organics and nutrient removal in one sequencing batch reactor.

Existing studies concerning AGS technology are mainly done on a well control laboratory scale sequencing batch reactor (SBR) with a height to diameter ratio (H/D) of over 10. This kind of practice will limit the practical application of aerobic granule since the existing SBR at a real site has mostly a low reactor H/D ratio. In practice, factors like maintenance problems and the impacts of natural disaster will be critical and have to be considered in designing a long slender reactor. Moreover, most of the research works have been focusing on factors that affect the formation and characterization of AGS which are, based on different operational parameters and high substrate composition (mainly synthetic wastewater with organic loading rate of more than 2.5 kg COD/m³ d). Little is known about the stability and recovery of AGS system after being subjected under fluctuating loading rate, constrained conditions and the feasibility of long term granulation process.

Concerning the biological facts that aerobic bacteria has high growth rate, it can be expected that AGS would have low stability and subsequently limits its application in the wastewater treatment practice. Currently, most of the research works regarding stability are focusing on the ability of mature aerobic granules to resist the toxic shock

loading from the pharmaceutical products, ammonia inhibition, famine conditions, hydrodynamic and mechanical shear force, instead of the process of the aerobic granules formation itself. Collectively all the aforementioned problems interfere with the stability of aerobic granules during the formation process under constrained conditions and not after the aerobic granules are well developed, thereby urging researchers for their extensive contribution in this specific discipline.

1.2 Objective of the Study

The major objective of the present study is to evaluate the formation and stability of AGS system to achieve stable conditions after being tested with a series of constrained conditions, in which will be the critical factor to highlight the environmental biotechnology novelty of AGS. This research will be the first to elaborate the mechanism of aerobic granules formation with regards to intermolecular interactions and the manner in which these forces govern the stability through:

- Multi-layer structural model of AGS
- A conceptual of AGS formation and breakage.

This research also will be the first to describe the relationship between change in biokinetic parameters with organic loading rate (OLR) and reactor H/D ratio. This research significantly contributes to a new insight of the cycle in AGS formation and stability process that endorsed a full-scale application of AGS technology for the treatment of domestic sewage in Malaysia.

To achieve the said aim, the following objectives are performed:

- i. To determine the effect of low and variable organic loading rate, and reactor height/diameter (H/D) ratio on formation of AGS.
- ii. To determine the formation and stability mechanism of AGS process via the usage of long term storage aerobic granules as seed.
- iii. To assess the microbial community dynamics in AGS at different phases (seed, aggregation, stability, disintegration and re-aggregation) of formation process.
- iv. To determined biokinetic parameters of aerobic granules develop in SBR with various configuration and sewage as substrate.

1.3 Research Scope

This research covers the design and application of a laboratory-scale reactor as indicated below:

- i. A modified bubble column with a presence of divided draft tubes (airlift reactor) was designed at a laboratory-scale and operated based on the sequencing batch system.
- ii. Two laboratory-scale bubble reactors with different height over diameter ratio (H/D) were used as controls.

- iii. Raw sewage (after the primary screening process) which was collected from Pantai STP (Control, Batch1 and Batch2) and Damansara STP (Batch3 and Bath4) were used as the substrate for the cultivation of AGS.
- iv. The performance of AGS in each reactor was determined by the means of effluent quality, biomass volumes and AGS characteristic.
- v. All analytical measurements performed in this research were conducted according to the Standard Methods for the Examination of Water and Wastewater (APHA, 2005).

1.4 Thesis overview

Chapter 1 starts with the introduction on the technological advancement in sewage treatment plants and the environmental issues on major source of river pollutions which were constantly being polluted by the sewage in Malaysia. This is followed by an introductory note on the negative side effects of biological treatments in treating wastewater and how aerobic granular technology helps to tackle these problems. The major limitations in aerobic granular sludge technology are signified and specific research hypotheses are sculptured. This is succeeded through major scopes and precise objectives with detailed steps.

Chapter 2 elaborates the background of aerobic granular sludge technology, the development of multi-layer structural model of aerobic granules, the various report on the factors that affect the formation of aerobic granules in treating low-strength wastewater particularly sewage and finally contribute to a structural concept on

mechanism of aerobic granules formation with regard to others intermolecular interactions, and how these forces will govern the stability of aerobic granules. The merits of different approaches in the formation and stability of AGS are highlighted and compared to identify the critical aspects in the treatment of low strength wastewater, particularly sewage.

Chapter 3 outlines the details on the experimental setup and operational conditions adopted for the formation of aerobic granules under constrained conditions. The formation is followed with characterization techniques that are involved in understanding the intermolecular interaction or the so called physicochemical and microbiological interactions of different tropic bacteria that keep the aerobic granules stable. Mechanism and the current state of aerobic granules performance can be described if intermolecular interaction is well identified.

Chapter 4 presents the outcome of the thesis findings with comprehensive discussions. This chapter necessitates the insights, importance and influence of organic loading rate and the reactors types and configurations, on the formation and stability of aerobic granules. The performances of aerobic granules are developed in different types of SBRs and organic loading rate are categorized as Control Batch, Batch1, Batch2, Batch3 and Batch4. The summary and recommendations are included in **Chapter 5**.

CHAPTER 2

LITERATURE REVIEW

2.1 AGS Background

Biological treatment is considered as a promising technique for biodegradation of wastewater, since it can degrade organic pollutant in the wastewater (Metcalf & Eddy, 2014). According to Schwarzenbeck et al. (2005), the performance of a biological treatment unit is significantly dependent upon the metabolic capabilities of microbial community in the system and the efficiency of biosolid-liquid separation at the last stage of the treatment procedure. Biodegradation is carried out by microorganisms which can degrade organic compounds to carbon dioxide and sludge under aerobic conditions and to biogas (a mixture comprising CO₂ and CH₄) under anaerobic conditions (Renou et al., 2008).

During the last 20 years, intensive research in the field of biological wastewater treatment and other applications demonstrated that biofilms (Adav et al., 2008a) have the potential to be an alternative to conventional activated sludge system (Liu & Tay, 2004). Granular sludge was first described as anaerobic system in 1980 (Lettinga et al., 1980). Only by the late 1990, the first report about the cultivation of AGS in a continuous aerobic upflow sludge blanket (AUSB) reactor linked to an oxygen dissolving tank was given by Mishima and Nakamura (1991). At the end of 1990, Morgenroth et al. (1997) reported the formation and application of AGS using discontinuous fed system. Since then, the development of AGS as a technology for wastewater biological treatments has been extensively reported using SBR systems (Arrojo et al. 2004; Yuan & Gao, 2010). SBR has been widely applied because the

operational parameters required to stimulate the formation of AGS can only be easily manipulated in SBR (Wagner & da Costa, 2013). The first patent of AGS was granted to Heijnen and van Loosdrecht (1998). Whilst, a comprehensive review of the art of AGS process was reported by Liu and Tay (2004).

2.2 Factors Effecting Formation of AGS

AGS formation has been extensively reported in SBR and is tailored for treating a wide variety of wastewater (Arrojo et al., 2004; de Kreuk, 2006; Liu & Liu, 2006). SBR is a wastewater treatment system based on activated sludge and operated in a fill-and-draw cycle. The most important difference between SBR and the conventional activated sludge systems is that reaction and settle take place in the same reactor. The main feature of SBR process is its cyclic operation. Each cycle consists of five common phases, which are carried out in fill, react, settle, drain and idle sequences (Fabregas, 2005; Mace & Mata-Alvarez, 2002). An example of the cycle operation of a SBR is given in Figure 2.1.

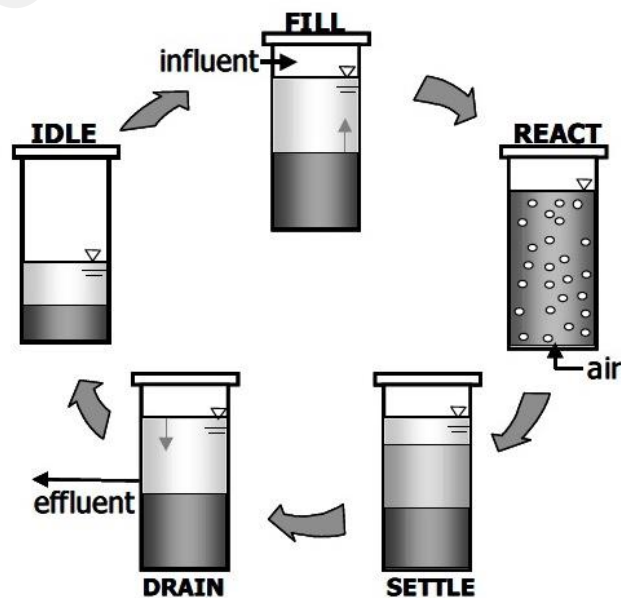


Figure 2.1: Schematic of SBR operating during 1 cycle (de Kreuk, 2006)

Granulation is an aggregation process of suspended biomass to form discrete well-defined granules with no use of carrier material. It is a self-immobilization of bacteria, involving physical agitation, physicochemical and microbiological interactions of different trophic bacteria groups (Lee et al., 2010; Liu et al., 2009; Liu & Tay, 2004; Zhu et al., 2013a). The dense-spherical structure of granules led to limited diffusion gradient of dissolved oxygen (DO) inside aerobic granules. As a result, aerobic, anoxic and anaerobic zones will exist simultaneously (Figure 2.2). Due to the different metabolic requirements, the stratification of microbial population inside aerobic granules at different zones existed. Hence, this will subsequently be providing simultaneous carbon, nitrogen and phosphorus removal (de Kreuk, 2006; Liu & Tay, 2006; Wagner & da Costa, 2013).

Figure 2.2 shows the schematic view of the multi-layer structure of aerobic granules based on previous schematic illustration developed by de Kreuk (2006), Bassin et al. (2012) and Winkler et al. (2013). Image analysis of granule central slices via scanning electron microscopy (SEM) coupled with energy dispersive x-ray detector (EDX) by Angela et al. (2011) show that mineral cluster, mainly calcium and phosphorus are present in the core of granules. Simultaneous nitrification and denitrification (SND) process takes place at the second and third layer, governed by ammonium-oxidising bacteria (AOB), nitrite-oxidising bacteria (NOB), glycogen-accumulating organisms (GAO) and phosphate-accumulating organisms (PAO). Cell-internally stored substrate, polyhydroxybutyrate (PHB) will be used as carbon source for growth and cell maintenance during famine (carbon source not available) period (de Kreuk, 2006).

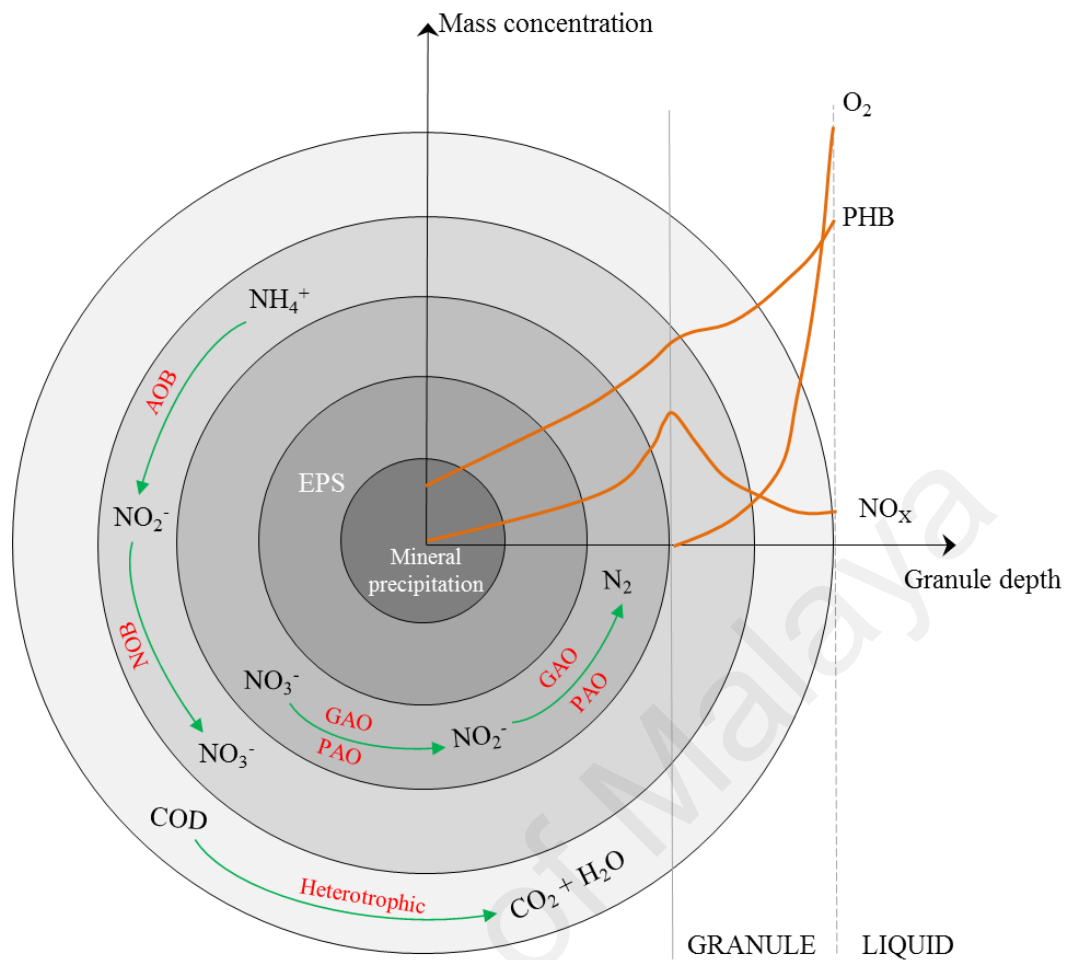


Figure 2.2: Schematic view of multi-layer structural of aerobic granules in biological wastewater treatment (Modified from de Kreuk, 2006).

As illustrated in Figure 2.2, the organic and inorganic substance and DO are initially transferred from liquid phase to the external surface of granule, before diffusing or being carried by an advective flow into granule interior for oxidation (Chiu et al., 2007). The oxidation or conversion process in aerobic granule is likely to be affected by external (bulk liquid to granule surface) and internal (surface to the interior of granules) mass transfer resistance (Skiadas et al., 2003). Mass transfer resistance in aerobic granules will result in a significant drop in microbial activity and growth rate, where larger aerobic granule will be affected even more severely (Li et al., 2008a).

Theoretically, mass transfer resistance increase with increasing granule size (Skiadas et al., 2003). For example, Jang et al. (2003) and Chiu et al. (2007) cultivated aerobic granules with glucose (300 mg COD/L) and phenol (500 mg COD/L) as carbon source, and where, diffusion limitation of DO is likely to occur at 300 μm and 120 μm depth, for mature granules with size of 1.0-1.3 mm and 1.5 mm, respectively. In contrast, Tay et al. (2002) claimed that the diffusion limitation of DO for 2.4 mm mature aerobic granules cultivated with glucose (4000 mg COD/L) occurred at 800 μm depth. By comparing only the size factors, the diffusion limitation of DO for 2.4 mm mature aerobic granules should be less than 120 μm . However, if concentration of substrate and granule size is taken into account, diffusion limitation of DO for 1.0-1.3 mm granules should be less than 120 μm . Hence, it shows that diffusion of substrate and DO in aerobic granules is an interrelated dynamic process and is interrelated (Li et al., 2008a). It can be concluded that apart from granule size, the influence of mass transfer resistance also depends on other factors like granule morphology, substrate concentration and diffusion, and degree of turbulence in reactor (Li et al., 2008a; Skiadas et al., 2003).

2.2.1 Substrate Composition and Concentration

Substrate composition and concentration has been reported to be the decisive factors in aerobic granules formation (Adav et al., 2010; Beun et al., 1999; Peyong et al., 2012; Tay et al., 2004). Substrate composition and concentration could exert the granulation process by selecting and enriching different microbial species and thus, influencing the size, morphology and kinetic behaviour of aerobic granules (Moy et al., 2002).

Various substrates based on organic and inorganic carbon sources had been used to cultivate aerobic granules. Result showed that the carbon source positively dictates the diversity and dominance of the bacterial species and microstructure of aerobic granules (Lee et al., 2010; Liu & Tay, 2004). Previous finding by Adav et al. (2009) and Li et al. (2008b) suggested that granules cultivated with acetate and glucose as carbon source demonstrated dominance genus of *Zoogloea* and *Flavobacterium*, respectively. Whilst, granules cultivated in swine slurry characterized by high carbon to nitrogen ratio (1.9 – 9.4 g COD_s/ g N) is mainly composed of genus *Nitrosomonas* (Morales et al., 2013). These diversity and dominance of the bacteria species are believed to be caused by the physiological characteristics of the bacteria itself. For example, a review of the physiology of filamentous bacteria in activated sludge by Martins et al. (2004) showed that *M. parvicella* sp. was able to use a wide range of different substrate including organic acids, complex substrates and fatty acids as carbon source, whilst Eikelboom type 0092 was capable to degrade only certain proteins. Thus, these subsequently affected the kinetics and stoichiometry coefficients during microbial degradation of organic substrate.

When granules are growing at a low substrate concentration, it is foreseen that filamentous bacteria will have a higher specific growth rate than floc forming bacteria, due to the higher surface area to volume (A/V) ratio for filamentous bacteria. Whereas, a higher A/V ratio for filamentous bacteria will help to facilitate the accessibility of substrate to the filamentous cell as compared to the floc forming bacteria cell (Martins et al., 2004). At high substrate concentration, the floc forming bacteria utilize the substrate at a higher rate than filamentous bacteria, and thus will dominate the system (Liu and Liu, 2006).

As mentioned earlier in Section 2.2, the influence of mass transfer resistance was also depending on substrate concentration and diffusion. Under low substrate conditions, diffusion of substrate will become a limiting factor in aerobic granular sludge formation (Li et al., 2008a), and thus tend to decrease the substrate removal rate. Peyong et al. (2012) and Martins et al. (2003) indicated that compact granules subjected to low substrate conditions will end up as loose structure and the existence of filamentous. This might be attributed to the nature of filamentous to excellently fit in loose structure and lead to the development of irregular shape. Figure 2.3 depicted a transition of compact granules cultivated in acetate at OLR of 1.2 kg COD /m³ d to fluffy structure of granules with larger diameter after being fed with domestic wastewater at OLR of 0.13 kg/m³ d. Hence, it can be concluded that interrelationship between granule size as showed in Figure 2.2, substrate types, concentration and diffusional resistance of substrate, and DO in liquid phase and within the granule, dictates the diversity and dominance of the bacterial species and microstructure of aerobic granules.

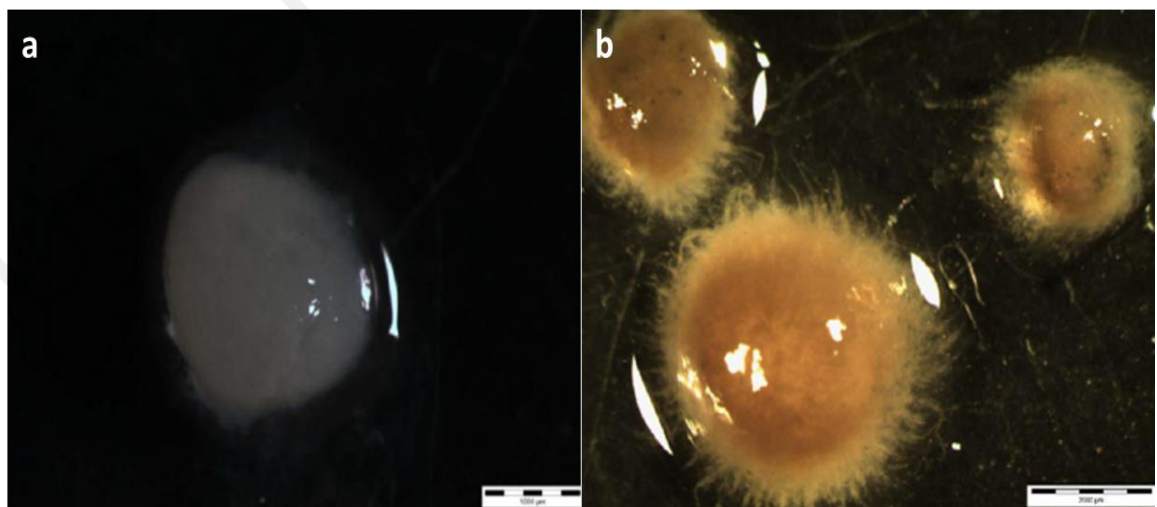


Figure 2.3: Microscopic images of aerobic granules develop in (a) acetate and (b) domestic wastewater (Peyong et al., 2012)

2.2.2 Operating Conditions

The presence of filamentous bacteria in moderate number is beneficial to serve as a binding material. However, proliferation of filamentous bacteria floating freely or extending from flocs will cause deterioration of sludge settleability and resulting in bulking sludge effect (Guo et al., 2012). As discussed in Section 2.2.1, formation aerobic granule sludge in low OLR is often subjected to the domination of filamentous bacteria. Hence, in order to control the growth of filamentous bacteria, manipulation of operating conditions depending on wastewater type are crucial. Since it is well accepted that sewage is a low type strength wastewater (low organic loading rate), review will not include control on operating conditions for high strength wastewater. Data in Table 2.1 will be used as a closed example to support the discussion in this section. Table 2.1 presents an overview of published data on various SBR configurations and operating conditions for domestic and synthetic wastewater treatment, resulting in different in MLSS volume, diameter of mature granule and period to achieve mature granules.

Table 2.1: Accumulation of SBR configurations and operating conditions for mature aerobic granules

wastewater	D (cm)	H/D	V (L)	V _{ER} (%)	Air flow rate (L/min)	SUA V (cm/s)	Cycle (h)	Settle (min)	Influent COD (mg/L)	COD OLR (kg/m ³ d)	MLSS (mg/L)	Granule diameter (mm)	Period to achieve mature granule (d)	Reference
Sewage	5	24	2.5	50	3.5	3	2	10	100-280	0.6	1300	0.63	20	Liu et al., 2007
Sewage	25	8	85	75	50.0	1.7	4	8	200	1.35	5900	0.75	60	Su et al., 2012
Sewage	50	12	1000	75	-	-	3	15	95-200	1.0	9500	0.2-0.8	300	Ni et al., 2009
Sewage	15	3.2	8	70	-	-	6	5	272-1423	2.0-3.5	5000-7000	-	34	Wang et al., 2009
Sewage	6.25	16	3	50	4.0	2.5	2	10	280	1.0	-	1.1	36	de Kreuk & van Loosdrecht, 2006
Sewage	9	22	11	40	4.0	1.1	4	15	412	1.0	-	0.7	140	Wagner & da Costa, 2013
Sewage	-	-	8	50	5.0	-	4	2	42-180	0.6	-	2.0	190	Peyong et al., 2012
Glucose	0.6	10	1.7	50	7.0	4.1	3	2	1400	4.0	-	0.88	52	Tay et al., 2004a
Glucose	5	16	1.5	50	1.5-2.0	1.6-1.7	6	5	300	0.6	2500-4500	0.75	70	Ma et al., 2013
Acetate & Propionate	10	4	3.2	50	2.83	0.6	4.5	3	200	0.58	5500	1.0	50	Zhang et al., 2011
Acetate	6	11	2	75	4.2	2.5	12	1.5	186	0.28	-	2.3±03	40	Zhu et al., 2013a

2.2.2.1 Hydrodynamic Shear Force

Similar to the formation of biofilm and anaerobic granule, hydrodynamic shear force resulting from hydraulics and particles collision is a key factor that involved in the formation, structure and stability of aerobic granules (Liu & Liu, 2008; Tay et al., 2001a). In a column-type upflow reactor like SBR, hydrodynamic shear force effect is oftenly governed by the strength of superficial upflow air velocity (SUAV). According to Tay et al. (2001a), higher shear force is preferable for the development of regular, rounder, strength and compact granules. It was found that bioflocs and regular granule were observed in reactors with SUAV of 0.3 cm/s and 1.2 cm/s, respectively. Therefore, the SUAV of 1.2 cm/s has become a threshold value for a successful cultivation of AGS (Liu & Tay, 2004). Based on the principles of thermodynamics, a review by Liu and Tay (2002) highlighted that column-type upflow reactor with higher H/D ratio can provide a longer circular flowing trajectory, which in turn creates an effective hydraulic attrition for microbial aggregation. This circular hydraulic attraction force helps to shape the microbial aggregates into regular granules that have a high cellular surface hydrophobicity and minimum surface Gibbs energy.

2.2.2.2 Organic Loading Rate (ORL)

Generally, in an SBR system, the OLR is dependent upon substrate concentration and hydraulic retention time (HRT) (Ni et al., 2009). HRT represents the retention time of substrate at a certain period of cycle time over volume exchange ratio (V_{ER}). A study by Muda et al. (2011) on the development of granular sludge for high strength wastewater (synthetic textile) proved that at 50% V_{ER} , increasing the HRT from 6 to 24 h resulted in the reduction of OLR. As the cycle time increases from 3 to 12 h, the

physical properties of granular sludge in terms of MLSS, mean size and settling velocity start to decrease from 35.3 to 23.3 g/L, 843 to 385 μm and 41.3 to 21.3 m/h, respectively. Whilst, as depicted in Table 1, for low strength wastewater, the typical value of cycle time and V_{ER} ranges from 2 to 4 h, and 50 to 75%, respectively. Hence, it is shown here that a balance between cycle time and V_{ER} will ensure enough time for system to suppress the suspended growth and optimize the substrate accumulation, and enough food for microbial growth (Wang & Liu, 2008). For an AGS system that is subjected under low strength wastewater or run over a long period, decreasing the cycle time or increasing the V_{ER} will ensure a high OLR, and hence will maintain a balance between food to microorganism ratio (F/M).

2.2.2.3 Settling Time

As mentioned earlier in section 2.1, effluent quality of biological wastewater treatment is highly dependent upon the efficiency of biosolids-liquid separation process. In SBR system, biosolids-liquid separation or so called the settling of biomass takes places before effluent being withdrawn at the end of each cycle (Figure 2.1). Biomass or sludge with a poor settleability will be washed out within the given settling time, leaving the fast settling bacteria to have more space for growth. In line with finding by Beun et al. (1999) and Qin et al. (2004b) that a short settling time was preferred for the growth of rapidly-settling bioparticles, a settling time within the range of 2 to 15 min has often being used by other researchers (Table 2.1) in order to enhance the granulation process. Gao et al. (2011) observed the rapid granulation of glucose granules occurring when reactor was run at the shortest settling time, which is from 15 to 1 min. Result showed that the granules had a better settling property (32-95 m/h) and storage stability (99%), and higher extracellular polymeric substance (EPS) (100.8 mg/g SS) content

than those developed under other conditions. Another study conducted by Adav et al. (2009) noted that selection of settling time was only crucial at the beginning of cultivation process, since most of the cyclic period was during aeration phase. Applying a short settling time at the beginning of cultivation process would ensure a washout of non-flocculating strains from sludge seed that corresponded to the shift of microbial community in granular sludge.

2.3 Stability of AGS

Based on discussion in Section 2.2.1 and 2.2.2, it is noteworthy that aerobic granule sludge could be formed under a variety of operating conditions and substrate types. Nevertheless, there are numerous reports marking the instability of aerobic granular sludge, especially during the long term operation period, which will become a major barrier to its practical application. The stability of sludge/flocs has recently drawn more attention in the field of biological wastewater treatment since it will directly influence the efficiency of solid-liquid separation process (clarification and dewatering).

As defined earlier, aerobic granules formed in reactor might consist of microbial communities performing nitrogen and phosphorus removal, glycogen accumulation, degradation of carbon source and autotrophic nitrogen removal via anammox process (Seviour et al., 2012). Herein, the stability of aerobic granules can also be defined as the ability of microbial granules to resist hydrodynamic and mechanical shear force (Sheng et al., 2010). The state of aerobic granules stability has often been described or measured in terms of bioactivity, microbial community, EPS composition and distribution, and granular characteristic (Chen et al., 2007a). Sheng et al. (2010)

proposed a multi-layer structural model of AGS (Figure 2.4) with two distinct regions which is identical with the proposed AGS multi-layer structural model as shown in Figure 2.2. As showed in Figure 2.4, the inner region provides the stability part, where the residual sludge cells are glued by non-readily extractable extracellular polymeric substances (EPS). The outer region is vice versa.

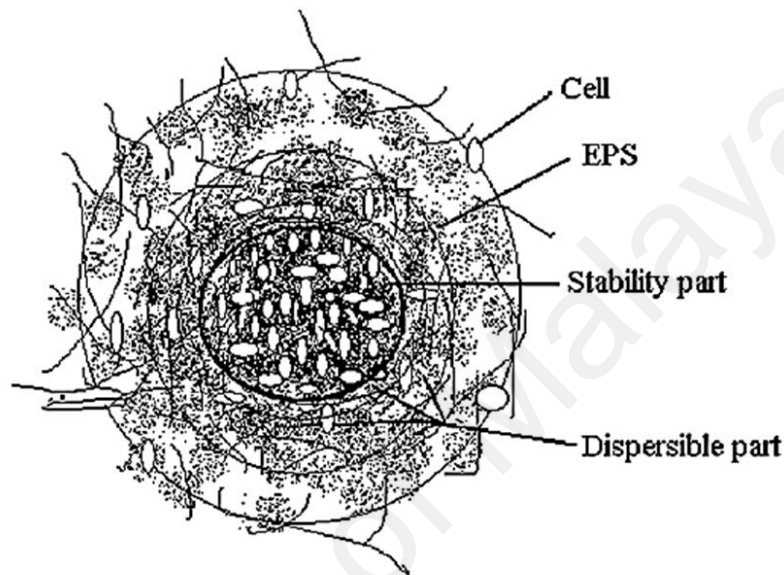


Figure 2.4: Multi-layer structural model of AGS in terms of stability (Sheng et al., 2010)

Although the effects of EPS on biofilm and anaerobic granule are well known, only in 2001, the first report that explored the role of EPS in the formation and stability of aerobic granules was presented by Tay, Liu and Liu (2001b). The following reports by Wang et al. (2005) and Mcswain et al. (2005) proved that EPS had a significant contribution to the microbial granules stability. Since then, intensive research effort has been dedicated to characterize the role of EPS in the formation and stability of aerobic granules. A comprehensive review with regard to the EPS extraction method, characteristic, spatial distribution in aerobic granule, and its role in governing the formation and stability of aerobic granules were reported by Sheng et al. (2010), Adav et al. (2008a), Lee et al. (2010) and Liu et al. (2004a). Nevertheless, none on this

author had clearly stated the mechanism of aerobic granules formation and stability with regard to others intermolecular interactions.

To date, only Liu and Tay (2002) had briefly described the interactive forces involved in aerobic sludge formation without further elaboration on the interactive mechanism or patterns. Thus, this study will demonstrate the mechanism of aerobic granules formation with regard to other intermolecular interactions, and how these forces will govern the stability of aerobic granules.

2.3.1 Mechanism of Aerobic Granules Formation and Stability

In wastewater, biomass or colloids are nearly always charged, in which electrical repulsion between them is responsible for their stability to remain in dispersion state for long periods rather than forming aggregates. Hydrophilic and hydrophobic are two terms that are coined to specify the classes of biomass. Hydrophilic infers a strong affinity for water molecules in the surface layer of the biomass to stay in stability rather than because of the slight charge that they might possess. Whilst, hydrophobic infers water repulsion that dependent on electrical charge or mutual repulsion for biomass stay in suspension (Bratby, 2006; Tebbutt, 1998). Thus, in order to alter the stability of biomass that remains in dispersion state, the interactive forces applied for self-immobilization of bacteria to form well-defined granules can be described as a two-step process.

The first step process is physical agitation to initiate bacterium-to-bacterium contact or attachment onto solid surface. The forces that might be involved in this step are hydrodynamic shear force, substrate diffusion, gravity force, Brownian movement

and cell mobility (Liu and Tay, 2002). Sources and effects of substrate diffusion and hydrodynamic shear force had been discussed in Section 2.2.1 and 2.2.2.1, respectively. Self-sedimentation via gravity force is only applicable for biomass down to a size of about 50 μm , depending upon self-density, where this method is not feasible for smaller biomass (Tebbut, 1998). Brownian movement caused by bombardment of water molecules and also when rapidly settling biomass overtakes more slowly settling particles (Tebbut, 1998) help to enhance the physical force of attraction in pulling the biomass together. However, if the forces of repulsion exceed those of attraction, the biomasses are not allowed to contact and remain dispersed indefinitely (Hammer & Jr Hammer, 1996). In terms of cell mobility, it is expected that cell can move by means of flagella, cilia or pseudopods to approach each other (Liu and Tay, 2002).

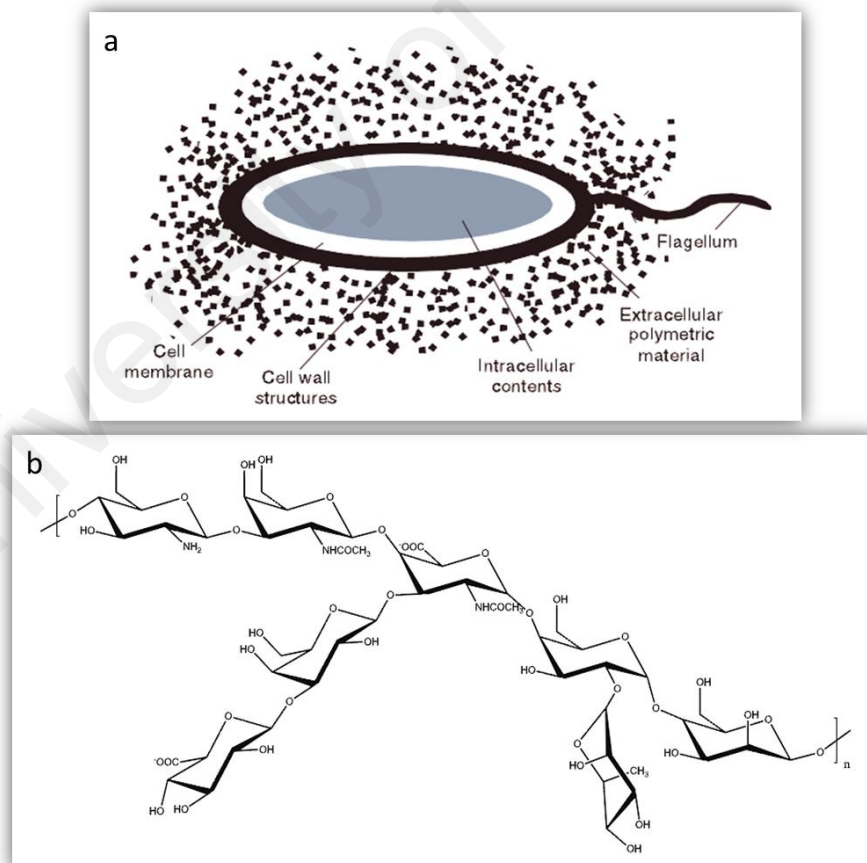


Figure 2.5: a) Illustration of EPS distribution around cell wall (Mittelman, 1985) and b) Proposed structure of repeat unit of exopolysaccharides from AGS (Seviour et al. 2011)

The second step process is intermolecular interaction or so called physicochemical and microbiological interactions of different trophic bacteria groups to keep the aerobic granule in stability. Mittelman (1985) illustrated the distribution of EPS around an individual cell wall (Figure 2.5a), with the structure of repeat unit of exopolysaccharides (one of synthesis component from EPS) that carries functional groups (Figure 2.5b) as hydroxyl (O-H), carboxyl (C=O) and amines (N-H) was given by Seviour et al. (2011). Component analysis on EPS using Fourier transform infrared spectroscopy (FTIR) by Zhu et al. (2012a) had further confirmed the proposed structure group by Seviour et al. (2011).

According to Flemming and Wingender (2010), the functional groups interact with each other in terms of hydrogen bonding, electrostatic and ionic attractive forces for the stability of EPS matrix (Figure 2.6). Apart from that, Van der Waals interaction that exists between any of two EPS components also helps to serve for EPS stability. As a result, the ionisable groups presented on cell aggregates surface will decrease, and subsequently lower the polar interaction of EPS with water molecules to promote cell hydrophobicity (Wang et al., 2006). Thus, in the sense of thermodynamic, an increase in cell hydrophobicity simultaneously causes a decrease in the excess Gibbs energy of the surface, which in turns promotes self-aggregation of cells from liquid phase to form a new solid phase (Liu et al., 2009; Liu & Tay, 2002).

As showed in Figure 2.4, the outer region of aerobic sludge is a dispersible sludge cells that are glued by the readily extractable EPS (Sheng et al., 2010). It is expected that cell aggregates will carry negative charges due to unbound functional groups. This is consistent with the report by Wang et al. (2014) that indicated a negative value in zeta potential of EPS was mainly due to the ionization of the anionic functional groups such

as carboxylic and phosphate. Since cell aggregates have the same charge, there will be a repulsive force that inhibits flocculation process. Here, filamentous bacteria help to bridge the individual cell or cell aggregates together. Besides, in order to promote the flocculation of cell aggregates for the formation of solid sludge, the forces involved in First step process is needed.

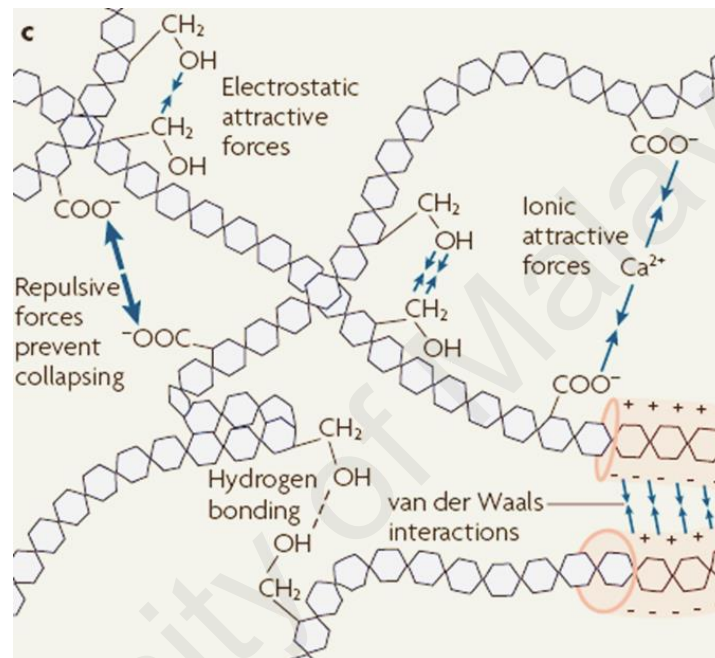


Figure 2.6: Physicochemical interaction and entanglement of EPS components from different cells that dominate the stability of EPS matrix (Flemming and Wingender, 2010)

Figure 2.7 depicts a summary of the aerobic granule formation based on the discussion above. Physical agitation force (First step process) helps to initiate individual cell (Step A) contacts, whilst intermolecular interaction (Second step process) will ensure the aggregation of individual cells (Step B). As the cell aggregates carry negative charges (Step C), bridging between filamentous bacteria, divalent (Ca^{2+} , Mg^{2+} , etc.) or monovalent (K^+ , Na^+ , etc.) metal cations from the particle surface of wastewater with the dissociated functional groups on the cell aggregates will enhance the flocculation process. In Step D, polymer (polymeric chains of EPS) entanglement tends to rearrange the position of cell aggregates to become more compact and strong cell flocs (Sheng et

al., 2010). Lin, Sharma, and van Loosdrecht (2013) had given a clear illustration of the strong gel structure developed from a crosslink between alginate-like exopolysaccharides (EPS components) and Ca^{2+} . On Step E, cell flocs approach each other's when there is an electrostatic attraction between positive and negative areas of cell flocs. Shear force would shape and densify the cell flocs (Step E) to become granular sludge as showed in Step F.

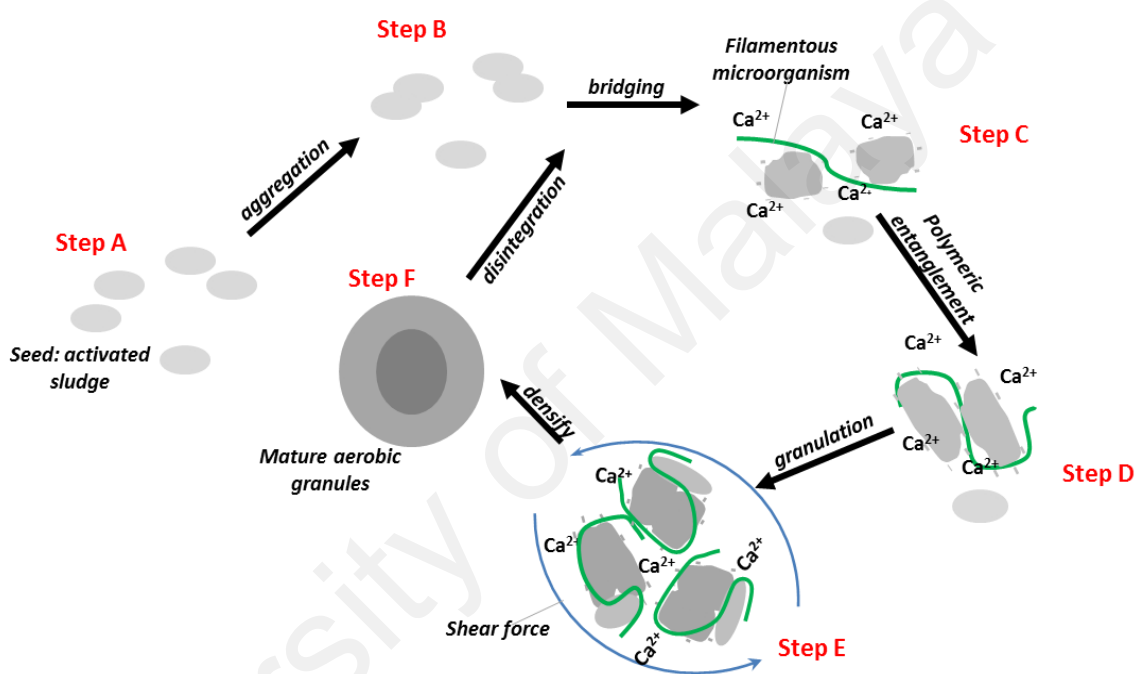


Figure 2.7: A conceptual of granule formation and breakage

The mature granular sludge will subsequently disintegrate after reaching a certain critical size and causing an overall reduction in granular sizes (Verawaty et al., 2013). According to Chiu et al. (2007), the critical size of the granules could be defined as diameter of the aerobic granule above an anaerobic zone or mass diffusion limitation would be present. In a low substrate/DO condition, the depth of diffusion limitation might occur at a depth of less than 1/3 from the granules diameter, in which the thickness of anaerobic zone will be twice that of aerobic zone.

2.3.2 Stability Loss

Lee et al. (2010) proposed four mechanisms to account for the loss of aerobic granule stability, which are outgrowth of filamentous organism, hydrolysis of the anaerobic core, losses of functional strains and role of EPS. Nevertheless, Luo et al. (2014) narrowed it down to two possible causes, which are reduction in net tyrosine production in the EPS and major microbial shift that leads to the collapse of granule structure. This can further be interrelated with the multi-layer structural model of aerobic granules as showed in Figure 2.2 which exhibit the stratification of EPS and microbial population at different zones. Mass transfer resistance at different zones will result in a significant drop in microbial activity and growth rate, where larger aerobic granule will be affected even more severely. Herein, it can be hypothesised that the sturdiness of aerobic granule structure plays an important part in ensuring its stability.

Under normal or static conditions, the size of aerobic granules will govern the microbial activity inside the aerobic granule (see section 2.2). Increase in aerobic granules size with time is an unstoppable process and will subsequently lead to the hydrolysis of anaerobic core. Whereas, the hydrolysis process is attributed to the gases and organic acids produced (Tay et al., 2002), and mass transfer resistance that hinders nutrient intake for microbial activity. Later, microbial shift to fit its own physiological requirement can be observed, in which filamentous organism will dominate the aerobic granule. Thus, this will alter the EPS matrix and lead to the loose structure of aerobic granule. At this point, an external force will disintegrate the aerobic granules becoming small flocs that will continue to regrow with time.

2.4 Research Gaps on AGS Formation and Stability

As shown in Table 2.1, in order to attain a successful development of aerobic granules, most researchers tend to manipulate either the aeration flow rate or reactor H/D ratio over 10 that will ensure a high shear force. Recently, Abdullah et al. (2013) and Zhu et al. (2013) used SBR with H/D ratio of 17 and 11, and managed to attain mature aerobic granules within 60 and 40 days of formation periods. This kind of practice will limit the practical application of aerobic granules since the existing SBR at working plant in Malaysia mostly has low H/D ratio and increase in operational cost for aeration energy requirement. In practice, factors like maintenance problems and impact of natural disaster will be critical and has to be considered in designing a high H/D ratio reactor.

The selection of reactor type and H/D ratio for applications at the real site vary depending on the characteristics of the wastewater itself. For example, Papadia et al. (2011), concluded that the air supply system has greatly influenced the efficiency of pilot scale bioreactors treating textile wastewater. The highest performance was achieved in Bioflotation and Fixed Bed Biofilm Reactors, which exhibited an H/D ratio of 5 and 3 respectively. The list presented by Liu et al. (2014) on aerobic granule reactors treating real wastewater showed that the H/D ratio for pilot scale reactors in both the Netherlands and China was 10. Meanwhile, the H/D ratio for pilot scale reactors treating synthetic wastewater in Spain was 8. However, at full scale application, Gansbaai WWTP, located in South Africa, demonstrates that the lowest H/D ratio is 0.39. **Thus, although the main criteria that ensures the successful formation of aerobic granules is the high H/D ratio reactor, in the case of dealing with real site applications, the low H/D ratio reactor is preferable.**

Apart from increasing the reactor H/D ratio, Zhou et al. (2014) and Liu and Tay (2007) used airlift type reactor to expedite the granulation process at low SUAV of 1.4 cm/s and 1.2 cm/s, respectively. Airlift reactor can deliver high shear force although the aeration rate is low and better mixing as compared to bubble column like SBR. Study by Kong et al. (2009) reported that reactor H/D ratio has no effect on operational conditions and aerobic granule characteristics. **However, the study neglected the difference in reactor working volume and organic loading rate (OLR) that may influence hydrodynamic properties and balance between foods to microorganism (F/M) ratio.**

In addition, tabulated result in Table 2.1 showing that the difference in SBR configurations and operating conditions will yield a significant impact on period to achieve mature granules and MLSS volume, and a slight difference in mature granule diameter. For example, de Kreuk and van Loosdrecht (2006), Ni et al. (2009), and Wagner and da Costa (2013) applied similar OLR of 1.0 kg COD/m³ d, and running at different SBR configurations especially in aspect of diameter ratio and operating conditions. Result showed that Ni et al. (2009) took the longest time (300 d) to acquire mature granule as compared to de Kreuk and van Loosdrecht (2006) and Wagner and da Costa (2013), was 36 d and 140 d, respectively. The obvious diversity in period to achieved mature granules could be due to the different in working volume and hydrodynamic properties which govern by SUAV. It should be noted that, the similar pattern also occurred when comparing result of Liu et al. (2007) and Peyong et al. (2012), which is running at similar OLR of 0.6 kg COD/m³ d, with different working volume of 2.5 L and 8.0 L, and air flow rate of 5 L/min and 3.5 L/min, respectively. Thus, it is apparent that the intensity of SUAV is control by air flow rate and reactor diameter as a function of surface area. Reactor with low H/D ratio which running at

high working volume and low SUAV will subsequently exhibited inadequacy in mixing or hydrodynamic efficiency. **In this context, study to compare and optimize the performance of aerobic granules develops in reactor with low H/D ratio and high H/D ratio should be carried out to address this issues.**

When comparing result of Liu et al. (2007) and Ma et al. (2013) that use different type of wastewater, but similar OLR of 0.6 kg COD/m³ d, it was an anomalous to note that the period to achieve mature granule was much longer in easily utilized substrate (glucose) than in complex substrate (domestic wastewater). This is likely to be caused by the different SBR configurations and operating conditions as discussed in Section 2.2.2 and above. Besides, in order to expedite the formation of aerobic granules, both Liu et al. (2007) and Ma et al. (2013) used aerobic granules that pre-cultivated at 1000 mg/L acetate and glucose, respectively, as seed. Su et al. (2012), Ni et al. (2009) and Wagner and da Costa (2013) provided the complete research results of AGS formation that utilized solely domestic wastewater. Whilst, other researcher tend to use pre-cultivated AGS from high concentration synthetic wastewater as seed or inoculation that adapted to and stabilized easily in new environments as compared to fresh activated sludge. Once again, this will not be a good practice for the practical application of aerobic granule since a large volume of AGS seed cultivated in high synthetic wastewater will be needed to accommodate the requirements of real site of SBR. **Despite being costly, the environmental factor like temperature, low and variable OLR vary on site, while these parameters can be precisely controlled in lab-scale reactor.**

The stability of AGS has been questioned by a few recent achievements. Liu and Tay (2012) suggested controlling the OLR in a specific optimal range to benefit the

growth of aerobic granules over flocculent sludge during long term operation. However, controlling the OLR in the operation of real wastewater will be challenging due to the variation in influent parameters. Furthermore, report by Adav et al. (2010) on biological nature for aerobic granules breakdown showed that a reduction in protein production in extracellular polymeric substances (EPS) was correlated with OLR range. Another study by Isanta et al. (2012) on a successful simultaneous nitrification and denitrification by granular SBR at pilot scale treating low strength wastewater during long term operation was solely using synthetic wastewater with fix COD concentration. Although Pronk et al. (2015) have successfully implemented AGS technology for the treatment of sewage at full scale with detailed description of the process, conversions, energy usage and design consideration, relatively, less information was obtained regarding the characteristics of AGS with respect to OLR variations. **Thus, further enhancements to characterize the behaviour of AGS developed using real wastewater, with respect to low and OLR variations have to be established.**

Nevertheless, Table 2.1 showed that aerobic granules cultivated from domestic wastewater could be developed at OLR as low as 0.6 kg COD/m³ d up to 1.35 kg COD/m³ d. Whilst, this study will attempt to cultivate AGS at fluctuating OLR as low as 0.10 kg COD/m³ d up to 0.81 kg COD/m³ d without pH and temperature control. It can be concluded that there is not much diversity in diameter of mature granules developed in either domestic or low strength synthetic wastewater. The typical size of mature granules could be assumed to be around 0.75 mm to 0.80 mm, and can reach up to 2.00 mm depending on selection of operating conditions. Table 2.2 present a detail on the literature reports in designing the experimental works for aerobic granules treating sewage.

Table 2.2: Accumulation of experimental design on aerobic granules for sewage treatment

Reactor Design	Operating Condition	Experimental Design	Reference
Types: SBR V _w : 2.5 L H: 120 cm D: 5 cm V _{ER} : 50 % DO: mg/L Air flow rate: 3.5 L/min	Cycle: 4 h Feed: 5 min Aerate: 200-220 min Settling: 10-30 min Discharge: 5 min Period: 1 and 4 month Temperature: 25 & 35 °C HRT: 8 OLR: 0.6 kg COD/m ³ d (200mg/L)	<p> Started-up/Acclimation 1.2 L activated + acetate synthetic w/w sludge (1000 mg/L COD) → Steady state (after 5 week) → R₃ (synthetic w/w) Operated with same condition as R₁ </p> <p> To test long term stability Stop after 3 month ← R₂ Domestic w/w R₁ </p> <p> Phase 1: 4 h cycle, 30 min fill, 195 min aerate, Period; 12 day Phase 2: 2 h cycle, 15 min fill, aerate 90 min, Period; day 13 onwards </p>	Liu et al., 2007 “ COD removal and nitrification of low strength domestic wastewater in aerobic granular sludge SBR”
Objective	Treating low strength domestic wastewater with COD removal and nitrification by seeding aerobic granules in SBR at 35 C° and 25°C.		
Result	<ul style="list-style-type: none"> Since seeded granules were first cultivated with 1000 mg/L COD, 200 mg/L COD in domestic w/w was easily utilized. Little change of settleability of granular sludge due to the disturbance of wastewater type, OLR and temperature can resume quickly. 		

Table 2.2, continued

Reactor Design & Operating Condition	Experimental Design	Reference																									
Types: SBR V _w : 85 L H: 2 m D: 25 cm DO: - mg/L Air flow rate: 50 L/min Temperature: Ambient COD in raw domestic w/w: 200 mg/L	<p style="text-align: center;">Operational strategies before day 70.</p> <table border="1" style="margin-left: auto; margin-right: auto;"> <thead> <tr> <th>Time (days)</th> <th>Cycle time (h)</th> <th>Exchange ratio (%)</th> <th>Settling time (min)</th> <th>OLR (kg COD/m³ d)</th> </tr> </thead> <tbody> <tr> <td>1-8</td> <td>12</td> <td>50</td> <td>20</td> <td>0.35</td> </tr> <tr> <td>9-12</td> <td>8</td> <td>60</td> <td>15</td> <td>0.54</td> </tr> <tr> <td>13-19</td> <td>6</td> <td>75</td> <td>12</td> <td>0.90</td> </tr> <tr> <td>20-70</td> <td>4</td> <td>75</td> <td>8</td> <td>1.35</td> </tr> </tbody> </table> <p style="margin-left: 20px;"> <i>Acclimatization</i> ← <i>Granulation fully achieved after 45 days</i> ← </p> <p style="margin-left: 100px;"> Seed sludge (anaerobic digested sludge) → R₁ (20 g/L) → R₂ (4 g/L) </p>	Time (days)	Cycle time (h)	Exchange ratio (%)	Settling time (min)	OLR (kg COD/m ³ d)	1-8	12	50	20	0.35	9-12	8	60	15	0.54	13-19	6	75	12	0.90	20-70	4	75	8	1.35	Su et al., 2012 “Optimal cultivation and characteristic of aerobic granules with typical domestic sewage in an alternating anaerobic/aerobic SBR”
Time (days)	Cycle time (h)	Exchange ratio (%)	Settling time (min)	OLR (kg COD/m ³ d)																							
1-8	12	50	20	0.35																							
9-12	8	60	15	0.54																							
13-19	6	75	12	0.90																							
20-70	4	75	8	1.35																							
Objective	To study the effect of High sludge loading rate and low sludge loading rate (at acclimatization stage) on cultivation of AGS																										
Method	<ul style="list-style-type: none"> ▪ Particle size distribution was determined by Master sizer 2000 (Malvern) (average diameter of granular ranging from 700 to 800 μm) ▪ Sludge concentration (MLSS) was maintained at approximately 4 ± 0.5 g/L until granulation fully achieved after 45 days operation by manually discharging the upper slow-settling sludge. 																										
Result	<ul style="list-style-type: none"> ▪ High sludge concentration (12.3-20 g/L) and low sludge lading rate (0.021-0.056 kgCOD/kgSSd) is the effective method for the formation of initial particles at the start-up phase. ▪ A 4 h cycle with an 1 h anaerobic stage was selected as Optimize condition for AGS granulation. 																										

Table 2.2, continued

Reactor Design & Operating Condition	Experimental Design			Reference	
<p>Types: SBR V_w: 85 L Bioreactor and an 8 L external Aeration column. H_{Reaction}: 1.8 m Internal D_{Reaction}: 50 cm</p> <p>DO: In aeration column, change gradually from 4.5 to 8 mg/L with recirculation rate ranged 8:1 to 10:1 and DO near the outlet of bioreactor was below 0.5 mg/L.</p> <p>COD in raw domestic w/w: 144-628 mg/L</p>	Period	O_{influx} (g/L·d)	HRT (h)	MLSS(g/L)	Liu & Dong, 2011 “Simultaneous COD and nitrogen removal in a micro-aerobic granular sludge reactor for domestic wastewater treatment”
	I	0.11/0.13/0.17/0.20/0.22/0.25	8	15~16	
	II	0.20	5/6/7/8/10	15~16	
	III	0.20	8	11/5.9	
	Seed: Anaerobic granules + aerobic activated sludge → ratio 4:1 MLSS concentration = 16 g/L				
Objective	To optimize the simultaneous COD and nitrogen removal in a micro-aerobic granular sludge reactor with external oxygenation.				
Method	<ul style="list-style-type: none"> ▪ A part of effluent was oxygenated and recirculated together with influent into the bottom of bioreactor reactor. 				
Result	<ul style="list-style-type: none"> ▪ Nitrogen removal in way of SND needs longer HRT than COD degradation in the micro-aerobic system. ▪ High biomass concentration is benefit for nitrogen removal because lower SLR and longer sludge retention can support the increase of slow-growing autotrophic nitrifiers. ▪ Excess sludge at high biomass concentration serve as carbon source of denitrification through endogenous metabolism when the influent organic was not enough. ▪ The ration of BOD:TN in influent is recommended more than 4 to sustain nitrogen removal in the conventional process. Otherwise addition of carbon source is needed. 				

Table 2.2, continued

Reactor Design & Operating Condition	Experimental Design	Reference																												
<p>Types: SBR V_w: 1000 L H: 6 m Internal D: 50 cm DO: 2 mg/L. COD in raw domestic w/w: 95-200 mg/L</p>	<p>Seed: Aerobic activated sludge. Characteristic; sludge age of 10 d, MLSS of 6.6 g/L, SVI of 75.5 ml/g, specific gravity of 1.004, settling velocity of 6.8 m/h.</p> <p>Inoculated: 700 L activated sludge → MLSS of 4 g/L</p>	<p>Ni et al., 2009</p> <p>“Granulation of activated sludge in a pilot-scale SBR for the treatment of low-strength municipal wastewater”</p>																												
<table border="1"> <thead> <tr> <th>Phase</th> <th>V_{ER} (%)</th> <th>Cycle (h)</th> <th>Fill (min)</th> <th>Aerate (min)</th> <th>Settle (min)</th> <th>Draw (min)</th> </tr> </thead> <tbody> <tr> <td>Initial</td> <td>50</td> <td>4</td> <td>5</td> <td>185-200</td> <td>15-30</td> <td>20</td> </tr> <tr> <td>After 1 month</td> <td>60</td> <td>3</td> <td>5</td> <td>124-140</td> <td>15-30</td> <td>20</td> </tr> <tr> <td>Day 80 onwards</td> <td>70</td> <td>3</td> <td>5</td> <td>124-140</td> <td>15-30</td> <td>20</td> </tr> </tbody> </table>			Phase	V_{ER} (%)	Cycle (h)	Fill (min)	Aerate (min)	Settle (min)	Draw (min)	Initial	50	4	5	185-200	15-30	20	After 1 month	60	3	5	124-140	15-30	20	Day 80 onwards	70	3	5	124-140	15-30	20
Phase	V_{ER} (%)	Cycle (h)	Fill (min)	Aerate (min)	Settle (min)	Draw (min)																								
Initial	50	4	5	185-200	15-30	20																								
After 1 month	60	3	5	124-140	15-30	20																								
Day 80 onwards	70	3	5	124-140	15-30	20																								
Objective	To optimize the granulation of activated sludge by selecting the optimum V_{ER} AND settling time.																													
Method	<ul style="list-style-type: none"> Anoxic phase was not included in SBR cycles to favour the conversion (N-removal) efficiency. 																													
Result	<ul style="list-style-type: none"> The OLR is dependent on both influent substrate concentration and hydraulic loading rate. The HLR of an SBR is governed by its volume exchange ratio and cycle period. A short settling time preferentially selects for the growth of rapidly-settling bioparticles and bioparticles with a poor settleability are washed out. For low strength wastewater, granulation could be achieved and accelerated when the SBR was operated at a high V_{ER} and low settling time. 																													

Table 2.2, continued

Reactor Design	Operating Condition	Experimental Design			Reference																
Types: SBR V _w : 8 L H: 48 m Internal D: 15cm	Cycle: 6 h Feed: 5 min Anaerobic stirring: 90 min Aerobic reaction: 240 min Settling: 5 min Discharge: 10 min Idle: 10 min V _{ER} : 70% SRT: 20-40 d DO: 2-3 mg/L. COD in raw domestic w/w: 272-1423 mg/L OLR: 0.75-3.41 kg COD/m ³ d	<p>Seed: Granular sludge cultivated using synthetic wastewater. Characteristic; size of 0.8-1.5 mm, MLSS of 3000 mg/L, SVI₅ of 20-40.</p> <table border="1"> <thead> <tr> <th>Period</th> <th>Cycle count</th> <th>Day count</th> <th>Medium</th> </tr> </thead> <tbody> <tr> <td>1</td> <td>1-32</td> <td>8</td> <td>40% Domestic w/w + 60% synthetic w/w</td> </tr> <tr> <td>2</td> <td>33-132</td> <td>25</td> <td>60% Domestic w/w + 40% tap water</td> </tr> <tr> <td>3</td> <td>133-705</td> <td>143</td> <td>100% Domestic w/w</td> </tr> </tbody> </table> <p>Acclimatization: Period 1 and 2 1 day = 4 cycle</p>			Period	Cycle count	Day count	Medium	1	1-32	8	40% Domestic w/w + 60% synthetic w/w	2	33-132	25	60% Domestic w/w + 40% tap water	3	133-705	143	100% Domestic w/w	Wang et al., 2009 “ Characteristic of aerobic granules and nitrogen and phosphorus removal in a SBR”
Period	Cycle count	Day count	Medium																		
1	1-32	8	40% Domestic w/w + 60% synthetic w/w																		
2	33-132	25	60% Domestic w/w + 40% tap water																		
3	133-705	143	100% Domestic w/w																		
Objective	Cultivation of AGS using synthetic wastewater (sodium acetate as carbon source) to treat domestic wastewater																				
Method	<ul style="list-style-type: none"> Sludge particle size distribution was determined by laser particle size, Malvern Master Sizer and granulometry procedure. From cycle 649 to 680, shock loading effect on SBR was investigated, and influent COD increased to 1000 mg/L by adding sodium acetate. 																				
Result	<ul style="list-style-type: none"> MLVSS/MLSS ratio increased with the particle size increasing. High influent COD volumetric loading rate was favourable for granule stability, increasing of sludge concentration and sludge particle size. SBR has a certain shock loading resistance ability. Influent TOC/TN ratio, 0.42-2.26 was lower than theoretical value of 2.86. Thus, removal of TN subsequently low which is around 47%. TOC was mainly removed during the anaerobic stage, and microorganism stored TOC as poly-β-hydroxybutyrate (PHB) under anaerobic condition for later use during aerobic stage. 																				

Table 2.2, continued

Reactor Design & Operating Condition	Experimental Design	Reference																					
Types: SBAR V _w : 3 L H _{dc} : 98 cm D _{dc} : 6.25 cm H _r : 90 cm Dr: 4cm Air flow rate: 4 L/min Superficial up-flow velocity: 0.025 m/s pH: 7.0 Temperature: 20 °C HRT: 5.6 h V _{ER} : 50% OLR: 1.0 kg COD/m ³ d	<p>Seed: activated sludge and SS (<0.2 mm) from the effluent of a lab scale granular sludge reactor fed with synthetic influent (OLR = 1.6 kg COD/m³ d)</p> <p>Medium: Pre-settled sewage</p> <table border="1" data-bbox="678 638 1655 791"> <thead> <tr> <th>Phase</th> <th>Cycle (h)</th> <th>Fill (min)</th> <th>Anaerobic period (min)</th> <th>Aerobic (min)</th> <th>Settle (min)</th> <th>Draw (min)</th> </tr> </thead> <tbody> <tr> <td>1</td> <td>3</td> <td>60</td> <td>-</td> <td>115^a</td> <td>6-15</td> <td>5</td> </tr> <tr> <td>2</td> <td>2</td> <td>30^b</td> <td>15</td> <td>70^a</td> <td>6-10</td> <td>5</td> </tr> </tbody> </table> <p>^a: minus the applied settling time for aeration ^b: anaerobic feeding</p>	Phase	Cycle (h)	Fill (min)	Anaerobic period (min)	Aerobic (min)	Settle (min)	Draw (min)	1	3	60	-	115 ^a	6-15	5	2	2	30 ^b	15	70 ^a	6-10	5	De Kreuk & van Loosdrecht, 2006 “Formation of aerobic granules with domestic sewage”
Phase	Cycle (h)	Fill (min)	Anaerobic period (min)	Aerobic (min)	Settle (min)	Draw (min)																	
1	3	60	-	115 ^a	6-15	5																	
2	2	30 ^b	15	70 ^a	6-10	5																	
Objective	To cultivate AGS																						
Method	<ul style="list-style-type: none"> ▪ Oxygen concentration was to 100% (= 9.1 mg/L) of oxygen saturation during the whole aeration time. ▪ Particles and biomass with settling velocity lower than 2 m/h were washed out. ▪ No stirring during anaerobic time. 																						
Result	<ul style="list-style-type: none"> ▪ Short cycle times and concentrated wastewater are preferred to form granules in a SBR when low strength wastewater is used. ▪ Filamentous and finger type structures overgrown granules grown which can be explained by the presence of COD during aerobic period and lack of shear stress. ▪ A considerably longer start up time is needed. 																						

Table 2.3 present a summary of research works regarding the operating conditions strategized to enhance the stability of aerobic granules. During long term-operation, applying appropriate operational condition like selective sludge discharge, settling time (Liu & Tay, 2012; Zhu et al., 2013a), aerobic-anaerobic phase (Isanta et al., 2012), shear force (Chen et al., 2007a) and cycle time (Liu and Tay, 2008) are necessary for granular sludge stability. Result from selective sludge discharge controls had proven that aerobic granular size played an important role in its stability. In order to alleviate the problems with filamentous bacteria, aerobic granules growth rate was controlled by an intentional increase in the N/COD ratio (Liu et al., 2004b; Wang et al., 2007b). In addition, a positive recovery of aerobic granules after being exposed to toxic shock loading (Amorim et al., 2014; Zhu et al., 2013b), breakage (Liu et al., 2014), drying (Lv et al., 2013) and storage (Xu et al., 2010) had ascertained its stability.

Table 2.3: Strategies controls to serve the stability of concern from AGS formation.

Operating periods (d)	Stability of concern	Operating conditions control	Findings remark	Reference
60	Long term operation	The SRT of flocs and granular sludge was controlled simultaneously by selective sludge discharge from different location of SBR.	Long SRT of granular sludge will leads to sludge destabilization. An appropriate discharge of proportional aging granular sludge and retention of enough new-born flocs are necessary for granular sludge stability.	Zhu et al. 2013a
800	Long term operation	Control of settling time (2 to 4 min) accordingly, when the volume percentage of flocculent sludge (size below 200 μm) was over 35%.	The specific growth rate of flocculent sludge decreased with the increase in initial flocculent sludge concentration.	Liu & Tay 2012
330	Long term operation (removing C-N-P simultaneously)	Combination of a long static feeding phase followed by aeration phase. Sludge was regularly purged to maintain the SRT around 20 d (From days 180 to 230)	BNR via nitrite was successfully achieved due to low DO/ammonium ratio (0.45 to 0.9). Regular purged based on mineral content (hydroxyapatite) of granular sludge rather than SRT help to avoid destabilization.	Isanta et al. 2012
70	High growth rate	The N/COD ratio of wastewater or substrate was controlled in order to enrich the slow-growing nitrifying bacteria.	Substrate with high N/COD ratio leads to high nitrifying population that slow down the growth rate. Aerobic granule with low growth rates showed strong structure and good settleability.	Liu et al. 2004b
280	Free ammonia (NH_3) inhibition	Stepwise increased of substrate NH_4^+ -N concentration (50 to 200 mg/L) to avoid inhibition of both heterotrophic and nitrifying activities by NH_3 which was reported to be at 42 mg/L.	Stepwise method increased microbial selection pressure adjustment of microorganism and triggered gradual improvements in performance of aerobic granules.	Wang et al. 2007b
120	Shear force	Shear force in terms of SUAV in four SBR were controlled at 0.8, 1.6, 2.4 and 3.2 cm/s by manipulating the air flow rate intensity.	Granules develop at high shear force (2.4 and 3.2 cm/s) can maintain a sturdy structure and have the potential of long-term operation.	Chen et al. 2007a

Table 2.3, continued

Operating periods (d)	Stability of concern	Operating conditions control	Finding remarks	Reference
180	Starvation	It was expected that the depletion of 500 mg/L acetate COD occurred during the first half hour of aerobic phase. The starvation period in three SBR were controlled by manipulating the length of cycle time, which were 1.5, 4 and 8 h.	The short starvation time (cycle of 1.5 h) played a negative role on the stability of aerobic granules although the short starvation time could speed up the formation of granules.	Liu & Tay, 2008
70	Toxic shock by 4-Chloroaniline (4-CIA)	Stepwise increased of substrate 4-CIA concentration was applied during the operation.	The growth of functional microbes would be inhibited when the influent 4-CIA concentration was above 180 mg/L. Decreased in EPS production (especially PN) and C=O stretching vibration were observed as the 4-CIA increased, led to AGS disintegration.	Zhu et al., 2013b
340	Toxic shock by fluoroquinolones (FQs)	Single and continuous FQs shock loadings were applied under different cycle time (3 and 8 h) and concentration (32 and 9 µm).	Exposure to the FQs will disintegrated aerobic granules. The system promptly recovered from FQ inhibition within 1 month after removing the FQs in the feed.	Amorim et al., 2014
7	Drying and Re-cultivation	Fresh granule were dried by means of acetone gradient method and stored for 40 d. Dried granule letter be used for re-cultivation under previous operational conditions of fresh granule.	Dried granules can be reactivated through a re-cultivation process to recover their organic degradation capacity within 12 h, or appearance in 5 d.	Lv et al., 2013
160	Re-formation after breakage	20 g/L poly (PAC) was mixed with aerobic granular sludge which had deteriorated during the last phase of granule cultivation.	Augment of aluminium chloride (PAC) reduced the granule re-formation time and enhanced the stability of the regenerated granule.	Liu et al., 2014
21	Storage	Stable granules seeded with pellets after operation for 25 days was stored at room temperature (25 ± 1 °C) for 21 day without aeration and nutrients.	Aerobic granules seeded with pellets were more resistant against storage than those seeded with activated sludge.	Xu et al., 2010

CHAPTER 3

METHODOLOGY

3.1 Study Outline

As mentioned earlier in Chapter 1, in Malaysia, sewage has become a major source of river pollution due to the unstandardized design and operation of small STP, and the use of obsolete technology that failed to cope with the expansion of social economics requirements. In order to counter this problem, Indah Water Konsortium (IWK) Sdn. Bhd. embarked upon a program to rehabilitate and refurbish the old STPs. However, land acquisition will become a major issue in selecting or upgrading the new STPs. Advanced technology like SBR is best suited in urban areas, in which land prerequisite has become more stringent. For example, Jelutong STP (1.2 million PE) that utilized SBR technology only required 12 ha land as compared to 16 ha by the new Pantai 2 STP (1.4 million PE and utilized advance A2O technology). Thus, by looking at the benefits of the combination of AGS and SBR technology, it is hoped that this system will be pervasive soon in Malaysia. It is noted from the literature review in Chapter 2, that numerous studies have been directed on AGS formation and characterization. However, very few studies are done regarding the stability of AGS developed in real wastewater, especially domestic sewage have been reported. This study will enlighten the formation and stability of AGS develops in SBR with a low H/D ratio, which is similar to a real site application. The formation and breakage cycle in AGS system is something that cannot be avoided. Thus, this study will expose the ability of AGS system to recover from breakage through AGS characterization. Figure 3.1 exhibits a flowchart illustrating on the overall outline of work for this study.

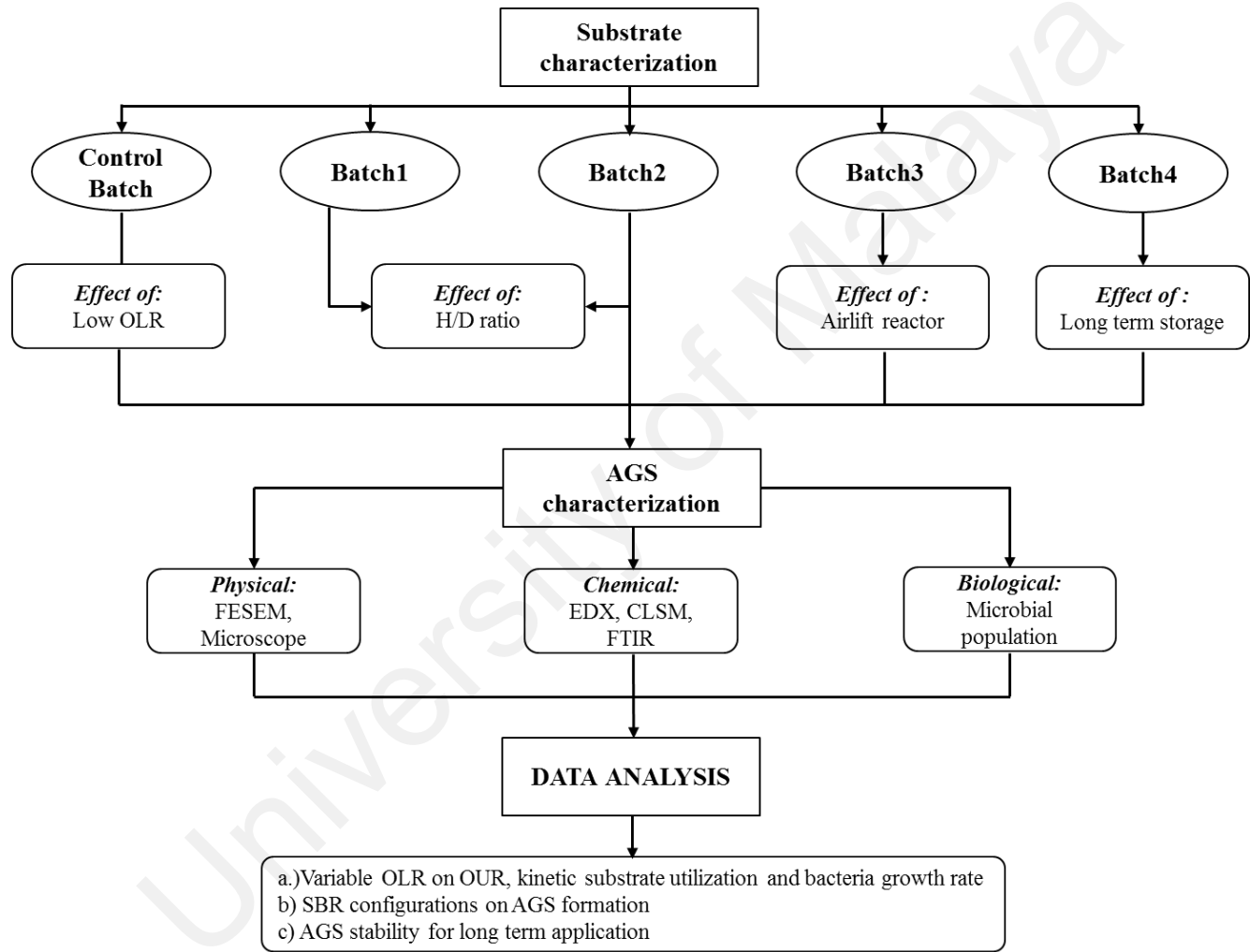


Figure 3.1: Flowchart of study outline

3.2 Experiments Set-Up

3.2.1 Sewage and Activated Sludge Collection Site

Sewage (substrate) for this study was collected from Pantai 1 STP and Damansara STP (KLR354). Pantai 1 STP is located at Pantai Dalam at the south central end of Kuala Lumpur city, which is closed to the new Pantai 2 STP and Klang River. Pantai 1 STP was designed based on an activated sludge system to treat sewage from a contributing PE to 377, 000. The development of new Pantai 2 STP has resulted in low influent intake/loading at Pantai 1 STP, where the problems remained prolonged for 4 to 6 months. Hence, the location for sewage collection was shifted from Pantai 1 STP to Damansara STP. Damansara STP is located at Jalan Pintasan Damansara and is situated on the border of Kuala Lumpur and Selangor. Damansara STP was constructed to treat sewage up to 100, 000 PE using an oxidation ditch process.

Sewage from Pantai 1 STP was used as substrate for the cultivation of Control Batch, Batch1 and Batch2. Batch3 and Batch4 used sewage from Damansara STP as substrate. Sewage was taken directly from primary clarifier (after coarse screening) and stored at 5 °C for a maximum of 18 days. During this time, the settled suspended solids from sewage collection tanks were removed. Influent for the SBRs was replaced every 2 or 3 days. Activated sludge collected from Pantai 1 STP was used as seed for formation process for all Batches except for Batch4. The seed for Batch4 was aerobic granules which was stored for 8 months at 5 °C. Before the start-up, seed will be aerated for 1 day without addition of external carbon source. This will result in an initial concentrated mixed liquor suspended solids (MLSS). The volume of active sludge added to SBR prior to the formation process is 50% from reactor working volume.

3.2.2 Reactor Design

Experiments were performed in 3 open, column-type SBRs, constructed identically from plexiglass with working volume of 4.5 L. The schematic diagram of basic SBR operation is illustrated in Figure 3.2. Influent was fed into the reactor from the bottom of the column, whilst, effluent standpipe was fixed for a 50% volumetric exchange ratio (V_{ER}). Rate and volume of influent and effluent during static FILL and DRAW phase, respectively, were controlled by peristaltic pumps (Model no. 775221-57, Master Flex Cole Parmer Ins.).

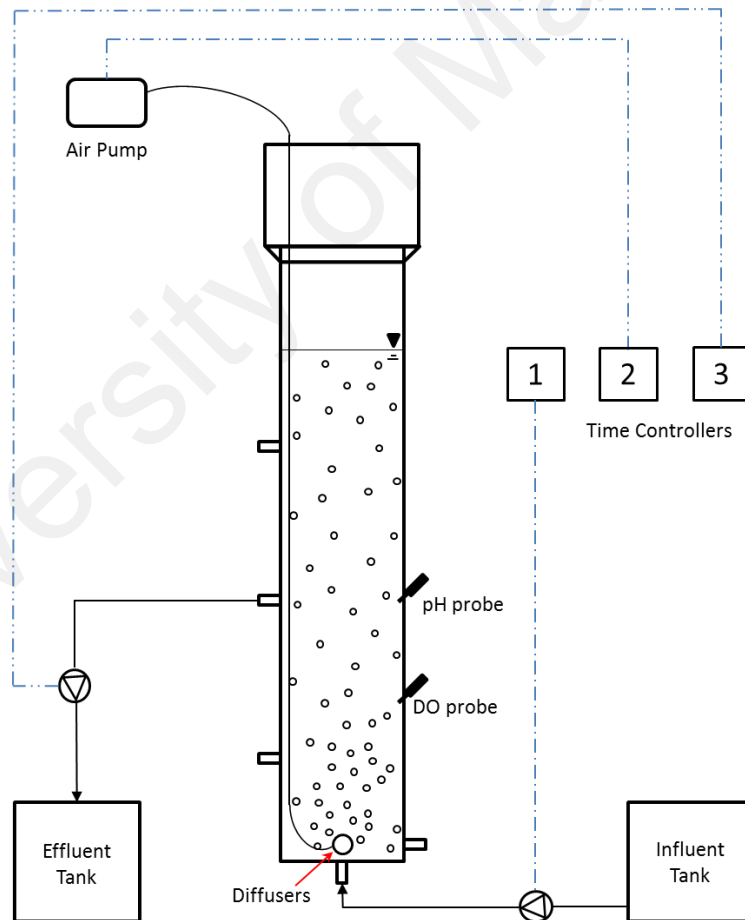


Figure 3.2: Schematic diagram of SBR operation

Mixing during REACT was accomplished by the aeration from a porous stone at the bottom of each reactor. Air was supplied to the system by air pump (Model ACO-

9720, HAILEA) and the rate was controlled by a flow meter in terms of litre per hour. Control of aeration, FILL and DRAW pumps associated with each SBR operating strategy were programmed into and controlled by digital timer (Model no. 601, THEBAN). Dissolved oxygen (DO) and pH of the system was monitored using DO meter (HI 9146) and pH meter (HI 8424), respectively, without further adjustment.

Figure 3.3 illustrates 3 different configurations of SBRs namely SBR1, SBR2 and SBR3 that were used throughout this study. SBR1 and SBR2 were counted as bubble column type reactor with difference in terms of H/D ratio, which is 11.3 and 4.4, respectively. Whilst, SBR3 had the exact configuration of SBR2, except for the draft tubes inside (airlift type reactor). Thus, in order to keep the V_w at 4.5 L, there was a slight difference in working height for both reactors due to volume added by draft tubes, which were 48 cm and 49 cm for SBR2 and SBR3, respectively. The V_{ER} for SBR2 and SBR3 were counted as approximately closed to 50%.

3.3 Experimental Phases and Operational Conditions

As shown in Figure 3.1, four main experimental phases were performed in this study with the aim to oppose common acceptances regarding the disadvantages in formation and stability of AGS. The four main experimental phases are listed as follow:

- i. Impact of low OLR on AGS formation
- ii. Impact of reactor H/D ratio on AGS formation
- iii. Formation of AGS in airlift reactor with divided draft tubes
- iv. Reformation and stability mechanism of long term storage AGS

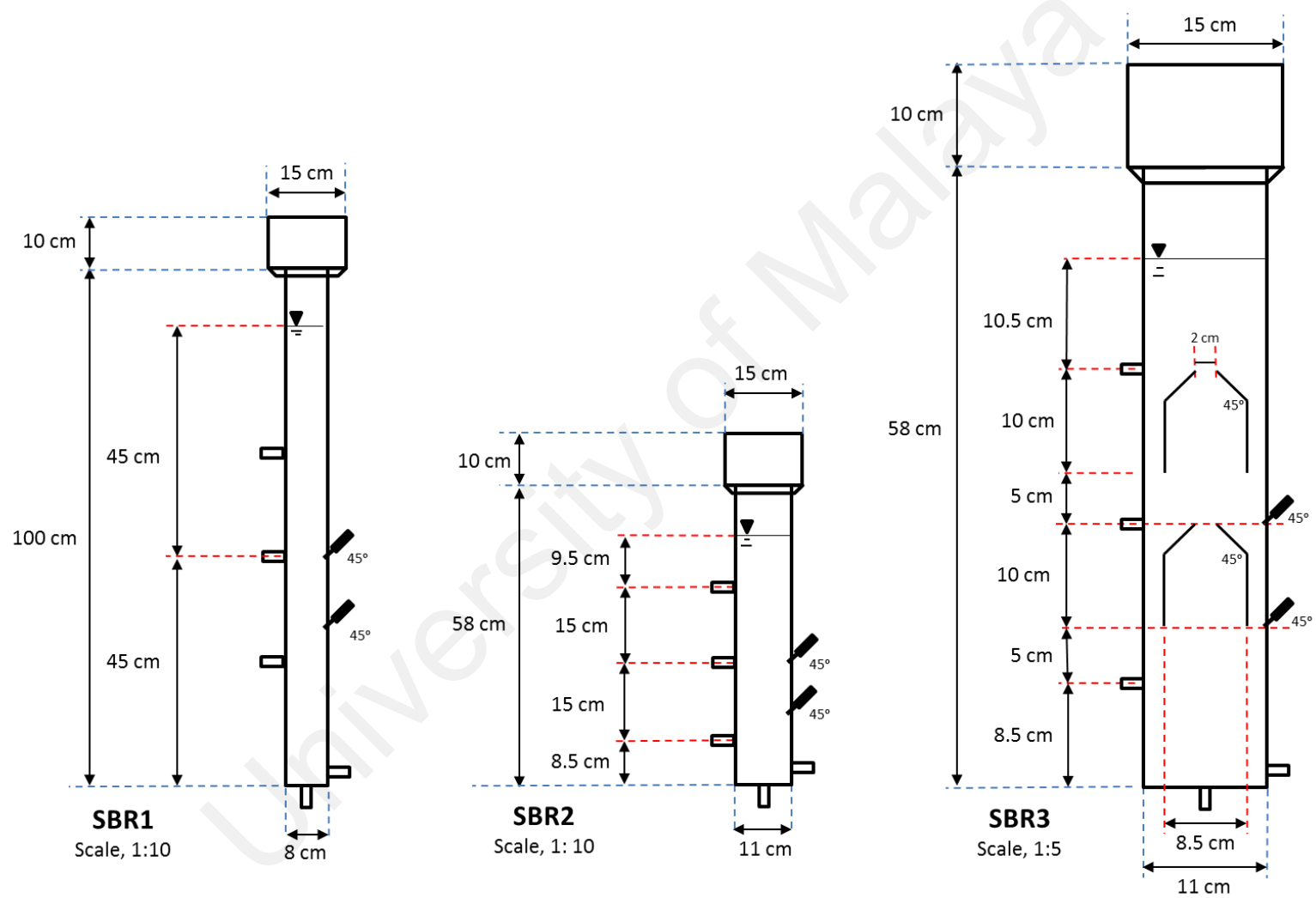


Figure 3.3: Schemes of SBRs with 3 different configurations

The operating conditions applied to achieve the targeted experimental phases are listed in Table 3.1. A minor modification for SBR1 due to crack at the bottom of reactor wall has result in different working volume for Batch4. The operating conditions for Control Batch remained the same until the end of formation process except for cycle time. The React, Settle and Fill time for Batch1, Batch2, Batch3 and Batch4 were changed accordingly to the performance of effluent quality and sludge volume index (SVI). The aeration rate for all batches were fixed at 4 L/min and thus resulted with dissolved oxygen within 7.0 and 9.0 mg/L range. Superficial air velocity (SUAV) was calculated using Equation 3.1 which is given by Beun et al., (1999).

$$SUAV \left(\frac{cm}{s} \right) = \frac{Aeration\ rate}{\pi \left(\frac{D}{2} \right)^2} \quad \text{Equation 3.1}$$

It is important to note that, OLR during formation of all batches was variable throughout the formation process. Once aerobic granules had completed the formation-breakage cycle, and steady state was achieved, the reactor would be turned off. Further analysis on AGS characteristic was carried out. Reactor maintenance was carried out only when excessive proliferation of filamentous microorganisms on the reactor wall occurred.

Table 3.1: Operating conditions applied for formation of AGS

<i>Batches</i> →	<i>Control</i>		<i>Batch1</i>		<i>Batch2</i>		<i>Batch3</i>		<i>Batch4</i>		
<i>Experimental date</i>	2 April 2013 to 22 July 2013		31 Oct 2013 to 10 Jan 2014		31 Oct 2013 to 25 March 2014		22 Jan 2015 to 7 May 2015				
Operating Conditions ↓	<i>Influent</i>	Pantai 1 STP					Damansara STP				
	<i>Reactor</i>	SBR1			SBR2		SBR3		SBR1		
	<i>H/D</i>	11.3			4.4			10.0			
	<i>V (L)</i>	4.5							4.0		
	<i>OLR (kg CODs/m³ d)</i>	0.20 -	0.20 -	0.10 -	0.12 -	0.10 -	0.12 -	0.26 -	0.48 -	0.26 -	0.48 -
		0.28	0.48	0.34	0.49	0.34	0.49	0.69	0.81	0.69	0.81
	<i>Phase</i>	1	2	1	2	1	2	1	2	1	2
	<i>HRT (h)</i>	8	6	8	6	8	6	8	6	8	6
	<i>Cycle (h)</i>	4	3	4	3	4	3	4	3	4	3
	<i>React (min)</i>	195	135	195-229	135	195-220	150-160	185	125-145	170	110-145
	<i>Settle (min)</i>	30		30-15	30	30-5	15-5	15		30	30-15
	<i>Fill (min)</i>	6					30	30-10	30	30-10	
	<i>Idle (min)</i>	3					4				
	<i>Draw (min)</i>	6									
	<i>Aeration rate (L/min)</i>	4									
	<i>SUAV (cm/s)</i>	1.33			0.7			1.33			
<i>Seed (stored at 5 °C)</i>	Fresh activated sludge		Activated sludge					8 months AGS			

In this study, aerobic granules which cultivated or develop under different operating conditions were name according to a series of batches namely as Control, Batch1, Batch2, Batch3 and Batch4. In order to study solely on the impact of low OLR in AGS formation, only HRT which acted as variant parameter was adjusted, while other invariants parameters like Settle, Fill, Idle, Draw and aeration rate remained constant. The produce aerobic granule was name as Control. At 50% volumetric exchange rate, variance HRT was adjusted by reducing the cycle time from 4 h during Phase 1 to 3 h for Phase 2. The study on impact of reactor H/D ratio on AGS formation was carried out by comparing the result obtained from Batch1 and Batch2 which were cultivated in SBR1 and SBR2. Since the main features that differentiate between SBR1 and SBR2 is the settling distance for biomass inside reactor, only Settle time was adjusted. The optimum Settle time for SBR1 and SBR2 during Phase 1 was used for Phase 2, with only React time was adjusted according to the change in Settle time.

The advantages and disadvantages of reactor with low H/D ratio (SBR2) were list out and new reactor namely as SBR3 was fabricated to optimize the system performance. SBR3 is an airlift reactor with divided draft tubes was designed for Batch3 formation to conquer the problem of longer period to achieve mature aerobic granules in bubble column reactor (SBR2) at low superficial air velocity of 0.7 cm/s compare to 1.33 cm/s in SBR1. Batch4 was cultivated in SBR1 with the applied operating conditions were gathered when Control and Batch1 at optimum system performance. Result from Batch4 was used to determine the reformation process and stability mechanism of long term storage aerobic granules.

3.4 Analytical Procedures

The physical and chemical characteristic of influent, mixed liquor and effluent were measured two to three times per week, all according to Standard Methods for the Examination of Water and Wastewater (APHA, 2005). Standard closed reflux titrimetric method (5220 C) was used to measure the COD which is in values between 40 to 400 mg/L. Spectroquant TR420 Merck was used as heating block for COD vial. 5-Day biochemical oxygen demand (BOD₅) method (5210 B) was used to measure the BOD₅ of influent. Others analytical methods and parameters were as follows: Method 2540 D for Suspended solid (SS), method 2540 E for volatile suspended solid (VSS), method 2710 D for sludge volume index (SVI) and method 2710 B for specific oxygen uptake rate (SOUR). Mixed liquor suspended solid (MLSS) and mixed liquor volatile suspended solids (MLVSS) followed method 2540 D and 2540 E, respectively. 0.45 µm glass microfiber filters (934-AH Whatman) was used as filtered for tests on solids or sludge.

Ammonium (NH₄⁺), nitrite (NO₂⁻) and nitrate (NO₃⁻) were determined by photometric determination using Merck test kit, with reference numbers of 114752.0002, 114776.0001, and 114773.0001, respectively. The procedure of the Merck test kits was in accordance with ISO 8466-1 and DIN 38402 A51 for calibration of analysis method during the production control process. Spectrophotometer Spectroquant® Pharo 100 (catalogue no. 100706) with a wavelength range of 320-1100 nm was used to measure the photometric absorbance.

3.5 Physical Characterization of AGS

3.5.1 Evaluation of AGS Size

The morphology and structural of aerobic granules were observed under a digital microscope, DSX500 Opto with 5x magnification lenses. Geometric shapes and angles on screen were measured automatically at an image acquisition of 2D. Microscope slide with double concave ($\text{Ø}15 - 18 \text{ mm}$) was used, considering that the samples were in wet condition and have the tendency to shrink or hydrate on normal microscope slide. Due to the lacks of grant money, suitable slide accessories for wet sample and time constraint, only Batch3 and Batch4 size were measured using microscope.

3.5.2 Morphology of AGS

The microstructure and microbial distribution within the granules were observed with field emission scanning electron microscope (FESEM). Sample preparation of aerobic granules for FESEM was carried out at Electron microscope unit Laboratory, Faculty of Medicine, University of Malaya. Aerobic granules were fixed with 4% glutaraldehyde in 0.1 M phosphate buffer for minimum of 4 h at 4 °C and post-fixed in 1% osmium (OsO_4) at room temperature for 1 h. Later, fixed aerobic granules were washed in distilled water for 20 min and dehydrated in ascending series of ethanol (30% - 50% - 70% - 80% - 90% - 95% -100%, 15 min per step). Dehydration processed was continued in ethanol-acetone mixture (3:1 - 1:1 - 1:3, 15 per step), and finished up with pure acetone for 3 x 20 min. Subsequently, aerobic granules were dry by means of critical point drying (CPD) with CO_2 for 1 h before being mounted on tubes with carbon adhesive for gold coating.

3.6 Chemical Characterization of AGS

3.6.1 Extraction of Extracellular Polymeric Substances (EPS)

A number of methods have been developed and applied to extract EPS from pure or undefined cultures. Each method is highly effective in extracting specific EPS components, whereby, a combination and repetition of extraction method to obtain high extraction efficiency are necessary (McSwain, 2005; Sheng et al., 2010). In this study, the extraction method was Ultrasound → Formamide → NaOH technique which followed the procedure as described by Adav and Lee (2008). Study by Adav and Lee (2008) has firmly assured that EPS collected from ultrasound, followed by formamide and NaOH method has outperformed other methods in extracting EPS from aerobic granules. The collected EPS revealed no contamination by intracellular substances and consisted of mainly proteins, polysaccharides, humic substances and lipid. Initially, 0.06 mL formamide (36.5% GC, Sigma) were added to 10 mL aerobic granules, and the mixture was leave for 1 h at 4 °C. Later, the mixture was sonicated at 50 W for 5 min in ice bath. 1mL 1N NaOH was added to the mixture and then leave for 1 h at 4 °C. The mixture was centrifuged for 20 min at 10, 000 g and 4 °C. The supernatant were filtered through 0.2 µm membrane to collect soluble components or known as EPS. The extracted EPS was stored at -20 °C prior to performing chemical analysis to determine functional groups. The functional groups in EPS were analysed using Fourier transform infrared (FTIR) at a spectral range of 4000 – 400 cm/s. Due to the lacks of grant money and time constraint, EPS extraction and FTIR analysis were carried out only for Batch3 and Batch4.

3.6.2 Elements Composition in AGS

Elements compositions for aerobic granules were analysed using energy dispersive X-ray spectrometer (EDX).

3.6.3 Distribution of Active Cells, Protein and β -polysaccharides in AGS

General principles in designing a multicolour staining scheme for granules have been presented by Chen et al. (2007b) with special precautions taken to avoid overlapping of excitation and emission wavelengths of fluorophores (dyes) as shown in Table 3.2. In this study, SYTO 63 (Product ID, S11345) and FITC (Product ID, F6434) were purchased from Life technologies. Calcofluor white (Product ID, 18909) was purchased from Sigma.

Table 3.2: Excitation and emission wavelengths of fluorophores
(Chen et al., 2007b)

Dye	Excitation (nm)	Emission (nm)	Targets
SYTO 63	633	650-700	Nucleic acids
FITC	488	500-550	Protein, amino-sugars
Calcofluor white	400	410-480	Polysaccharides

The staining scheme procedures are as followed. **Sample preparation:** aerobic granules were suspended in distilled water. The water was removed by decantation and re-washed again with distilled water for 2 times and then suspended in 200 μ L phosphate buffer (PBS, pH 7.2). **First staining scheme:** 20 μ M SYTO 63 was added to the prepared sample and placed on rotary shaker (rpm 100) for 30 min. The excess dye solution was removed by washing with PBS buffer. **Second staining scheme:** 0.1 M

sodium bicarbonate buffer (pH 9.0) was added to maintain the amine group in non-protonated form, followed by FITC solution (1 mg/mL in DMSO). Aerobic granules were incubated on a rotary shaker for 30 min. The excess dye solution was removed by washing with PBS buffer. **Third staining scheme:** The aerobic granules were stained with 30 mg /mL Calcofluor white for 30 min. The excess dye solution was removed by washing with PBS buffer. The stained aerobic granules were kept in cold room at temperature of 5 °C.

The whole aerobic granules images were visualized under confocal laser scanning microscope (CLSM; Leica Tcs Sp5 li model) with corresponding excitations and emissions as showed in Table 3.2. Z-sectioning was performed on whole granules and rendered three-dimensionally by using Las Af Lite software. Only Batch3 AGS and Batch4 AGS were tested using CLSM.

3.7 Biological Characterization of AGS

The evolution of microbial population in aerobic granules at different phase of formation process was determined using polymerase chain reaction (PCR) coupled with next-generation sequencing (NGS). Compared with denaturing gradient gel electrophoresis (DGGE), NGS is a new method that helps to identify microbial community based on percentage quantity rather than percentage similarity. With the use of NGS, the dominant and minor groups of microbial community in aerobic granules can be straightforwardly identified. This is in agreement with work reported by Abdullah et al. (2013) that showed uncertainty in deciding the relationship between the abundance and band intensity in DGGE profile. The platform for NGS used in this

study was based on Illumina Miseq. Methods described for DNA quality control, bioinformatics analysis and taxonomic classification were provided by Sango Biotech (Shanghai) Co., Ltd.

3.7.1 DNA Extraction

Biomass from reactor was collected at the end of the React phase. Since biomass has high water content, an appropriate amount of biomass was centrifuged (using D3024 High speed microcentrifuge, Dragon Lab) at room temperature for 30 s at 10,000 g. Water was removed as much as possible with a pipet tube to provide approximately 0.25 g of biomass or aerobic granules samples. DNA was isolated from aerobic granules using PowerSoil[®] DNA isolation kit (catalogue no. 12888, MoBio). The pure extracted DNA was kept in a freezer at temperature of -20 °C until microbial identification was carried out.

3.7.2 Quality Control of Extracted DNA

DNA concentration and purity were measured using agarose gel electrophoresis technique. DNA concentration required for PCR reaction was quantified using Qubit 2.0 DNA kit. The primer for PCR was designed using a blend of universal primer of Illumina Miseq sequencing platform. Henceforth, agarose gel electrophoresis was run to test the PCR products and DNA was recovered by Sangon agarose recover kit. Once again, Qubit 2.0 was used to quantify the recovered products based on a mixture of 1:1 ratio with DNA concentration. Mixed sample was shaken and later used as subsequent sample for library construction and sequencing.

3.7.3 Bioinformatics Analysis and Taxonomic Classification

At first, PRINSEQ software was used to truncate low-quality data in order to improve merge ratio for subsequent sequences. Then, Flash software was used to fuse dual-terminal sequences and split the data to samples by barcodes. Primer and barcodes were then trimmed from the resulting sequences using PRINSEQ software. UCHIME software and sequences in Silva data as template were used to filter out PCR chimeras. Finally, only samples with sequences length of over 450 bp were used for taxonomic classification analysis.

The sequences readings were clustered into operational taxonomic units (OTU) based on the distance between sequences. OTU clustering software use was UCLUST. Sequence similarity was set at 0.97 and OTU was considered to be as close as possible to genus. The representative sequences from each OTU were subjected to RDP Classifier software, and Greengenes database was used to classify taxonomic assignment based on Bergey's taxonomy. Bergey's taxonomy organized the sequences into six taxonomic levels of domain, phylum, class, order, family and genus. Due to the lacks of grant money and time constraint, analyses on microbial populations were carried out only for Batch3 and Batch4.

CHAPTER 4

RESULTS AND DISCUSSION

4.1 Sewage Characterization

The characteristics of raw sewage collected from Pantai 1 STP and Damansara STP are given in Table 4.1 with all parameters being measured in mg/L. The results indicated that concentration of all parameters (except for SS and VSS) was almost two times higher in Damansara STP than Pantai 1 STP. Sewage characteristic especially SS was highly depending on the weather during the collection time. This might be associated with the system collection point in sewer. Rubbish like plastic bags and dry leaves were found in primary clarifier during rainy day or season at Pantai 1 STP.

Table 4.1: Characteristics of raw sewage

Parameter	Pantai 1 STP			Damansara STP			Standard ³	
	Min	Max	Average ¹	Min	Max	Average ²	A	B
BOD ₅	41	60	53	54	140	97	20	50
Total COD	60	230	180	163	470	270	120	200
Soluble COD	39	120	83	86	231	150	60	100
SS	58	195	97	32	136	80	50	100
VSS	40	145	78	26	122	78	-	-
NH ₄ ⁺	13	33	20	22	53	41	5	5
NO ₂ ⁻	0.02	0.08	0.05	0.01	0.07	0.01	-	-
NO ₃ ⁻	0.30	0.40	0.38	0.1	0.2	0.11	20	50
PO ₄ ³⁻	3.3	20.8	10.0	7.2	19.5	15.4	-	-

¹ Average of 12 samples collected from April 2013 till March 2014.

² Average of 6 samples collected from Jan 2015 till April 2015

³ Acceptable conditions of sewage discharge of Standard A and B from Environmental Quality (Sewage) Regulation 2009, Malaysia.

Analysis on relationship between total COD and soluble COD (CODs) with SS as show in Figure 4.1 exhibit a huge increment for total COD compare to CODs when SS value is increasing. High SS contributed to the increasing in COD value since more

organic and inorganic materials were oxidized by potassium dichromate. Result showed that total COD values for influent were exceptionally high due to increase in SS when sewage was collected during rainy day or season. Thus, CODs was used as a parameter to assess the quality of effluent instead of the total COD. Based on Table A.3 from Guidelines for Developers, Volume IV (Ministry of housing & local government, 1998) and the total COD average values, sewage from Pantai 1 STP and Damansara STP could be classified as low and medium, respectively. BOD/CODs ratio for Pantai 1 STP and Damansara STP which were more than 0.5 indicated that sewage could be easily treated by biological means.

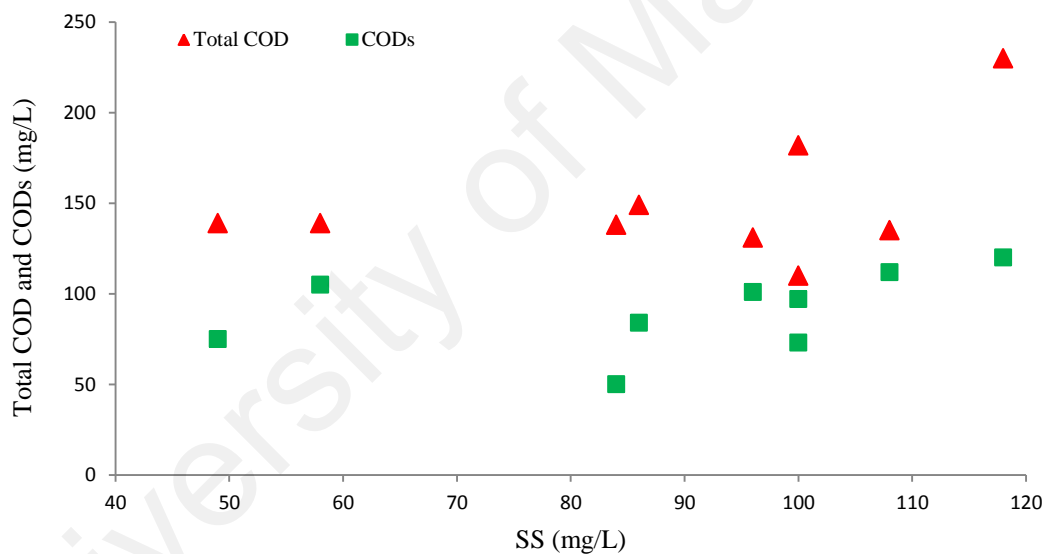


Figure 4.1: Relationship between total COD and CODs with SS increment. Data obtained between June 2013 and November 2013.

4.2 Impact of Low OLR on AGS Formation (Control)

Peyong et al. (2012) and Liu et al. (2007) has successfully developed aerobic granules at the lowest range of OLR applied for AGS formation in sewage, which was 0.6 kg COD/m³ d as previously discussed in Section 2.2.1 and 2.2.2. Therefore, throughout the formation process, a Control without any changes in operating conditions except for cycle time was set-up. Control was used as a baseline to study the feasibility of AGS development at OLR as low as 0.20 kg CODs/m³ d to 0.48 kg CODs/m³ d without pH and dissolved oxygen control. The SBR configuration and operating conditions for Control were fixed as close as possible with other researcher's works (Table 2.1) so that a parallel comparison can be made.

4.2.1 Profile of Biomass Concentration and Settling Properties

Figure 4.2 depicted the profiles of MLSS, MLVSS, OLR and CODs influent for Control, developed in SBR1 from the start-up until the end of the study. Within 24 hours of start-up, most of the sludge from the concentrated activated sludge was being washed out from SBR1, causing a rapid decreased in the MLSS from 5.8 g/L to 1.43 g/L. An excessive elimination of poor settling activated sludge during day 1 affected the performance of SS removal but not COD removal as exhibited in Figure 4.3.

From an observation, the proliferation of filamentous microorganisms on the reactor wall started on day 4 hindered the settling process which caused a decrease in MLVSS and increase in SS effluent. Filamentous microorganisms interfered the settling process by floating freely or protruding from small flocs. This was in conjunction with the result on SVI profile (Figure 4.4) that showed relatively high different concentrations in

between 5 min intervals settling time during the start-up. The length of the bar with different colour (represent different settling time) could be used as an alternative to assess the current state of settling properties for aerobic granules.

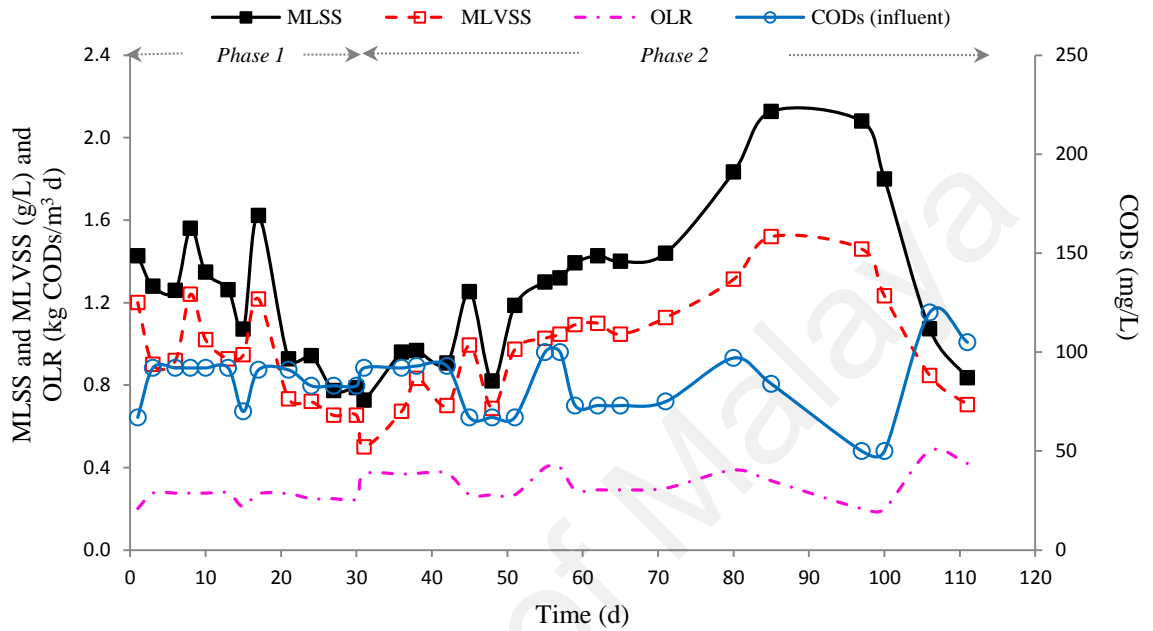


Figure 4.2: Profile of biomass concentration, OLR and CODs influent for Control

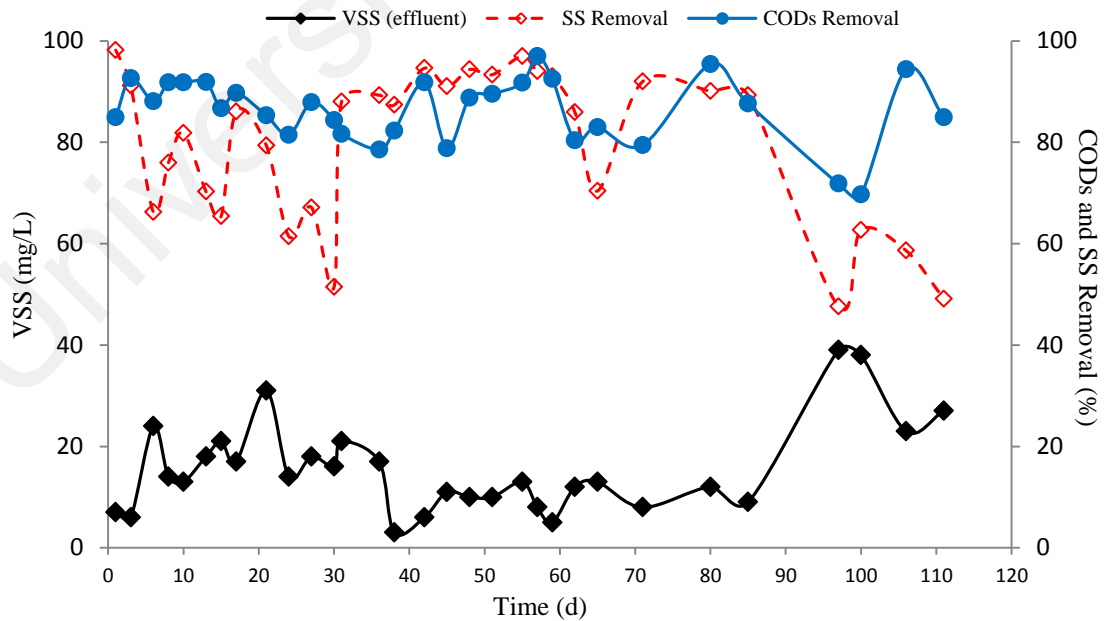


Figure 4.3: Removal of CODs and SS by Control

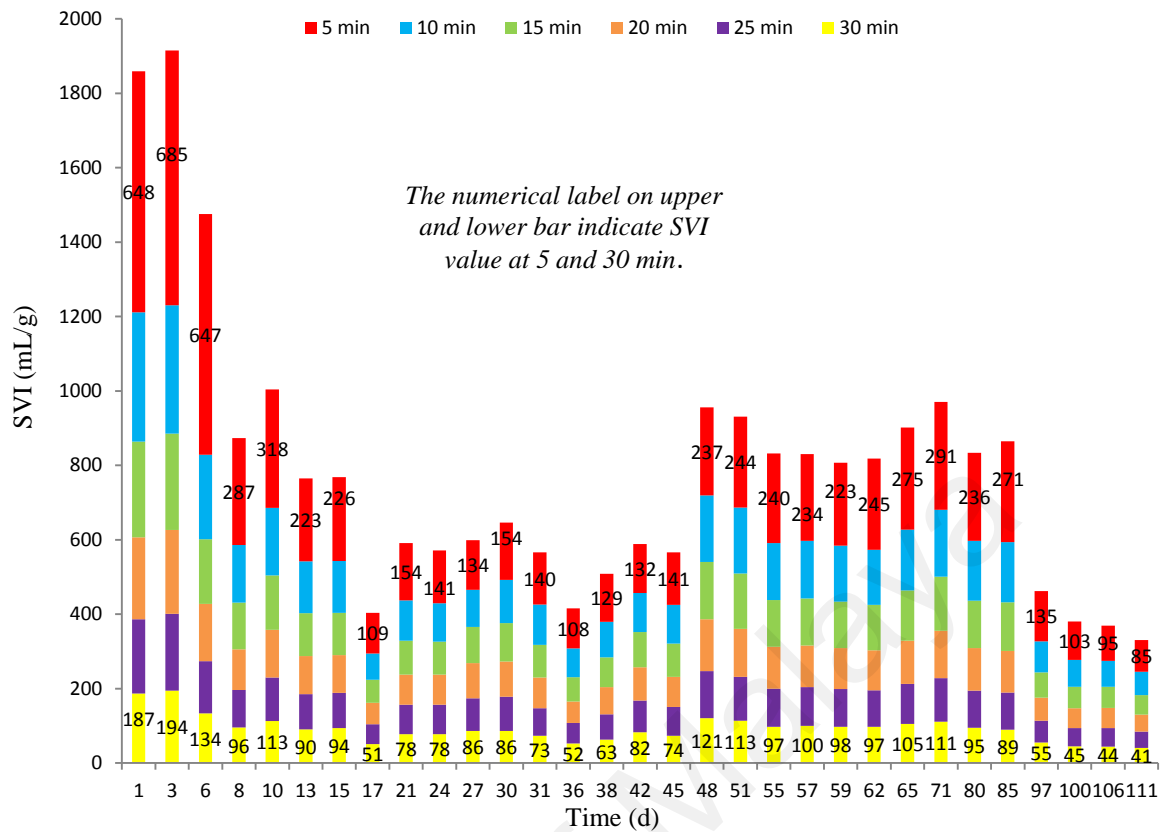


Figure 4.4: Profile of SVI at 5 min intervals of settling time for Control

The occasional sporadic increased on day 8 and 17 for MLSS and SS removals were resulted from the reactor maintenance on the day before the analytical procedure was carried out. By removing the biofilm which had grown on the reactor wall during the reactor maintenance, aerobic granules did not have to outcompete for food with biofilm anymore. As the reactor maintenance occasion took place on day 7 and 16, more than 50% of SVI_5 decreased on the following day of analysis. However, filamentous microorganisms continued to proliferate within 4 to 5 days after the reactor maintenance occasion took places on day 7 and 16. These observations were consistent with SVI_5 result that showed sudden increases from 287 mL/g on day 8 to 318 mL/g on day 10 and 109 mL/g on day 17 to 154 mL/g on day 21.

Although MLSS and SS removal continued to decrease after 30 days of the formation process, the removal efficiency of CODs stayed high at 84%. The analysis on Food to microorganism (F/M) ratio increased from 0.22 g COD/ g MLVSS d on day 8 to 0.38 g COD/ g MLVSS d on day 30, even though OLR remained at 0.28 to 0.25 kg COD/m³ g. Thus, this was suggested as a signal to indicate that OLR or the amount of microbial responsible for substrate degradation was not sufficient. According to Wang and Liu (2008), decreasing the cycle time or increasing the volumetric exchange rate would ensure a high OLR and keep a balance between F/M ratio for an AGS system that subjected under low strength wastewater to run over a long time. Thus, in order to increase the OLR in Control Batch AGS system, cycle time was adjusted from 4 hours to 3 hours (Phase 2) after the analysis on day 30 with the other operating conditions to remain unchanged.

A slight decrease in MLVSS concentration observed on day 31 was normally expected due to the adaptation process of microbial to a new selection pressure. Nevertheless, F/M ratio increased up to 0.74 g COD/ g MLVSS d with the increment of OLR on day 31. The removal of CODs and SS reached above 90% in line with the increase of MLSS and MLVSS on day 42. A sudden increase in MLSS up to 1.25 g/L was observed on day 45 due to reactor maintenance on day 43. However, MLSS had slightly decreased to 0.82 g/L on day 48 due to a low OLR which was from 0.37 kg COD/m³ d on day 42 to 0.27 kg COD/m³ d on day 45.

At a stable condition, SBR system should be comprised of mature aerobic granules that could easily adapt and stabilize in variable substrate concentration and changes of operating conditions. As shown in Figure 4.2, MLSS did not substantially alter with significant changes in influent CODs between days 55 to 71. This was in conjunction

with the analysis on F/M ratio that varied distinctively between 0.17 to 0.74 g CODs/g MLVSS d at an early stage of the formation process. Instead, F/M ratio was slightly varied between 0.27 to 0.39 g CODs/g MLVSS d at a stable condition. During a stable period, profile of SVI between 5 min intervals of settling time started to plateau off and distributed uniformly. Control Batch stabilized at an average MLSS of 1.38 g/L, F/M ratio of 0.31 g CODs/g MLVSS d, CODs and SS removal of 87% and 89%, respectively.

4.2.2 Ammonium Removal Efficiencies

The removal efficiencies of ammonium (NH_4^+), nitrite (NO_2^-) and nitrate (NO_3^-) by Control Batch from the beginning until the end of the formation period were illustrated in Figure 4.5. It was noted that the removal of ammonium remained high at 100% from start-up until day 97. It was suggested that a complete nitrification process took place accompanied with the CODs utilization during the reaction time. This was consistent with the result on nitrate effluent (Figure 4.5f) which was almost equivalent to ammonium influent from start-up until day 97. The trend in nitrate effluent (Figure 4.5e) results also indicated that denitrification process was likely not occurred at all. It was expected that denitrification process should occurred during the idle and settling time (anoxic conditions). This might be attributed by the insufficient of carbon source (CODs) after the reaction time took place.

It had been reported by Metcalf and Eddy (2014) that optimal nitrification process occurred at pH 7.5 to 8.0 and the culture pH below 6.8 would inhibit a nitrifying bacteria. A pH of 7.0 to 7.2 was normally used to maintain reasonable nitrification rates. In fact, a complete nitrification in turn leads to the accumulation of hydrogen ion in the

reactor and decreased the pH inside the reactor. Since the pH of the raw sewage from Pantai 1 STP varied within 7.4 to 7.9, it would take sometimes for the accumulation of hydrogen ion to disturb the pH at the start of the reaction time inside the reactor. As shown in Figure 4.5, pH decreased below 6.8 between days 6 to 17 and 71 to 111. Whilst, the average pH at the end of the reaction time during a stable conditions was 7.0.

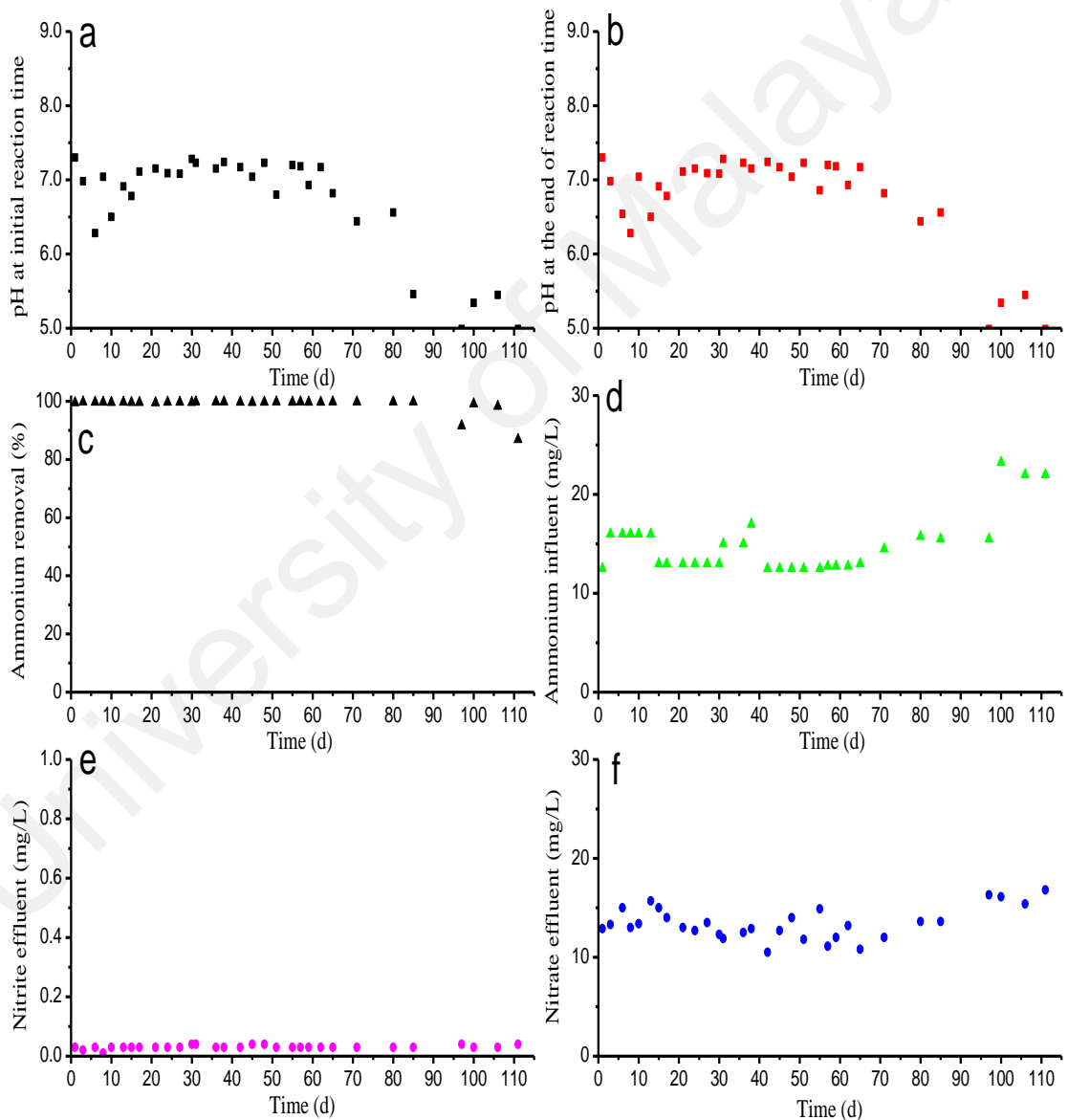


Figure 4.5: Profile of pH, ammonium, nitrite and nitrate effluent for Control

It was anticipated that certain microbial species which were responsible for the granule formation might have decayed due to the acidic condition and the proliferation of filamentous microorganisms that took place. This was consistent with the result on SS removal and MLSS profile that significantly decreased after day 97. Alkalinity was not added to maintain acceptable pH values since pH should not be controlled during the formation process of Control Batch. Hence, as in between day 6 to 17, it was predicted that the performance of aerobic granule system would continue to increase if the formation period was to extend for more than 111 days.

4.2.3 Morphology Observation of Control

FESEM examination was used to characterize the microstructure of Control Batch. Figure 4.6 exhibited the morphology of the activated sludge and the mature aerobic granule collected on day 80, just before the performance of the aerobic granule system dropped. As shown in Figure 4.6(f), the activated sludge exhibited a loose-structure morphology and had a relative abundance of filamentous microorganisms. In contrast, the mature aerobic granules (Figure 4.6; a-e) were consisted of bacteria-dominant granules with a few filamentous microorganisms. The aerobic granules for Batch Control were mainly comprised of cocci-shape and bacilli-shape bacteria which were uniformly and tightly cross-linked between one another to form a compact structure. A similar result was reported by Ma et al. (2013) who found the suppression of filamentous microorganism at low OLR (0.6-1.2 kg COD/m³ d) for the mature aerobic granules to develop in synthetic (glucose based) wastewater.

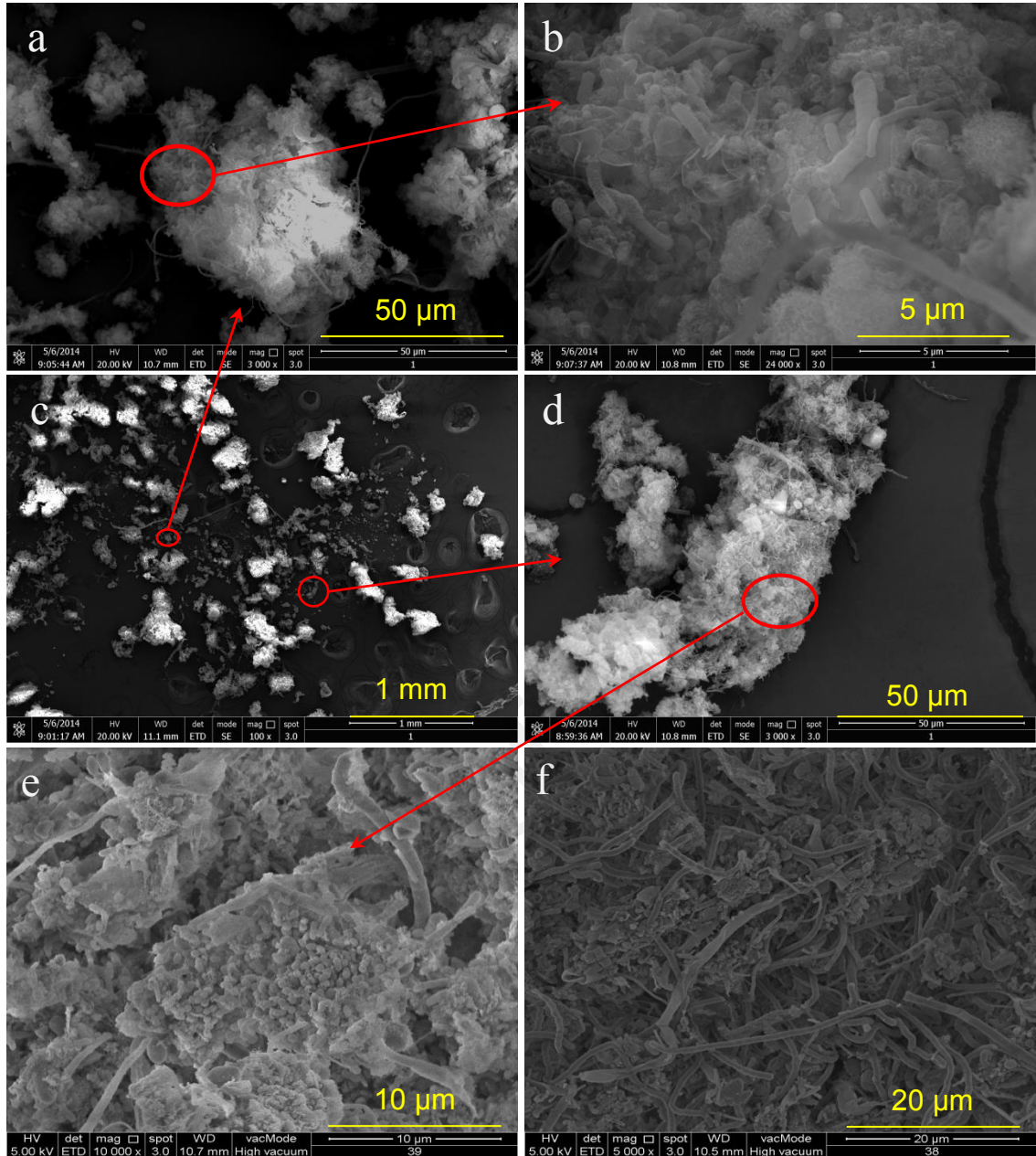


Figure 4.6: FESEM images of mature granules from Control at day 80 (a, b, c, d, e) and activated sludge (f).

4.2.4 Chemical Composition of Control

EDX analysis was carried out on the surface of the aerobic granules and the activated sludge with the selected area as shown in Figure 4.6(b) and 4.6(f). The localized elements spectra for the activated sludge showed that only carbon, oxygen and

nitrogen were present with weight percentages of 65%, 22% and 13%, respectively. As illustrated in Figure 4.7, an analysis of the localized spectra also clearly showed that carbon and oxygen were the major components observed on the surface of the aerobic granules. However, the EDX spectra for the activated sludge did not show any characteristic signal of magnesium, iron, calcium, sodium and titanium as present in the aerobic granules. Elemental EDX mapping image analysis by Angela et al. (2011) on the central slice mature aerobic granules depicted that carbon majorly present on the surface, whilst calcium and phosphate were formed in the core of the aerobic granules. Thus, this explained why the presence of magnesium, iron, calcium, sodium and titanium signals was lesser on the surface of the aerobic granules.

4.2.5 Summary on Result Analysis

In this study, Control Batch was successfully developed even though OLR were exceptionally low, which were in range of 0.2 to 0.48 kg COD/m³ d. Mature aerobic granules were attained after 55 days of formation process with an average MLSS of 1.38 g/L, F/M ratio of 0.31 g CODs/g MLVSS d, CODs and SS removal of 87% and 89%, respectively. The findings by Li et al. (2011) and Tay et al. (2004a) had remarked that the maturity periods for aerobic granules developed under a low OLR or F/M ratio were relatively longer than the one developed in high a OLR or F/M ratio. A cross reference with tabulated findings in Table 2.1 for aerobic granules formation using sewage and this study were in conjunction with the overview in Section 2.2.3, where apart from OLR, different working volumes and reactor H/D ratio also could affect the maturity period of aerobic granules.

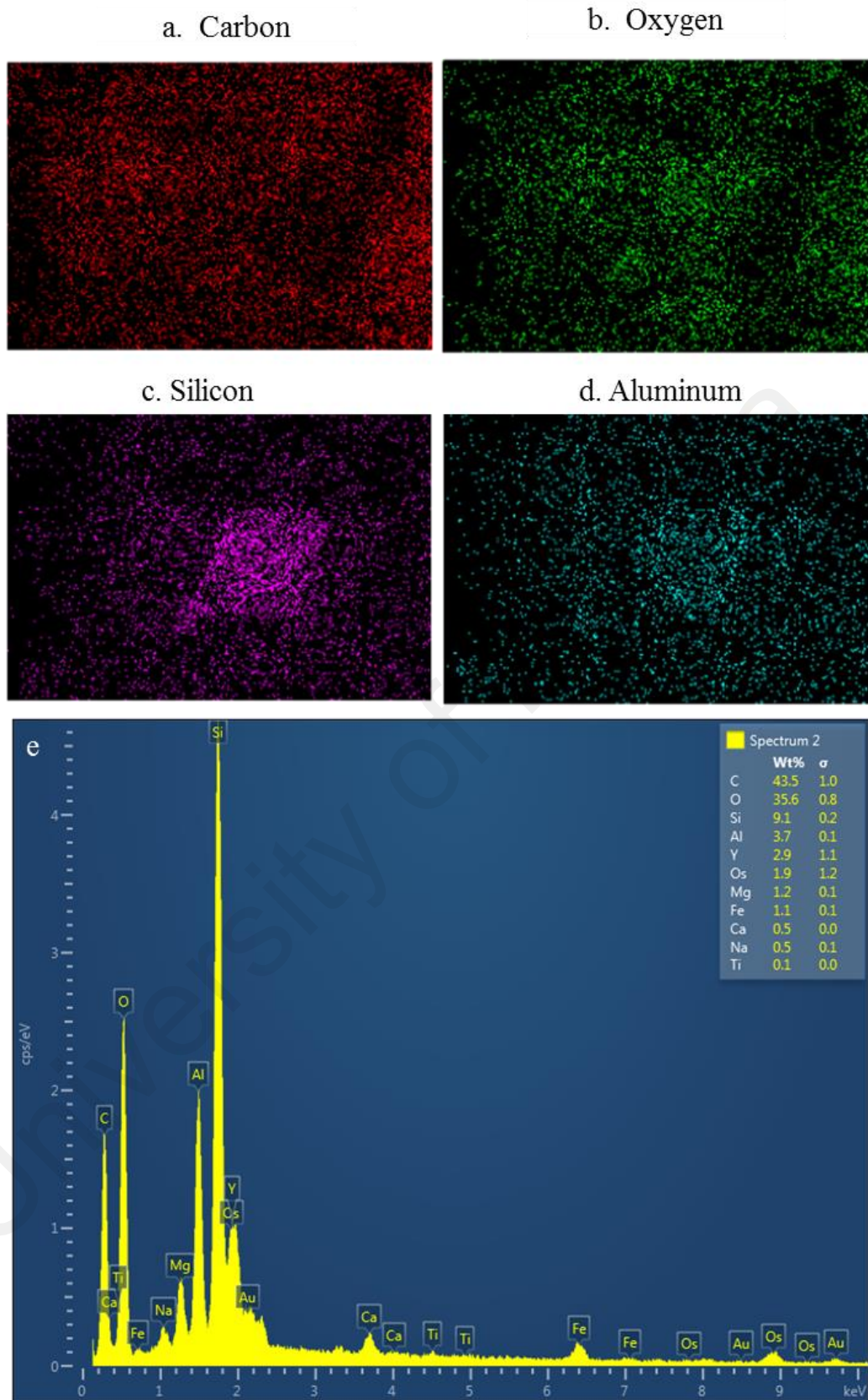


Figure 4.7: Elemental mapping images (a, b, c, d) and localized elements spectra (e) from EDX analysis for Figure 4.6b surface area.

4.3 Impact of Reactor H/D Ratio on AGS Formation (Batch1 and Batch2)

The development of AGS has been extensively reported to use SBR system. A review by Liu and Tay (2002) had highlighted that column-type upflow reactor with a higher H/D ratio could provide a longer circular flowing trajectory, which in turn creates an effective hydraulic attrition for microbial aggregation. Based on Table 2.1 and references on other researcher's works, existing studies concerning aerobic granules formation were mainly established on well-controlled laboratory scale SBR with H/D ratio of over 10. This kind of practice would limit the practical application of aerobic granule since the existing SBR mostly had low H/D ratio. In practice, factors like maintenance problems and the impacts of natural disaster would be critical and had to be considered in designing a long slender reactor.

Currently, only Kong et al. (2009) published a research work regarding the formation of aerobic granules at different H/D ratios (diameters were fixed to 5 cm). Kong et al. (2009) concluded that H/D ratio or reactor minimal settling velocity did not have any influence on granulation or granule properties. However, since the difference in the aspect of working volume and organic loading rate ($\text{kg COD/m}^3 \text{ day}$) were neglected, this study was aimed to address this issues. In this study, Batch1 and Batch2 were developed in two SBR with different H/D ratio of 11.3 and 4.4, respectively. The details of the operating conditions were given in Table 3.1.

4.3.1 Effect of Reactor H/D Ratio on Period to Achieved Mature Granules

Theoretically, the configuration of SBR2 seemed to be unfavourable for the development of compact aerobic granules that required a high shear force and H/D ratio. At an aeration rate of 4 L/min, the SUAV for SBR1 was two times higher than in SBR2, which were 1.33 and 0.7 cm/s, respectively. Figure 4.8 showed an MLSS profile for the aerobic granule cultivated in SBR1 and SBR2 being called as Batch1 and Batch2, respectively. As shown in Figure 4.8, the biomass concentration measure of MLSS for both Batch1 and Batch2 were altered according to the change in influent CODs for the first 63 days of the formation process. Batch1's formation was stopped on day 63 after analyses on effluent quality since day 49 showed a constant efficiency with an average of 84% CODs removal and effluent SS to be lower than 26 mg/L (Figure 4.9). As shown in Figure 4.9, Batch2 was mostly stable in period between days 89 to 103, with the highest CODs removal up to 90% being recorded on day 95, followed by low SS effluent of 10 mg/L.

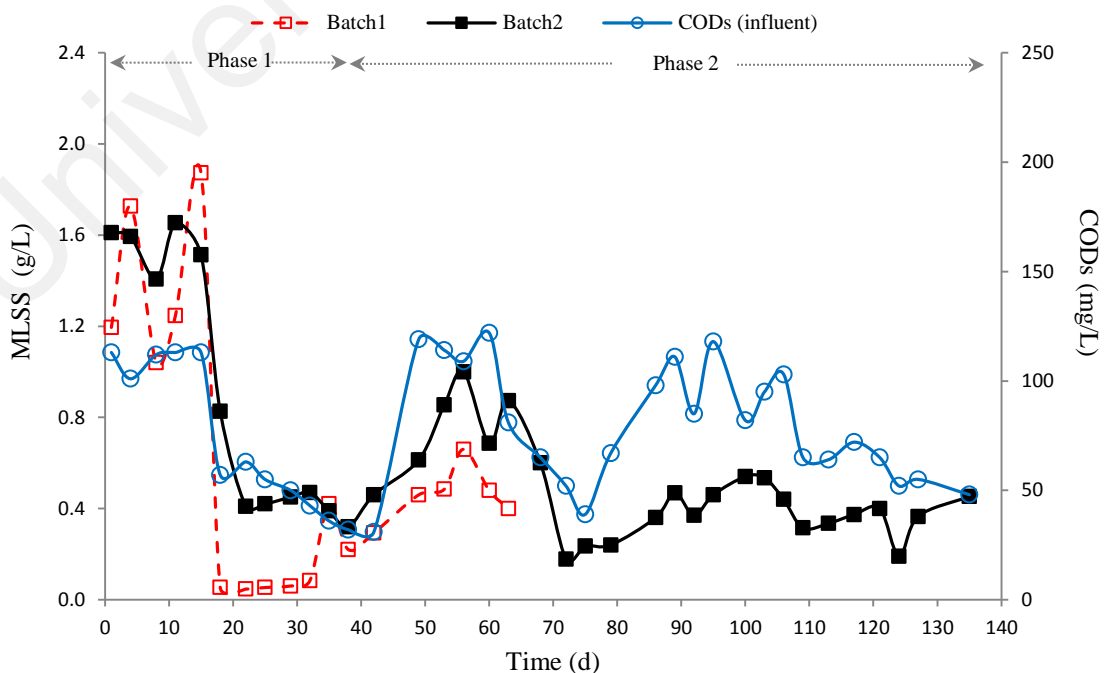


Figure 4.8: Profile of MLSS and CODs influent for Batch1 and Batch2

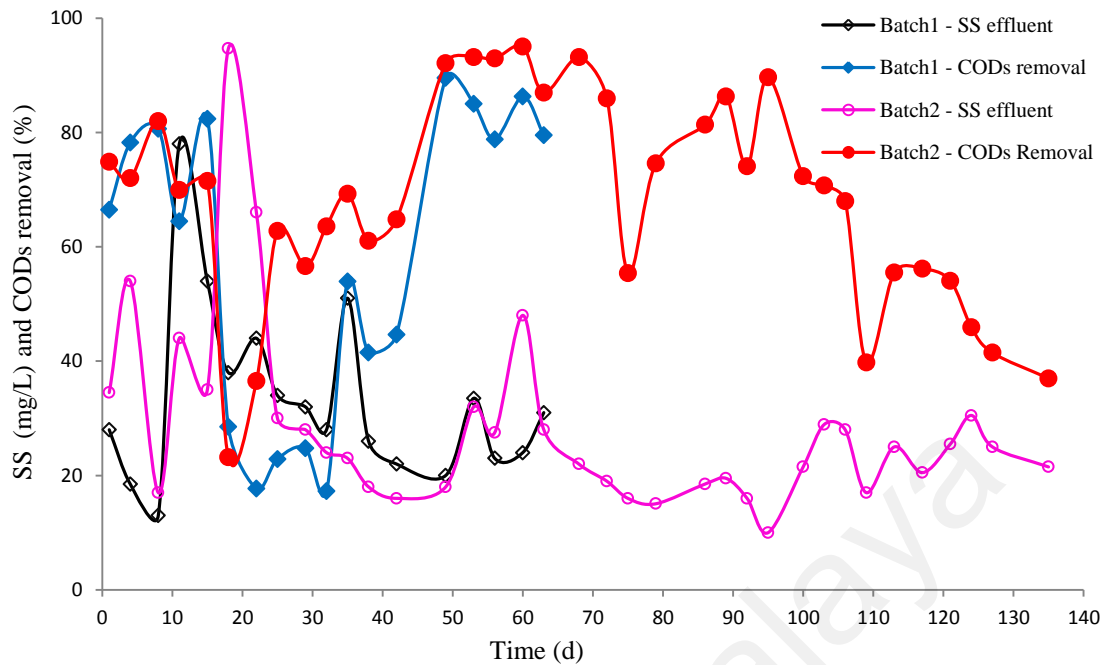


Figure 4.9: CODs removal and SS effluent for Batch1 and Batch2

At stable conditions, SBR system should be comprised of mature aerobic granules that could easily adapt and stabilize in variable substrate concentration and changes of operating conditions. As shown in Figure 4.8, MLSS concentration for both batches did not substantially increase with significant changes in influent CODs during and after the stable period. This was in conjunction with the analysis on food to microorganism ratio (F/M) as indicated in Figure 4.10. The F/M ratio varied distinctively at the early stage of Batch 1 (the first 30 day) and Batch2 (the first 70 day). Batch1 stabilized at an average MLSS of 440 mg/L, F/M ratio of 1.10 g CODs/g MLVSS d and sludge retention time (SRT) of 5 d. Whilst, Batch2 stabilized at an average MLSS of 412 mg/L, F/M ratio of 0.96 g CODs/g MLVSS d and SRT of 6 d.

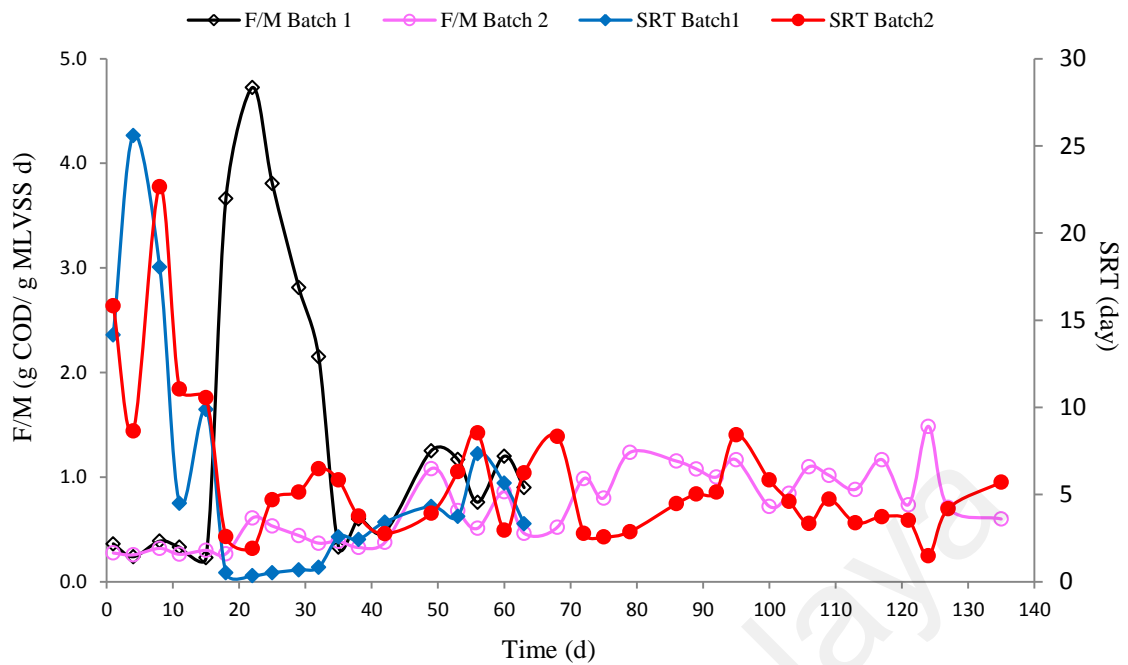


Figure 4.10: Profile of F/M ratio and SRT for Batch1 and Batch2

A longer period to achieve stable conditions for Batch2 as compared to Batch1 was expected based on the consideration of SUAV and F/M ratio factors. According to Tay et al. (2001a), a higher shear force was preferable for the development of regular, rounder, strong and compact granules. It was found that bioflocs and regular granule were observed in reactors with SUAV of 0.3 cm/s and 1.2 cm/s, respectively. Since then, the SUAV of 1.2 cm/s had become a threshold value for a successful cultivation of AGS (Liu & Tay, 2004) in SBR. A study by Li et al. (2011) also reported that F/M ratio as high as 1.1 g CODs/g SS d initiated a rapid formation of large granules within 15 d. Meanwhile, a low F/M ratio of 0.3 g CODs/g SS d would result in a slow granulation process of more than 40 d.

4.3.2 Effect of Reactor H/D Ratio on Settling Properties of Biomass

4.3.2.1 Formation of Batch1 in Reactor With High H/D Ratio (SBR1)

Figure 4.11 exhibited profiles of SVI for Batch 1 at 5 min intervals of settling time. The coloured arrows above the graphs' area specified the settling time applied during a certain period of the formation process. From an observation, the proliferation of filamentous microorganisms on the SBR1 wall had started on day 5 and this resulted in a decrease of MLSS concentration on day 8. Hence, in order to discharge off the filamentous microorganisms that were floating freely or extending from small flocs, settling time was reduced from 30 to 15 min on day 9.

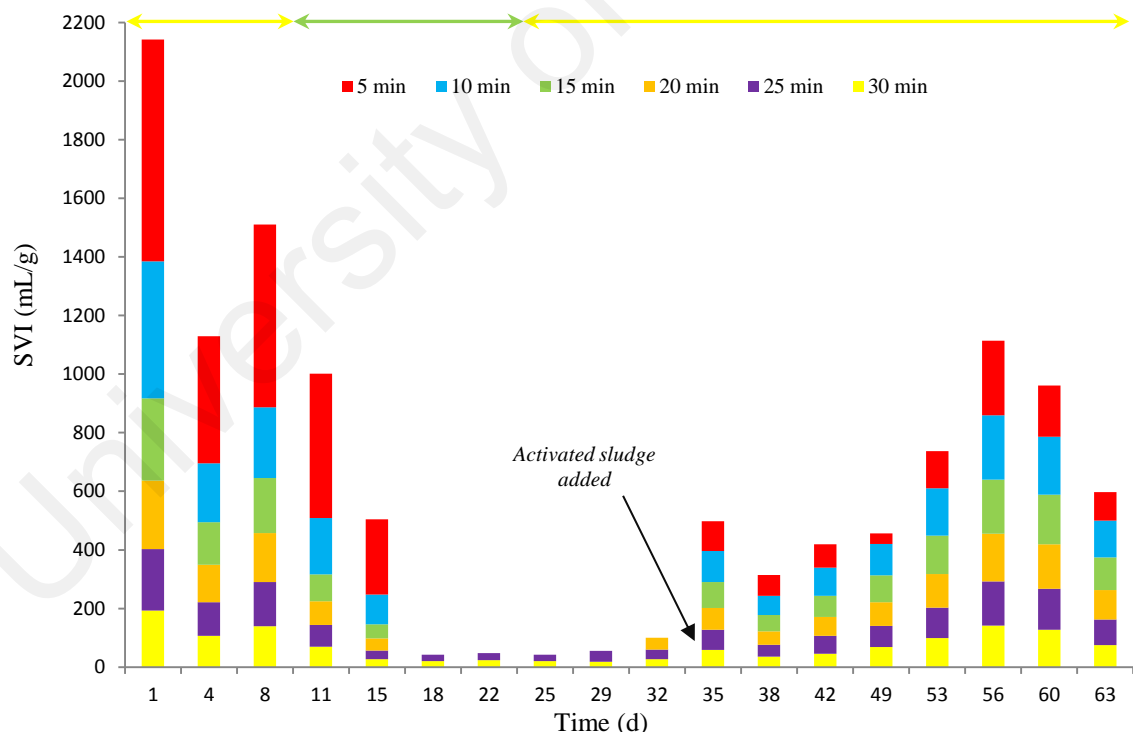


Figure 4.11: Profile of SVI at 5 min intervals of settling time for Batch1

As a result, effluent SS increased relatively higher on day 11 which was 78 mg/L as compared to 13 mg/L on day 8. In fact, the percentage removal for SS on day 11 was -30% signifying small flocs that were used to settle within 30 min started to

disintegrate and were discharge off. SRT of 5 d on day 11 was consistent with decreases in SVI_5 and SVI_{30} on day 15. As of day 15, more than 50% of the biomass from day 11 was discharged off and this can noted based on the SVI_5 and SVI_{30} profile. Nevertheless, MLSS concentration continued to increase in line with the improvement of effluent performance until day 15.

A sharp decrease in OLR (the first low shock OLR) from 0.34 to 0.17 kg COD/m³ d on day 16 (Figure 4.12) practically caused a complete washed out of MLSS in SBR1. Even after the settling time was reset to 30 min on day 23, MLSS concentration remained low until day 32, in which was around 0.06 g/L. Although SOUR (Figure 4.12) had greatly increased up to 394 mg O₂/g MLVSS h, CODs removal receded to less than 30% with high concentration of SS effluent due to insufficient amount of microbial (MLVSS) in reactor to degrade CODs influent. Hence, by looking at MLVSS and OUR's result that remained linearly low but with slightly increase, SOUR's value at this point was not a decent indicator to reflect the microbial activity in SBR1. SVI profile for the biomass indicated that small flocs or granules took 25 to 30 mins to settle in order to maintain at least a minimum of 21 mL/g active biomass in SBR1.

As present in Figure 4.10, F/M ratio for Batch1 was exceptionally high between days 18 to 32 due to the loss of active biomass. Thus, in order to recover the loss of biomass in SBR1, 0.6 L of activated sludge was added on day 33. OUR during day 35 increased drastically from 0.20 to 0.84 mg O₂/L min, suggesting an active competition between newly added bacteria from the activated sludge and aerobic sludge to present in the reactor. However, since the availability of food was still limited (low OLR), MLSS concentration was reduced from 0.42 g/L on day 35 to 0.22 g/L on day 38. In order to

increase the OLR, the cycle time was adjusted from 4 to 3 h (Phase 2) after an analysis on day 38 with the other operating conditions remained unchanged. On day 38 onwards, MLSS concentration in SBR1 had gradually improved in line with the effluent performance. Despite of the high OLR increment on day 49, SVI₃₀ and MLSS concentration showed a slightly increase since system was already in a stable condition.

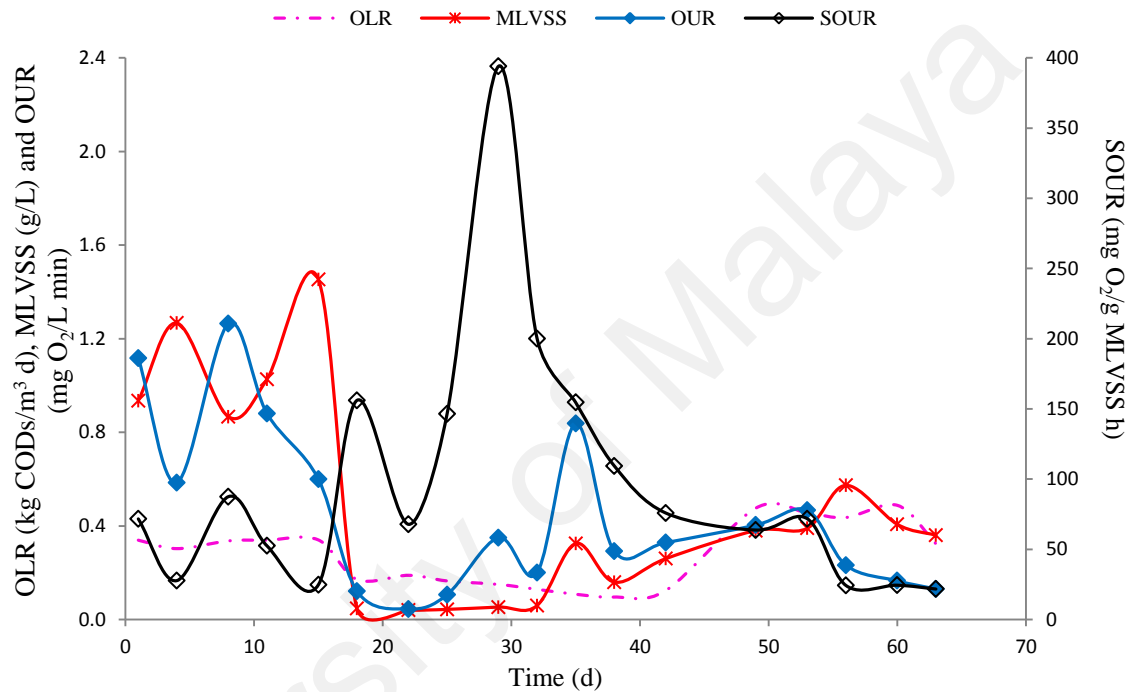


Figure 4.12: Profile of OLR, MLVSS, OUR and SOUR for Batch1

At the end of the formation process, aerobic granules in SBR1 continued to recover from variable shock OLR and achieved stable conditions between days 49 to 60. This was consistent with the result on SRT that showed an increment from 40 mins on day 22, to 7 d on day 56 onwards. Based on Table 5.9 from Guidelines for Developers, Volume IV (Ministry of housing & local government, 1998), the optimal SRT for conventional activated sludge system was from 5 to 10 days. Outside this range (too short or long SRT), the reactor performance would deteriorate (Zhu et al., 2013a). Beside, Muda et al. (2011) had concluded that sludge biomass would lose bioactivity characteristics based on the overall specific biomass growth rate, endogenous decay rate

and biomass yield when SRT was increased. A system with long SRT would favour filamentous growth because of a low specific growth rate of filamentous microorganism (Liu & Liu, 2006).

4.3.2.2 Formation of Batch2 in Reactor With Low H/D Ratio (SBR2)

In contrast to SBR1, after 1 day of a formation process at identical operating conditions, SBR2 managed to retain a higher MLSS due to the short settling distance for SS. Even after the settling time was reduced to 15 mins on day 5, MLSS remained high but with a slender different in concentration until day 15. In SBR1, the proliferation of filamentous microorganism started after 5 days of a formation process. However in SBR2, filamentous microorganisms started to proliferate on day 11 attributed to changes in the settling time from 30 to 15 mins on day 5. As of day 11, more than 50% of the biomass from day 8 was discharged off and this can be noted based on the profile of SVI as shown in Figure 4.13.

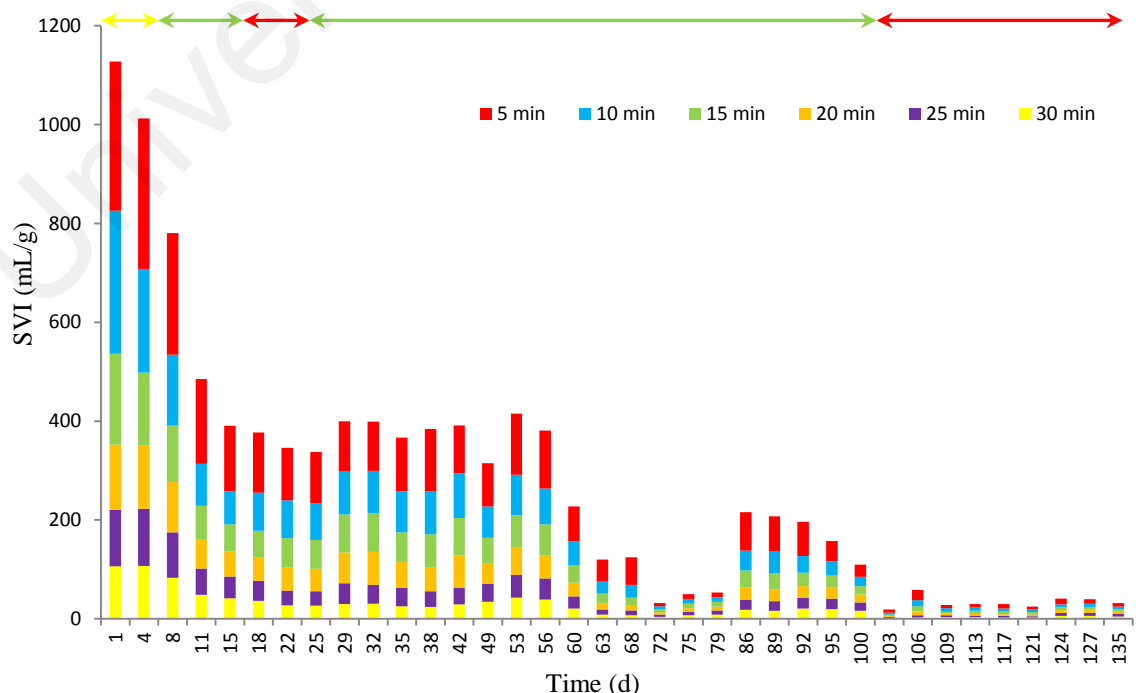


Figure 4.13: Profile of SVI at 5 min intervals of settling time for Batch2

The highest effluent SS concentration from SBR2 was recorded on day 18 due to the change in settling time from 15 to 5 min on day 16, and followed with a relatively lower OLR of $0.17 \text{ kg/m}^3 \text{ d}$ as compared to $0.34 \text{ kg/m}^3 \text{ d}$ on day 15 (the first low shock OLR). In fact, the percentage removal for SS on day 18 and 22 was around -16% signifying small flocs that was used to settle within 15 mins started to disintegrate and were discharge off. In order to avoid the washed out of small flocs that started to disintegrate due to the low OLR, the settling time was changed back to 15 mins on day 23, and the cycle time was adjusted from 4 to 3 h on day 38.

From observation, the proliferation of filamentous microorganism on SBR1 wall was severe as compared to SBR2. Thus unlike Batch1, an excessive low OLR up to $0.10 \text{ kg/m}^3 \text{ d}$ that continued until day 42 did not significantly affect the performance of Batch2. Instead, the result on MLSS and SVI profile between days 18 to 42 were rather plateaued. It was anticipated that this was caused by the ability of SBR2 to retain sufficient biomass in reactor and changes in a short settling time at the beginning of the formation process. A study conducted by Adav et al. (2009) had noted that the selection of settling time was only crucial at the beginning of the cultivation process, since most of the cyclic period was during the aeration phase. Applying a short settling time at the beginning of the cultivation process would ensure a washout of non-flocculating strains from sludge seed that corresponded to the shift of microbial community in granular sludge.

Batch2 encountered the second low shock OLR from $0.49 \text{ kg CODs/m}^3 \text{ d}$ on day 60 to $0.16 \text{ kg CODs/m}^3 \text{ d}$ on day 75 (Figure 4.14). Although the second shock OLR had resulted in a decrease of SVI_{30} from 21 to 9 mL/g on day 63, CODs removal remained high with SS removal and vice versa. This indicated that F/M ratio was low. In order to

avoid being washed out from the reactor due to a low F/M ratio of 0.46 g CODs/g MLVSS d, the microbial activity during this period was high. This indeed was in conjunction with OUR and SOUR (Figure 4.14) profile between day 68 to 89. In contradiction, OUR exhibited a decreasing trend when the first low shock OLR (days 16 to 42) with an average F/M ratio of 0.4 g CODs/g MLVSS d occurred. The identical decreasing of OUR trend between days 16 to 42 for Batch2 could also be observed in Batch1. This was presumably attributed by the maturity state of aerobic granules or microbial species within the time frame. Mature aerobic granules were attained after 89 days of formation process. The highest CODs removal up to 90% was recorded on day 95, followed by a low effluent SS of 10 mg/L.

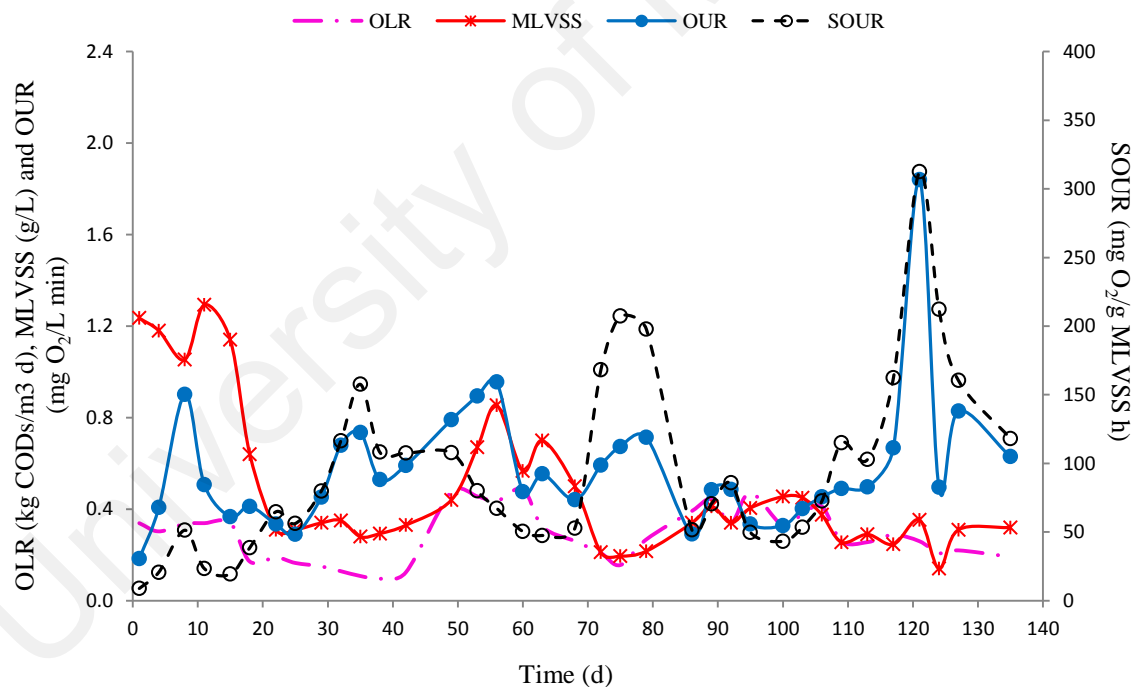


Figure 4.14: Profile of OLR, MLVSS, OUR and SOUR for Batch2

Reducing the settling time from 15 to 5 mins on day 103 onwards, and followed by the changes in aeration rate from 4 to 2 L/min on day 106 and low OLR (0.41 to 0.26 kg CODs/m³ d) on day 109 had extremely altered the performance of Batch2. It was estimated that consecutive changes in operating parameters within short period

interfered the capability of mature aerobic granules to fit in with the new conditions. Due to low sewage intake, collection point was shifted to new inlet that consisted of mixture of sewage with leachate and industrial wastewater on day 117. Thus, the system performance continued to decline after the sewage was exchanged with sewage mixture that were consisted of leachate and industrial wastewater on day 118 onwards. An analysis on BOD concentration indicated that the sewage mixture (BOD₅ of 24 mg/L) was less biodegradable than the sewage (BOD₅ of 53 mg/L). SRT had decreased from 6 d (at stable conditions) to 1 day on day 124.

Based on an analysis for effluent SS, CODs removal and SVI, the optimum settling time for SBR1 and SBR2 under shock OLR was 30 and 15 min, respectively. Followed by findings from Beun et al. (1999) and Qin et al. (2004a and 2004b) regarded that a short settling time was preferred for the growth of rapidly-settling bioparticles and a settling time within the range of 2 to 15 mins had often being used by other researchers in order to enhance the granulation process.

4.3.3 Effect of Reactor H/D Ratio on Efficiencies of Ammonium Removal

The removal efficiencies of ammonium (NH₄⁺), nitrite (NO₂⁻) and nitrate (NO₃⁻) by Batch1 and Batch2 from the beginning until the end of the formation period were illustrated in Figure 4.15 and 4.16. Based on the profile of ammonium influent and nitrate effluent, it could be noted that a complete nitrification process could only happened at certain days. However, the removal of ammonium remained high at above 80% from days 1 to 60 for Batch1 and 86% from days 1 to 72 for Batch2, indicate that nitrification process was not inhibited in both batches. Reported by Metcalf and Eddy (2014), it was stated that the optimal nitrification process should occurred at pH 7.5 to

8.0 and the culture pH below 6.8 would inhibit the nitrifying bacteria. Since, the pH of the raw sewage from Pantai 1 STP varied within 7.4 to 7.9, a drop in pH at the end of the reaction time (Figure 4.15b and Figure 4.16b) which was closed to 5.0 between day 4 to 18 for both batches did not disturb the nitrification process.

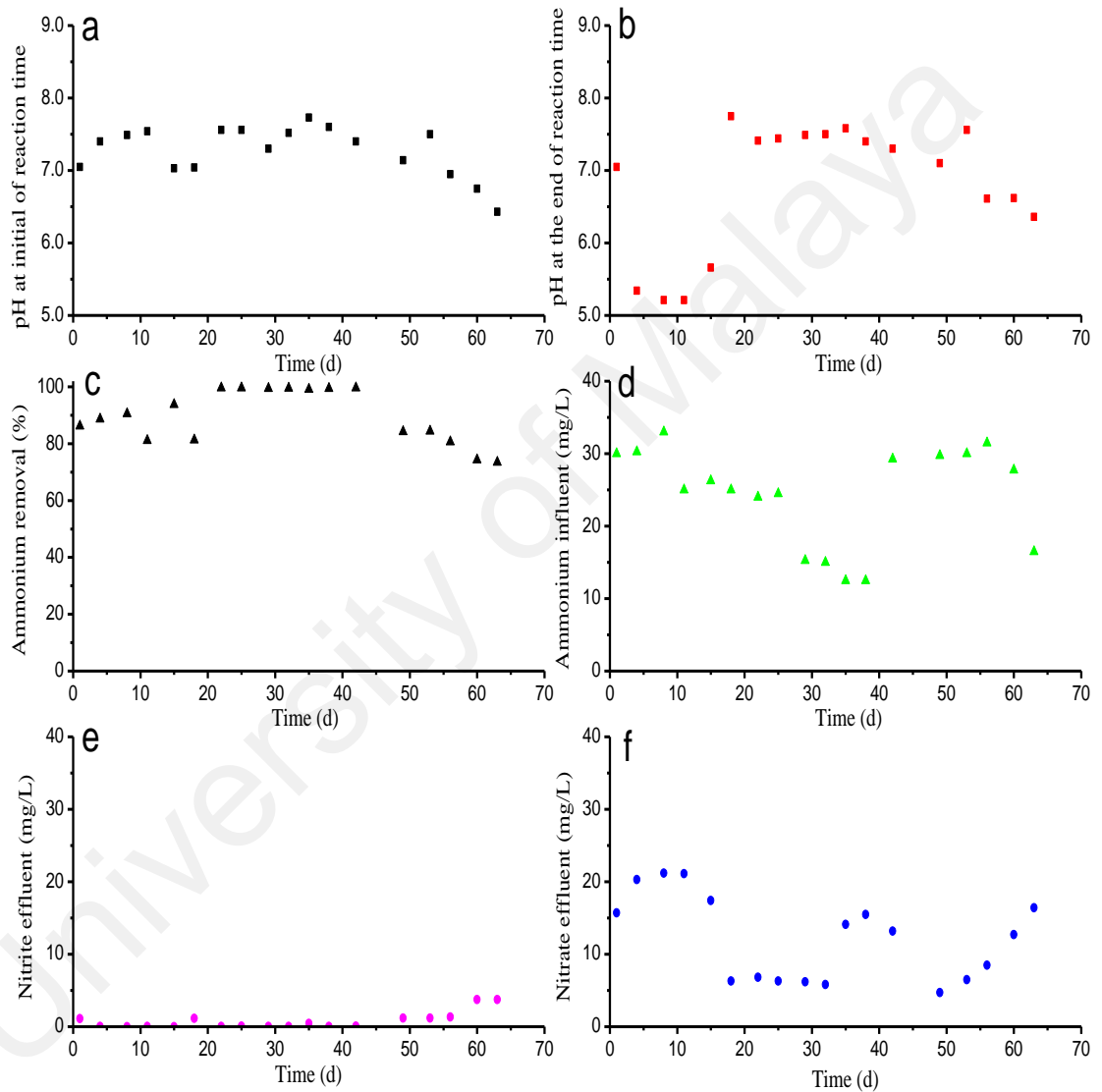


Figure 4.15: Profile of nitrogen effluent and pH at the end of reaction time for Batch1

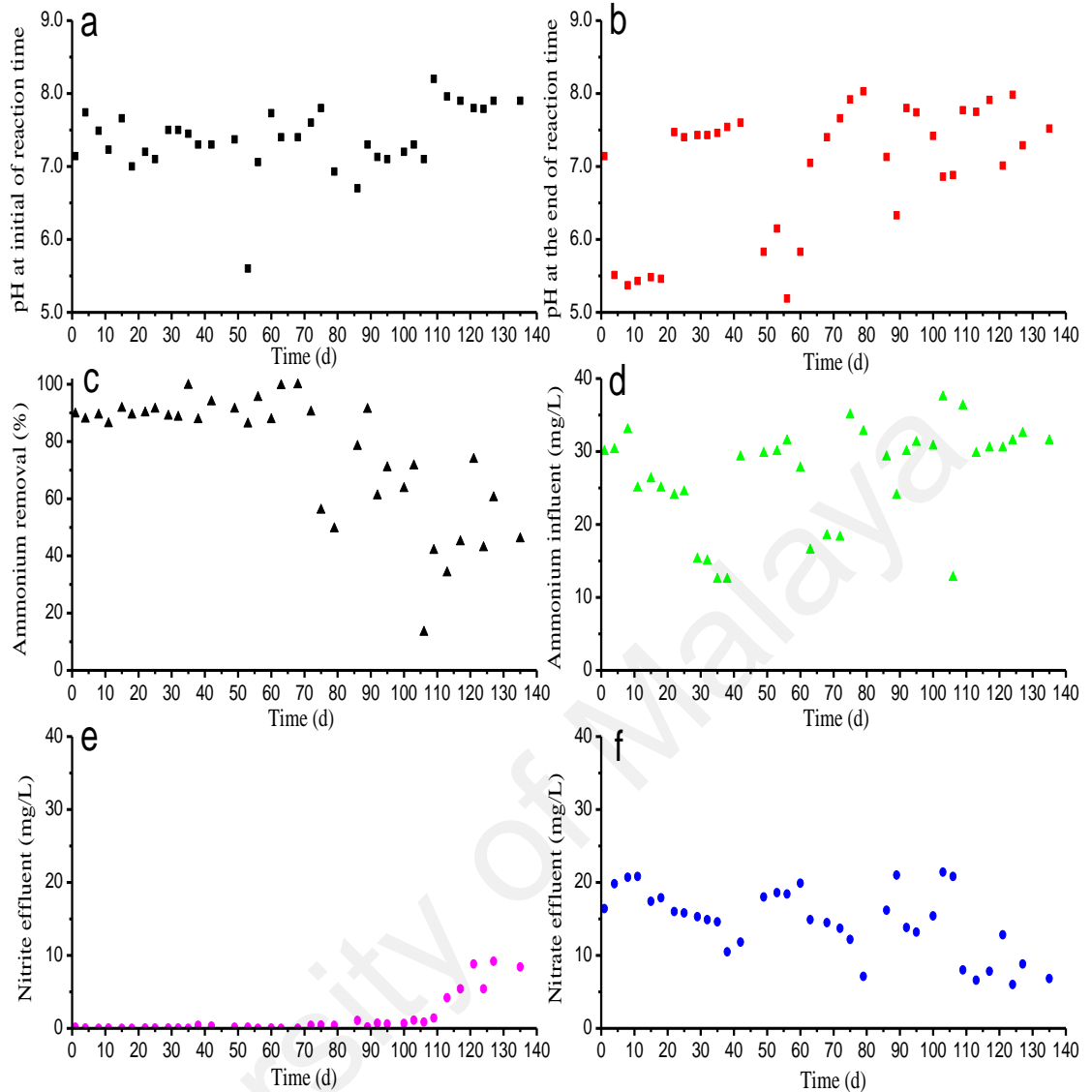


Figure 4.16: Profile of nitrogen effluent and pH at the end of reaction time for Batch2

The removal of ammonium (Figure 4.15c and Figure 4.16c) started to decrease after 60 and 72 days of the formation process for Batch1 and Batch2, respectively. During this period, the pH at the start of the reaction time varied outside the optimal range for nitrification process. The result showed that the pH at the start of the reaction time for Batch1 and Batch2 varied within 6.4 to 6.8 (Figure 4.15a) and 6.7 to 8.2 (Figure 4.16a), respectively. This might be attributed by the accumulation of hydrogen ion from the nitrification process that intrudes the pH at the start of the reaction time after a certain period of the formation process. The minimum DO concentration

observed in Batch1 and Batch2 at the start of reaction time was about 8.5 mg/L. For nitrification to proceed, the DO level should not be less than 2.0 mg/L. In this study, the minimum DO at the end of the reaction time was 8.11 mg/L. These seemed to specify that reactor H/D ratio did not influences the removal efficiencies of nitrogen by AGS directly.

4.3.4 Morphology observation of Batch1 and Batch2

The morphology of aerobic granules was affected by a number of operational parameters such as seed, substrate composition, OLR, reactor configuration and hydrodynamic shear force (Liu et al., 2009). Figure 4.17 exhibited morphology of Batch1 collected on day 38 and 61. Despite of a noteworthy differences in size at 300 μm image scale (a, b), both aerobic granules had displayed straggler shaped and loose structure.

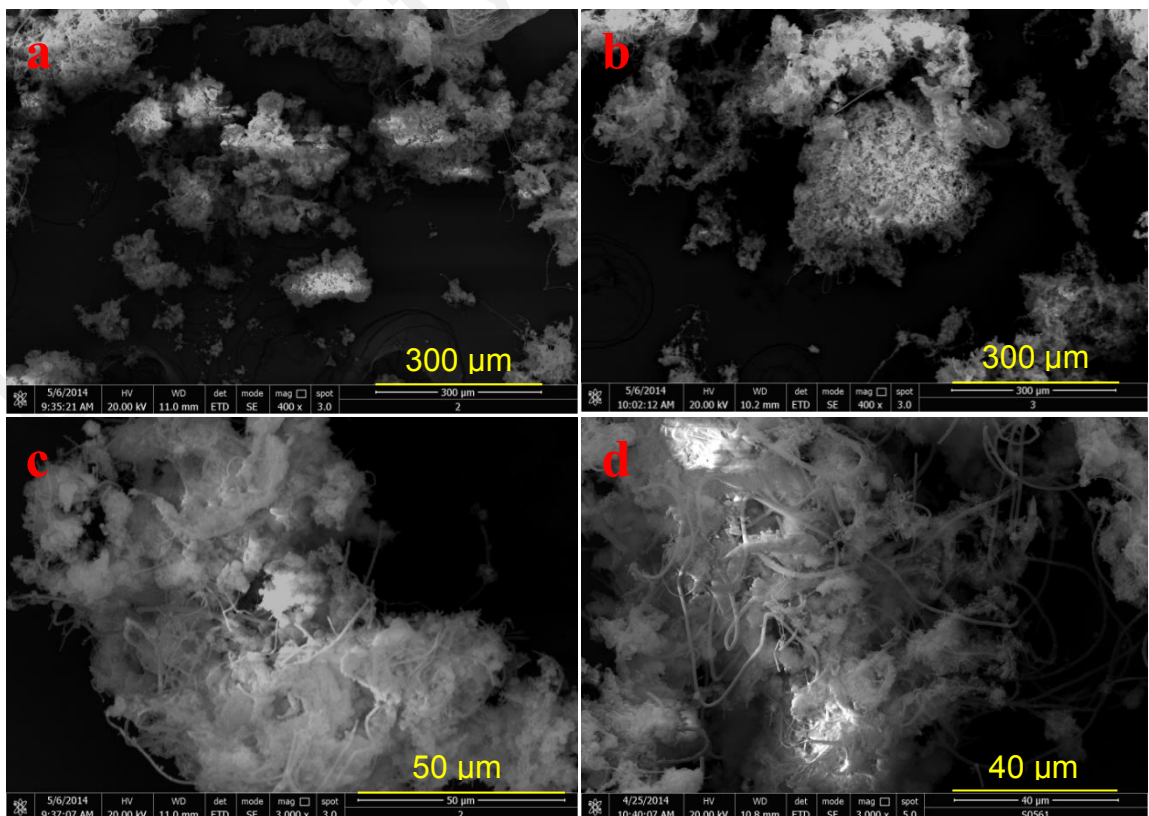


Figure 4.17: FESEM images for Batch1 on day 38 (a, c) and day 60 (b, d)

A closed up image at 50 and 40 μm illustrated that the aerobic granules on day 38 and 60 were consisted of bacteria-dominant granules with abundant of filamentous microorganism especially on day 60. A loose structure of aerobic granules expected since Batch1 was developed under a low substrate concentration. Under the low substrate conditions, the diffusion of substrate would become a limiting factor in aerobic granular sludge formation (Liu et al., 2008a) and thus it tended to decrease the substrate removal rate. Peyong et al. (2012) and Martins et al. (2003) had reported that compact granules subjected to low substrate conditions would end up with loose structure and the existence of filamentous microorganism. This was attributed by the nature of filamentous to excellently fit in loose structure and lead to the development of irregular shape.

Like Batch1, aerobic granules for Batch2 (Figure 4.18) on day 38 and 93 also displayed straggler shapes. Closed-up image indicated that aerobic granules for Batch2 AGS were likely more sturdy than Batch1. Microscopic observations of Batch1 and Batch2 revealed that the granules were typically comprised of filamentous microorganism that linked with one another via bridging to serve as a backbone for the development of AGS. According to Wang et al. (2004), filamentous microorganisms would associate with varying degrees of rod and cocci shape bacteria, bacterial morphotypes that occurred in micro colonies as single cells or in flora forms that distributed randomly in granules. As illustrated Figure 4.19, it appeared that protozoa like vorticella campanula (a), peritrichous ciliates (b) and acineta tuberosa (c) were present in Batch2 on day 93. According to Li et al. (2013), Weber et al. (2007) and Lemaire et al. (2008), vorticella and ciliates contributed to reduce SS effluent and turbidity by removing a certain amount of non-flocculated bacteria and fine suspended biomass particles.

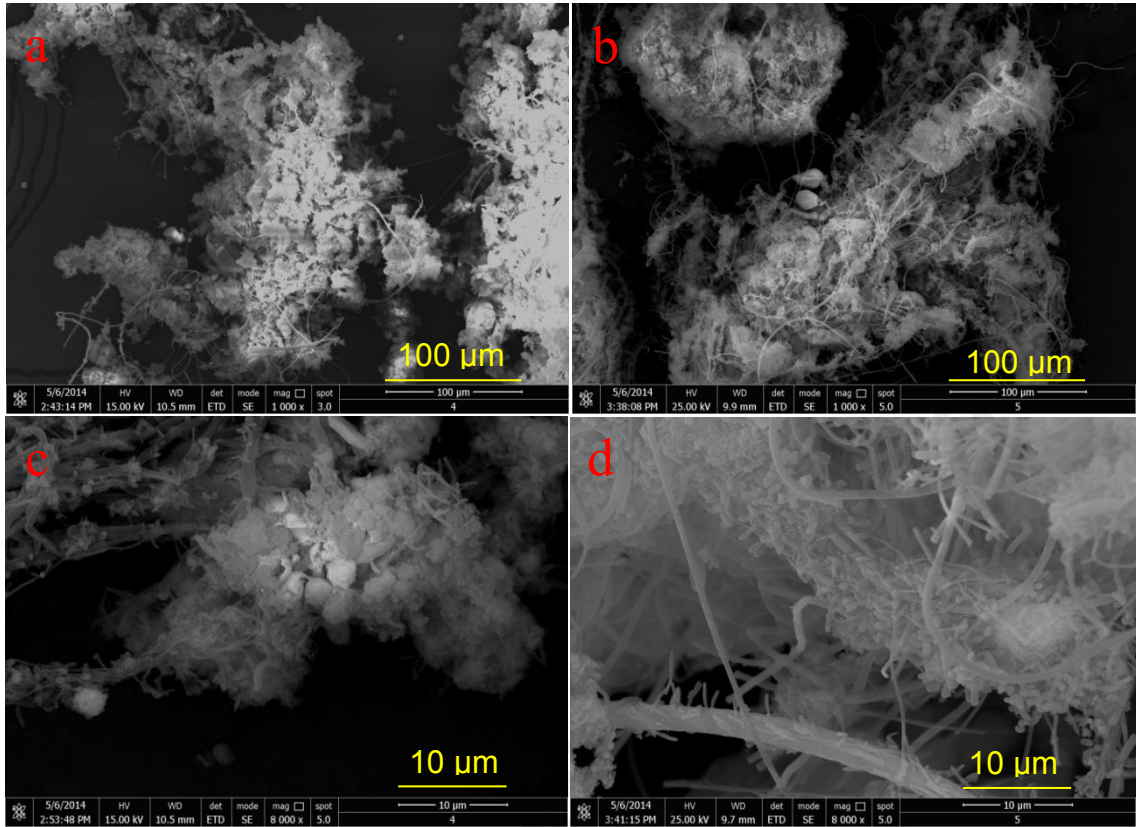


Figure 4.18: FESEM images for Batch2 on day 38 (a, c) and day 93 (b, d)



Figure 4.19: Presence of protozoa in Batch2 on day 93

4.3.5 Chemical Composition of Batch1 and Batch2

EDX analysis was carried out on the surface of aerobic granules for Batch1 and Batch2 and the image analysis were as exhibited in Figure 4.20 and Figure 4.21, respectively. The selected area for the surface mapping for Batch2 was as showed in Figure 4.18(d). The result on the localized and map spectra indicated that carbon and oxygen were the major components observed on the surface of aerobic granules with a slight presence of elements like iron, sodium and calcium. EDX analysis could be a useful tool in understanding the distribution of elements if aerobic granules could be sliced. However, slicing an aerobic granule required a precise technique and equipment that could ensure the aerobic granules structure would not be disrupted during the process. Currently, only Angela et al. (2011) had published the result for EDX analysis on slice mature aerobic granules.

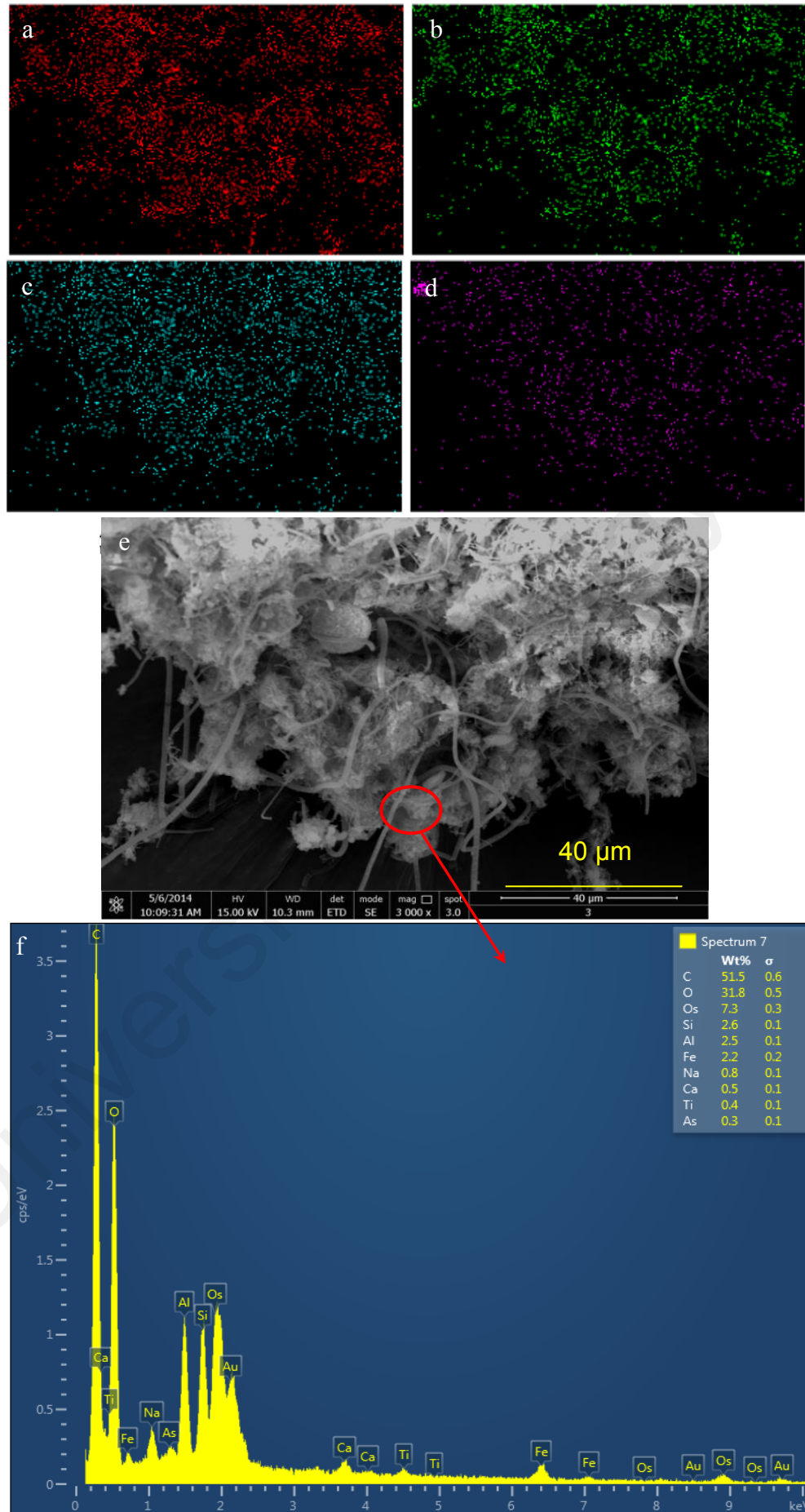


Figure 4.20: Elemental mapping images (a: carbon, b: oxygen, c: silicon, d: aluminium) and localized elements spectra (f) from EDX analysis for (e) surface area of Batch1 on day 60

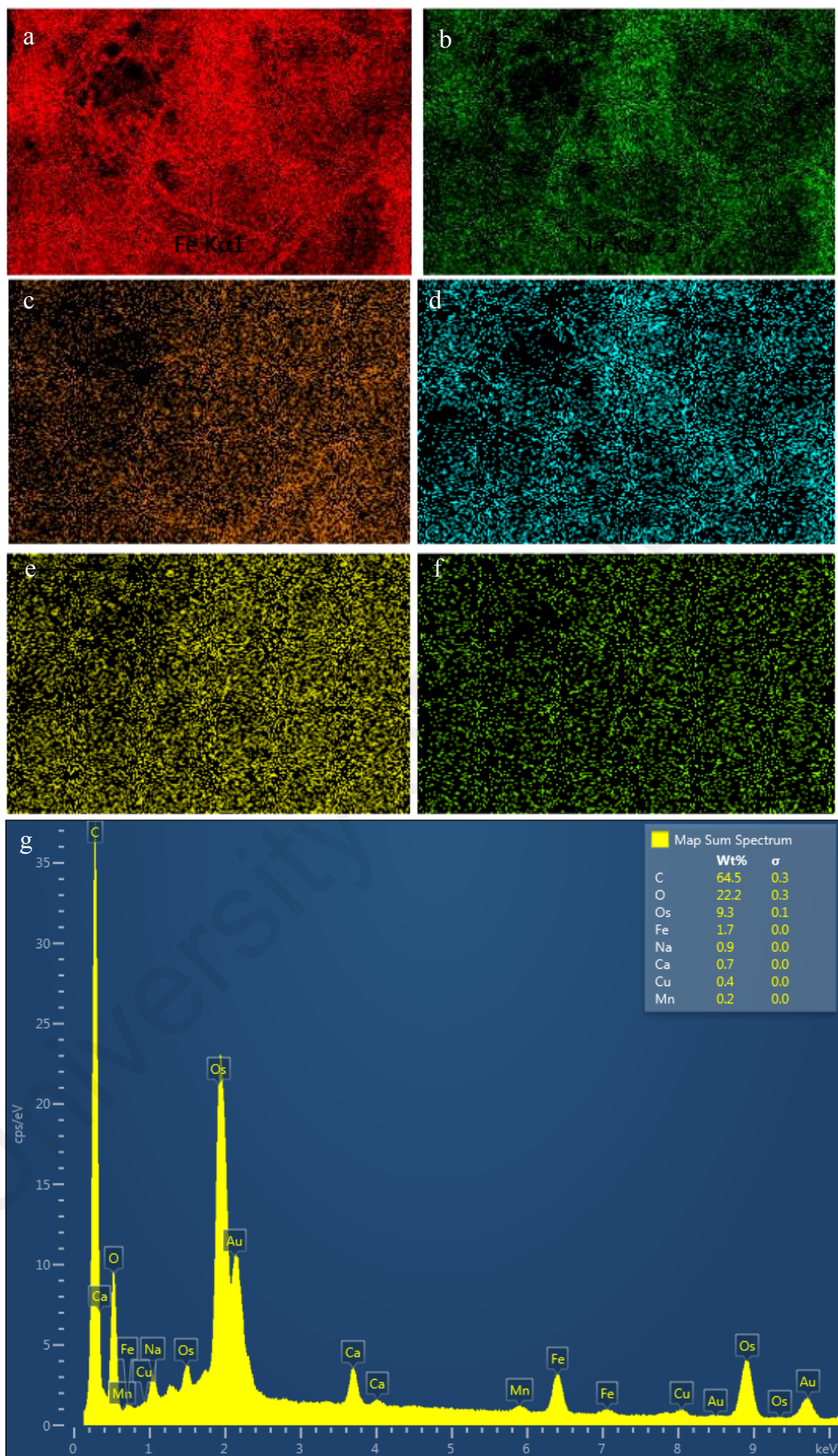


Figure 4.21: Elemental mapping images (a: carbon, b: oxygen, c: iron, d: sodium, e: calcium, f: copper) and map elements spectra (g) from EDX analysis for Figure 4.18(d) surface area of Batch2 on day 93

4.3.6 Advantages and Disadvantages of Reactor with Low H/D Ratio

In this study, aerobic granules were successfully developed in SBR2 with low H/D ratio and SUAV of 4.4 cm/cm and 0.7 cm/s, respectively. The advantages and disadvantages of reactor with low H/D ratio (SBR2) as compared to reactor with high H/D ratio (SBR1) that could be pointed out from the results and discussion were as follows:

- i. At a similar working volume, the periods to achieve stable conditions or mature aerobic granules in SBR1 with high H/D ratio was shorter than in SBR2 even after fresh activated sludge was added on day 33.
- ii. Biological AGS reactor was needed to retain sufficient amount of biomass (MLSS and MLVSS) in order to recover the loss prior to excessive washed out. In comparison to SBR1, at a similar settling time which was 15 mins, SBR2 provided short settling distance for biomass in facing unfavorable circumstances.
- iii. Both Batches exhibited a decrease in SV_{15} to SVI_{15} in which was due to the densifying process in line with formation periods.
- iv. SVI_{30} indicated that SBR1 produced more sludge than SBR2 meanwhile the effluent performances in both reactors were high.
- v. An analysis on effluent quality showed that under the variable OLR, 30 and 15 mins were the optimum settling times for SBR1 and SBR2 respectively.

4.4 Formation of AGS in Airlift Reactor with Divided Draft Tubes (Batch3)

To date, the development of aerobic granules that has been extensively reported is the one using bubble column with sequencing batch operation. This is because the formation process of aerobic granules itself depending upon the flowing trajectory inside reactor influenced by reactor height and SUAV. This was firmly confirmed by Liu and Tay (2002) who had stated that microbial granulation has hardly been reported in complete mixed tank reactor in the past one hundred years of conventional activated sludge operation practice. SUAV governs the formation process by exerting the rate of oxygen supply and intensity of hydrodynamic shear force. Apart from bubble column, numerous reports on the formation of aerobic granules in airlift column with sequencing batch operation are also available. This is due to the fact that airlift reactor can deliver higher shear force although the aeration rate is low and better mixing as compared to bubble column. Currently, only Liu and Tay (2007) had reported formation of aerobic granules in a novel airlift reactor with divided draft tubes with the aim to alleviate the problems of unequal discharge from riser and downcomer compartments.

Result from Section 4.3 showed that optimal settling time and biomass production of SBR2 with H/D ratio of 4.4 was shorter and lesser than of SBR1 with H/D ratio of 11.3. However, aerobic granules produced in SBR2 took 89 days to achieve mature conditions compared to 41 days in SBR1. Thus, the aim of this work is to optimize the performance of reactor with low H/D ratio. An airlift reactor with divided draft tubes (SBR3) was designed to solve the problem of long period needed to achieve mature aerobic granules. The result in this study enlightened that aerobic granules formation only requires a definite critical height for an effective flowing trajectory take places, could give a different insight for researchers in designing reactor H/D ratio.

4.4.1 Flow Pattern of Liquid in SBR3

The details of SBR3 design was shown in Figure 3.3. The internal diameter of SBR3 was 11 cm and the diameter of the draft tube was 8.5 cm. The draft tube comprised two sections with the same length (10 cm) and effluent discharging point located between the gaps of draft tubes. Figure 4.22 shows the comparison between the flow patterns of liquid in bubble column and airlift type reactors. The given flow pattern for bubble column (Figure 4.22a and 4.22b) were based on report by Liu and Tay (2002) which described liquid upflow pattern as a homogenous circular flow along the reactor height. Hence, it is expected that the circular flowing trajectories in SBR1 are longer than in SBR2 and SBR3.

The internal liquid circulation between the riser and downcomer of the airlift reactor were based on reports by Jin et al. (2008) and Chan et al. (2009) for Figure 4.22c and by Liu and Tay (2007) for Figure 4.22d. The given flow pattern for Figure 4.22e was based on assumption derived from reports by Liu and Tay (2002; 2007), Jin et al. (2008) and Chan et al. (2009). As showed in Figure 4.22e, liquid turns flow direction when reaches an inclined part of the draft tubes resulting in circular flowing trajectory. SBR3 is expected to have two phases of circular flowing trajectories compare to SBR1 and SBR2.

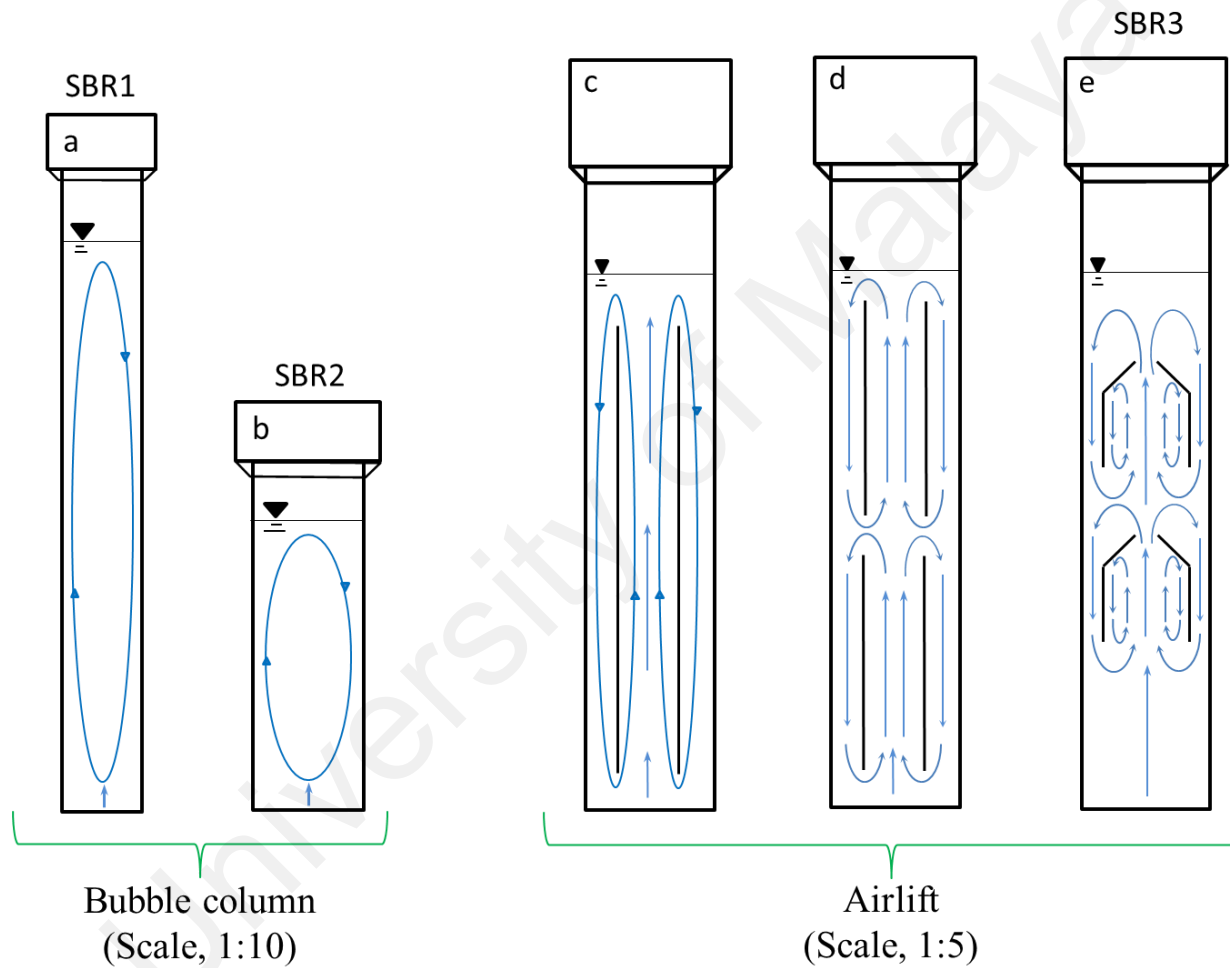


Figure 4.22: The flow pattern of liquid in bubble column and airlift type reactor based on report by Liu and Tay (2002; 2007), Jin et al. (2008) and Chan et al. (2009).

4.4.2 Size and Morphology Evolution of Aerobic Granules

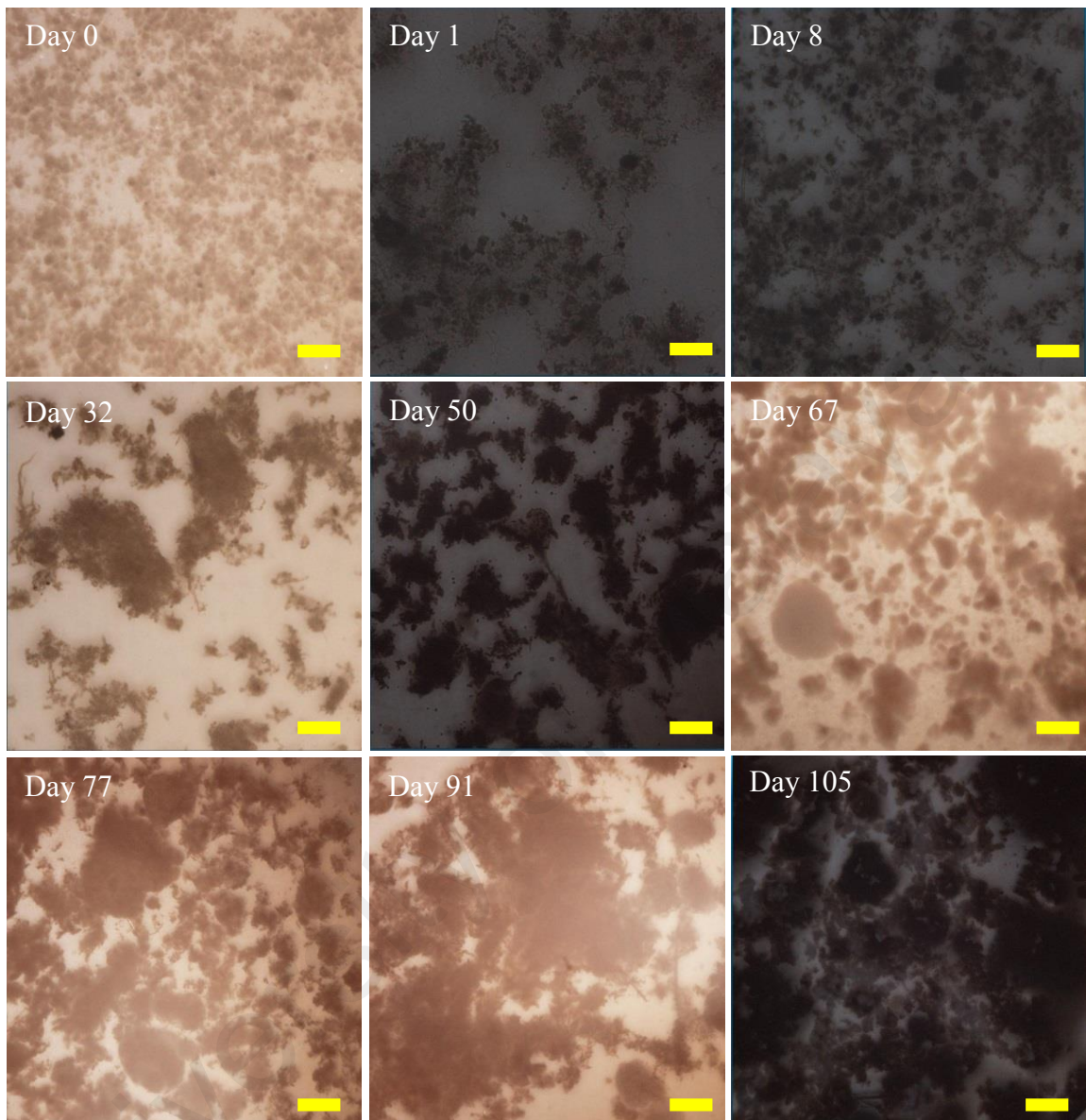


Figure 4.23: Evolution of aerobic granules in SBR3. Bar = 500 μm

Figure 4.23 exhibits the evolution of inoculate seed on Day 0 to mature aerobic granules on different days of formation period. Whilst, the deviation in aerobic granules size on different days was reflected in the length of the box plot as presented in Figure 4.24. As shown on day 0, the inoculate seed was activated sludge with median size of 154 μm , having fluffy structure. Dissipation of activated sludge occurred within 24 h of start-up and resulted in the formation of pin flocs on day 1. It appears that aggregation of pin flocs started since day 1, and by day 8, the median size of pin flocs started to

increase from 24 to 99 μm , respectively. Fluffy aerobic granules started to appear after 32 days, but with apparent existence of filamentous microorganism protruding from aggregates.

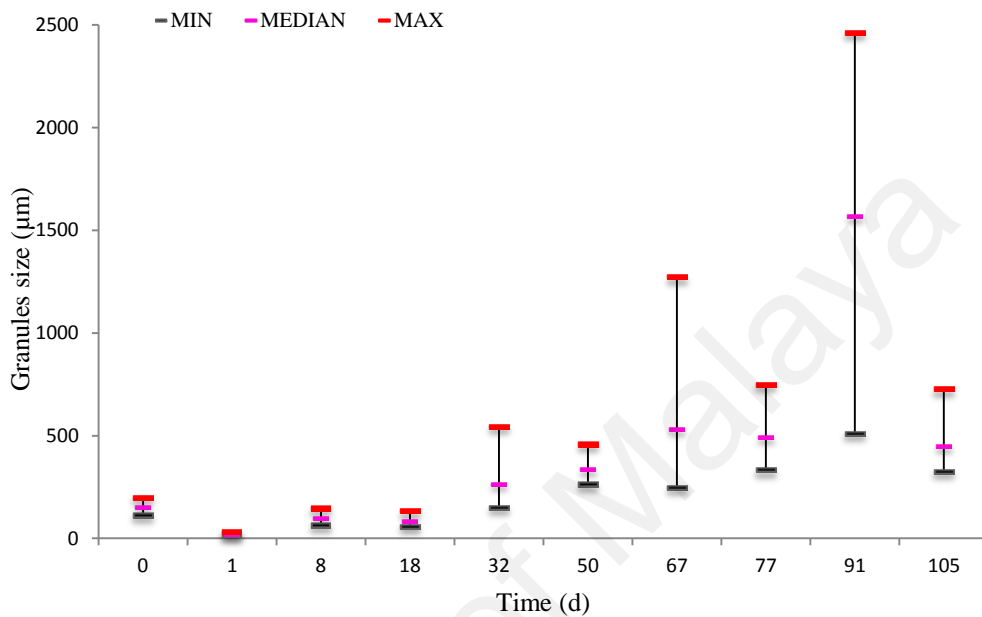


Figure 4.24: Deviation in aerobic granules size for Batch3.

The deviation in aerobic granules size on day 50, which was between 264 and 459 μm were within the range on day 32 (151 to 545 μm) and this suggests that densified process for fluffy aerobic granules has started. This is in line with pattern of SVI profile (Figure 4.25) that exhibited small deviations between 5 min intervals of settling time after 22 days of formation process. Moreover, as shown in Figure 4.26(b), the morphology of aerobic granules on day 50 exhibited a cauliflower-like structure compared to aerobic granules on day 32 (Figure 4.26a) that displayed long straggler shape which might indicate aggregation of small aerobic granules along the filamentous microorganism as backbone. Similar cauliflower-like structure was observed by Liu et al., (2004) and Lemaire et al. (2008) when aerobic granules were developed at substrate COD/N ratio less than 5 and 6, respectively. Liu et al. (2004) remarked that the

cauliflower-like structure of densely slow-growing nitrifying bacteria would contribute to the stability of aerobic granules developed at low substrate COD/N ratio.

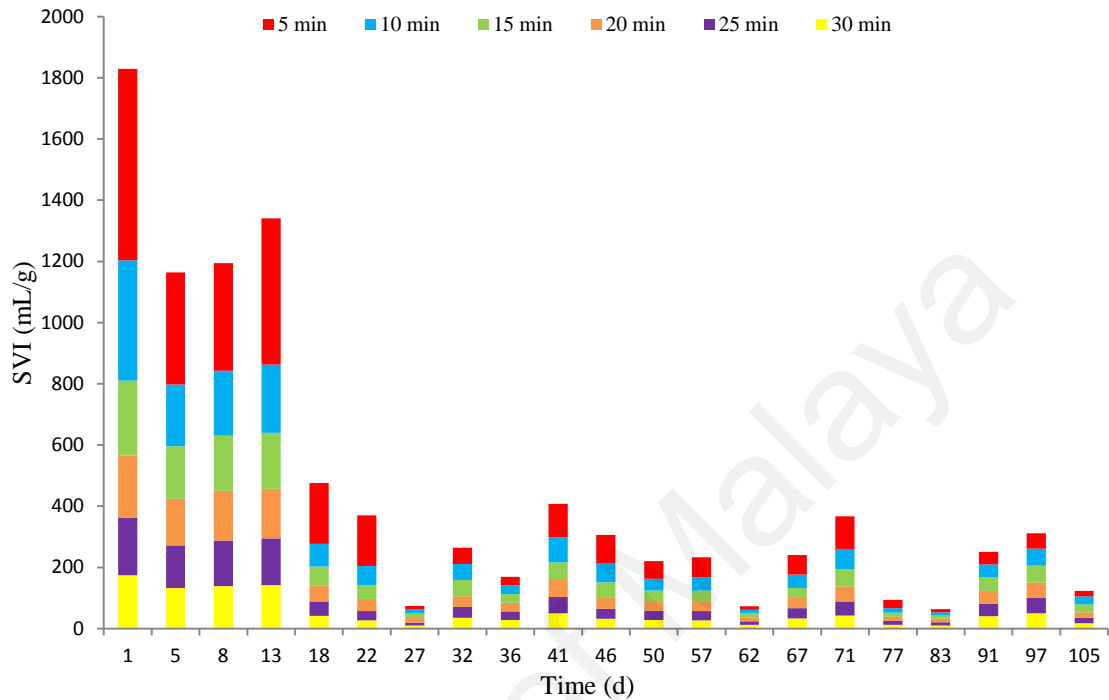


Figure 4.25: Profile of SVI at 5 min intervals of settling time for Batch3

Aerobic granules size continued to increase up to 1237 μm on day 67 with the numbers of small aerobic granules of less than 532 μm , being predominant in the reactor. This might be attributed to densified process. Arrangement of aerobic granules position becomes more compact and strong aggregates during densified process (Sheng et al., 2010) contribute to a clear outline boundary of aerobic granules. Thus, it can be concluded that mature aerobic granules were achieved on day 67. According to Verawaty et al. (2013), mature aerobic granules will subsequently disintegrate after reaching a certain critical size and causing an overall reduction in granular sludge. This indeed occurred on day 77 in which the size of mature aerobic granules on day 67 decreased and varied between 333 and 750 μm . Microscopic image for aerobic granules on day 77 also indicated an apparent existence of filamentous microorganism protruding from the aggregates.

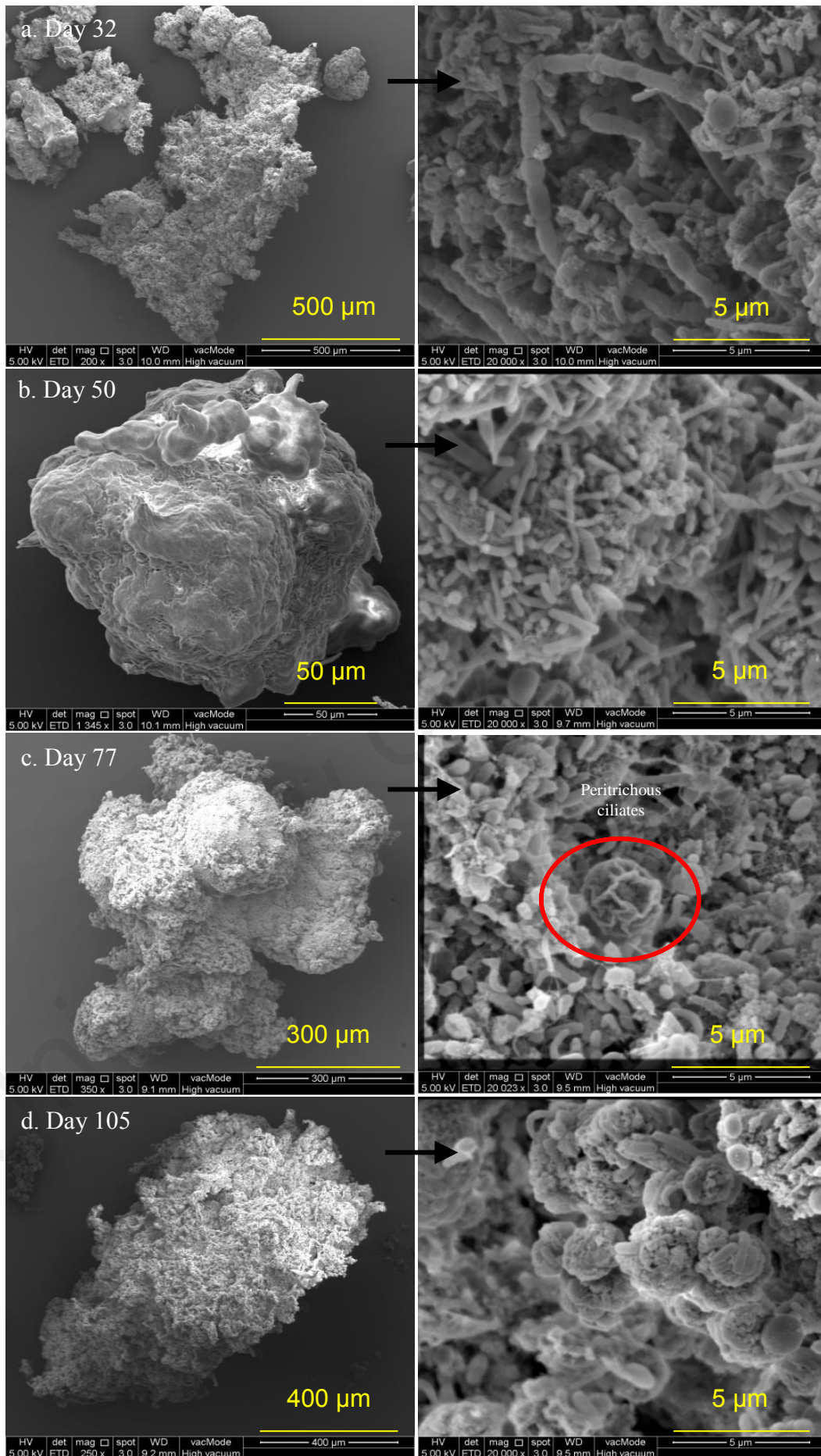


Figure 4.26: Morphological development of aerobic granules during the experimental run

The morphology of aerobic granules on day 77 (Figure 4.26c) was likely exhibited the detachment of biomass from parents aerobic granules, and this further confirmed the disintegration of mature aerobic granules on day 67. A close-up image on aerobic granules morphology at day 77 demonstrated the appearance of peritrichous ciliates surrounded by varying degrees of rod and cocci shape bacteria. According to Weber et al. (2007), ciliates stalks serve as backbone in the granule-forming process since bacteria use them as a substratum to grow. Weber et al. (2007) and Lemaire et al. (2008) remarked that ciliates contribute to the reduction of SS effluent and turbidity by removing certain amount on non-flocculated bacteria and fine suspended biomass particle

By day 91, aerobic granules continue to increase in size, with diameter varying between 511 and 2463 μm . This signifies that filamentous microorganism protruding out from the aggregates helps to promote aggregation between small and big granules via bridging. This in turn leads to irregular shape and diffused granular structure as depicted in microscopic image on day 91. Mature aerobic granules again dominate in the reactor on day 105 with diameter varying between 326 and 728 μm . A clear outline boundary of mature aerobic granules was accompanied by small granules from partial disintegration of aerobic granules on day 91. Based on microscope and FESEM images, the mature aerobic granules produced on day 105 exhibited a tinny oval or rod shape form instead of the desired sphere shape. Chiu et al. (2007) reported that the critical size of aerobic granules could be defined as the diameter of the aerobic granule above an anaerobic zone or else, mass diffusion limitation would be present. Based on an analysis of the pattern of aerobic granules image, size deviations and SVI, it can be concluded that the critical size of aerobic granules in this study was around 1200 μm

As presented in Figure 4.25, SVI profile showed a decreasing pattern along with the formation of aerobic granules. SVI profile for the first 13 days of formation process was noticeably higher compared to the rest of the formation days. However, biomass concentration in terms of MLSS and MLVSS (Figure 4.27) was comparatively high between day 1 and 13 and day 41 to 77. These results demonstrated that the transient phase in formation process was strongly related to the settling properties of aerobic granules.

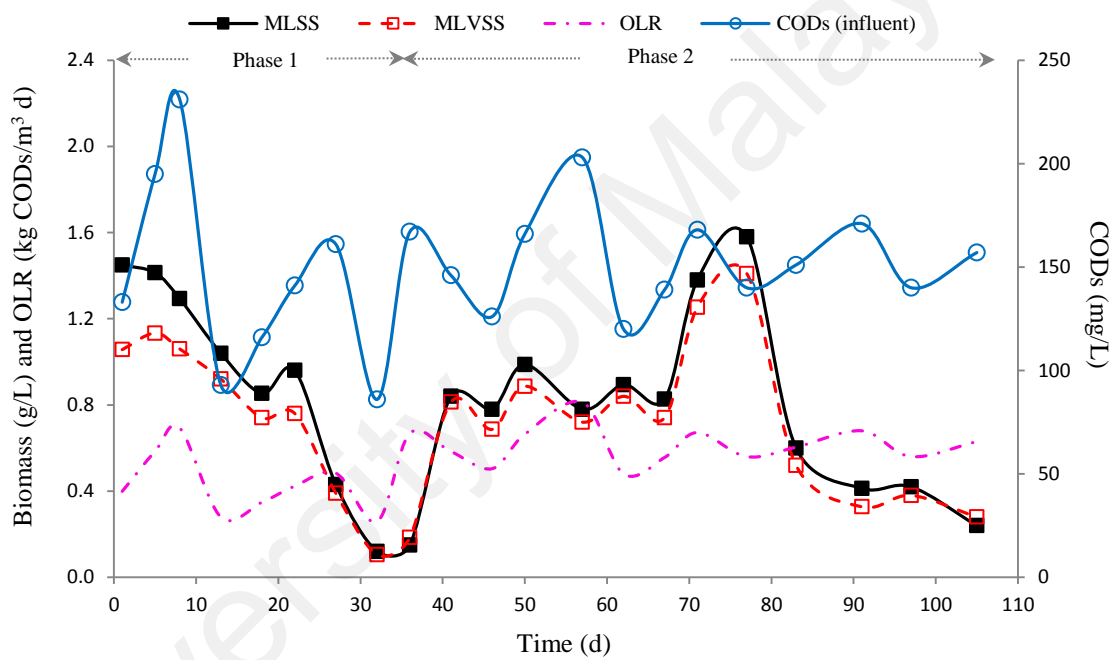


Figure 4.27: Profile of biomass (MLSS and MLVSS), OLR and CODs influent for Batch3

Based on microscopic observation and SVI profile, it is more likely that aerobic granules on day 1 to 36 and day 41 to 67 were in aggregation and stability phase, respectively. During aggregation phase, formation of aerobic granules was highly dependable on OLR or substrate concentration. This matches well with profile of MLSS and MLVSS which varied according to changes in CODs influent from day 1 to 36. Cycle time was adjusted from 4 to 3 h on day 33 when analysis on F/M ratio (Figure 4.28) indicated that the biomass decreased due to insufficient food since 22 days of

formation process. Changes in CODs influent during stability phase did not significantly affect MLSS and MLVSS profile. By removing the biofilm which has grown on reactor wall during reactor maintenance on day 69, aerobic granules did not have to outcompete for food with biofilm anymore. Thus, in turn MLSS promptly increased from 0.83 g/L on day 67 to 1.38 g/L on day 71. An increase in MLSS on day 71 also indicated that partial disintegration of mature aerobic granules as depicted on microscopic image on day 77 was not solely due to critical size effect.

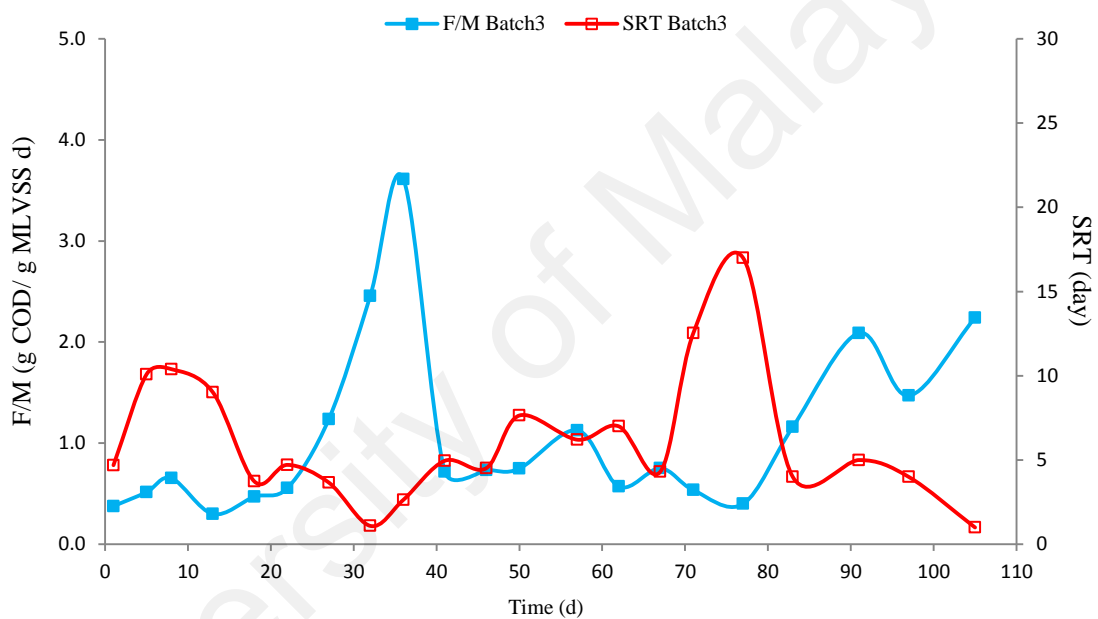


Figure 4.28: Profile of F/M ratio and SRT for Batch3

Along with the increase in MLSS and partial disintegration of mature aerobic granules, it appears that some aerobic granules were floated and entrapped into effluent discharge pipe during long feeding time of 30 min. As a result, MLSS promptly decreased from 1.58 g/L on day 77 to 0.60 g/L on day 83. It is expected that hydrolysis of anaerobic core during disintegration of mature aerobic granules release gases and organics acids (Tay et al., 2002) which were entrapped within sludge layer at static condition. Other than that, long feeding time may create an anoxic condition inside reactor and this governs the denitrification process which releases nitrogen gas within

sludge layer. From observation, aerobic granules started to float after 20 min of feeding time. Hence, the feeding time was changed from 30 to 10 min on day 82 with settling time remained at 15 min throughout the formation process.

Afterwards, a reduction in biomass concentration and sludge retention time (Figure 4.28) was observed. This is in agreement with studies reported by Thanh et al. (2009) and Wagner and da Costa (2013) that signified disintegration of aerobic granules leads to the washout of the generated flocs and particles, and subsequently reducing the biomass concentration on the following days. Anyhow, mature aerobic granules were successfully re-dominated in the reactor on day 105. The formation of Batch3 was mostly stable between day 41 to 67 and this is in line with result on F/M ratio that varied slightly between 0.57 to 1.13 g CODs/g MLVSS d. During stable periods, the differences of SVI between 5 min intervals of settling time started to plateau off and evenly distributed. Batch3 AGS stabilized at average MLSS of 0.85 g/L and SRT of 6 d.

Microscopic observation of aerobic granules size evolution was in accordance to the dynamic granulation model developed by Zhou et al. (2014). The model helps to explain the enormous deviation in aerobic granules size obtained in this study which might be caused from the self-aggregation of aerobic granules and re-granulation of the detached bioflocs, newborn cells and crushed aged aerobic granules. The final aerobic granules size obtained in was in the range of 326 to 728 μm , and were comparable with results demonstrated by Liu et al. (2007), Su et al. (2012), Ni et al. (2009) and Peyong et al. (2012) for aerobic granules developed in sewage. The typical size of mature granules developed in sewage were assumed to be around 750 to 800 μm , and can reach up to 2000 μm , depending on the selection of operating conditions. The variations in OLR will intrusive the formation process particularly during low OLR required longer period

to achieve mature aerobic granules or full granulation of biomass in the reactor. Result showed that the use of divided draft tubes for formation of aerobic granules in low H/D ratio SBR3 and under variable OLR and low SUAV has successfully expedited the formation period. In SBR2 with similar H/D ratio of SBR3, mature aerobic granules were formed after 89 days instead of 67 days, respectively.

4.4.3 Effect of low COD/N Ratio on Reactor Performance

Besides the formation process, the performance of SBR3, in terms of CODs, SS and nitrogen removal were also determined. Figure 4.29 and Figure 4.30 depict influent and effluent concentration as well as the removal efficiency of CODs, SS and ammonium during the formation process. During the first 36 days, aerobic granules were in formation stage and thus led to poor CODs and SS removal. Negative removal for SS at an early stage indicated that the biomass was excessively washed out from the reactor. Afterwards, the reactor's performance improved continuously and was at stable condition, within days 41 to 67, the average of CODs, SS and ammonium removal reached 71%, 64% and 78% respectively. As for the concentration of nitrite and nitrate in the effluent during stable periods, the respective average values of 14 mg/L and 13 mg/L were obtained, respectively.

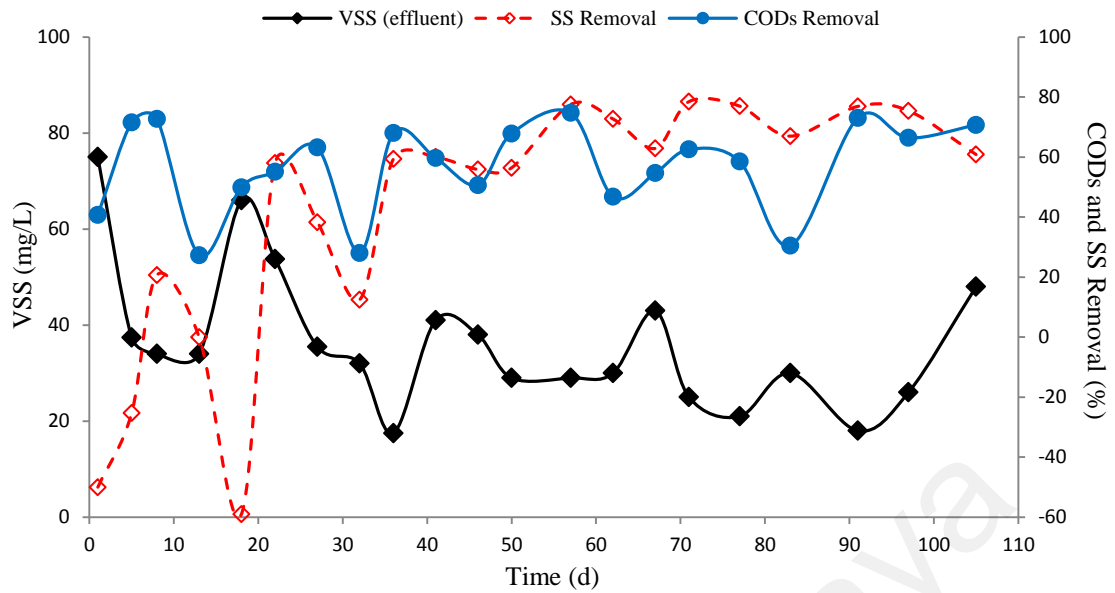


Figure 4.29: VSS effluent, SS and CODs removal for Batch3

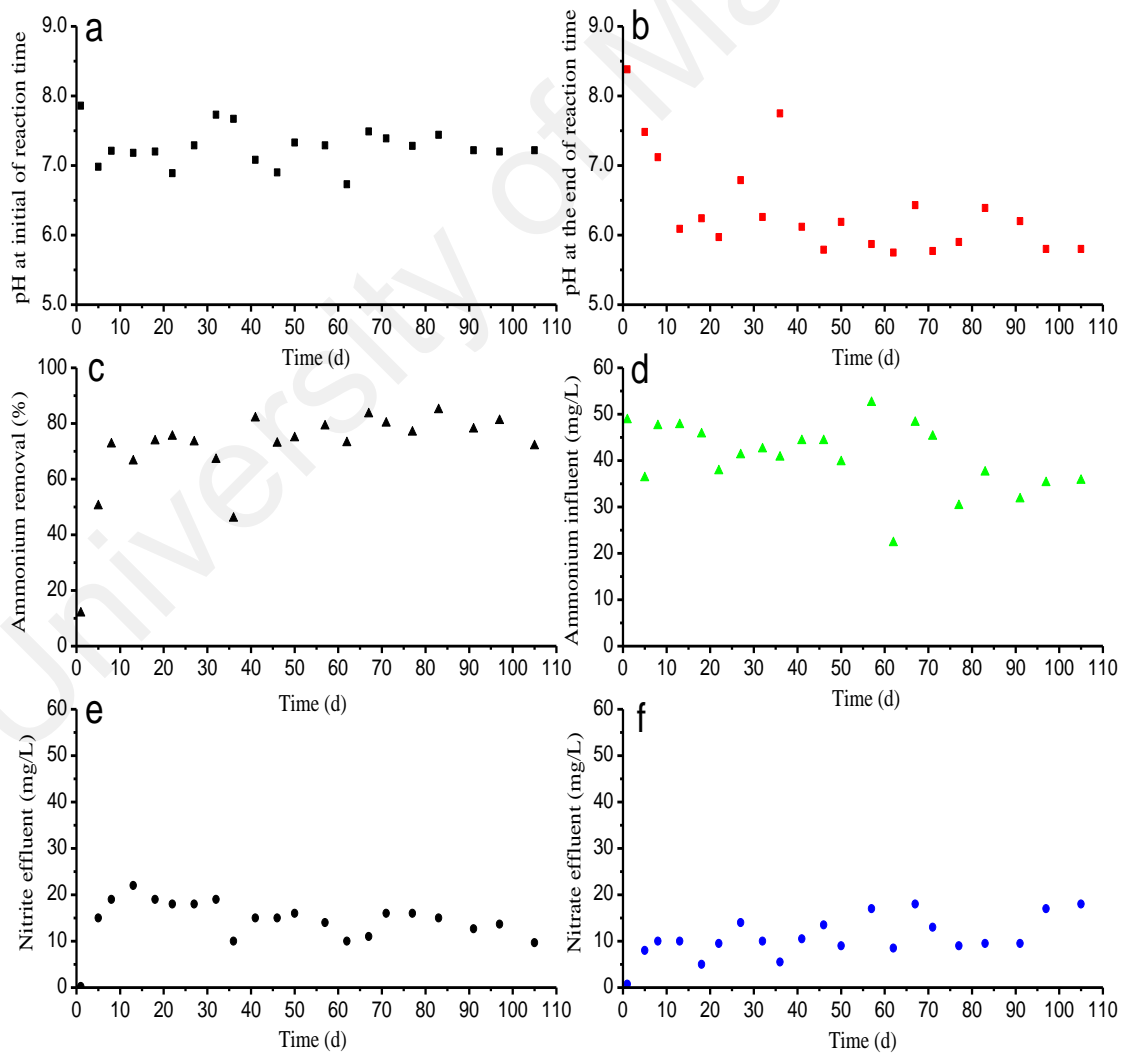


Figure 4.30: Profile of pH, ammonium, nitrite and nitrate effluent for Batch3

Throughout the formation process, it is noted that partial nitrification of ammonium was switched in-between high or equal nitrite and nitrate accumulation corresponding to the changes in ammonium influent. Ammonium removal increased as the cycle time reduced to 3 h on Phase 2 and remained high even though the reaction time increased from 124 to 145 min on day 82. Thus, this suggests that the difference in reaction times will not affect nitrogen removal. In fact, Wagner and da Costa (2013) proved that COD and ammonium in sewage were mainly degraded within 30 min of reaction time. According to Ruiz et al. (2003), complete nitrification occurs at pH 6.45 to 8.95, and the culture over that range would inhibit both ammonia oxidizing bacteria and nitrite oxidizing bacteria (NOB).

As depicted in Figure 4.30(a), pH at the start of reaction time throughout the formation period was above 6.45. Thus, this confirms that pH is not the main reason for partial nitrification in SBR3. Reports by Ruiz et al. (2003), Yang et al. (2004), Wang et al. (2007) and Liu et al. (2008) have claimed that accumulation of nitrite is likely due to inhibition of NOB either by low dissolve oxygen (DO) or high level of free ammonia (FA). The minimum DO concentration observed at the start and end of reaction time in this study was about 6.3 mg/L and 7.50 mg/L, respectively. Thus, it seems that DO concentration also did not contribute to inhibition of NOB. Liu et al. (2008) remarked experimental results on NOB inhibition which was done by Anthonisen et al. (1976). It is reported that *Nitrobacter* was inhibited at unionized of free nitrous acid (FNA) concentration as low as 0.2 mg/L. Increase in FNA concentration along with accumulation of nitrite resulted in a decrease in pH. Indeed, as presented in Figure 30(b), pH at the end of reaction time decreased to 5.8 except for day 1 to 13 and day 32 to 41.

Low CODs removal and decrease in pH at the end of reaction time to 5.8 was attributed to low COD/ammonium ratios during Phase 1 and Phase 2, which were 3.4 and 3.9, respectively. This finding is supported by Yang et al. (2004) and Wang et al. (2007) that suggested aerobic granulation and nitrification process are closely related to the COD/N ratios applied to the reactors, in which COD/N ratio lower than 10 will inhibit both heterotrophic and nitrifying bacteria. This is indeed in line with tabulated result compiled in Table 4.2.

Table 4.2: Effect of COD/NH₄⁺ ratio on COD and ammonium removal

COD		Ammonium (NH ₄ ⁺)		COD/ NH ₄ ⁺	References
Influent (mg/L)	Removal	Influent (mg/L)	Effluent		
5850	-	450	Almost all NH ₄ ⁺ influent converted into NO ₂ ⁻ . Removal of NH ₄ ⁺ ≈ 100%.	13	Liu et al. 2008
3900	-	300	Complete nitrification.	13	
430	≈ 78%	91	Removal of NH ₄ ⁺ ≈ 23%. NO ₂ ⁻ and NO ₃ ⁻ accumulation are low.	4.7	Wagner and da Costa 2013
412	≈ 82%	83	Removal of NH ₄ ⁺ ≈ 69%. NO ₂ ⁻ accumulation higher than NO ₃ ⁻ .	5	
849	≈ 96%	76	Removal of NH ₄ ⁺ ≈ 96%. NO ₂ ⁻ accumulation lower than NO ₃ ⁻ .	11.2	
1000	≈ 95%	100	Removal of NH ₄ ⁺ ≈ 50%. NO ₂ ⁻ accumulation.	10	Yang et al. 2004
1000	≈ 95%	200	Removal of NH ₄ ⁺ ≈ 25%. NO ₂ ⁻ and NO ₃ ⁻ not present.	5	
1000	≈ 95%	300	Removal of NH ₄ ⁺ ≈ 17%. NO ₂ ⁻ and NO ₃ ⁻ not present.	3.3	
145 ^a	≈ 51%	43 ¹	Removal of NH ₄ ⁺ ≈ 61%. NO ₂ ⁻ accumulation higher than NO ₃ ⁻ .	3.4	This study
153 ^b	≈ 60%	39 ²	Removal of NH ₄ ⁺ ≈ 76%. NO ₂ ⁻ accumulation ≈ NO ₃ ⁻ .	3.9	

≈: nearly closed to, ¹: Average for Phase 1, ²: Average for Phase 2

Although influent ammonia concentration was less than 91 mg/L, a decrease in COD removal from 96% to 78% when COD/N ratio decreased from 11.2 to 4.7 was observed during aerobic granules formation (Wagner and da Costa, 2013). Thus, it can

be concluded that the rate of nitrification inhibition should not be estimated solely based on ammonium influent concentration. Complete nitrification could occur even when the wastewater has high in ammonium influent and COD/N ratio is over 10 (Yang et al. 2004). As shown in Figure 4.29 and Table 4.2, average of CODs removal can be considered as low with 51% and 60% during Phase 1 and Phase 2, respectively. This result was expected since low COD/ammonium ratio would inhibit both heterotrophic and nitrifying bacteria (Wang et al. 2007b; Yang et al. 2004).

4.4.4 Composition and Distribution of EPS

The chemical functional groups of the freezing Batch3 extracellular polymeric substances (EPS) were characterized by FTIR analysis. FTIR spectrum was monitored in order to evaluate the variations of EPS functional groups changing from day 0 to day 105 as depicted in Figure 4.31. The characteristic assignments for FTIR spectrum were based on studies carried out by Schmitt and Flemming (1998), Omoike and Chorover (2004) and Badireddy et al. (2010). The strong presence of protein was confirmed by the typical amide band I and amide band II at 1637 and 1505 cm^{-1} , respectively. The presence of polysaccharides and phosphodiester (asymmetric PO_2^- stretch) was confirmed within 1134 to 1137 cm^{-1} and 1259 to 1263 cm^{-1} range, respectively. The FTIR spectrum also confirmed a strong presence of hydroxyl at 3303 cm^{-1} .

Compared to the seed, FTIR spectrum revealed that transmittance intensity signals increased throughout the formation period. This can be used as an indicator to reflect an improved stability of the properties of aerobic granules upon formation period. According to Badireddy et al. (2010) and Zhu et al. (2012a), the bands within 1630 to 1640 cm^{-1} that exist in all EPS samples, are specifically associated with $\text{C}=\text{O}$

stretching vibration of β -sheet in secondary protein structures that favor bio flocculation. EPS spectrum exhibited weak signal for amide II (1505 cm^{-1}) indicating that C=O stretching was predominant compared to C-N stretching, N-H bending and O=C-N bending. Weak vibrations from broad phosphodiester bonds were detected at 1263 cm^{-1} indicating low amounts of nucleic acids. Badireddy et al. (2010) explained that broad ester band ranging 1270 and 1230 cm^{-1} helps to promote cell aggregation, adhesion and biofilm integrity. Bands between the range of 900 to 1200 cm^{-1} that result from bonds vibration of polysaccharides as well as DNA/RNA (Omoike and Chorover, 2004) are associated with the vibrational stretching of O-H and C-O (Zhu et al., 2012a).

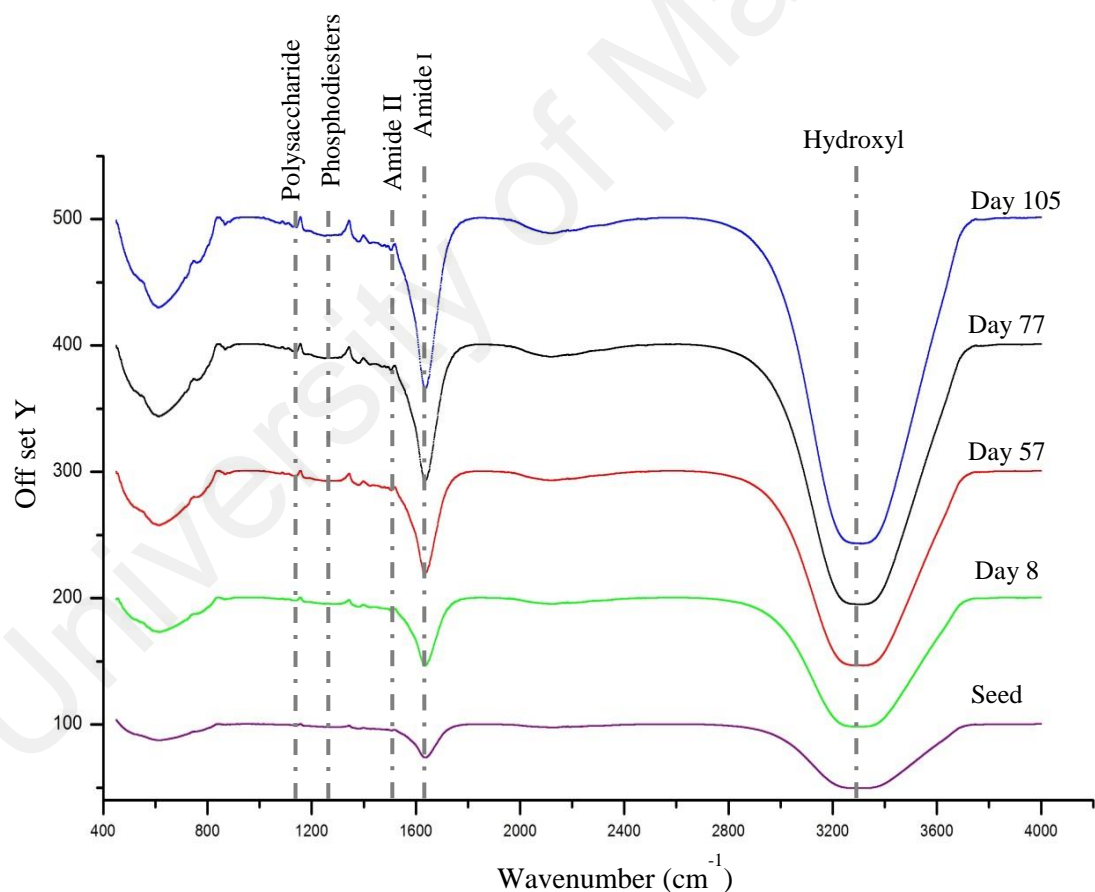


Figure 4.31: FTIR spectrum of freezing EPS from seed to day 105 for Batch3

Compounds such as proteins, polysaccharides and alcohol that carry functional groups of C=O, C-O and O-H, help to promote microorganism aggregation (Badireddy et al., 2010) by means of ionic and electrostatic attractive forces and hydrogen bonding,

for the stability of EPS matrix (Flemming and Wingender, 2010). Whilst, functional groups like carbonyl, carboxylate, acetal, or hemiacetal and hydrocarbons hinder the aggregation process (Badireddy et al., 2010). As exhibited in Figure 4.32, EDX analysis on localized spectrum at different days of formation period showed that carbon and oxygen were the major components observed on the surface of aerobic granules with a slight presence of elements like iron, sodium, calcium, aluminium and zinc. This suggest that ionic attractive forces between dissociated C=O and divalent metal cations (Ca^{2+} , Fe^{2+}), and -H bonding between O-H and monovalent cations (K^+ , Na^+) exist at all stages of formation periods.

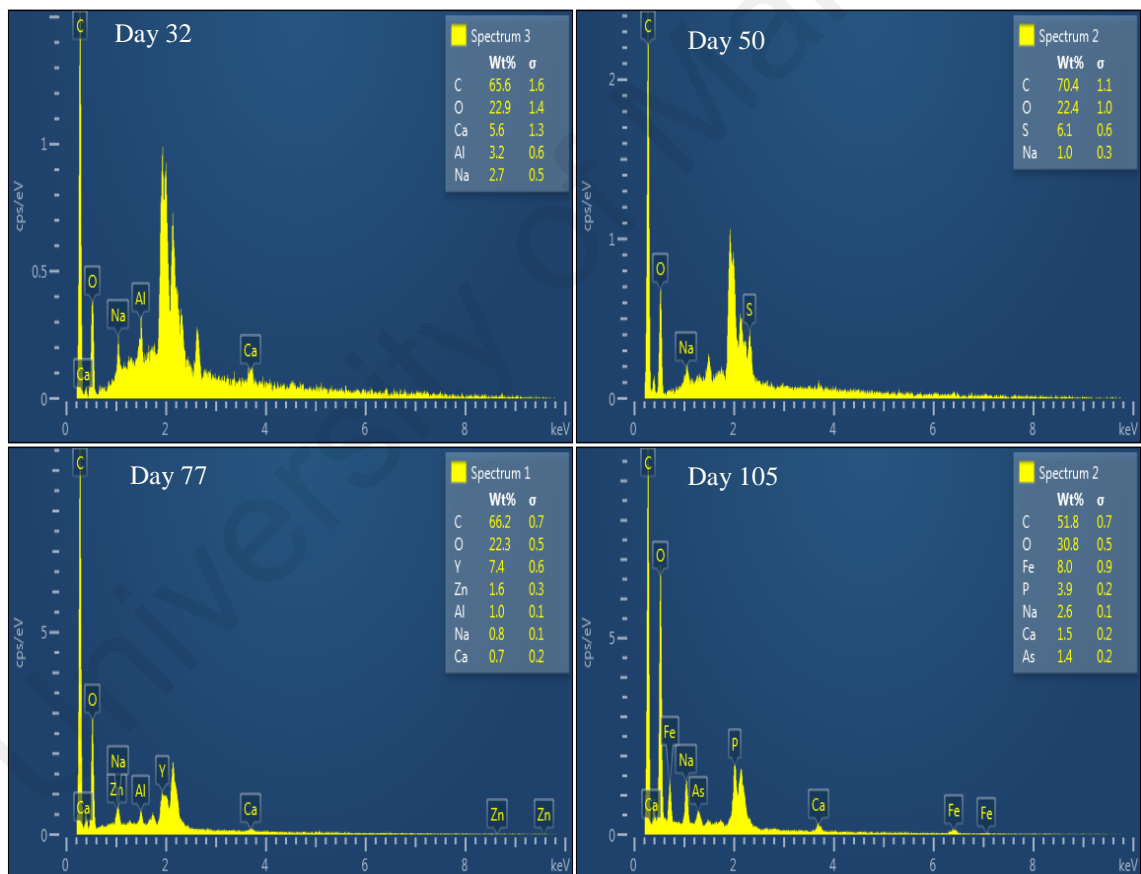


Figure 4.32: localized elementals spectra from EDX analysis for Batch3 on day 32, 50, 77 and 105

Figure 4.33(a) shows the appearance of contrast image, while Figure 4.33(b-e) display fluorescent staining results of whole aerobic granules on day 77 and 105. Fluorescent images were probed at the centre ($-72\mu\text{m}$) of aerobic granules for day 77, and $7\mu\text{m}$ from the centre of aerobic granules for day 105. The thicknesses of whole aerobic granules used for CLSM image analysis on day 50, 77 and 105 were reflected on the length of Z-sectioning as illustrated in Figure 4.33(f). The condition of selected aerobic granules for CLSM image viewing for day 77 was mature aerobic granules with apparent existence of filamentous microorganism protruding from aggregates. Whilst, selected aerobic granules for CLSM image viewing for day were from partial disintegration of aerobic granules on day 91.

Based on the image analysis at different Z-sectioning on day 77, it can be concluded that the core of aerobic granules was formed by protein, whereas the active cells (nucleic acid) and β -D-glucopyranose polysaccharides were also within the core of the granule but to a lesser extent than protein. This finding is consistent with reports by Chen et al. (2007b) and McSwain et al. (2005). Chen et al. (2007b) reported that β -D-glucopyranose polysaccharides are concentrated not only in the outer layer but they spread throughout the granules interior. Meanwhile, McSwain et al. (2005) spotted few signals of active cells from aerobic granule centre and suggested that the sample was either in flocs or small aerobic granules formed when cells and EPS existed together at centre.

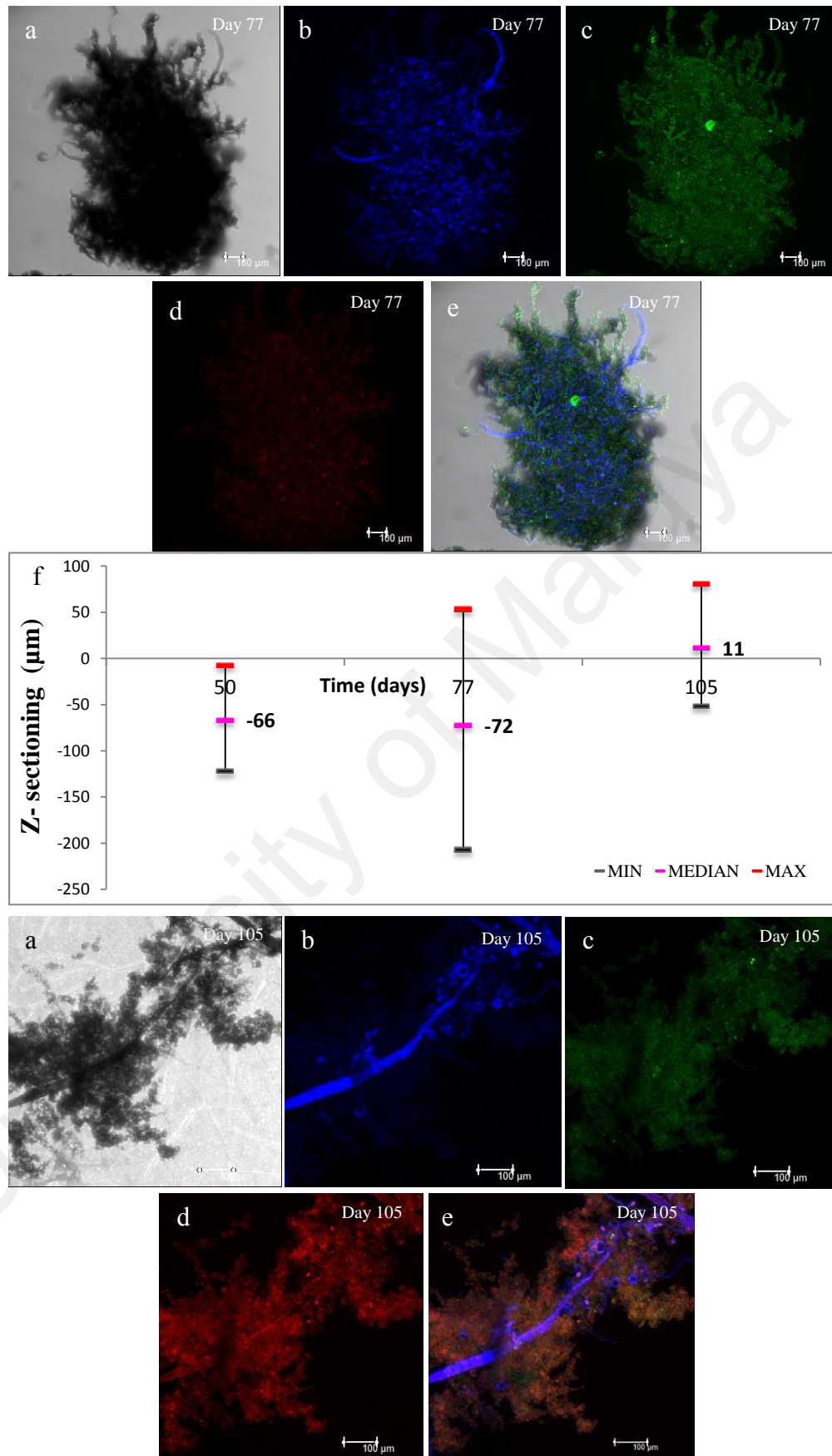


Figure 4.33: CLSM images of Batch3 on day 77 and 105; **a.** contrast images, **b.** β -D-glucopyranose polysaccharides (calcofluor white), **c.** protein (FITC), **d.** nuclei acid (SYTO 63), **e.** overlap images of b-d, **f.** Z-sectioning on whole aerobic granules on day 50, 77 and 105

Zhu et al. (2012b) described a report by Wang et al. (2005) on β -polysaccharides forming a continuous shell and integrated structure that held the soft core of aerobic granules as mesh skeleton which favoured the formation of stable granular structure. This is in conjunction with overlapped images on day 77 which revealed that β -D-glucopyranose polysaccharides were likely to entrench the protein surface with traces of active cell almost completely covered. Whilst, overlapped images on day 105 signified that β -D-glucopyranose polysaccharides were likely to act as the backbone for protein and active cells layer embedment. This observation supported by Adav et al. (2008), in their study revealing large fragments which may have originated from the outer layers of aerobic granules prior to hydrolysis. The β -polysaccharides were likely to form the backbone of a network like outer layer of embedded proteins, lipids, α -polysaccharides and cells, whose elasticity supported granule mechanical stability.

Image analysis at different Z-sectioning on day 50 (image not included) was also similar to day 77. Only protein with few spots of β -D-glucopyranose polysaccharides was present on the overlapped images of day 50. In contrast, overlapped image on day 105 which was probed at 7 μm from the centre of aerobic granules indicated the significant presence of active cells. Further image analysis at different Z-sectioning on day 50, 77 and 105 showed that high fluorescent intensity for active cells was present between β -D-glucopyranose polysaccharides and protein in a very thin layer depending on the thickness and form of aerobic granules. Outer surface and core of aerobic granules were mainly composed of β -D-glucopyranose polysaccharides and protein, respectively.

This study reveals that EPS components can also be qualitatively determined based on correlation between FTIR spectrum and CLSM images. The strong presence of protein marked by typical amide band I at 1637 cm^{-1} was in line with high intensity of fluorescent FITC in the overlapped images on day 50 and 77. The weak vibration from broad phosphodiester bonds were detected at 1263 cm^{-1} , indicating low amounts of nucleic acids (active cells) which was in line with low intensity of fluorescent SYTO 63 on whole aerobic granules except at specific thin layer between β -D-glucopyranose polysaccharides and protein. Bonds vibration for polysaccharides within 1134 to 1137 cm^{-1} range was more intense than phosphodiester bonds, and this was in line with high presence of fluorescent calcofluor white at outer surface as well as core of aerobic granules compared to SYTO 63.

Although EPS components were not quantitatively determined in this study, analysis from FTIR spectrum and CLSM images strongly suggested that protein is the main component that governed the stability of aerobic granules. The result are in agreement with reports by Zheng et al. (2005), Wang et al. (2006) and Zhu et al. (2012b) which suggested high protein/polysaccharide ratio is in positive correlation with the hydrophobicity. In the sense of thermodynamic, an increase in cell hydrophobicity simultaneously causes a decrease in the excess Gibbs energy of the surface, which in turn promotes self-aggregation of cell from liquid phase to form a new solid phase (Liu and Tay, 2002; Liu et al., 2009).

4.4.5 The Diversity in Microbial Community

An analysis of microbial community was performed to demonstrate the evolution of microbial population in aerobic granules at different phases in the formation of aerobic

granules by using PCR-NGS method. In order to demonstrate the evolution of microbial population, a total of 58,679 effective sequencing readings were assigned to known phylum, class, order, family and genus based on Bergey's taxonomy. Analysis was carried out on day 0, 8, 50, 77 and 105, each representing seed, aggregation, stability, disintegration and re-aggregation phase, respectively. Most of the effective sequencing readings were affiliated to 3 major phyla out of 25 detected phyla in total, which were *Proteobacteria*, *Bacteroidetes* and *Firmicutes*. Previous literature reported phyla of *Proteobacteria* (Zhang et al., 2011; Zhao et al., 2013; Zhou et al., 2014), *Bacteroidetes* (Abdullah et al., 2013), *Flavobacterium* (Li et al., 2008) and *Actinobacteria* (Song et al., 2010) were dominant in aerobic granules formation.

Cluster analysis as shown in Figure 4.34 was used to scrutinize the similarity of microbial community that represented different phases in aerobic granules formation. It is noted that *Betaproteobacteria* and *Sphingobacteriia* classes, which belong to the *Proteobacteria* and *Bacteroidetes* phyla, were always dominant throughout the formation period. The rapid increase in total sequences percentage for *Betaproteobacteria* and *Sphingobacteriia* classes from 42% in seed to 74%, 68% and 62% on day 50, 77 and 105, respectively, indicated a significant shift in microbial population. Dominant classes have outcompeted minor classes in which 18% of *Bacilli* classes was markedly existed only on day 8, suggesting that this class is beneficial to the aggregation process at an early stage. *Bacteroidia* and *Nitrospira* classes existed noticeably in seed, with *Flavobacteriia* class increased steadily throughout the formation period. It demonstrates that only certain microbial community is beneficial to aerobic granules formation.

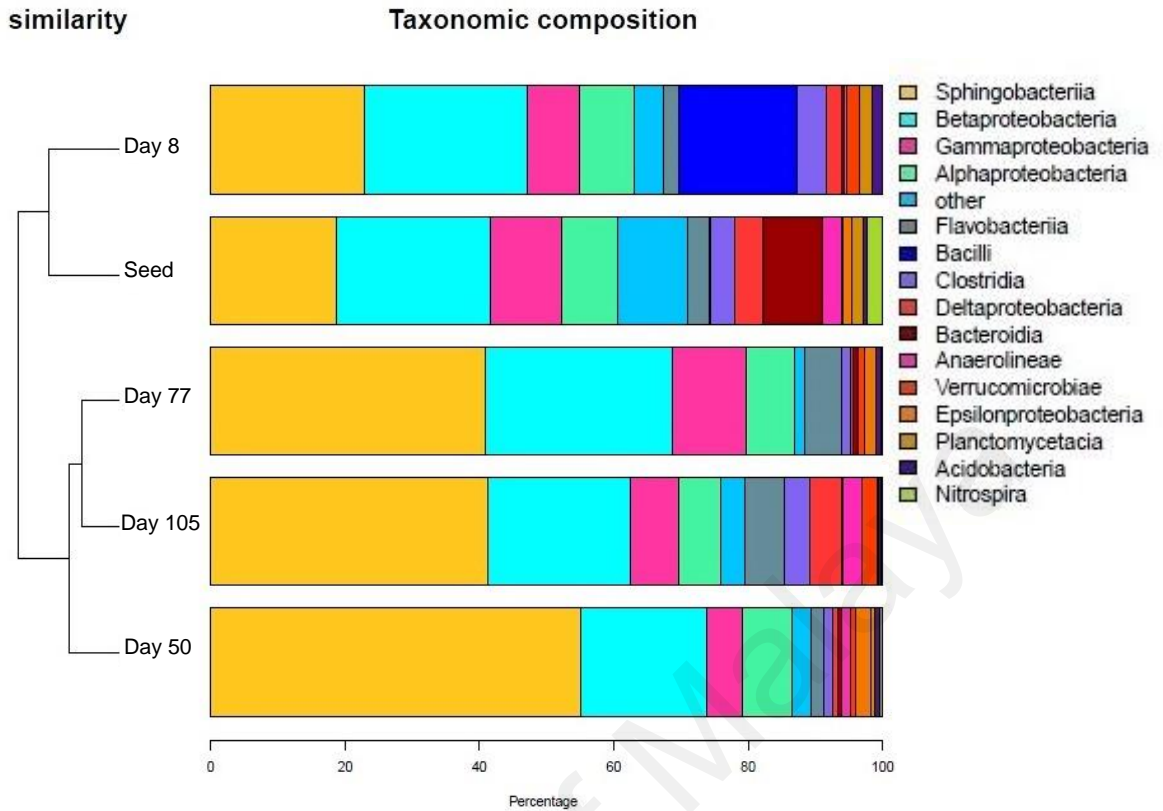


Figure 4.34: Cluster analysis for the first 15 taxonomic classifications from bacterial community of seed, day 8, 50, 77 and 105 at the class level for Batch3

Xie et al. (2014) defined the abundance percentage of a given phylogenetic group with less than 1% of the total sequences in a sample as a minor group. Thus, as shown in Figure 4.35, the taxonomic classification of pyrosequences from bacterial community at genus level revealed that seed contained a greater microbial diversity than aerobic granules. For example, the presence of *Candidatus_vadinBC27*, *unclassified_Rhodocyclaceae* and *Sulfuritalea* genera in seed were over 3% as compared to 1% in aerobic granules which formed afterwards. Except for several dominant genus, most of the microbial community from seed was suppressed to less than 1% during the aggregation, stability, disintegration and re-aggregation phases. *Bacillus* genus was markedly present in aggregation phase (day 8) but almost non-existent in the late formation process, suggesting that this genus was dominant in the small aerobic granules with median size of 99 μm and eventually was eliminated as the aerobic granules size increased.

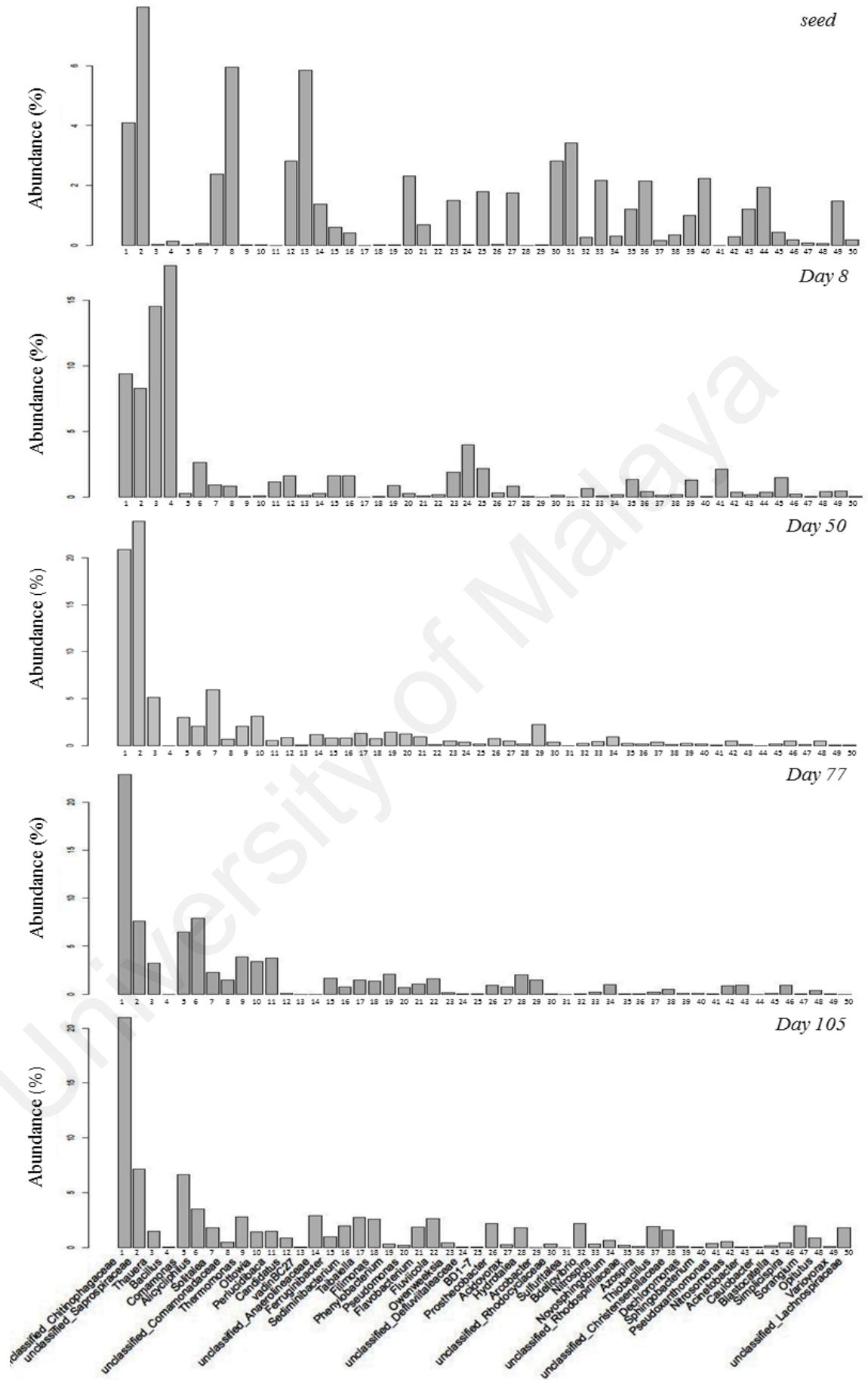


Figure 4.35: Taxonomic classification of pyrosequences from bacterial community of seed, day 8, 50, 77 and 105 at the genus level for Batch3.

Genus of *Thauera* from *Rhodocyclaceae* family also was significantly prevalent on day 8 with nearly 15% abundance, but continued to decrease to less than 5% on day 50 when median aerobic granules size was 336 μm . Afterwards, *Comamonas*, *Alicyclophilus* and *Ottowia* genus from *Comamonadaceae* family increased with the decrease in *Rhodocyclaceae* class on day 50, 77 and 105 with total abundance accounted at 8%, 18% and 10%, respectively. Thus, this highlights the shift in microbial community for denitrification process from *Rhodocyclaceae* to *Comamonadaceae* family was accommodated with changes in aerobic granules size. The result was in agreement with work by Allen et al. (2004) that demonstrated *Thauera* as an aerobic denitrifies and floc-forming bacteria. Whilst, Adav et al. (2009) suggested that the members of *Comamonadaceae* family plays a major role in denitrification process with contribution of polar flagellum of *Comamonas* genus to the stability of aerobic granules (Lv et al. 2013).

Result has confirmed an increasing trend in the dominant abundance of *unclassified_Chitinophagaceae* and *unclassified_Saprospiraceae* from *Sphingobacteriia* class throughout the formation period. Further investigation on the phylogenetic analysis using MEGAN software showed a shift in *Chitinophagaceae* family, from *Ferruginibacter* genus in seed, to *Sediminibacterium* genus on day 8 and *Taibaiella* genus on day 50 and 77, and *Filimonas* genus on day 105. Previous report by Rosenberg et al. (2014) showed that *Sphingobacteriia* class are Gram-negative non-spore-forming bacilli with smooth and convex colonies. In particular, *unclassified_Saprospiraceae* demonstrates the ability for the hydrolysis and utilization of complex organic compounds with the helical gliding strains. Whilst, *unclassified_Chitinophagaceae* are rods cells with rounded corners, called microcysts, despite do not form fruiting bodies like myxobacteria. The closed up morphology image for aerobic granules on day 105

(Figure 4.26d) proved the domination of *unclassified_Chitinophagaceae* genus, where rods cells with rounded or so called microcysts were tightly linked together to form a compact flora structure.

Comparing the result of microbial community in this study with other research works further proves that the dominance of particular microbial is governed by substrate composition (type of wastewater) and concentration (OLR). The dominant microbial in seed will suppress the existence of other species over the formation period and result in low microbial species diversity in mature aerobic granules. A study by Li et al. (2008) confirmed that reactor with high OLR has the lowest microbial species diversity as compared to reactor with low OLR. The diversity and dominance of the microbial species are caused by the physiological characteristics of the microbial itself. Whilst, Zhou et al. (2014) proved that microbial selection pressure is not a prerequisite for aerobic granulation from both the dynamic granulation steps and molecular biology aspects. For example, the domination of *Sphingobacteriia* class in this study is similar with the work by Zhou et al. (2014) on the formation of aerobic granules in sewage. Findings by Adav et al. (2009) and Li et al. (2008) suggested that the aerobic granules cultivated with acetate and glucose as carbon source demonstrates dominance genus of *Zoogloea* and *Flavobacterium*, respectively. Abdullah et al. (2013) claimed the existence of *Propionibacteriaceae* family is associated with the presence of phenolic compounds in palm oil mill effluent.

4.4.6 Advantage of Airlift Reactor

The period to achieve stable condition or mature aerobic granules in airlift with divided draft tubes (SBR3) was shorter compared to bubble column (SBR2). However, since substrate loading rate is distinctively different in both reactors, direct comparison on the effect of flow pattern cannot be made. Report by Liu and Tay (2007) had concluded that aerobic granules cultivated in bubble column showed instability at the same SUAV with that of airlift reactor and no big difference of average granule size could be observed in both reactors. Considering the satisfactory removals performance in low OLR (average of 0.54 kg CODs/m³ d) and SUAV (0.7 cm/s) as compared to previous research works (De Kreuk and van Loosdrecht, 2006; Liu et al. 2007; Ni et al. 2009; Su et al. 2012; Wagner et al. 2013; and Wang et al. 2009) on aerobic granulation in sewage, the use of divided draft tubes has been proven to be beneficial.

The typical size of mature granules developed in sewage based on previous research works was around 630 to 1110 µm depending on selection of operating conditions. Whilst, the size of mature aerobic granules during stability phases in this study was around 500 µm and could reach 1273 µm. Although EPS components were not quantitatively determined in this study, analysis from FTIR spectrum and CLSM images strongly suggested that protein as the main component that governed the stability of aerobic granules. Result was in agreement with report by Wang et al. (2006), Zheng, Yu and Sheng (2005), and Zhu et al. (2012a) which suggested high protein/polysaccharide ratio was in positive correlation with the hydrophobicity. In the sense of thermodynamic, an increase in cell hydrophobicity simultaneously causes a decrease in the excess Gibbs energy of the surface, which in turns promotes self-

aggregation of cell from liquid phase to form a new solid phase (Liu et al., 2009; Liu & Tay, 2002).

This study supports the advantage of using airlift reactor with divided draft tubes (SBR3) in optimizing the performance of reactor with low H/D ratio. The main conclusions derived from the obtained result are as follows:

- i. Aerobic granules were successfully developed in SBR3 with low H/D ratio and under variable OLR of 0.26 to 0.81 kg CODs/m³ d and low SUAV of 0.7 cm/s. The used of divided draft tubes has successfully expedited the formation period of mature aerobic granules within 67 days compared to 89 days in SBR2 with equal H/D ratio.
- ii. The final aerobic granules size obtained on day 105 was in the range of 326 to 728 µm and can be considered as smaller compared to that of reported by other researches utilizing sewage as substrate which was around 750 to 800 µm, and can reach up to 2000 µm. This is mainly attributed to short flowing trajectories in SBR3.
- iii. Small size of aerobic granules in the range of 333 to 750 µm was relatively stable. This is based on CLSM analysis that showed active cells, β-D-glucopyranose polysaccharides and protein that existed together at aerobic granules core.
- iv. The NGS analysis result indicated the shift in microbial community performing denitrification process from *Rhodocyclaceae* to *Comamonadaceae* class was accommodated with the changes in aerobic granules size from 147 µm to more than 336 µm.

- v. The dominant microbial in seed suppressed the existence of other species over the formation period and resulted in low microbial species diversity in mature aerobic granules.

4.5 Reformation and Stability of Long Term Storage AGS (Batch4)

The stability of aerobic granules can be defined as the ability of microbial granules to resist hydrodynamic and mechanical shear force (Sheng et al. 2010). Whereas, the state of aerobic granule stability were measure based on bioactivity, microbial community, EPS composition and distribution, and granular characteristic (Chen et al. 2007a). Based on result and discussion in Section 4.2 to 4.4, it is noteworthy that aerobic granule sludge could be formed under a variety of operating conditions. Nevertheless, there are numerous report had marked the loss of aerobic granules stability in long term operation as the bottleneck that limits it practical application in the field of biological wastewater treatment particularly sewage. A few recent achievements on successful operating conditions strategized to enhance the stability of aerobic granules were mostly focusing on mature aerobic granules instead of the development process.

Thus, this work aims to demonstrate the reformation process of aerobic granules after subjected to long term storage in liquid at 5 °C, under low SUAV of 1.33 cm/s and OLR variations. The reformation indices of aerobic granules were determined based on the physical size, biomass production and reactor performance evaluation. The characteristic of AGS in terms of EPS components and distribution, microbial community structure, and morphology were monitored throughout the reformation process to demonstrate the stability state of aerobic granules at different phase of

reformation indices. This will benefit in validating the reformation ability of aerobic granules and to demonstrate that system operation was not in total failure conditions when aerobic granules started to disintegrate due to the variations in OLR.

4.5.1 The Reformation Indices for Batch4

During long term-operation, applying appropriate operational conditions like selective sludge discharge (Zhu et al., 2013a), settling time (Liu & Tay, 2012), aerobic-anaerobic phase (Isanta et al., 2012), shear force (Chen et al., 2007a) and cycle time (Liu & Tay, 2008) are necessary to ascertain granular sludge stability. Results from these authors proved that the aerobic granules size plays an important role in exhibiting its stability. Figure 4.36 exhibits the evolution of inoculated seed on day 0 to mature aerobic granules on different days of formation period. The deviation in aerobic granules size at different days was reflected on the length of the box plot was presented in Figure 4.37.

As showed in day 0, the inoculate seed that previously kept in cold room at temperature of 5 °C for 8 months were aerobic granules with median size of 245 µm and fuzzy structure. Disintegration of aerobic granules occurred within 24 h of start-up had resulted in formation of pin flocs started from day 1. By the 8th day, the median size of pin flocs promptly increased from 13 to 326 µm. Although aerobic granules size continued to increase, most of the sludge was washed out from SBR from day 1 due to the excessive disintegration process resulting in a rapid decrease in MLSS from 0.45 g/L to 0.1 g/L (Figure 4.38). A sharp decrease in CODs influent from 231 mg/L on day 8 to 93 mg/L on day 13 has resulting in low MLSS and MLVSS.

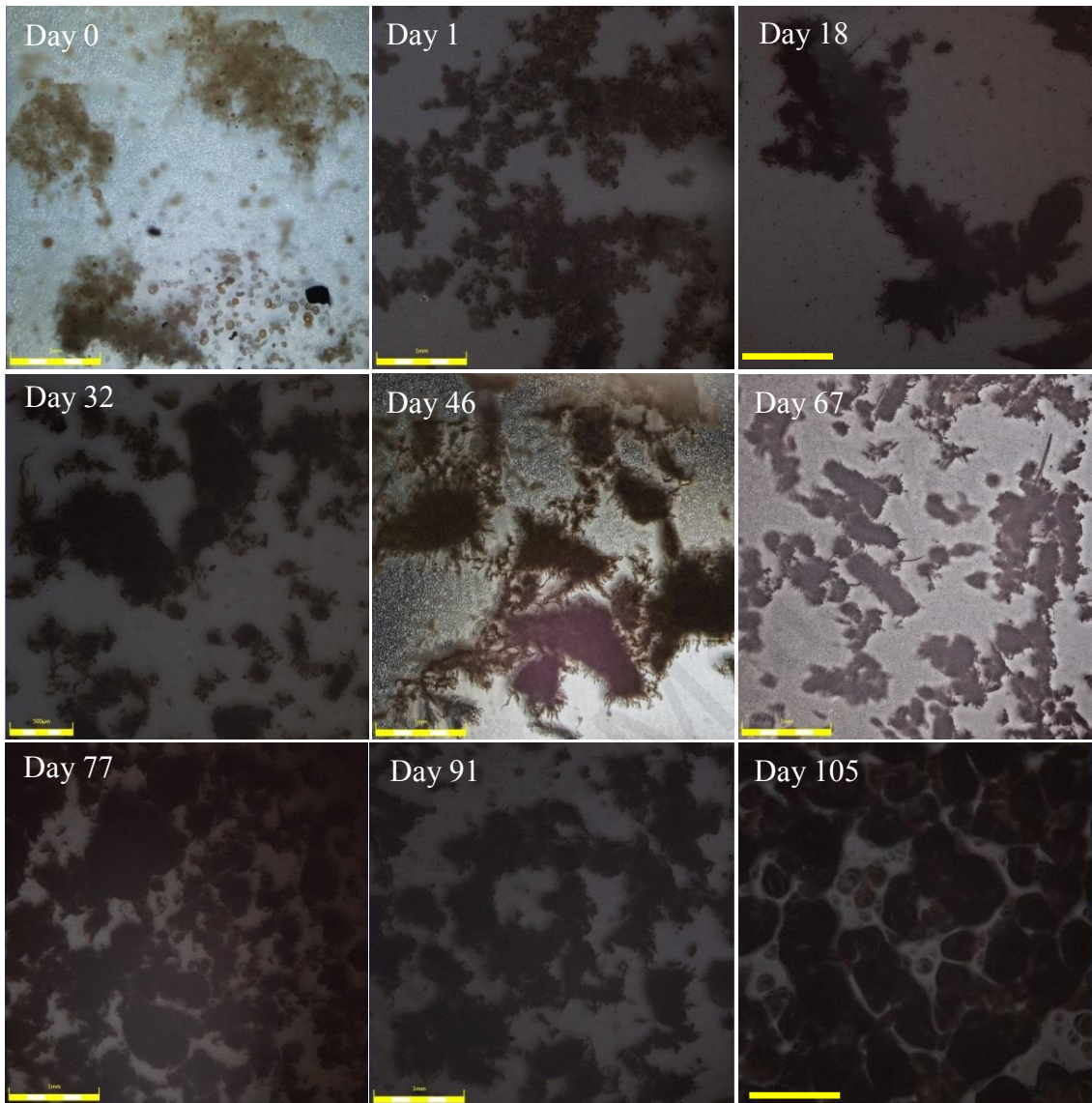


Figure 4.36: Evolution of aerobic granules in SBR4. Bar = 1 mm for day 0, 1, 67, 77, 91, and 105. Bar = 500 μm for day 18, 32 and 46 for Batch4

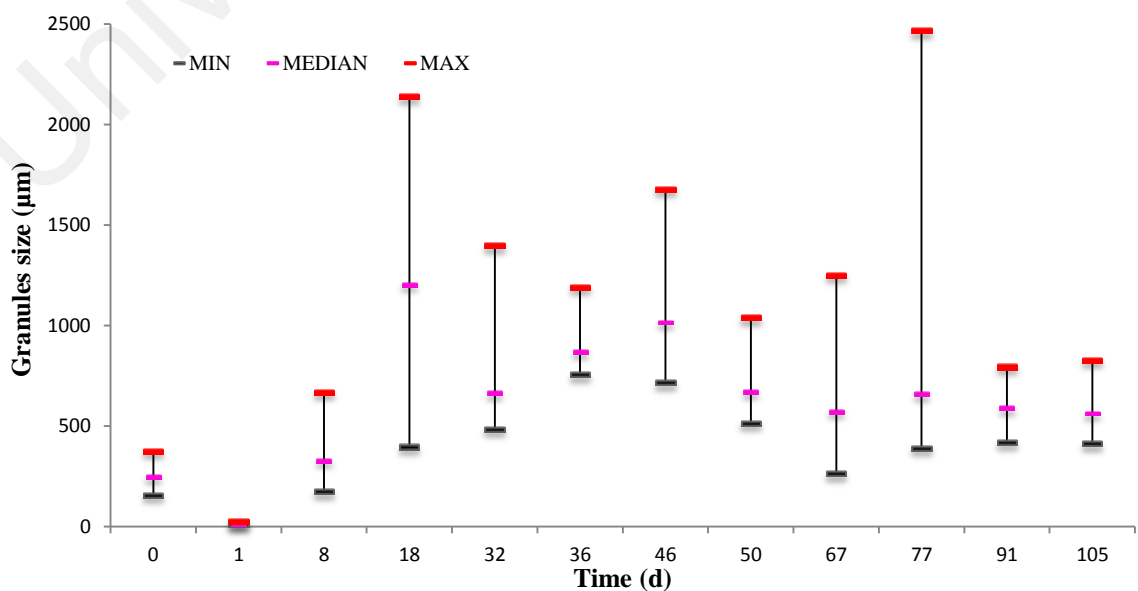


Figure 4.37: Deviation in aerobic granules size for Batch4

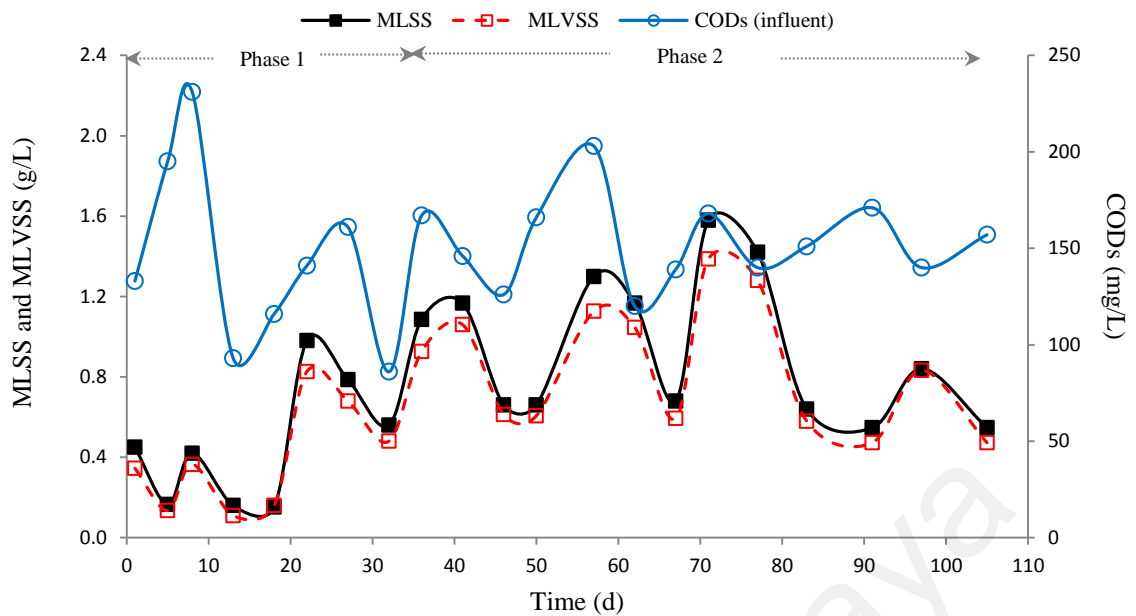


Figure 4.38: Profile of biomass (MLSS and MLVSS), OLR and CODs influent for Batch4

On day 18, aerobic granules exhibited a fluffy structure without indistinct shape and the pattern continued until day 32. It is apparent that deviation of box plot on day 18 which was between 395 to 2137 μm compared to 482 to 1396 μm on day 32 has indicated that the densified process for fluffy aerobic granules has started. The Results are in line with the pattern of SVI profile (Figure 4.39) that illustrated small deviation between 5 min intervals of settling time after 27 days of formation process. The MLSS decreased when the CODs influent decreased from 161 mg/L on day 27 to 86 mg/L on day 32, hence, this leads to a reduction of 50% of SVI_{30} on day 36 and 41. This suggests that the small aerobic granules with minimum size of 482 μm were predominant in the reactor on day 32 and were washed out afterwards due to the substrate limitation. According to Wang and Liu (2008), decreasing the cycle time or increasing the volumetric exchange rate will ensure a high availability of substrate for an AGS system subjected to low strength wastewater or run over a long time. Thus, cycle time was adjusted from 4 h to 3 h (Phase 2) after analysis on day 33 with other operating conditions remained unchanged.

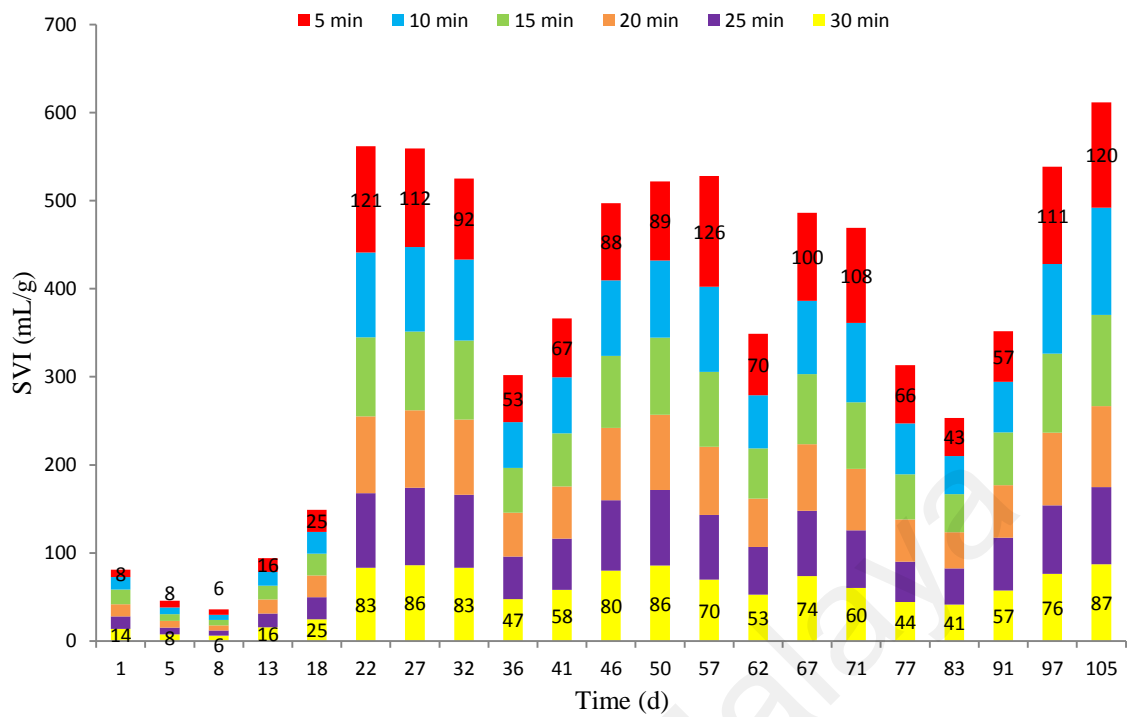


Figure 4.39: Profile of SVI at 5 min intervals of settling time for Batch4

Afterwards, predomination of aerobic granules with size within 714 to 1014 μm range on day 46 exhibited a starting point on formation of a sturdy structure and oval shape. Microscopic image of aerobic granules on day 46 also indicated an apparent existence of filamentous microorganism protruding from aggregates and similar pattern was exhibited on day 50 and 67 when CODs influent was reduced to 144 mg/L. This Result is in line with review by Martins et al. (2004) on aerobic granules that grow in a low substrate concentration. Filamentous microorganism will have a higher specific growth rate rather than floc forming bacteria due to the higher surface area to volume (A/V) ratio for filamentous microorganism. Peyong et al. (2012) and Martins et al. (2003) indicated that the compact granules subjected to low substrate conditions will end up with loose structure and the existence of filamentous. This might be attributed to the nature of filamentous that excellently fit in loose structure leading to the development of irregular shape.

It appears that some aerobic granules were floating and entrapped into effluent discharge point during feeding time on day 57. In turns, SVI_{30} was noticeably reduced from 70 mL/g on day 57 to 53 mL/g on day 62. This is expected due to the hydrolysis effect of anaerobic core since day 46. According to Tay et al. (2002), hydrolysis of anaerobic core during disintegration of mature aerobic granules produces gases and organics acids which are entrapped within sludge layer at static condition. Moreover, long feeding time of 30 min may create an anoxic condition inside reactor and helps to govern the denitrification process which releases nitrogen gas within the sludge layer. From observation, aerobic granules started to float after 10 min of feeding time. Similar floating event also occurred on day 71 resulting in decrease of SVI_{30} and MLSS on day 77. Hence, in order to avoid the floating event, the feeding time was changed from 30 to 10 min on day 82. Settling time was also changed from 30 to 15 min on day 82 after considering SVI profile for settling properties of aerobic granules and high CODs influent.

Despite the floating event, aerobic granules size continued to increase on day 77 indicating the occurrence of re-aggregation process. The changes in feeding and settling time contributed to a sharp decrease of MLSS on day 83, from 1.42 g/L on day 77 to 0.64 g/L. However, MLSS continued to increase afterwards. Large aerobic granules with maximum size of 2463 μm on day 77 were disintegrated due to the change in operating conditions which led to the fraction of aerobic granules with 400 to 800 μm size range on day 91 and 105. From the results, MLSS was only reduced to 0.55 g/L in line with the decrease in CODs influent and change in operating conditions. It is suggested that aerobic granules system was able to retain sufficient amount of biomass or active microbial to recover from shock loading and change in operating conditions within a short time. Compare to Control Batch, Batch1, Batch2 and Batch3 AGS,

biomass profile analysis showed that showed Batch4 was highly dependent on CODs influent attributed by size and the maturity state of aerobic granules itself. The results are in accordance to Li et al. (2008a), a study on mass transfer resistance in aerobic granules that result in a significant drop in microbial activity and growth rate, where larger aerobic granule will be affected more severe.

As showed in Figure 4.40, F/M ratio did not substantially increase with significant changes in CODs influent and MLSS between days 40 to 83. This indicate that SBR system was in stable conditions and comprised of mature aerobic granules that easily adapt and stabilize in variable substrate concentration and changes of operating conditions. In addition, SRT during stable conditions was between 5 and 10 days which are suitable for the aerobic granules system. Zhu et al. (2013a) mentioned that the reactor performance will deteriorate if SRT is beyond the range of 5 to 10 days. Rapid granulation was successfully obtained within 8 days of reformation process with the use of aerobic granules as seed instead of activated sludge that being kept at temperature of 5 °C for 8 months.

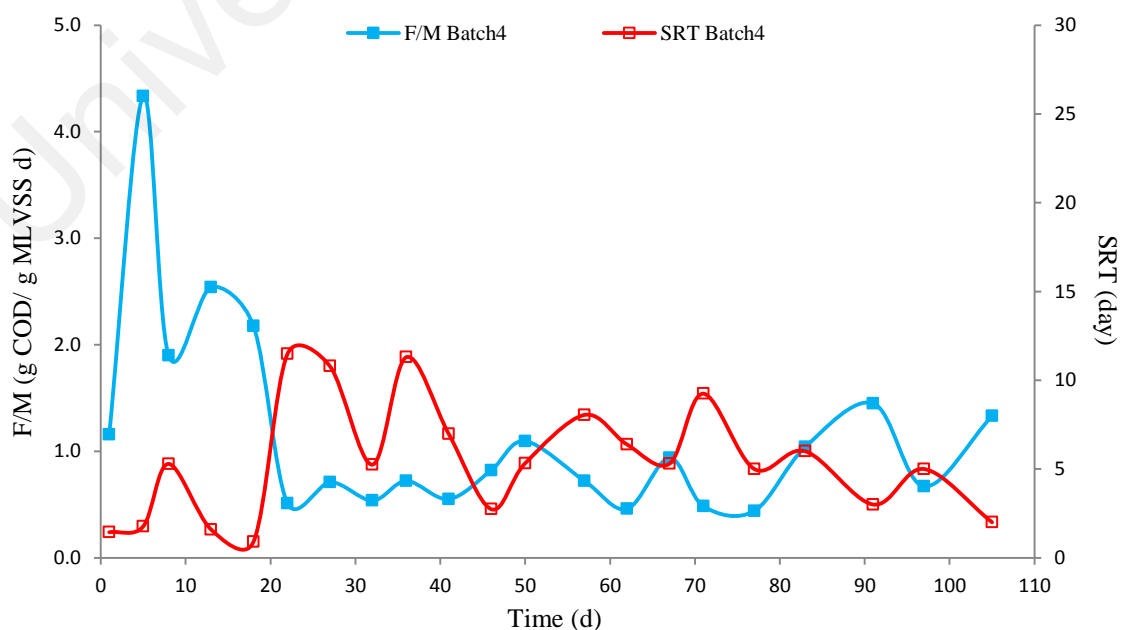


Figure 4.40: Profile of F/M ratio and SRT for Batch4

In this study, the Microscopic observation of aerobic granules size evolution is accordance to the dynamic granulation model developed by Zhou et al. (2014). The model helps to explain the enormous deviation in aerobic granules size obtained in this study which might be caused from the self-aggregation of aerobic granules and re-granulation of the detached bioflocs, newborn cells and crushed aged aerobic granules. The final Aerobic granules size obtained in this study was in the range of 410 to 825 μm and were comparable with results demonstrated by other researcher that using sewage as substrate. The typical size of mature granules developed in sewage were assumed to be around 750 to 800 μm , and can reach up to 2000 μm , depending on the selection of operating conditions. It can be concluded that the formation indices of aerobic granules developed using sewage will be far more complex than in synthetic wastewater. The variations in OLR will intrusive the formation process particularly during low OLR and resulting in longer period to achieve mature aerobic granules or full granulation of biomass in the reactor. The aerobic granules produced exhibited a tinny oval or rod shape form instead of desired sphere shaped due to the occurrence of substrate limitation before aerobic granules was well developed.

4.5.2 Reactor Performance

During the reformation process, the performances of Batch4 AGS in terms of CODs, SS and nitrogen removal were determined. Figure 4.41 and Figure 4.42 depict the influent and effluent concentration as well as the removal efficiency of CODs, SS and ammonium during the reformation process. During the first 18 days, aerobic granules were in aggregation stage and poor CODs and SS removals were expected. Negative removal for SS at an early stage indicated that the biomass was excessively being washed out from reactor. Afterwards, Batch4 performance has improved

continuously. At stable condition, the highest removal of CODs, SS and ammonium were marked at day 57 with 69%, 72% and 83%, respectively. As for the concentration of nitrite (Figure 4.42e) and nitrate (Figure 4.42f) in the effluent during stable periods, average values of 17 mg/L and 11 mg/L were obtained, respectively.

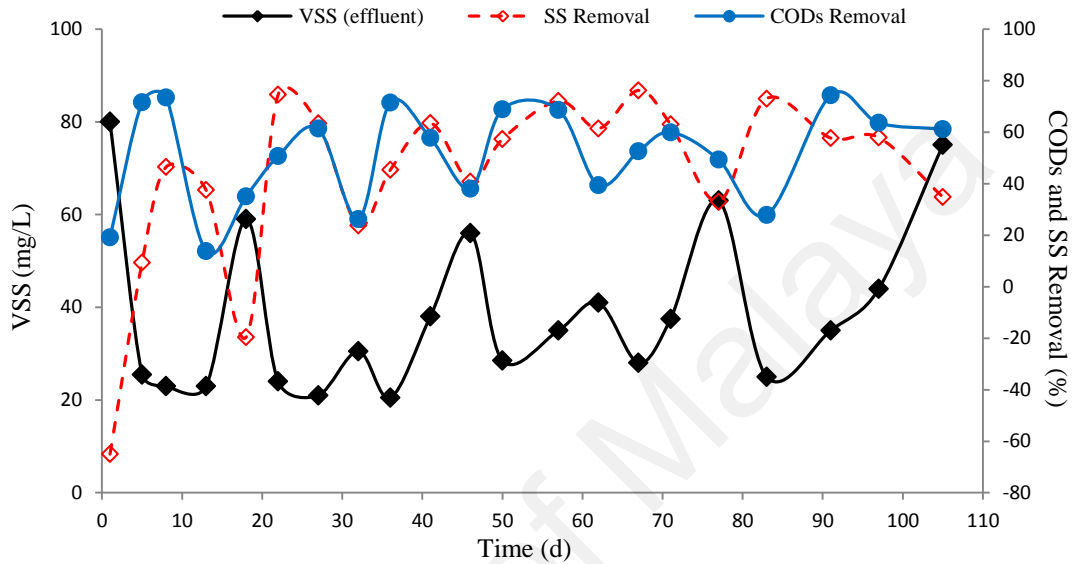


Figure 4.41: VSS effluent, SS and CODs removal for Batch4

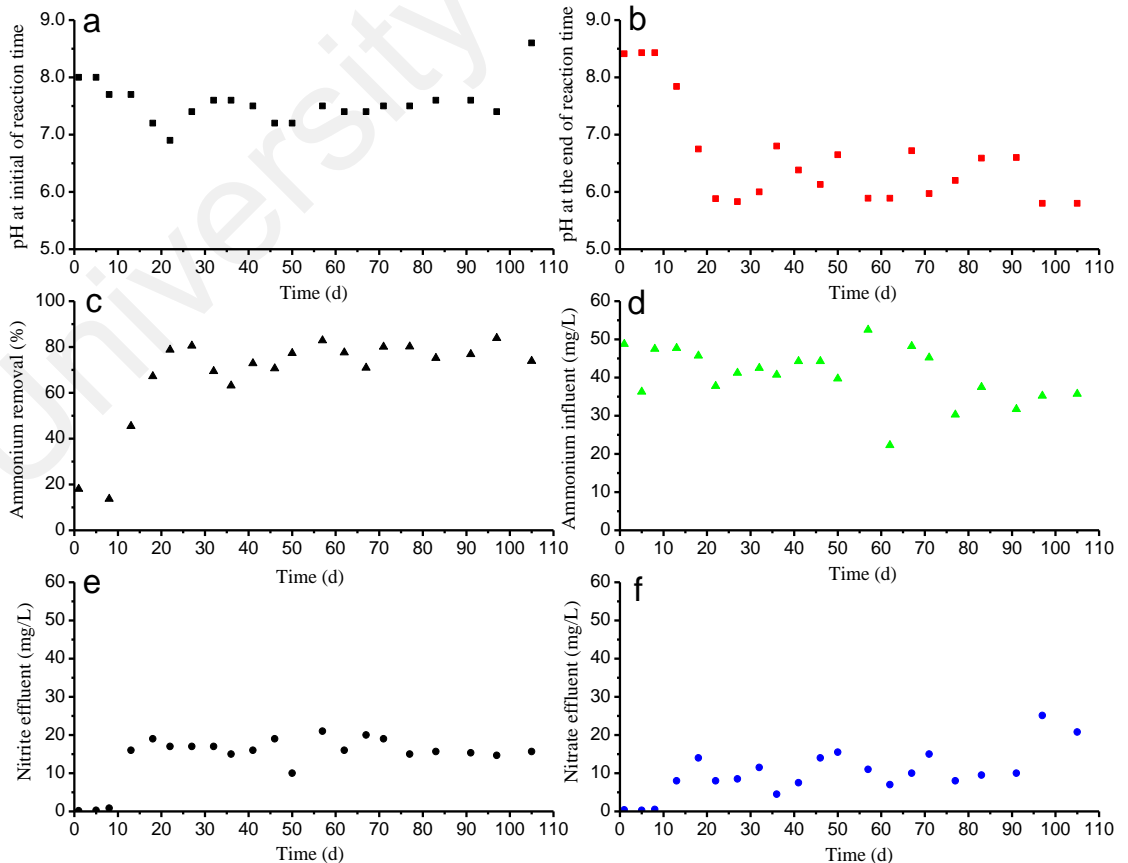


Figure 4.42: Profile of pH, ammonium, nitrite and nitrate effluent for Batch4

Throughout the reformation process, it was noted that the partial nitrification of ammonium had resulted in accumulation of nitrite and nitrate in effluent. Low DO did not contribute to partial nitrification of ammonia since minimum reading for DO at the beginning and the end of reaction time was over 7.10 mg/L. Besides, pH at the initial of reaction time (Figure 4.42a) was observed to be above 6.9, indicating that pH was not the main reason for partial nitrification. Thus, as has been discussed in Section 4.4.3, partial nitrification occurred due to inhibition of NOB by high level of FA. High FA which was due to low COD/ammonia ratio will inhibit both heterotrophic and nitrifying bacteria (Wang et al., 2007b; Yang et al., 2004) and resulted with pH decreased. Hence, low CODs removal and decrease in pH to 5.8 at the end of reaction time (Figure 4.42b) was expected since COD/ammonium ratio during Phase 1 and Phase 2 were 3.4 and 3.9, respectively. In addition, Li et al. (2008a) stated that the diffusion of substrate will become a limiting factor for aerobic granular sludge formation under low substrate conditions, and tends to decrease the substrate removal rate. Indeed, CODs removal was at its lowest when CODs influent decreased sharply on days 13, 32, 46, 62 and 77.

4.5.3 Characteristic of AGS at Different Phase of Reformation Indices

Characterization of aerobic granules characteristic is crucial to understand the intermolecular interaction or so called physicochemical and microbiological interactions of different tropic bacteria that keep the aerobic granules in stability. Mechanism and the current state of aerobic granules performance can be described if the intermolecular interaction was well identified.

4.5.3.1 Composition and Distribution of EPS in Batch4

Although the effects of EPS on biofilm and anaerobic granule are well known, it was only in 2001 the first report about the role of EPS in the formation and stability of aerobic granules was discussed by Tay et al. (2001b). The following reports by Wang et al. (2005) and McSwain et al. (2005) proved that EPS contributes significantly to the stability of microbial granules. Since then, intensive research effort was studied to characterize the role of EPS in the formation and stability of aerobic granules. Characterization of chemical functional groups is important in defining the active chemical functional groups that interact with each other by hydrogen bonding, electrostatic and ionic attractive forces for the stability of EPS matrix. The variations in functional groups of aerobic granules EPS are characterized by analyzing the FTIR spectrum from day 0 to day 105 as depicted in Figure 4.43. The characteristic assignment for FTIR spectrum is based on the studies by Schmitt and Flemming (1998), Omoike and Chorover (2004) and Badireddy et al. (2010).

The presence of protein in all EPS samples was confirmed by strong vibration of amide band I at 1638 cm^{-1} and weak vibration of amide band II at 1505 cm^{-1} . The amine band I (1630 to 1640 cm^{-1} range) was specifically associated with C=O stretching vibration of β -sheet in secondary protein structures that favored bio flocculation (Badireddy et al., 2010; Zhu et al., 2012a). Whilst weak signal from amide band II indicated that C=O stretching was predominant compared to C-N stretching, N-H bending and O=C-N bending. The functional group of polysaccharides within 1134 to 1136 cm^{-1} range also appeared in all EPS sample. According to Omoike and Chorover (2004), bands between the range of 900 to 1200 cm^{-1} is a result of bonds vibration of polysaccharides as well as DNA/RNA that is associated with vibrational stretching of

O-H and C-O (Zhu et al., 2012a). Weak vibrations from broad phosphodiester bonds were detected on day 50, 77 and 105 within 1259 to 1263 cm^{-1} range indicating that the amounts of nucleic acids in samples were low. Badireddy et al. (2010) showed that broad ester band between 1270 to 1230 cm^{-1} helps to promote cell aggregation, adhesion and biofilm integrity. The FTIR spectrum also confirmed a strong presence of hydroxyl at 3303 cm^{-1} .

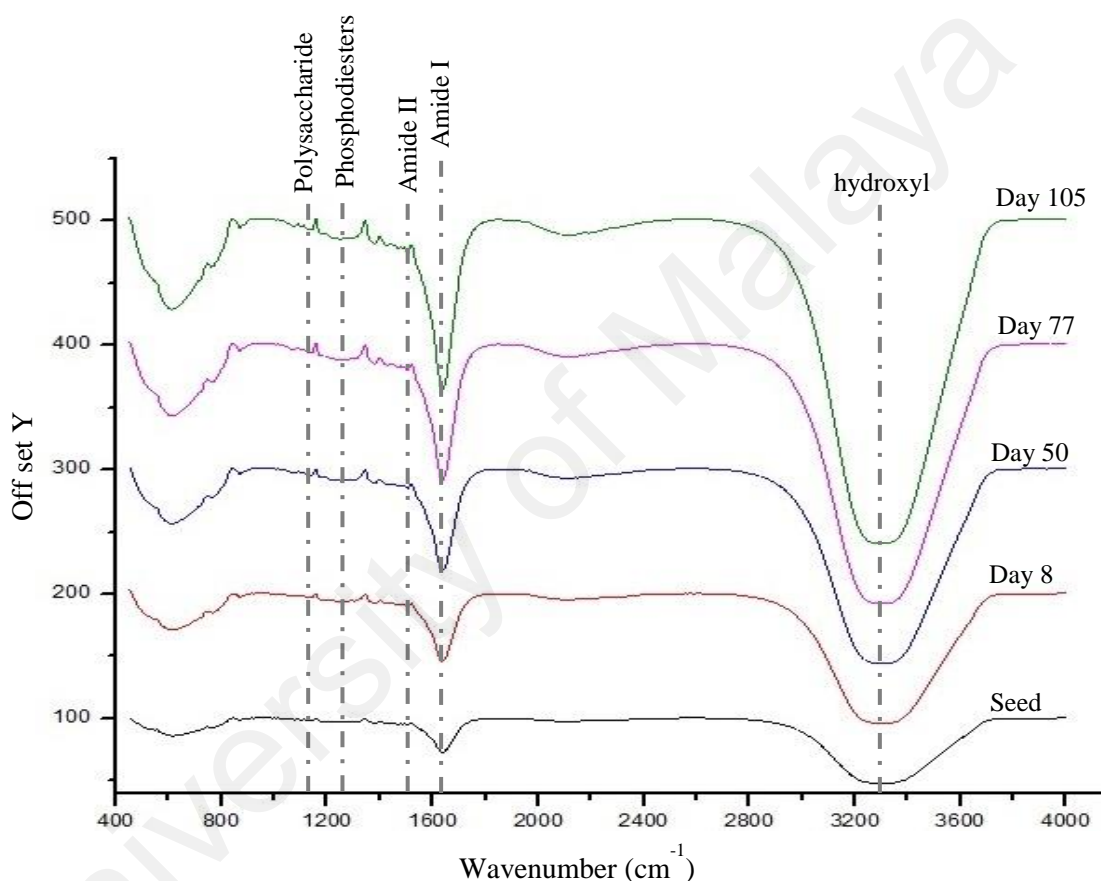


Figure 4.43: FTIR spectrum of freezing EPS from day 0 (seed) to 105 for Batch4

Compared to the seed, FTIR transmittance intensities of amide band I, amide band II and polysaccharides in aerobic granules appeared to be increased along with the re-formation period. This can be used as an indicator for improving the stability properties of aerobic granules upon formation period. Compounds such as proteins, polysaccharides and alcohol that carries functional groups of C=O, C-O and O-H, helps to promote microorganism aggregation (Badireddy et al., 2010) by means of ionic and electrostatic attractive forces and hydrogen bonding, for the stability of EPS matrix

(Flemming & Wingender, 2010). On the other hand, functional groups like carbonyl, carboxylate, acetal, or hemiacetal and hydrocarbons hindered the aggregation process (Badireddy et al., 2010). Apart from that, Van der Waals interaction that exists between the EPS components also helps to serve for EPS stability. As a result, the ionisable groups presented on cell aggregates surface will decrease, and subsequently lower the polar interaction of EPS with water molecules to promote cell hydrophobicity (Wang et al., 2006). Thus, thermodynamically, an increase in cell hydrophobicity simultaneously causes a decrease in the excess Gibbs energy of the surface, which in turn promotes self-aggregation of cells from liquid phase to form a new solid phase (Liu et al., 2009; Liu & Tay, 2002).

EDX analysis on localized spectrum showed that the total percentage of carbon and oxygen elements for seed was nearly 90%. Increase in presence of elements like iron, sodium, calcium, aluminium and zinc afterwards suggested the existence of ionic attractive forces between dissociated C=O and divalent metal cations (Ca^{2+} , Fe^{2+} , etc.), and -H bonding between O-H and monovalent cations (K^+ , Na^+) in aerobic granules. Combining the results of FTIR and EDX prove that the intermolecular interaction assisted the EPS stability.

In this study, multicolor fluorescence experiments were conducted to investigate the distribution of EPS and cells in the granules. Figure 4.44 exhibited the appearance of contrast image (a) and fluorescent staining results (b-e) of whole aerobic granules on day 0 (seed), 50 and 105. Fluorescent images for Figure 4.44 were probed at the centre for day 0 (7.8 μm) and day 50 (14 μm), and 6.3 μm from the centre for day 105. The thickness of whole aerobic granules used for CLSM image analysis was reflected on the length of Z-sectioning as illustrated on Figure 4.45.

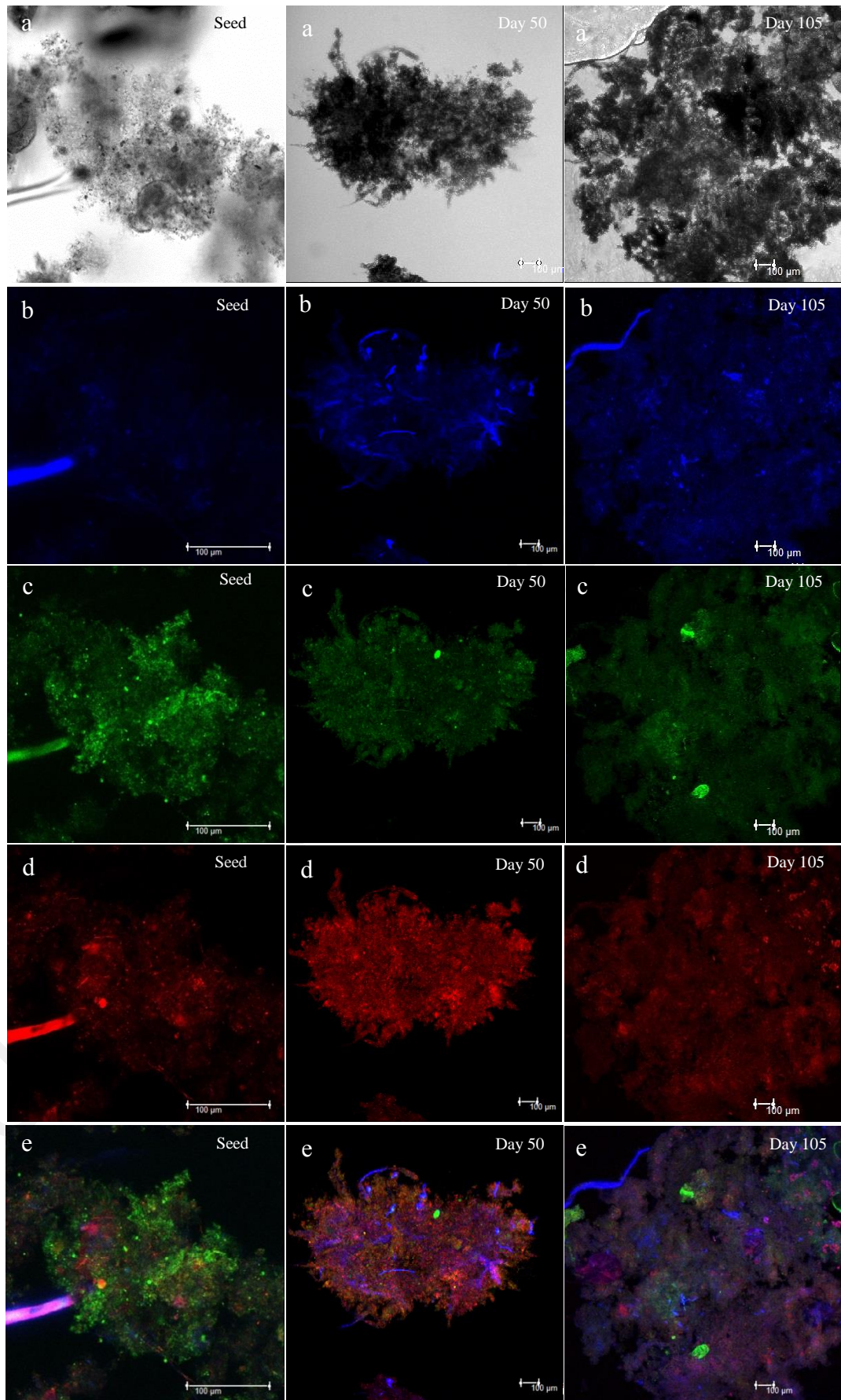


Figure 4.44: CLSM images of Batch4 on day 0 (seed), 50 and 105; **a.** contrast images, **b.** β -D-glucopyranose polysaccharides (calcofluor white), **c.** protein (FITC), **d.** nuclei acid (SYTO 63), **e.** overlap images of b-d.

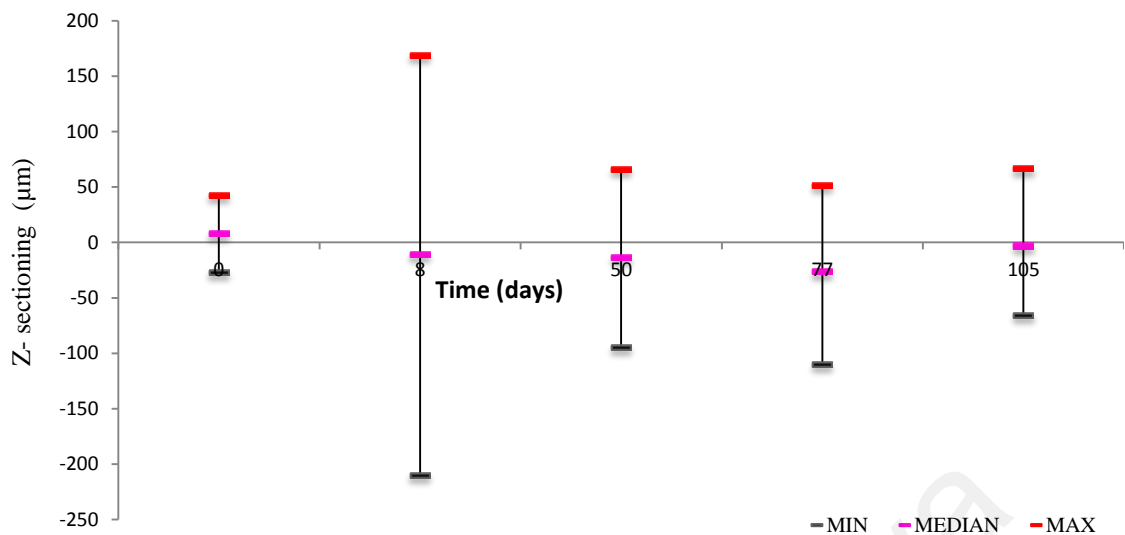


Figure 4.45: Z-sectioning on whole aerobic granules on day 0 (seed), 8, 50, 77 and 105 for Batch4

As shown in contrast image (a), a long storage of aerobic granules at 5 °C may have contributed to rarefy structure for seed (day 0). In contrast, aerobic granules on day 50 and 105 exhibited dense structure. Image analysis at different Z-sectioning on day 0 and 50 exhibited distribution of β -D-glucopyranose polysaccharides throughout the entire aerobic granules, while aerobic granules core was composed of protein and active cells (nucleic acid). Image analysis at different Z-sectioning on day 105 showed that the high fluorescent intensity for protein and active cells was located within 56 μ m from the outer surface. The thickness of protein and active cells layer was around 7 μ m with β -D-glucopyranose polysaccharides was distributed throughout the entire aerobic granules. From observation, the fluorescence intensity of β -D-glucopyranose polysaccharides was higher in core layer compare to outer layer for all aerobic granules tested.

These results are consistent with report by Chen et al. (2007c) and McSwain et al. (2005). Chen et al. (2007c) reported that β -D-glucopyranose polysaccharides was not concentrated only in the outer layer but was spread throughout the granules interior. Whilst, McSwain et al. (2005) spot few signals of active cells from aerobic granule centre and suggesting that the sample was either in flocs or smaller aerobic granules

formed when cells and EPS existed together at centre. Indeed, as previously showed in Figure 4.37, the average size for aerobic granules on day 0, 50 and 105 were less than 700 μm and can be classified as small. Contrast image on day 50 (a) was in conjunction with the microscope images for aerobic granules on day 46 to 67 in which the apparent existence of filamentous microorganism protruding out from dense aggregates was due to the low CODs influent. The overlap images on day 50 (e) further revealed that protein and active cell surface were likely entrenched by β -D-glucopyranose polysaccharides in order to avoid disintegration of aerobic granules. This is confirming the remarked by Zhu et al. (2012b) based on the report by Wang et al. (2005) for β -polysaccharides which had formed a continuous shell and integrated structure that held the soft core of aerobic granules as mesh skeleton that favours the formation of stable granular structure. Similar to FTIR spectrum result, the fluorescence intensities of calcofluor white, FITC and SYTO 63 in aerobic granules also increased along with the re-formation period.

4.5.3.2 Role of Microbial Community and Morphology Change

Analysis on microbial community demonstrated the evolution of microbial population in aerobic granules at different reformation phase using PCR-NGS method. In order to demonstrate the evolution of microbial population, 55,495 total effective qualifies sequences were assigned to known phylum, class, order, family and genus based on Bergey's taxonomy system. Analysis was carried out on day 0, 8 and 50 to represent seed, aggregation and disintegration phase while day 77 and 105 denoted re-aggregation phase. Most of the sequence reads were affiliated to 2 major phyla out of 25 detected phyla in total, namely *Proteobacteria* and *Bacteroidetes*. The result was consistent with a study conducted by Zhao et al. (2015) who report *Proteobacteria* and

Bacteroidetes as two predominant flora that have excellent adaptation in response to changes of the external environment.

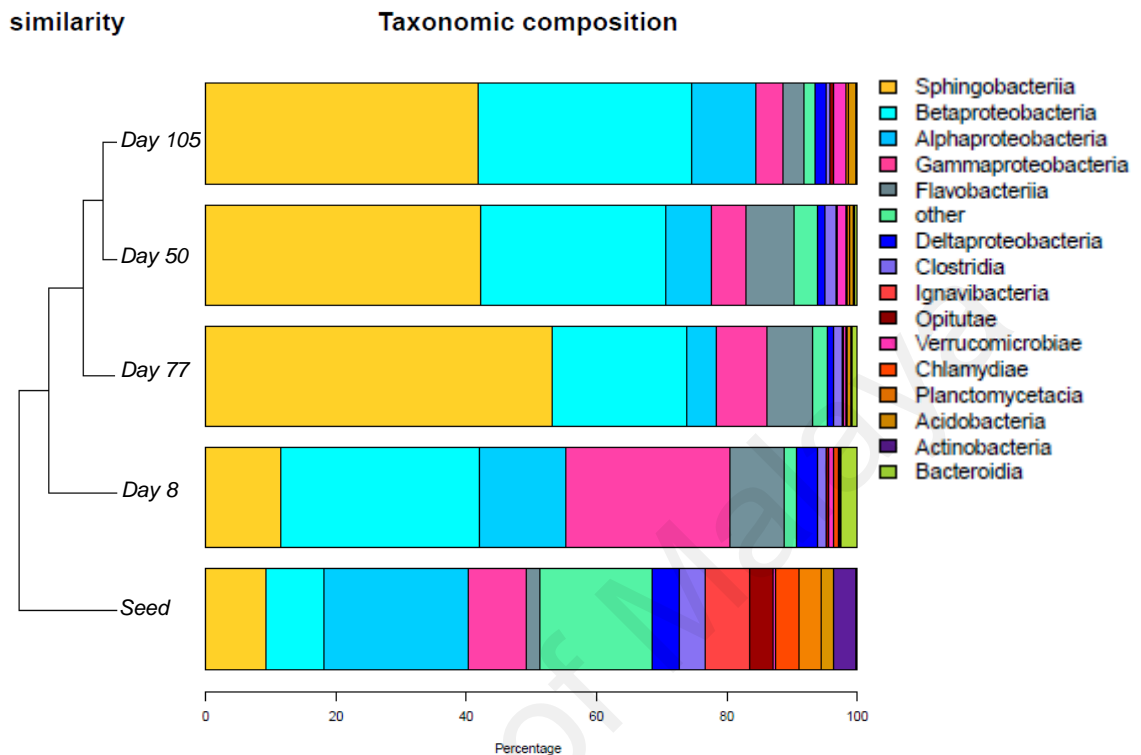


Figure 4.46: Cluster analysis for the first 15 taxonomic classifications from bacterial community of seed, day 8, 50, 77 and 105 at the class level for Batch4

The similarity of microbial community at class level from day 0 (seed) to the end of re-formation process was showed on Figure 4.46. In Figure 4.46, *Betaproteobacteria* and *Sphingobacteriia* which belong to *Proteobacteria* and *Bacteroidetes* phyla dominated after 8 days of formation process, although they were not the dominant groups in the seed. Total sequences percentage for the first 5 taxonomic classifications (*Sphingobacteriia*, *Betaproteobacteria*, *Alphaproteobacteria*, *Gammaproteobacteria* and *Flavobacteriia*) from *Proteobacteria* and *Bacteroidetes* phyla indicate a shift in microbial domination in seed from 52% to 86%, 92%, 94% and 93% on day 8, 50, 77 and 105, respectively. While, *Gammaproteobacteria* was subdominant class on day 8 with sequences percentage of 25% and promptly decrease to 10% on day 105, suggesting that this class only beneficial at an early stage of

aggregation process. Guo et al. (2011) supported the statement by Yang et al. (2004), that the domination of certain microbial groups in formability of AGS was due to the specific culture condition required in biogranulation.

At genus level, the pyrosequencing taxonomic classification of bacterial community (Figure 4.47) revealed that seed and aerobic granules on day 8 contained a greater microbial diversity compare to the develop aerobic granules on day 50, 77 and 105. Except for several dominants genus (*unclassified_Chitinophagaceae*, *unclassified_Saprospiraceae*, *Alicyclophilus* and *Comamonas*), most of the genus existed in seed and day 8 were suppressed to less than 1% of abundance sequences. Xie et al. (2014) had reported that the abundance sequences of a given phylogenetic group with less than 1% of the total sequences in a sample as a minor group and not significant.

Ignavibacterium which belong to *Chlorobi* phyla appeared to be the most dominant in seed and followed by *Candidatus*, *Caulobacter* and *unclassified_Chitinophagaceae*, which accounted for 6.7%, 5.6%, 4.7% and 4.3% of the abundance sequences, respectively. *Ignavibacterium* is known as facultative anaerobic organism suggesting its survival as heterotrophic bacteria (Rosenberg et al. 2014) during long term storage. Other genus like *Caulobacter* and *Nitrospira* (3.4%) also were significantly detected only in seed showing that this genus could thrive under comparatively resource scarcity (Rosenberg et al. 2014) due to long term storage. The abundance of *Perlucidibaca*, *Acinetobacter* and *Pseudomonas* genus from *Gammaproteobacteria* class was dominant in day 8, while it was almost non-existent in late reformation process.

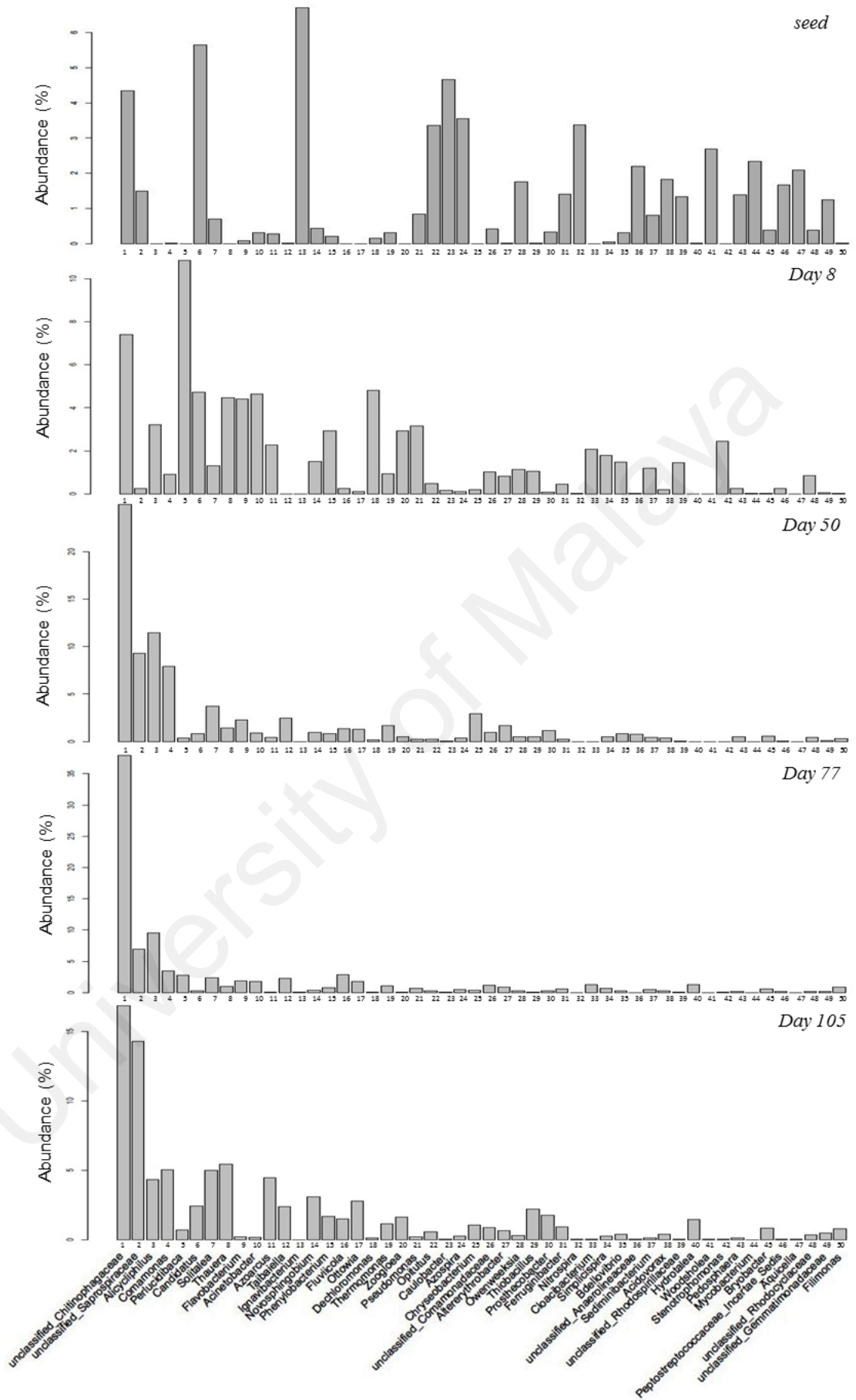


Figure 4.47: Taxonomic classification of pyrosequences from bacterial community of seed, day 8, 50, 77 and 105 at the genus level for Batch4

Result in Section 4.4.5 remarked that the shift in microbial community for denitrification process from *Rhodocyclaceae* to *Comamonadaceae* family can accommodate with change in aerobic granules size. Indeed, the total abundance of *Thauera*, *Dechloromonas* and *Zoogloea* genus which belong to *Rhodocyclaceae* class was prevalent on day 8 with 12.4 % when median aerobic granules size was 326 μm and reduced to less than 3% on day 50 and 77 when median aerobic granules size was more than 600 μm . *Comamonas* and *Alicyclophilus* genus from *Comamonadaceae* increased with a decreased in *Rhodocyclaceae* on day 50 and 77 with total abundance accounted at 19.8% and 13%, respectively. As fraction of aerobic granules size on day 105 ranging from 410 to 825 μm , *Rhodocyclaceae* and *Comamonadaceae* family are nearly in balance with 7.2% and 9.5% of the total abundance. Thus, it can be concluded that the shift in microbial community from *Rhodocyclaceae* to *Comamonadaceae* family for denitrification process can accommodate with changes in aerobic granules size.

This result supported the work by Allen et al. (2004), which demonstrated that *Thauera* as aerobic denitrifiers and floc-forming bacteria that could secrete EPS. Result from this study also suggesting that the given stability period was within day 46 to 83 and contributed by *Comamonas*. This is based on findings by Lv et al. (2013) on re-cultivation of drying aerobic granules, where polar flagellum of *Comamonas* might contribute to the stability of aerobic granules. Results suggested that the dominance of particular bacteria was not dependable on the period of aerobic granules formation process. Instead, the formation of aerobic granules was governed by the substrate composition and concentration by selecting and enriching different microbial species and thus, influencing the size, morphology and kinetic behaviour of aerobic granules (Moy et al., 2002).

The result confirmed an increasing trend in the dominant abundance of *unclassified_Chitinophagaceae* and *unclassified_Saprospiraceae* from *Sphingobacteriia* class throughout the formation period. Further inquiry on the phylogenetic analysis using MEGAN software showed a shift in *Chitinophagaceae* family, which is from *Ferruginibacter* genus in seed, to *Sediminibacterium* genus on day 8 and *Taibaiella* genus afterwards. *Solitalea* genus which belongs to *Sphingobacteriaceae* family was clearly present on day 105 with total abundance of 5%. Previous report by Rosenberg et al. (2014) showed that *Sphingobacteriia* class are Gram-negative non-spore-forming bacilli with smooth and convex colonies. In particular, *unclassified_Saprospiraceae* had demonstrated ability for the hydrolysis and utilization of complex organic compounds with the helical gliding strains. Whilst, *unclassified_Chitinophagaceae* are rods cells with rounded corners and had been called microcysts despite do not formed fruiting bodies like myxobacteria.

Guo et al. (2011) confirmed that the hydrophobic nature of *Sphingobacteriales*, *Rhodocyclaceae* and dominant bacterial groups that will exhibit intra-group diversity in their cell hydrophobicity and functions. Thus, it is anticipated that the dominance of *Sphingobacteriales* and *Rhodocyclaceae* help to increase cell hydrophobicity, hence promote self-aggregation of cell from liquid phase to form a new solid phase. Comparing the result of microbial community in this study with other research works proves that the dominance of particular bacteria is govern by substrate composition (type of wastewater) and concentration (OLR). For example, the domination of *Sphingobacteriia* class in this study is similar with the work by Zhou et al. (2014) on formation of aerobic granules in sewage. Finding by Adav et al. (2009) and Li et al. (2008b) suggested that the aerobic granules cultivated with acetate and glucose as carbon source demonstrated dominancy genus of *Zoogloea* and *Flavobacterium*,

respectively. Whilst, granules cultivated in swine slurry characterized by high carbon to nitrogen ratio (1.9 – 9.4 g COD_s/ g N) was mainly composed by genus *Nitrosomonas* (Morales et al., 2013). These diversity and dominancy of the bacteria species are caused by the physiology characteristic of bacteria itself. The study by Zhou et al. (2014) also has confirmed that microbial selection pressure was not a prerequisite for aerobic granulation from both the dynamic granulation steps and molecular biology aspects

Figure 4.48 shows the morphological transformation from seed to aerobic granules at different days of re-formation phase which were aggregation (day 32), disintegration (day 50) and re-aggregation (days 77 and 105). The close up images was taken between 5 to 50 µm image scales. Seed with excessive cell lysis displayed long limper structure which obviously indicated effect from long term storage at cold temperature. An apparent existence of filamentous microorganism protruding from aerobic granules that has ready to form oval shape was shown on day 32 and this pattern continued to day 50. The outer appearance of the aerobic granules started to form a smooth surface as showed on day 77 and at 105th day, the cauliflower-like structure was observed. Similar structure was observed by Liu et al. (2004b) and Lemaire et al. (2008) when aerobic granules was developed at substrate COD/N ratio less than 5 and 6. The close up images demonstrated the appearance of protozoa vorticella (seed and day 50) and ciliates (day 77) which has previously proven to be beneficial to the aerobic granules formation by Li et al. (2013). A close up image on day 77 demonstrated peritrichous ciliate stalks serve as backbone in the granule-forming process since the bacteria used them as a substratum to grow, and this is supported by Weber et al. (2007). Weber et al. (2007) and Lemaire et al. (2008) had remarked that ciliates contributed to reduce of SS effluent and turbidity by removing certain amount of non-flocculated bacteria and fine suspended biomass particle.

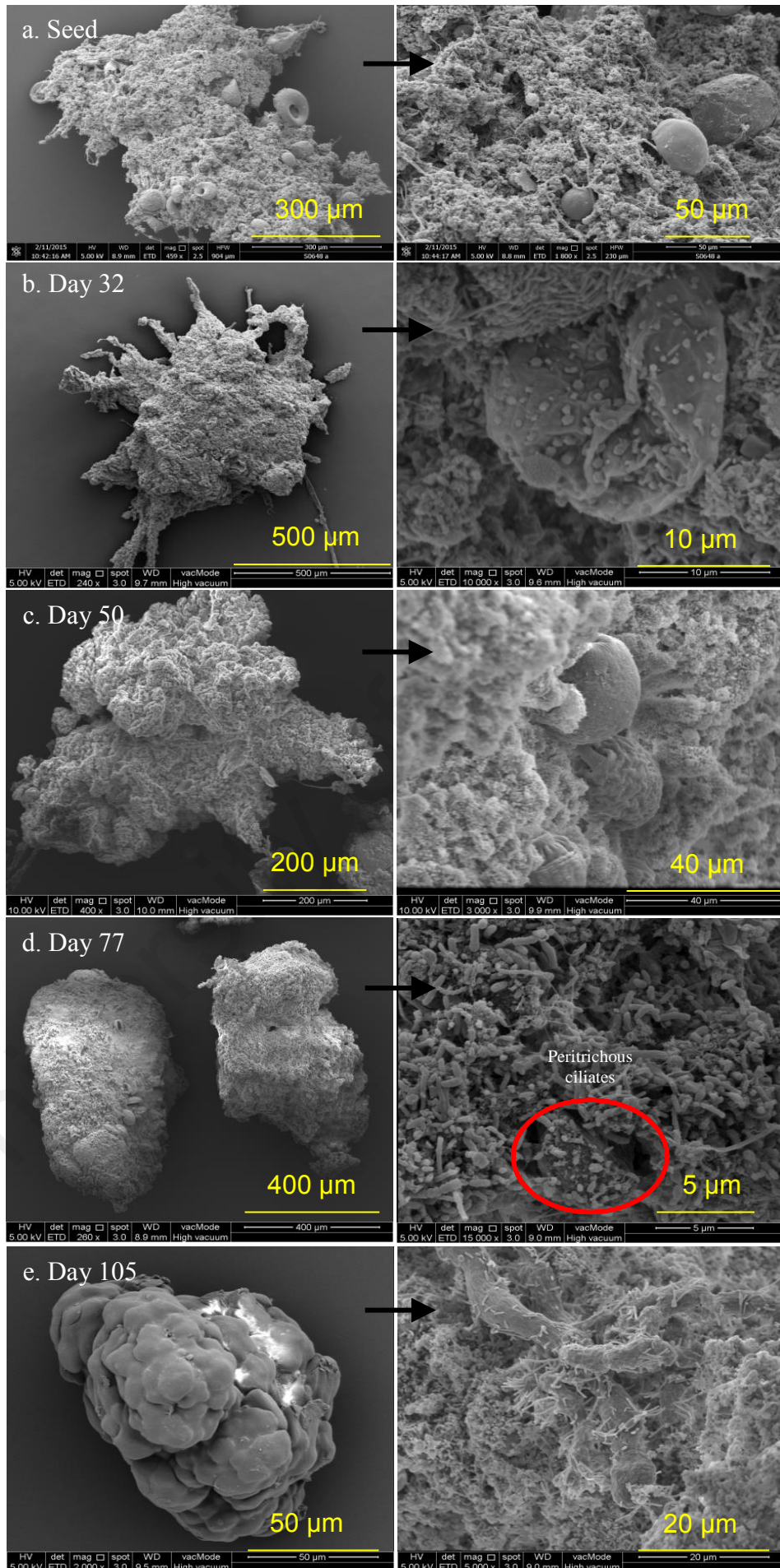


Figure 4.48: FESEM images of aerobic granules for Batch4

4.5.4 Summary on Result Analysis

Aerobic granular sludge was successfully developed under OLR of 0.26 to 0.81 kg CODs/m³d and low SUAV of 1.33 cm/s. Low CODs/N ratio of 3.4 for phase 1 and 3.9 for phase 2 contributed to the inhibition of pollutant removals with the highest CODs, SS and ammonium removals that were marked at day 57 with 69%, 72% and 83%, respectively. Variation in OLR has intruded the development of aerobic granules and resulting in longer period to achieve the stable conditions, which is after 40 days of formation process. Analysis from CLSM considered the aerobic granules with size of 700µm as small and relatively stable. This is contributed by β-D-glucopyranose polysaccharides that spread throughout the granules interior. The NGS analysis result indicated that the shift in microbial community from *Rhodocyclaceae* to *Comamonadaceae* class for denitrification process was accommodated with the changes in the aerobic granules size from 326 µm to more than 600 µm.

4.6 Bioactivity of Aerobic Granules

The stability of aerobic granules can be defined as the ability of microbial granules to resist hydrodynamic and mechanical shear force (Sheng et al., 2010). The state of aerobic granule stability is measured in terms of bioactivity, microbial community composition and aerobic granules characteristic (Chen et al., 2007a). Currently, comprehensive review and research works with regard to aerobic granules characteristic and microbial community are well reported. However, there are only a few reports concerning bioactivity of aerobic granules in treating real wastewater, especially sewage. Bioactivity of aerobic granules often has been quantified based on

SOUR and biokinetic parameters. Biokinetic parameters help to describe the rate of substrate utilization and biomass production or growth by microbial (Muda et al., 2011), which are important to process design and optimization of system performance (Chen et al., 2008). As mentioned in Section 4.2 to 4.5, the observed performance of aerobic granules from different batches was influenced greatly by OLR and reactor H/D ratio. Therefore, this section aims to determine the relationship between change in kinetic coefficients with OLR and reactor H/D ratio. Result presented for each batch was selected at conditions when aerobic granules system was in a steady state

4.6.1 Development of Kinetic Equation for Biokinetic Parameters

The proposed equations for substrate utilization and microbial growth below are based on the study conducted by Han and Levenspiel (1988), Kaewsuk et al. (2010), Liu et al. (2005a), Metcalf and Eddy (2004) and Okpokwasili and Nweke (2005). Under steady state, the mass balance for substrate utilization in SBR can be expressed as:

$$r_{su} = \frac{dS}{dt} \quad \text{Equation 4.1}$$

Equation 4.1 can also be expanded as:

$$r_{su} = \frac{dS}{dt} = -\frac{Q(S_o - S_e)}{V} = -\frac{(S_o - S_e)}{\tau} \quad \text{Equation 4.2}$$

where r_{su} represent substrate utilization rate (mg CODs/L d), Q = influent flow rate (L/d), V = reactor working volume (L) S_o = influent substrate concentration (mg CODs/L), S_e = effluent substrate concentration (mg CODs/L) and τ = hydraulic retention time (d).

Based on the assumption that the rate of substrate (sewage) utilization is generally proportional to the biomass concentration and dependent on substrate

concentration in bioreactor characteristics (first order reaction), Equation 4.2 can also be expressed using modified Monod equation as:

$$\frac{dS}{dt} = -\frac{kSX}{K_s+S} \quad \text{Equation 4.3}$$

where S represents concentration of substrate in reactor (mg CODs/L), X = biomass concentration in reactor (mg MLVSS/L), k = maximum specific substrate utilization rate (mg CODs/mg VSS d) and K_s = half saturation coefficient (mg CODs/L).

Substituting Equation 4.2 into Equation 4.3:

$$U = \frac{(S_o - S_e)}{\tau X} = \frac{kS}{K_s + S} \quad \text{Equation 4.4}$$

where U represents specific substrate utilization rate (mg CODs/mg VSS d). In double reciprocal form Equation 4.4 can be changed to the following form:

$$\frac{\tau X}{(S_o - S_e)} = \frac{K_s}{k} \frac{1}{S} + \frac{1}{k} \quad \text{Equation 4.5}$$

A liner plot of $(\tau X/S_o - S_e)$ versus $1/S_o$ yields a positive slope of K_s/k and intercept of $1/k$. Thus, K_s and k can be obtained.

Under steady state, the mass balance for microbial growth in SBR can be expressed as:

$$r_g = \frac{dX}{dt} \quad \text{Equation 4.6}$$

Equation 4.6 can also be expended as:

$$r_g = \frac{dX}{dt} = \frac{Q(X_o - X_e)}{V} \quad \text{Equation 4.7}$$

where r_g represent microbial growth rate (mg VSS/L d), Q = influent flow rate (L/d), V = reactor working volume (L), X_o = influent biomass concentration (mg VSS/L) and X_e = effluent biomass concentration (mg VSS/L).

The relationship between rate of microbial growth and rate of substrate utilization in SBR can be expressed as:

$$r_g = -Yr_{su} - k_d X \quad \text{Equation 4.8}$$

Substituting Equation 4.7 into Equation 4.8, we obtain:

$$\frac{Q(X_o - X_e)}{VX} = Y \frac{(S_o - S_e)}{\tau X} - k_d \quad \text{Equation 4.9}$$

where Y represents synthesis yield coefficient (mg VSS/mg CODs), K_d = endogenous decay coefficient (1/d) and X = biomass concentration in reactor (mg MLVSS/L). The inverse of the term on the left-hand side of Equation 4.9 is defined as sludge retention time (SRT). Thus, Equation 4.9 can be written as:

$$\frac{1}{SRT} = Y \frac{(S_o - S_e)}{\tau X} - k_d \quad \text{Equation 4.10}$$

A liner plot of $1/SRT$ versus $(S_o - S_e/\tau X)$ yields a positive slope of Y and intercept of k_d . Thus, k_d and Y can be obtained. Maximum specific microbial growth rate (μ_{max}) can be determined from multiplication between k and Y .

4.6.2 Determination of Process Kinetic Coefficients

In this study, steady state period is defined as a condition in which SBR system was consists of mature aerobic granules that could easily adapt and stabilize in variable substrate concentration and changes in operating parameters. Result from MLSS, F/M ratio and quality of effluent were used as benchmark to determine steady state period. Equations 4.5 and 4.10 were used to compute the kinetic coefficients of k , K_s , Y , K_d and μ_{max} during steady state through plotted linear graph as shown in Figure 4.49 and Figure 4.50, and result is presented in Table 4.3.

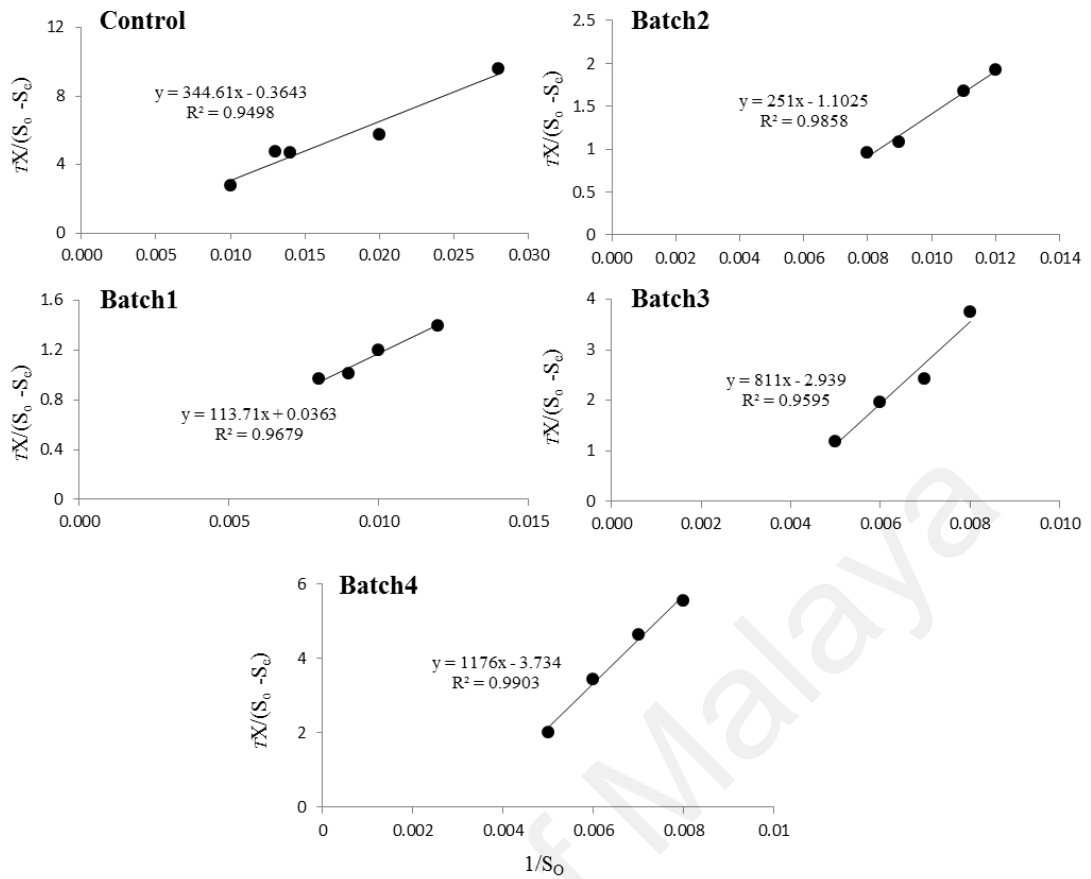


Figure 4.49: Linear plot of substrate utilization for determination of k and K_s coefficient during steady state.

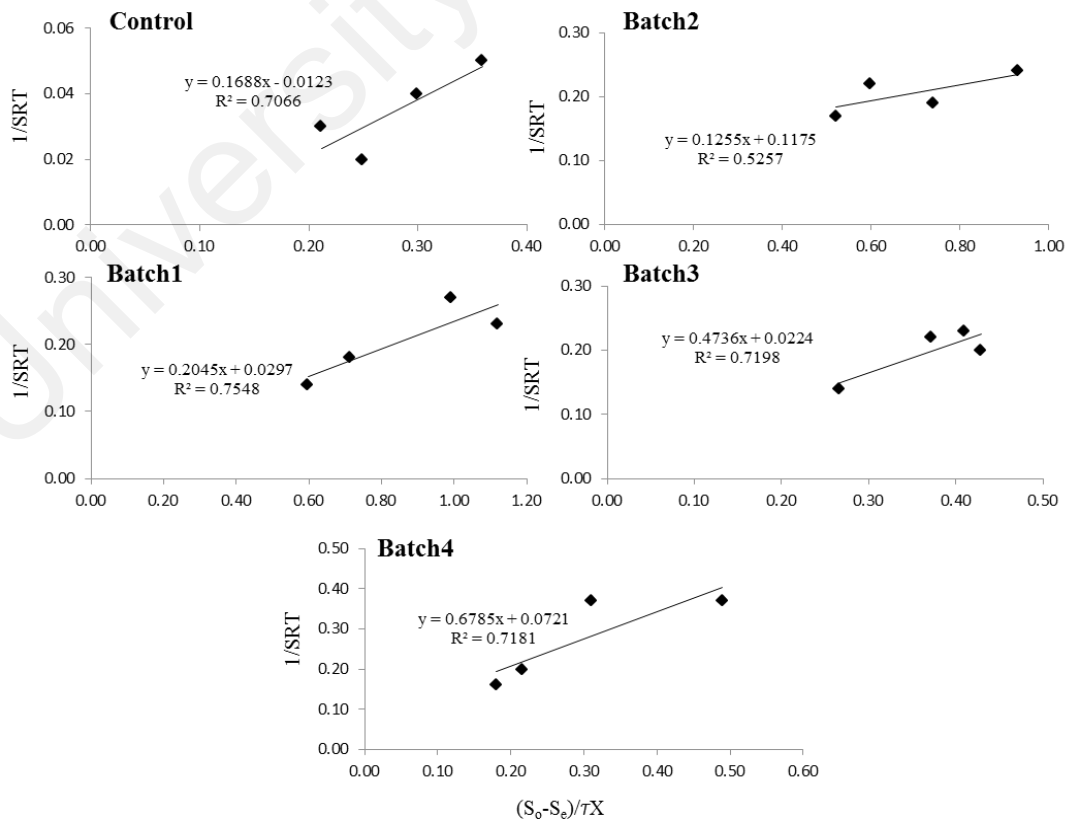


Figure 4.50: Linear plot of microbial growth for determination of Y and K_d coefficients during steady state

Table 4.3: Corresponding kinetic coefficient of substrate utilization and microbial growth for this study

Batch	SBR	H/D ratio	Period ¹ (days)	Average OLR ^a (kg CODs/m ³ d)	<i>k</i> (1/d)	<i>K_s</i> (mg/L)	<i>Y</i> (mg/mg)	<i>K_d</i> (1/d)	<i>μ_{max}</i> (1/d)
Control	SBR1	11.3	55-71	0.32	2.74	946	0.17	0.01	0.46
Batch1	SBR1	11.3	49-63	0.43	27.55	3133	0.20	0.03	5.63
Batch2	SBR2	4.4	89-103	0.41	0.91	228	0.13	0.12	0.11
Batch3	SBR3	4.4	41-67	0.63	0.34	276	0.47	0.02	0.16
Batch4	SBR1	10.0	40-83	0.63	0.27	315	0.68	0.07	0.18

¹ during steady state

The R^2 value for substrate utilization fit line is above 0.90 and this indicates that kinetic coefficients of k and K_s are accurate in this study. In contrast, the R^2 reading for microbial growth fit line is lower, in which 0.52 for Batch2 AGS and above 0.70 for the rest. Asadi et al. (2014) reported R^2 reading of 0.62 for determination of μ_{max} and K_s , and suggested the lack of fit was due to low biodegradability of COD. Indeed, although the biodegradability of sewage for all sample based on BOD/CODs ratio is over 0.5, during steady state CODs/NH₄⁺ ratio for Batch2 is the lowest, which is 3.3 followed by Batch3, Batch4 and Batch1 that are around 4 and over 6.3 for Batch1. Thus, this explains why the fit line for substrate utilization is much higher than microbial growth.

4.6.3 Effect of OLR and Reactor H/D ratio on Kinetic Coefficients

As shown in Table 4.3, the values of k , K_s and μ_{max} are exceptionally high for Batch1 which are 27.55 1/d, 3133 mg/L and 5.63 1/d, respectively. This could be attribute to active competition between newly added microbial from activated sludge and aerobic sludge present in reactor on day 33 (Section 4.3.2.1), which is 16 days just before Batch1 in steady state. Result is in line with report by Kaewsuk et al., (2010) on

high K_s value that demonstrated the activeness of aerobic microbial. However, Asadi et al. (2014) found that a process or system with high value of K_s as less efficient. Thus, a plot of μ_{max} versus K_s is plotted (Figure 4.51) to determine the activeness of aerobic granules produced in SBR with different H/D ratio.

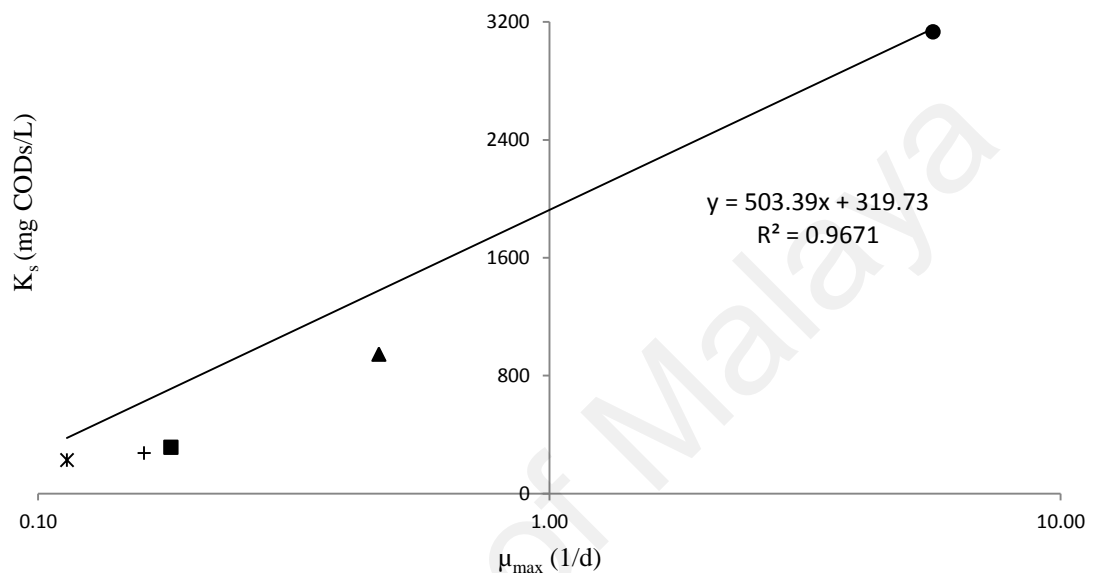


Figure 4.51: Relationship between maximum specific microbial growth rate (μ_{max}) and half saturation coefficient (K_s); Control = ▲, Batch1 = ●, Batch2 = *, Batch3 = +, Batch4 = ■

Result shows that the activeness of aerobic granules produces in SBR with H/D ratio of 4.4 (Batch 2 and Batch3) is lower than in SBR with H/D ratio of 10 (Batch4) and 11.3 (Control and Batch1). This explains why at equal OLR and operational conditions, period to achieve steady state in SBR1 with high H/D ratio is shorter than in SBR2, which has a low H/D ratio (Section 4.3.6). Thus, it can be concluded that period to achieve steady state is governed by reactor H/D ratio. Despite that, in comparison with Batch4, the use of divided draft tubes for SBR3 proved to be beneficial in reducing the time period of setup for Batch3 (Section 4.4.6). The performance of SBR with low H/D ratio appears to have a higher resistant to variable and lower OLR by providing the

short settling distance for biomass in facing the unfavorable circumstance (Section 4.3.6).

A plot of OLR versus Y is shown in Figure 4.52 to determine the influence of OLR on the development of aerobic granules. Considering the differences in sewage composition since sewage were collected at Pantai STP and Damansara STP and operating conditions applied, the reading for R^2 linear fit line of 0.82 is as shown in Figure 4.50 can be considered as reliable. Thus, this indicates that biomass production depended proportionally on OLR, and this fits well with earlier assumption of first order reaction characteristic of sewage. Result also revealed that for comparatively equal effluent performances, the production of biomass in SBR with high H/D ratio is always greater than in low H/D ratio.

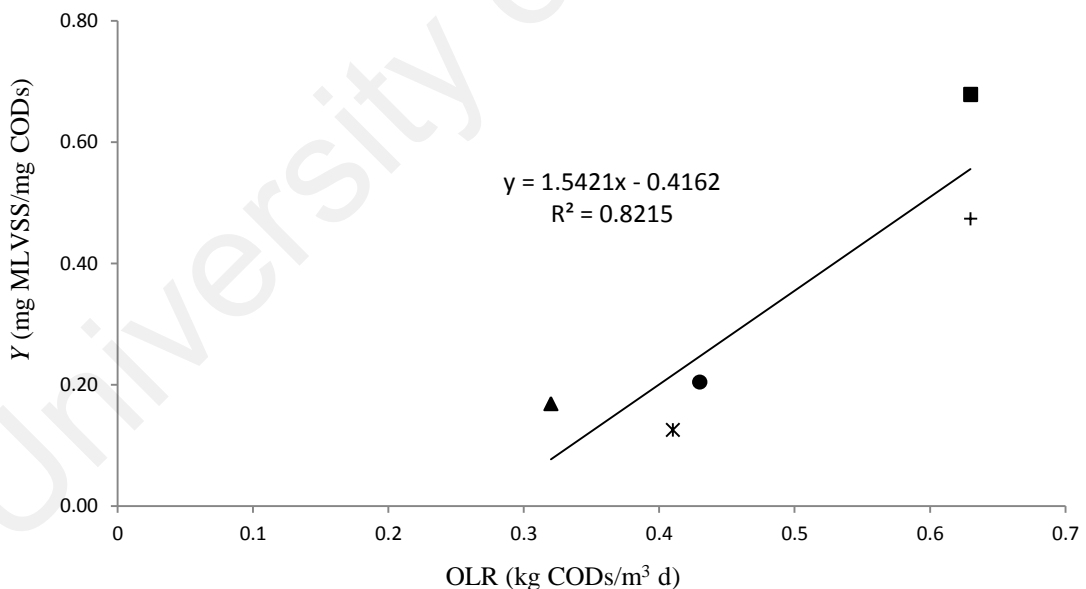


Figure 4.52: Relationship between OLR and synthesis yield coefficient (Y);
Control = ▲, Batch1 = ●, Batch2 = *, Batch3 = +, Batch4 = ■

Furthermore, Y of this study is almost comparatively within the reported range for sewage as shown in Table 4.4, which are 0.3 to 0.6 mg/mg by Metcalf and Eddy (2004) and 0.7 mg/mg by Pala and Bölükbaş (2005). It appears that values of Y is higher

for sewage than in other type of substrates (Table 4.4) although concentration of influent COD is much lower in sewage (maximum 231 CODs mg/L in this study). Liu et al. (2005b) related that the low Y value was caused by the diversity of microorganism in completing the oxidation process with complicated food chains. Thus, it can be concluded that substrate utilization and bacteria growth are highly dependent on the characteristics of substrate itself.

Table 4.4: Corresponding kinetic coefficients of substrate utilization and microbial growth from others study based on Monod equation

Reactor	System	Substrate	COD (mg/L)	k (1/d)	K_s (mg/L)	Y (mg/mg)	K_d (1/d)	μ_{max} (1/d)	References
SBR-AGS	Batch	Sewage form Pantai 1	39	0.91	228	0.13	0.01	0.11	This study
			to 120	to 27.5	to 3133	to 0.20	to 0.12	to 5.63	
SBR-AGS	Batch	Sewage from Damansara	86	0.27	276	0.47	0.02	0.16	This study
			to 231	to 0.34	to 315	to 0.68	to 0.07	to 0.18	
SBR-AGS	Batch	Acetate	2000	-	-	0.142	0.065	0.075	Chen et al., 2008
			to 4000			0.231	0.069	0.027	
SBR-AGS	Batch	Glucose	3342	13.2	276	0.183	0.023	-	Liu et al., 2005a
						to 0.250	to 0.075		
SBR-AGS	Batch	Synthetic textile	1200	-	-	0.217	0.006	0.013	Muda et al., 2011
			to 1600			0.412	0.010	0.036	
MBSR	Batch	Dairy	2584 ±794	7.42	174	0.228	0.138	1.69	Kaewsuk et al., 2010
UAASB	Batch	Industrial Estate	945 to 1200	0.41	180	0.161	0.039	0.07	Asadi et al., 2014
Batch Test	Batch	Sewage	100 to 500	-	343	0.70	0.053	1.13	Pala & Bölükbaş, 2005
CSTR	Continuous	Petroleum refinery	172 to 1617	0.81	111	0.049	0.004	0.04	Mizzouri & Shaaban, 2013
Activated Sludge	Continuous	Sewage	-	2 to 10	10 to 60	0.3 to 0.6	0.06 to 0.15	-	Metcalf & Eddy, 2004

From the study by Kaewsuk et al. (2010), the determination of kinetic coefficients of Mixed-PnSB using dairy wastewater as substrate, the value of K_s was determined to be 174 mg/L instead of 8000 mg/L as reported by Kantawanichkul (1990), which using coconut cream. Kaewsuk et al. (2010) confirmed that higher organic substance and oil and grease concentration in coconut cream compare to dairy wastewater and acetate had caused the increased in K_s value. Thus, this show that substrate with complicated structure organic matter will subsequently has a high K_s value compare to the simple structure. However, the K_s value in this study is higher comparing to results by Asadi et al. (2014), Kaewsuk et al. (2010) and Mizzouri and Shaaban (2013), that using substrate with more complicated structure than sewage. Besides, the K_s value in this study is significantly higher than that reported by Metcalf and Eddy (2004) and relatively equal to the study by Pala and Bölükbaş (2005), which both using sewage as substrate. Hence, this shows that the type of reactor, system and reactor scale has influence on K_s value.

Comparing the data in Table 4.4 with results in Table 4.3, the values of K_d in this study are normally within the reported range of conventional activated sludge (Metcalf & Eddy, 2004) and SBR-AGS system (Chen et al., 2008; Liu et al., 2005a; Muda et al., 2011). Further analysis reveals that K_d values gradually increase with an increase in period to achieve steady state (Figure 4.53). This can most probably be attributed to the linear relationship between K_d and cell age. Result reported by Chen et al. (2008) demonstrated an increasing trend of K_d value from 0.065 1/d on the first 118 days of aerobic granules formation period to 0.069 1/d for the last 335 days. While, Muda et al. (2011) considered that an increase in K_d values from 0.0075 to 0.0076 1/d between days 140 to 280 as constant.

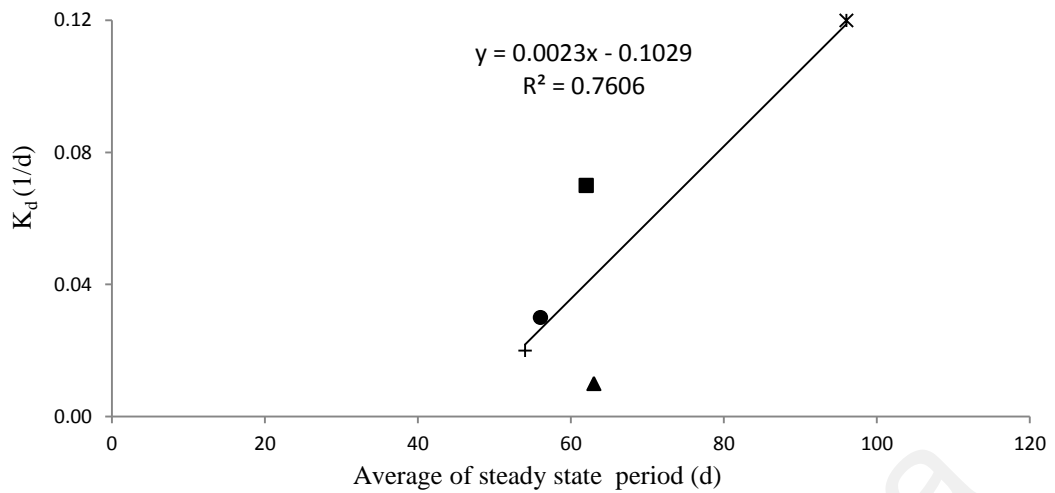


Figure 4.53: Relationship between steady state period and endogenous coefficient (K_d); Control = ▲, Batch1 = ●, Batch2 = *, Batch3 = +, Batch4 = ■.

Substrate characterization is important in understanding bioactivity of aerobic granules especially when equivalent operating conditions is applied to the sequencing batch reactor (SBR) system. Repetition of identical experiment would not lead to the same result because of variability in substrate constituent particularly real wastewater. Bioactivity can be quantified based on biokinetic parameters, which generally describes the rate of substrate utilization and biomass production or growth by microbial. Result revealed that biomass production (Y and μ_{max}) depended proportionally on the increase in OLR and reactor H/D ratio. This might be attributed to the effectiveness of aerobic granules measured by K_s values that are greater in high H/D ratio reactor. However, high K_s values do not guarantee an efficient system performance in which aerobic granules produced in low H/D ratio reactor appears to be more resistant to variable OLR and biomass floating event. At equal effluent performance and OLR, the production of biomass in low H/D ratio reactor was lesser than in high H/D ratio reactor. This could bring big benefits in terms of reducing cost involved in sludge thickening process for conventional activated sludge system.

4.6.4 Significance of Biokinetic Parameters

In this study, an independent sample t-test was performed to determine the significance of biokinetic parameter with the different in reactor H/D ratio and OLR. As showed in Table 4.5, by default, reactor with H/D ratio over 10 (N=3) was associated with high K_s value $M=1464.67(SD=1478.87)$. By comparison, reactor with H/D ratio less than 10 (N=2) was associated with a numerically smaller K_s value $M=252.00(SD=33.94)$. To test the hypothesis that reactor with the different H/D ratio of 10 were associated with statistically significantly different Mean K_s , an independent sample t-test was performed.

As can be seen in Table 4.6, the K_s distribution was sufficiently normal for the purpose of conducting a t-test, where Skewness and Kurtosis value are lower than |2.0| and kurtosis |9.0|, respectively (Schmider et al. 2010). Additionally, the assumption of homogeneity of variances was tested and satisfied via Levene's (Table 4.7) F test, $F(3)=6.430$, $p=0.085$. The independent sample t-test was associated with a no statistically significantly effect, $t(3)= 1.100$, $p=0.352$. Thus, it can be conclude that there is no statistically significant difference between reactor H/D ratio and K_s value. The differences between reactor H/D ratio Means are likely due to external factors like OLR range and operating conditions applied and not likely due to the reactor H/D ratio manipulation.

Table 4.5: Group Statistic for reactor with different H/D ratio

	Reactor H/D ratio	N	Mean	Std. Deviation	Std. Error Mean
K_s	Reactor H/D ratio > 10	3	1464.67	1478.865	853.823
	Reactor H/D ratio < 10	2	252.00	33.941	24.000
Y	Reactor H/D ratio > 10	3	.3500	.28618	.16523
	Reactor H/D ratio < 10	2	.3000	.24042	.17000
μ_m	Reactor H/D ratio > 10	3	2.0900	3.06892	1.77184
	Reactor H/D ratio < 10	2	.1350	.03536	.02500

Table 4.6: Descriptive statistic associated for kinetic coefficients

		K_s	Y	K	μ_m
N	Valid	5	5	5	5
	Missing	0	0	0	0
Mean		979.60	.3300	6.3620	1.3080
Variance		1534977.300	.056	141.288	5.856
Skewness		1.954	.981	2.198	2.219
Std. Error of Skewness		.913	.913	.913	.913
Kurtosis		3.811	-.891	4.855	4.935
Std. Error of Kurtosis		2.000	2.000	2.000	2.000

Independent sample t-test also was performed to test that reactor with the different H/D ratio of 10 were associated with statistically significantly different Mean Y and μ_m . Result from Table 4.7 showed that both Y and μ_m were associated with a no statistically significantly effect, $t(3)= 0.202$, $p=0.853$ and $t(3)= 0.855$, $p=0.456$, respectively. Thus, this showed that the formation and performance of aerobic granules in reactor with H/D ratio lower than 10 are similar to the higher one. This will be a good indicator for the practical application of aerobic granules since the existing SBR at working plant in Malaysia mostly has low H/D ratio.

Table 4.7: Independent Sample Test for reactor with different H/D ratio

		Levene's Test for Equality of Variances		t-test for Equality of Means						
		F	Sig.	t	df	Sig. (2-tailed)	Mean Difference	Std. Error Difference	95% Confidence Interval of the Differences	
									Lower	Upper
K_s	Equal variances assumed	6.430	.085	1.100	3	.352	1212.667	1102.426	-2295.746	4721.079
	Equal variances not assumed			1.420	2.003	.291	1212.667	854.160	-2456.940	4882.274
Y	Equal variances assumed	.484	.537	.202	3	.853	.05000	.24810	-.73958	.83958
	Equal variances not assumed			.211	2.615	.848	.05000	.23707	-.77137	.87137
μ_m	Equal variances assumed	.225	.056	.855	3	.456	1.95500	2.28752	-5.32490	9.23490
	Equal variances not assumed			1.103	2.001	.385	1.95500	1.77202	-5.66648	9.57648

As showed in Table 4.8, by default, organic loading rate (OLR) over 0.5 kg CODs/m³ d (N=2) was associated with high *Y* value M=0.5750(SD=0.14849). By comparison, OLR less than 0.5 kg CODs/m³ d (N=3) was associated with a numerically smaller *Y* value M=0.1667(SD=0.03512). To test the hypothesis that the different in OLR of 0.5 kg CODs/m³ d were associated with statistically significantly different Mean *Y*, an independent sample t-test was performed. As can be seen in Table 4.6, the *Y* distribution was sufficiently normal for the purpose of conducting a t-test, where Skewness and Kurtosis value are lower than |2.0| and kurtosis |9.0|, respectively (Schmider et al. 2010).

Table 4.8: Group Statistic for Organic Loading Rate

	Organic Loading Rate	N	Mean	Std. Deviation	Std. Error Mean
<i>Y</i>	Organic loading rate > 0.5	2	.5750	.14849	.10500
	Organic loading rate < 0.5	3	.1667	.03512	.02028
μ_m	Organic loading rate > 0.5	2	.1700	.01414	.01000
	Organic loading rate < 0.5	3	2.0667	3.09090	1.78453
<i>K</i>	Organic loading rate > 0.5	2	.3050	.04950	.03500
	Organic loading rate < 0.5	3	10.4000	14.88049	8.59126

Additionally, the assumption of homogeneity of variances was tested and satisfied via Levene's (Table 4.9) F test, F test, F(1)=34.657, p=0.010. The Sig. value for *Y* from Levene's F test was greater less than 0.05 indicated that the variability in the OLR is significantly different, which is contribute by fluctuated OLR range applied during the formation of aerobic granules. Whilst, the independent sample t-test was associated with a no statistically significantly effect, t(1)= 3.818, p=0.149. Thus, it can be conclude that there is no statistically significant difference between OLR and *Y*

value. The differences between OLR Means are likely due to external factors like operating conditions especially settling time applied and not likely due to the OLR manipulation.

Independent sample t-test also was performed to test that the different in OLR were associated with statistically significantly different Mean μ_m and K . Result from Table 4.9 showed that both μ_m and K were associated with a no statistically significantly effect, $t(3) = -0.823$, $p = 0.471$ and $t(3) = -0.910$, $p = 0.430$, respectively. Thus this showed that the applied OLR from 0.32 to 0.63 kg CODs/m³ d range are not wide and this lead to a no statistically significantly affect although a linear relationship between Y and OLR is equal to R^2 above 0.82 (Section 4.6.3)

Table 4.9: Independent Sample Test for Effect of OLR

		Levene's Test for Equality of Variances		t-test for Equality of Means						
		F	Sig.	t	df	Sig. (2-tailed)	Mean Difference	Std. Error Difference	95% Confidence Interval of the Differences	
								Lower	Upper	
<i>Y</i>	Equal variances assumed	34.657	.010	4.948	3	.016	.40833	.08252	.14571	.67096
	Equal variances not assumed			3.818	1.075	.149	.40833	.10694	-.74519	1.56186
μ_m	Equal variances assumed	9.252	.056	-.823	3	.471	-1.89667	2.30383	-9.22848	5.43515
	Equal variances not assumed			-1.063	2.000	.399	-1.89667	1.78456	-9.57453	5.78120
<i>K</i>	Equal variances assumed	9.226	.056	-.910	3	.430	-10.0950	11.09130	-45.39245	25.20245
	Equal variances not assumed			-1.175	2.000	.361	-10.0950	8.59133	-47.05933	26.86933

CHAPTER 5

CONCLUSIONS AND RECOMMENDATIONS

5.1 Conclusions

The foremost aim of this thesis was to identify the formation and stability of aerobic granules develop in reactor with low H/D ratio for a full-scale application at new or existing sewage treatment plant that utilize SBR in Malaysia. The foresaid goal was successfully achieved by conducting the experimental work in conditions which is similar to real site application like low volumetric conversion capacity, variable OLR and low reactor H/D ratio. The most conclusive findings drawn from the thesis are listed below:

- i. The effect of low and variable organic loading rate, and reactor height/diameter (H/D) ratio on formation of AGS.**
 - AGS (Control) was successfully attained after 55 days of a formation period although the applied OLR was exceptionally low and variable, which were in the range of 0.20 kg CODs/m³ d to 0.48 kg CODs/m³ d.
 - Although the periods to attain AGS (Batch1) in high H/D ratio reactor was shorter, AGS (Batch2) produced in low H/D ratio reactor appeared to be more resistant towards low and variable OLR by providing a short settling distance for biomass in facing the unfavourable circumstances.
 - The use of divided draft tubes proved to be beneficial in shortening the time period setup for aerobic granules formation in low H/D ratio reactor, which is from 89 days (Batch2) to 41 days (Batch3).

ii. Formation and stability mechanism of AGS process via the usage of long term storage aerobic granules as seed.

- Formation of aerobic granules is a cycle process in which SBR-AGS system was not in a total failure condition when at the disintegration phase.
- The variations in OLR will intrusive the formation process particularly during low OLR and resulting in longer period to achieve mature aerobic granules or full granulation of biomass in the reactor.

iii. Microbial community dynamics in AGS at different phases of formation process.

- The NGS analysis result indicated that the shift in microbial community performing denitrification process from Rhodocyclaceae to Comamonadaceae family was accommodated with the changes in the aerobic granules size from 147 μm to more than 336 μm for Batch3 and from 326 μm to more than 600 μm for Batch4.
- The dominant microbial in seed suppressed the existence of other species over the formation period and resulted in low microbial species diversity in mature aerobic granules.

iv. Biokinetic parameters of aerobic granules develop in SBR with various configuration and sewage as substrate.

- Biomass production (Y and μ_{max}) depended proportionally on the increase in OLR and reactor H/D ratio.
- Aerobic granules developed in reactors with high H/D ratio have a shorter setup time period and are more active compared to those in low H/D ratio reactors. This can be measured by greater K_s value in high H/D ratio reactors with values over 315 mg/L as compared to less than 276 mg/L in low H/D ratio reactors.

5.2 Recommendations for Further Work

Despite of the increasing number of studies on aerobic granules were carried out worldwide, many aspects of aerobic granule formation and stability for real wastewater treatment remained uncertain. Future studies should not be confined to the formation of aerobic granules in H/D ratio reactor of over 10 only. Since all the theories regarding the formation of aerobic granules had been well documented and described using synthetic wastewater, the technology must be ready to be taken to a pilot scale in treating real wastewater, and finally to a full scale implementation. Recommendations for future research are outlined as follows:

i. Hydrodynamic Study for Reactor Mixing

It is well accepted that shear force is the crucial factor in determining the formation of aerobic granules under hydrodynamic conditions where, high shear force can help to enhance the formation process and produce thinner and denser aerobic granules. Currently, research efforts regarding hydrodynamic study for aerobic granules are described based on continuous-flow instead of batch-flow. Thus this will be a limiting factor for practical application of aerobic granules in SBR. An analysis on hydrodynamic is useful in determining the flow pattern, mixture properties, diagnose dead zones and short circuits in reactors at a large scale.

ii. Stability of Aerobic Granules

Currently, most researches regarding stability are focused on the ability of mature aerobic granules to resist toxic shock loading from pharmaceutical products, ammonia inhibition, famine conditions, hydrodynamic and mechanical shear force instead of the process for aerobic granules formation itself. In addition, the period for aerobic granules

formation is enhancing by the addition of carrier or glucose. Thus, the stability of aerobic granules should be described during the formation itself since the final effluent and sludge quality will become a benchmark whether the aerobic granules technology is suitable for the industrial application.

University of Malaya

REFERENCES

- Abdullah, N., Yuzir, A., Curtis, T. P., Yahya, A., & Ujang, Z. (2013). Characterization of aerobic granular sludge treating high strength agro-based wastewater at different volumetric loadings. *Bioresource Technology*, *127*: 181–187.
- Adav, S. S., & Lee, D.-J. (2008). Extraction of extracellular polymeric substances from aerobic granule with compact interior structure. *Journal of Hazardous Materials*, *154*(1-3): 1120–1126.
- Adav, S. S., Lee, D.-J., & Lai, J.-Y. (2009). Aerobic granulation in sequencing batch reactors at different settling times. *Bioresource Technology*, *100*(21): 5359–5361.
- Adav, S. S., Lee, D.-J., & Lai, J.-Y. (2010). Potential cause of aerobic granular sludge breakdown at high organic loading rates. *Applied Microbiology and Biotechnology*, *85*(5): 1601–1610.
- Adav, S. S., Lee, D.-J., Show, K.-Y., & Tay, J.-H. (2008). Aerobic granular sludge: recent advances. *Biotechnology Advances*, *26*(5): 411–423.
- Adav, S. S., Lee, D.-J., & Tay, J.-H. (2008). Extracellular polymeric substances and structural stability of aerobic granule. *Water Research*, *42*(6-7): 1644–1650.
- Allen, M.S., Welch, K.T., Prebyl, B.S., Baker, D.C., Meyers, A.J., & Sayler, G.S. (2004). Analysis and glycosyl composition of the exopolysaccharide isolated from the floc-forming wastewater bacterium *Thauera sp. MZIT*. *Environmental Microbiology*, *6*(8): 780-790.
- Amorim, C. L., Maia, A. S., Mesquita, R. B. R., Rangel, A. O. S. S., van Loosdrecht, M. C. M., Tiritan, M. E., & Castro, P. M. L. (2014). Performance of aerobic granular sludge in a sequencing batch bioreactor exposed to ofloxacin, norfloxacin and ciprofloxacin. *Water Research*, *50*: 101–113.
- Angela, M., Béatrice, B., & Mathieu, S. (2011). Biologically induced phosphorus precipitation in aerobic granular sludge process. *Water Research*, *45*(12): 3776–3786.
- Anthonisen, A.C., Loehr, R.C., Prakasam, T.B.S., Srinarh, E.G. (1976). Inhibition of nitrification by ammonia and nitrous acid. *Journal of the Water Pollution Control Federation*, *48*(5): 835–852.
- APHA. (2005). Standard Methods for the Examination of Water and Wastewater, 21st ed. American Public Health Association/ American Water Works Association/ Water Environment Federation, Washington.
- Arrojo, B., Mosquera-Corral, A., Garrido, J. M., & Méndez, R. (2004). Aerobic granulation with industrial wastewater in sequencing batch reactors. *Water Research*, *38*(14-15): 3389–3399.

- Asadi, A., Zinatizadeh, A. A., & Sumathi, S. (2014). Industrial Estate Wastewater Treatment Using Single Up-Flow Aerobic /Anoxic Sludge Bed (UAASB) Bioreactor : A Kinetic Evaluation Study. *Environmental Progress & Sustainable Energy*, 0(0): 1-9.
- Badireddy, A. R., Chellam, S., Gassman, P. L., Engelhard, M. H., Lea, A. S., & Rosso, K. M. (2010). Role of extracellular polymeric substances in bioflocculation of activated sludge microorganisms under glucose-controlled conditions. *Water Research*, 44(15): 4505–4516.
- Bassin, J. P., Kleerebezem, R., Dezotti, M., & van Loosdrecht, M. C. M. (2012). Simultaneous nitrogen and phosphate removal in aerobic granular sludge reactors operated at different temperatures. *Water Research*, 46(12): 3805–3816.
- Beun, J. ., Hendriks, A, van Loosdrecht, M. C.M ., Morgenroth, E., Wilderer, P.A., & Heijnen, J.J.(1999). Aerobic granulation in a sequencing batch reactor. *Water Research*, 33(10): 2283–2290.
- Beun, J. J., van Loosdrecht, M. C. M., & Heijnen, J. J. (2002). Aerobic granulation in a sequencing batch airlift reactor. *Water Research*, 36(3): 702–712.
- Bratby, J., 2006. *Coagulation and Flocculation in Water and Wastewater Treatment*. 2nd ed., Vol. 2, London: IWA Publishing.
- Chan, Y. J., Chong, M. F., Law, C. L., & Hassell, D. G. (2009). A review on anaerobic–aerobic treatment of industrial and municipal wastewater. *Chemical Engineering Journal*, 155(1-2): 1–18.
- Chen, M. Y., Lee, D. J., & Tay, J. H. (2007c). Distribution of extracellular polymeric substances in aerobic granules. *Applied Microbiology and Biotechnology*, 73(6): 1463–1469.
- Chen, M.-Y., Lee, D.-J., Tay, J.-H., & Show, K.-Y. (2007b). Staining of extracellular polymeric substances and cells in bioaggregates. *Applied Microbiology and Biotechnology*, 75(2): 467–474.
- Chen, Y., Jiang, W., Liang, D. T., & Tay, J. H. (2007a). Structure and stability of aerobic granules cultivated under different shear force in sequencing batch reactors. *Applied Microbiology and Biotechnology*, 76(5): 1199–1208.
- Chen, Y., Jiang, W., Liang, D. T., & Tay, J. H. (2008). Biodegradation and kinetics of aerobic granules under high organic loading rates in sequencing batch reactor. *Applied Microbiology and Biotechnology*, 79(2): 301–308.
- Chiu, Z. C., Chen, M. Y., Lee, D. J., Wang, C. H., & Lai, J. Y. (2007). Oxygen diffusion and consumption in active aerobic granules of heterogeneous structure. *Applied Microbiology and Biotechnology*, 75(3): 685–691.
- De Kreuk, M.K. (2006). *Aerobic granular sludge: scaling up a new technology*. (Doctoral thesis, Technical University Delft, The Netherlands).

- De Kreuk, M. K., & van Loosdrecht, M. C. M. (2006). Formation of Aerobic Granules with Domestic Sewage. *Journal of Environmental Engineering*, 132(6): 694–698.
- Department of Environment, Malaysia. (2014). *Malaysia environmental quality report 2014*. Malaysia.
- Di Iaconi, C., Ramadori, R., Lopez, A., & Passino, R. (2007). Aerobic Granular Sludge Systems : The New Generation of Wastewater Treatment Technologies. *Ind. Eng. Chem. Res.*, 46: 6661–6665.
- Fabregas, T. V. (2005). *SBR technology for wastewater treatment: Suitable operational conditions for a nutrient removal*. (Doctoral thesis, Universitat de Girona, Spain).
- Flemming, H.-C., & Wingender, J. (2010). The biofilm matrix. *Nature Reviews. Microbiology*, 8(9): 623–633.
- Gao, D., Liu, L., Liang, H., & Wu, W.-M. (2011). Comparison of four enhancement strategies for aerobic granulation in sequencing batch reactors. *Journal of Hazardous Materials*, 186(1): 320–327.
- Guo, F., Zhang, S.-H., Yu, X., & Wei, B. (2011). Variations of both bacterial community and extracellular polymers: the inducements of increase of cell hydrophobicity from biofloc to aerobic granule sludge. *Bioresource Technology*, 102(11): 6421–6428.
- Guo, J., Peng, Y., Wang, Z., Yuan, Z., Yang, X., & Wang, S. (2012). Control filamentous bulking caused by chlorine-resistant Type 021N bacteria through adding a biocide CTAB. *Water Research*, 46(19): 6531–6542.
- Hamid, H., Narayana, D., Bai, S.A., 2009. Centralized and decentralized wastewater management in Malaysia – Experience and challenge. *The Ingenieur* 43, 37-44
- Hammer, M. J., & Jr Hammer, Mark J. (1996). *Water and Wastewater Technology. Bibliothek*. 3rd ed. New Jersey: Prentice-Hall.
- Han, K., & Levenspiel, O. (1988). Extended monod kinetics for substrate product and cell inhibition. *Biotechnology and Bioengineering*, 32: 430–437.
- Heijnen, J. J., & van Loosdrecht, M. C. M. (1998). Method for acquiring grain shaped growth of a microorganism in a reactor. European patent EP0826639.
- Indah Water Konsortium (2012). *2012 Facts & Figures*. Malaysia.
- Isanta, E., Suárez-Ojeda, M. E., Val del Río, Á., Morales, N., Pérez, J., & Carrera, J. (2012). Long term operation of a granular sequencing batch reactor at pilot scale treating a low-strength wastewater. *Chemical Engineering Journal*, 198-199: 163–170.
- Jang, A., Yoon, Y.-H., Kim, I. s, Kim, K. S., & Bishop, P. L. (2003). Characterization and evaluation of aerobic granules in sequencing batch reactor. *Journal of Biotechnology*, 105(1-2), 71–82.

- Jin, R.-C., Zheng, P., Mahmood, Q., & Zhang, L. (2008). Hydrodynamic characteristics of airlift nitrifying reactor using carrier-induced granular sludge. *Journal of Hazardous Materials*, 157(2-3): 367–373.
- Kaewsuk, J., Thorasampan, W., Thanuttamavong, M., & Tae, G. (2010). Kinetic development and evaluation of membrane sequencing batch reactor (MSBR) with mixed cultures photosynthetic bacteria for dairy wastewater treatment. *Journal of Environmental Management*, 91: 1161–1168.
- Kantawanichkul, S. (1990). *Application of hollow fiber membrane bioreactor to anaerobi treatment of oily wastewater treatment by Photosynthetic bacteria: Rhodobacter sphaeroides*. (Doctoral thesis, AIT, Bangkok, Thailand).
- Kong, Y., Liu, Y.-Q., Tay, J.-H., Wong, F.-S., & Zhu, J. (2009). Aerobic granulation in sequencing batch reactors with different reactor height/diameter ratios. *Enzyme and Microbial Technology*, 45(5): 379–383.
- Lee, D.-J., Chen, Y.-Y., Show, K.-Y., Whiteley, C. G., & Tay, J.-H. (2010). Advances in aerobic granule formation and granule stability in the course of storage and reactor operation. *Biotechnology Advances*, 28(6): 919–934.
- Lemaire, R., Webb, R. I., & Yuan, Z. (2008). Micro-scale observations of the structure of aerobic microbial granules used for the treatment of nutrient-rich industrial wastewater. *The International Society for Microbial Ecology Journal*, 2(5): 528–541.
- Lettinga, G., van Velsen, a F. M., Hobma, S. W., de Zeeuw, W., & Klapwijk, a. (1980). Use of the upflow sludge blanket (USB) reactor concept for biological wastewater treatment, especially for anaerobic treatment. *Biotechnology and Bioengineering*, 22: 699–734.
- Li, A., Li, X., & Yu, H. (2011). Effect of the food-to-microorganism (F/M) ratio on the formation and size of aerobic sludge granules. *Process Biochemistry*, 46(12), 2269–2276.
- Li, A., Yang, S., Li, X., & Gu, J. (2008b). Microbial population dynamics during aerobic sludge granulation at different organic loading rates. *Water Research*, 42(13): 3552–3560.
- Li, J., Ma, L., Wei, S., & Horn, H. (2013). Aerobic granules dwelling vorticella and rotifers in an SBR fed with domestic wastewater. *Separation and Purification Technology*, 110: 127–131.
- Li, Y., Wang, Z., & Liu, Y. (2008a). Diffusion of Substrate and oxygen in aerobic granules. In Y. Liu (Ed.), *Wastewater purification: Aerobic granulation in sequencing batch reactors* (1st ed., pp. 131–147). Taylor & Franchis Group.
- Lin, Y. M., Sharma, P. K., & van Loosdrecht, M. C. M. (2013). The chemical and mechanical differences between alginate-like exopolysaccharides isolated from aerobic flocculent sludge and aerobic granular sludge. *Water Research*, 47(1): 57–65.

- Liu, L., Wang, Z., Yao, J., Sun, X., & Cai, W. (2005a). Investigation on the formation and kinetics of glucose-fed aerobic granular sludge. *Enzyme and Microbial Technology*, 36: 712–716.
- Liu, L., Wang, Z., Yao, J., Sun, X., & Cai, W. (2005b). Investigation on the properties and kinetics of glucose-fed aerobic granular sludge. *Enzyme and Microbial Technology*, 36(2-3): 307–313.
- Liu, Q., & Liu, Y. (2008). Aerobic Granulation at different shear force. In Y. Liu (Ed.), *Wastewater purification: Aerobic granulation in sequencing batch reactors* (1st ed., pp. 25–36). Taylor & Franchis Group.
- Liu, X., & Dong, C. (2011). Simultaneous COD and nitrogen removal in a micro-aerobic granular sludge reactor for domestic wastewater treatment. *System Engineering Procedia*, 1: 99–105.
- Liu, X.-W., Sheng, G.-P., & Yu, H.-Q. (2009). Physicochemical characteristics of microbial granules. *Biotechnology Advances*, 27(6): 1061–1070.
- Liu, Y., & Liu, Q.-S. (2006). Causes and control of filamentous growth in aerobic granular sludge sequencing batch reactors. *Biotechnology Advances*, 24(1): 115–127.
- Liu, Y., Liu, Z., Wang, F., Chen, Y., Kuschik, P., & Wang, X. (2014). Regulation of aerobic granular sludge reformulation after granular sludge broken: effect of poly aluminum chloride (PAC). *Bioresource Technology*, 158: 201–208.
- Liu, Y., & Tay, J.-H. (2002). The essential role of hydrodynamic shear force in the formation of biofilm and granular sludge. *Water Research*, 36(7): 1653–1665.
- Liu, Y., & Tay, J.-H. (2004). State of the art of biogranulation technology for wastewater treatment. *Biotechnology Advances*, 22(7): 533–63.
- Liu, Y., Yang, S.-F., & Tay, J.-H. (2004b). Improved stability of aerobic granules by selecting slow-growing nitrifying bacteria. *Journal of Biotechnology*, 108(2): 161–169.
- Liu, Y.-Q., Liu, Y., & Tay, J.-H. (2004a). The effects of extracellular polymeric substances on the formation and stability of biogranules. *Applied Microbiology and Biotechnology*, 65(2): 143–8.
- Liu, Y.-Q., Moy, B. Y.-P., & Tay, J.-H. (2007). COD removal and nitrification of low-strength domestic wastewater in aerobic granular sludge sequencing batch reactors. *Enzyme and Microbial Technology*, 42(1): 23–28.
- Liu, Y.-Q., & Tay, J.-H. (2006). Variable aeration in sequencing batch reactor with aerobic granular sludge. *Journal of Biotechnology*, 124(2): 338–346.
- Liu, Y.-Q., & Tay, J.-H. (2007). Cultivation of aerobic granules in a bubble column and an airlift reactor with divided draft tubes at low aeration rate. *Biochemical Engineering Journal*, 34(1): 1–7.

- Liu, Y.-Q., & Tay, J.-H. (2008). Influence of starvation time on formation and stability of aerobic granules in sequencing batch reactors. *Bioresource Technology*, 99(5): 980–985.
- Liu, Y.-Q., & Tay, J.-H. (2012). The competition between flocculent sludge and aerobic granules during the long-term operation period of granular sludge sequencing batch reactor. *Environmental Technology*, 33(23): 2619–2626.
- Liu, Y.-Q., Wu, W.-W., Tay, J.-H., & Wang, J.-L. (2008). Formation and long-term stability of nitrifying granules in a sequencing batch reactor. *Bioresource Technology*, 99(9): 3919–3922.
- Luo, J., Hao, T., Wei, L., Mackey, H. R., Lin, Z., & Chen, G.-H. (2014). Impact of influent COD/N ratio on disintegration of aerobic granular sludge. *Water Research*, 62C: 127–135.
- Lv, Y., Wan, C., Liu, X., Zhang, Y., Lee, D.-J., & Tay, J.-H. (2013). Drying and recultivation of aerobic granules. *Bioresource Technology*, 129: 700–703.
- Ma, J., Quan, X., & Li, H. (2013). Application of high OLR-fed aerobic granules for the treatment of low-strength wastewater: Performance, granule morphology and microbial community. *Journal of Environmental Sciences*, 25(8): 1549–1556.
- Mace, S., & Mata-Alvarez, J. (2002). Utilization of SBR Technology for Wastewater Treatment: An Overview. *Industrial & Engineering Chemistry Research*, 41(23): 5539–5553.
- Martins, A. M. P., Heijnen, J. J., & van Loosdrecht, M. C. M. (2003). Effect of feeding pattern and storage on the sludge settleability under aerobic conditions. *Water Research*, 37(11): 2555–2570.
- Martins, A. M. P., Pagilla, K., Heijnen, J.J., & van Loosdrecht, M.C.M. (2004). Filamentous bulking sludge--a critical review. *Water Research*, 38(4): 793–817.
- McSwain, B.S., 2005. *Molecular investigation of aerobic granular sludge formation*. (Doctoral thesis, University of Notre Dame, Indiana).
- Mcswain, B. S., Irvine, R. L., Hausner, M., & Wilderer, P.A. (2005). Composition and Distribution of Extracellular Polymeric Substances in Aerobic Floccs and Granular Sludge. *Applied and Environmental Microbiology*, 71(2): 1051–1057.
- Metcalf and Eddy., Tchobanoglous, G., Stensel, H.D., Tsuchihashi, R., & Burton, F., (2014). *Wastewater engineering: Treatment and Resource Recovery*, 5th ed. Boston: McGraw-Hill.
- Ministry of Housing and Local Government. (1998). *Guidelines for developers: Sewage treatment plant, Volume IV*. 2nd ed. Malaysia.
- Mishima, K., Nakamura, M., 1991. Self-immobilization of aerobic activate sludge: A pilot study of the aerobic upflow sludge blanket process in municipal sewage treatment. *Water Sciences and Technology* 23: 981–990.

- Mittelman, M., 1985. Biological fouling of Purified-Water Systems: Part 1, Bacteria Growth and Replication. *Microcontaminat* 3(11): 51–55.
- Mizzouri, N.S., & Shaaban, G. (2013). Kinetic and hydrodynamic assessment of an aerobic purification system for petroleum refinery wastewater treatment in a continuous regime. *International Biodeterioration & Biodegradation*, 83: 1–9.
- Morales, N., Figueroa, M., Fra-Vázquez, a., Val del Río, a., Campos, J. L., Mosquera-Corral, a., & Méndez, R. (2013). Operation of an aerobic granular pilot scale SBR plant to treat swine slurry. *Process Biochemistry*, 48(8): 1216–1221.
- Morgenroth, E., Sherden, T., van Loosdrecht, M. C. M., Heijnen, J. J., & Wilderer, P. A. (1997). Aerobic granular sludge in a sequencing batch reactor. *Water Research*, 31(12): 3191–3194.
- Moy, B. Y.-P., Tay, J.-H., Toh, S.-K., Liu, Y., & Tay, S. T.-L. (2002). High organic loading influences the physical characteristics of aerobic sludge granules. *Letters in Applied Microbiology*, 34(6): 407–412.
- Muda, K., Aris, A., Razman, M., Ibrahim, Z., van Loosdrecht, M. C. M., Ahmad, A., & Zaini, M. (2011). The effect of hydraulic retention time on granular sludge biomass in treating textile wastewater. *Water Research*, 45: 4711–4721.
- Mulder, R., Vereijken, T. L., Frijters, C. T., & Vellinga, S. H. (2001). Future perspectives in bioreactor development. *Water Science and Technology: A Journal of the International Association on Water Pollution Research*, 44: 27–32.
- Ni, B.-J., Xie, W.-M., Liu, S.-G., Yu, H.-Q., Wang, Y.-Z., Wang, G., & Dai, X.-L. (2009). Granulation of activated sludge in a pilot-scale sequencing batch reactor for the treatment of low-strength municipal wastewater. *Water Research*, 43(3):
- Okpokwasili, G. C., & Nweke, C. O. (2005). Microbial growth and substrate utilization kinetics. *African Journal of Biotechnology*, 5(4): 305–317.
- Omoike, A., & Chorover, J. (2004). Spectroscopic Study of Extracellular Polymeric Substances from *Bacillus subtilis*: Aqueous Chemistry and Adsorption Effects. *Biomacromolecules*, 5(4): 1219–1230.
- Pala, A., & Bölükba, Ö. (2005). Evaluation of kinetic parameters for biological CNP removal from a municipal wastewater through batch tests. *Process Biochemistry*, 40: 629–635.
- Papadia, S., Rovero, G., Fava, F., Gioia, D.D. (2011). Comparison of different pilot scale bioreactors for the treatment of a real wastewater from the textile industry. *International Biodeterioration & Biodegradation*, 65, 396-403.
- Peyong, Y. N., Zhou, Y., Abdullah, A. Z., & Vadivelu, V. (2012). The effect of organic loading rates and nitrogenous compounds on the aerobic granules developed using low strength wastewater. *Biochemical Engineering Journal*, 67: 52–59.
- Pronk, M., de Kreuk, M.K., de Bruin, B., Kamminga, P., Kleerebezem, R., van Loosdrecht, M.C.M. (2015). Full scale performance of the aerobic granular sludge

process for sewage treatment. *Water Research* 84: 207-217.
Doi:10.1016/j.watres.2015.07.011

Qin, L., Liu, Y., & Tay, J.-H. (2004b). Effect of settling time on aerobic granulation in sequencing batch reactor. *Biochemical Engineering Journal*, 21(1): 47–52.

Qin, L., Tay, J.-H., & Liu, Y. (2004a). Selection pressure is a driving force of aerobic granulation in sequencing batch reactors. *Process Biochemistry*, 39(5): 579–584.

Renou, S., Givaudan, J. G., Poulain, S., Dirassouyan, F., & Moulin, P. (2008). Landfill leachate treatment: Review and opportunity. *Journal of Hazardous Materials*, 150(3): 468–493.

Rosenberg, E., DeLong, E. F., Lary, S., Stackebrandt, E., & Thompson, F. (2014). *THE PROKARYOTES other major lineages of Bacteria and the Archea*. (E. Rosenberg, Ed.) (4th ed.). Springer.

Ruiz, G., Jeison, D., Chamy, R. (2003). Nitrification with high nitrite accumulation for the treatment wastewater with high ammonia concentration. *Water Research*, 37: 1371-1377.

Schmider, E., Ziegler, M., Danay, E., & Buehner, M. (2010). Is it really Robust?. *Methodology European Journal of Research Methods for the Behavioral and Social Sciences*, 6: 147-151.

Schmitt, J., Flemming, H., 1998. FTIR-spectroscopy in microbial and material analysis. *International Biodeterioration and Biodegradation*, 41: 1-11.

Schwarzenbeck, N., Borges, J. M., & Wilderer, P. A. (2005). Treatment of dairy effluents in an aerobic granular sludge sequencing batch reactor. *Applied Microbiology and Biotechnology*, 66(6): 711–778.

Seviour, T., Yuan, Z., van Loosdrecht, M. C. M., & Lin, Y. (2012). Aerobic sludge granulation: a tale of two polysaccharides? *Water Research*, 46(15): 4803–4813.

Sheng, G.-P., Yu, H.-Q., & Li, X.-Y. (2010). Extracellular polymeric substances (EPS) of microbial aggregates in biological wastewater treatment systems: a review. *Biotechnology Advances*, 28(6), 882–894.

Skiadas, I. V, Gavala, H. N., Schmidt, J. E., & Ahring, B. K. (2003). Anaerobic granular sludge and biofilm reactors. *Advances in Biochemical Engineering/biotechnology*, 82: 35–67.

Song, Z., Pan, Y., Zhang, K., Ren, N., & Wang, A. (2010). Effect of seed sludge on characteristics and microbial community of aerobic granular sludge. *Journal of Environmental Sciences*, 22(9): 1312–1318.

Su, B., Cui, X., & Zhu, J. (2012). Optimal cultivation and characteristics of aerobic granules with typical domestic sewage in an alternating anaerobic/aerobic sequencing batch reactor. *Bioresource Technology*, 110: 125–129.

- Tay, J. H., Liu, Q. S., & Liu, Y. (2001b). The role of cellular polysaccharides in the formation and stability of aerobic granules. *Letters in Applied Microbiology*, 33(3): 222–226. Retrieved from <http://www.ncbi.nlm.nih.gov/pubmed/11555208>
- Tay, J., Pan, S., He, Y., Tiong, S., & Tay, L. (2004). Effect of Organic Loading Rate on Aerobic Granulation . I: Reactor Performance. *Journal of Environmental Engineering*, 130: 1094–1101.
- Tay, J.-H., Ivanov, V., Pan, S., & Tay, S. T.-L. (2002). Specific layers in aerobically grown microbial granules. *Letters in Applied Microbiology*, 34(4): 254–257.
- Tay, J.-H., Liu, Q.-S., & Liu, Y. (2001a). The effects of shear force on the formation, structure and metabolism of aerobic granules. *Applied Microbiology and Biotechnology*, 57(1-2): 227–233.
- Tebbutt, T. H. Y. (1998). *Principles of Water Quality control. Principles of Water Quality control*. 3rd ed. Pergamon Press: Oxford.
- Thanh, B. X., Visvanathan, C., & Aim, R. Ben. (2009). Characterization of aerobic granular sludge at various organic loading rates. *Process Biochemistry*, 44(2): 242–245.
- Verawaty, M., Tait, S., Pijuan, M., Yuan, Z., & Bond, P. L. (2013). Breakage and growth towards a stable aerobic granule size during the treatment of wastewater. *Water Research*, 47(14): 5338–5349.
- Wagner, J., & da Costa, R. H. R. (2013). Aerobic Granulation in a Sequencing Batch Reactor Using Real Domestic Wastewater. *Journal of Environmental Engineering*, 139(11): 1391–1396.
- Wang, B.-B., Peng, D.-C., Hou, Y.-P., Li, H.-J., Pei, L.-Y., & Yu, L.-F. (2014). The important implications of particulate substrate in determining the physicochemical characteristics of extracellular polymeric substances (EPS) in activated sludge. *Water Research*, 58(0): 1–8.
- Wang, F., Lu, S., Wei, Y., & Ji, M. (2009). Characteristics of aerobic granule and nitrogen and phosphorus removal in a SBR. *Journal of Hazardous Materials*, 164(2-3): 1223–1227.
- Wang, Q., Du, G., & Chen, J. (2004). Aerobic granular sludge cultivated under the selective pressure as a driving force. *Process Biochemistry*, 39(5): 557–563.
- Wang, S., Teng, S., & Fan, M. (2010). Interaction between Heavy Metals and Aerobic Granular Sludge. In S. Santosh (Ed.), *Environmental Management* (1st ed., pp. 173–188). Sciyo, Chapter published.
- Wang, S.-G., Liu, X.-W., Gong, W.-X., Gao, B.-Y., Zhang, D.-H., & Yu, H.-Q. (2007a). Aerobic granulation with brewery wastewater in a sequencing batch reactor. *Bioresource Technology*, 98(11): 2142–2147.

- Wang, X. H., Zhang, H. M., Yang, F. L., Xia, L. P., & Gao, M. M. (2007b). Improved stability and performance of aerobic granules under stepwise increased selection pressure. *Enzyme and Microbial Technology*, *41*(3): 205–211.
- Wang, Z., Liu, L., Yao, J., & Cai, W. (2006). Effects of extracellular polymeric substances on aerobic granulation in sequencing batch reactors. *Chemosphere*, *63*(10): 1728–1735.
- Wang, Z., & Liu, Y. (2008). Aerobic granulation at different SBR cycle times. In Y. Liu (Ed.), *Wastewater purification: Aerobic granulation in sequencing batch reactors* (1st ed., pp. 37–50). Taylor & Franchis Group.
- Wang, Z.-W., Liu, Y., & Tay, J.-H. (2005). Distribution of EPS and cell surface hydrophobicity in aerobic granules. *Applied Microbiology and Biotechnology*, *69*(4): 469–73.
- Weber, S. D., Ludwig, W., Schleifer, K.-H., & Fried, J. (2007). Microbial composition and structure of aerobic granular sewage biofilms. *Applied and Environmental Microbiology*, *73*(19): 6233–6240.
- Winkler, M.-K. H., Kleerebezem, R., Strous, M., Chandran, K., & van Loosdrecht, M. C. M. (2013). Factors influencing the density of aerobic granular sludge. *Applied Microbiology and Biotechnology*, *97*(16): 7459–7468.
- Xie, Z., Wang, Z., Wang, Q., Zhu, C., & Wu, Z. (2014). An anaerobic dynamic membrane bioreactor (AnDMBR) for landfill leachate treatment: performance and microbial community identification. *Bioresource Technology*, *161*: 29–39.
- Xu, H.-C., He, P.-J., Wang, G.-Z., Yu, G.-H., & Shao, L.-M. (2010). Enhanced storage stability of aerobic granules seeded with pellets. *Bioresource Technology*, *101*(21): 8031–7.
- Yang, S.-F., Liu, Q.-S., Tay, J.-H., & Liu, Y. (2004). Growth kinetics of aerobic granules developed in sequencing batch reactors. *Letters in Applied Microbiology*, *38*(2): 106–112.
- Yang, S.-F., Tay, J.-H., & Liu, Y. (2004). Inhibition of free ammonia to the formation of aerobic granules. *Biochemical Engineering Journal*, *17*(1): 41–48.
- Yuan, X., & Gao, D. (2010). Effect of dissolved oxygen on nitrogen removal and process control in aerobic granular sludge reactor. *Journal of Hazardous Materials*, *178*(1-3): 1041–1045.
- Zhang, B., Ji, M., Qiu, Z., Liu, H., Wang, J., & Li, J. (2011). Microbial population dynamics during sludge granulation in an anaerobic-aerobic biological phosphorus removal system. *Bioresource Technology*, *102*(3): 2474–2480.
- Zhao, X., Chen, Z., Wang, X., Li, J., Shen, J., & Xu, H. (2015). Remediation of pharmaceuticals and personal care products using an aerobic granular sludge sequencing bioreactor and microbial community profiling using Solexa sequencing technology analysis. *Bioresource Technology*, *179*: 104–112.

- Zhao, Y., Huang, J., Zhao, H., & Yang, H. (2013). Microbial community and N removal of aerobic granular sludge at high COD and N loading rates. *Bioresource Technology*, *143*: 439–446.
- Zheng, Y.-M., Yu, H.-Q., & Sheng, G.-P. (2005). Physical and chemical characteristics of granular activated sludge from a sequencing batch airlift reactor. *Process Biochemistry*, *40*(2): 645–650.
- Zhou, D., Niu, S., Xiong, Y., Yang, Y., & Dong, S. (2014). Microbial selection pressure is not a prerequisite for granulation: dynamic granulation and microbial community study in a complete mixing bioreactor. *Bioresource Technology*, *161*: 102–8.
- Zhu, L., Lv, M., Dai, X., Yu, Y., Qi, H., & Xu, X. (2012b). Role and significance of extracellular polymeric substances on the property of aerobic granule. *Bioresource Technology*, *107*: 46–54.
- Zhu, L., Lv, M., Dai, X., Zhou, J., & Xu, X. (2013b). The stability of aerobic granular sludge under 4-chloroaniline shock in a sequential air-lift bioreactor (SABR). *Bioresource Technology*, *140*: 126–130.
- Zhu, L., Qi, H., Lv, M., Kong, Y., Yu, Y., & Xu, X. (2012a). Component analysis of extracellular polymeric substances (EPS) during aerobic sludge granulation using FTIR and 3D-EEM technologies. *Bioresource Technology*, *124*: 455–459.
- Zhu, L., Yu, Y., Dai, X., Xu, X., & Qi, H. (2013a). Optimization of selective sludge discharge mode for enhancing the stability of aerobic granular sludge process. *Chemical Engineering Journal*, *217*: 442–446.

LIST OF PUBLICATIONS AND PAPERS PRESENTED

List of Publications published/submitted

1. Awang, N.A., & Shaaban, M.G. (2015). Impact of height to diameter (H/D) ratio on aerobic granular sludge (AGS) formation in sewage treatment. *Jurnal Teknologi (Sciences & Engineering)*, 77:32, 95-103. doi.org/10.11113/jt.v77.6990 - (Scopus Index Journal).
2. Awang, N.A., & Shaaban, M.G. (2016). Effect of reactor height/diameter ratio and organic loading rate on formation of aerobic granular sludge in sewage treatment. *International Biodeterioration & Biodegradation*, 112: 1-11. (Q1, ISI Index Journal). <http://dx.doi.org/10.1016/j.ibiod.2016.04.028>
3. Awang, N.A., Shaaban, M.G., Weng, L.C., Wei, B.C. (2016) Reformation and stability of aerobic granular sludge in sewage treatment under variations of organic loading rate. *International Biodeterioration and Biodegradation*. (under editor decision).
4. Awang, N.A., & Shaaban, M.G. (2016). Rapid formation of aerobic granular sludge in low Height/Diameter ratio reactor with divided draft tubes. *Journal of Environmental Sciences*, **in preparation for submission.**

List of conferences presented

1. Awang, N.A., & Shaaban, M.G. River Sustainability from domestic sewage pollution using AGS technology. *Comprehensive Symposium IV: Integrated Watershed Management*; UTM Skudai Campus, Johor, 3-4 December 2014.
2. Awang, N.A., & Shaaban, M.G. Effect of H/D ratio on development of AGS in sewage treatment. *The 6th International Conference on Postgraduate Education*; Main Hall UteM, Melaka, 17-18 December 2014.
3. Shaaban, M.G., Malek, M.I.A., Awang, N.A., & Shawkat, N. Microbial population and performance in SBR adapted for treating sewage, MSW leachate and petroleum effluents. *5th Comprehensive symposium on Asian core program integrated watershed management*; Kyoto University, Japan, Nov 2015.

APPENDIX A1

TABULATED DATA FOR INFLUENT VALUE AT EACH PHASE DURING FORMATION OF AGS NAMELY AS CONTROL

Period	HRT	Phase	CODs	NH ₄ ⁺	NO ₂ ⁻	NO ₃ ⁻	P	SS	VSS
(d)	(h)								
1	8	1	67	13	0.05	0.3	3	137	87
3	8	1	92	16	0.07	0.2	4	79	70
6	8	1	92	16	0.07	0.2	4	79	70
8	8	1	92	16	0.07	0.2	4	79	70
10	8	1	92	16	0.07	0.2	4	79	70
13	8	1	92	16	0.07	0.2	4	79	70
15	8	1	70	13	0.06	0.3	4	79	70
17	8	1	91	13	0.06	0.3	4	165	131
21	8	1	91	13	0.06	0.3	4	165	131
24	8	1	83	13	0.08	0.2	3	35	38
27	8	1	83	13	0.08	0.2	3	35	38
30	8	1	83	13	0.08	0.2	3	35	38
31	6	2	92	15	0.08	0.2	4	154	115
36	6	2	92	15	0.08	0.2	4	154	115
38	6	2	93	17	0.06	0.3	4	87	80
42	6	2	93	13	0.05	0.2	3	195	145
45	6	2	67	13	0.05	0.2	3	195	145
48	6	2	67	13	0.05	0.2	3	195	145
51	6	2	67	13	0.05	0.3	3	195	145
55	6	2	100	13	0.05	0.3	3	100	87
57	6	2	100	13	0.05	0.2	4	100	87
59	6	2	73	13	0.05	0.2	4	100	87
62	6	2	73	13	0.05	0.2	4	100	87
65	6	2	73	13	0.06	0.3	4	49	39
71	6	2	75	15	0.08	0.2	4	100	67
80	6	2	97	16	0.07	0.2	15	86	70
85	6	2	84	16	0.04	0.2	9	84	68
97	6	2	50	16	0.04	0.2	9	84	68
100	6	2	50	23	0.08	0.2	17	118	100
106	6	2	120	22	0.08	0.3	16	58	55
111	6	2	105	22	0.08	0.3	16	58	55

APPENDIX A2

TABULATED DATA FOR INFLUENT VALUE AT EACH PHASE DURING FORMATION OF AGS NAMELY AS BATCH1

Period	HRT	Phase	CODs	NH ₄ ⁺	NO ₂ ⁻	NO ₃ ⁻	P	SS	VSS
(d)	(h)								
1	8	1	113	30	0.03	0.3	14	96	67
4	8	1	101	30	0.04	0.3	16	108	70
8	8	1	112	33	0.04	0.3	18	160	96
11	8	1	113	25	0.02	0.3	9	60	38
15	8	1	113	26	0.01	0.3	9	60	42
18	8	1	57	25	0.02	0.4	10	80	60
22	8	1	63	24	0.02	0.4	9	58	40
25	8	1	55	25	0.02	0.6	9	56	40
29	8	1	50	15	0.02	0.6	9	34	26
32	8	1	43	15	0.02	0.7	8	30	22
35	8	1	36	13	0.01	0.8	8	26	22
38	8	1	32	13	0.01	0.8	8	36	28
42	6	2	31	29	0.02	0.3	21	112	100
49	6	2	119	30	0.02	0.3	21	100	91
53	6	2	114	30	0.03	0.3	20	96	90
56	6	2	109	32	0.05	0.2	19	38	36
60	6	2	122	28	0.03	0.2	15	92	76
63	6	2	81	17	0.05	0.3	11	72	58

APPENDIX A3

TABULATED DATA FOR INFLUENT VALUE AT EACH PHASE DURING FORMATION OF AGS NAMELY AS BATCH2

Period	HRT	Phase	CODs	NH ₄ ⁺	NO ₂ ⁻	NO ₃ ⁻	P	SS	VSS	
(d)	(h)		(mg/L)							
1	8	1	113	30.0	0.03	0.3	14.2	96	67	
4	8	1	101	30.3	0.04	0.3	16.3	108	70	
8	8	1	112	33.0	0.04	0.3	17.9	160	96	
11	8	1	113	25.0	0.02	0.3	8.7	60	38	
15	8	1	113	26.3	0.01	0.3	9.0	60	42	
18	8	1	57	25.0	0.02	0.4	10.1	80	60	
22	8	1	63	24.0	0.02	0.4	8.9	58	40	
25	8	1	55	24.5	0.02	0.6	8.5	56	40	
29	8	1	50	15.3	0.02	0.6	8.5	34	26	
32	8	1	43	15.0	0.02	0.7	7.8	30	22	
35	8	1	36	12.5	0.01	0.8	8.4	26	22	
38	8	1	32	12.5	0.01	0.8	8.4	36	28	
42	6	2	31	29.3	0.02	0.3	20.8	112	100	
49	6	2	119	29.8	0.02	0.3	20.8	100	91	
53	6	2	114	30.0	0.03	0.3	20.0	96	90	
56	6	2	109	31.5	0.05	0.2	19.0	38	36	
60	6	2	122	27.8	0.03	0.2	14.8	92	76	
63	6	2	81	16.5	0.05	0.3	10.6	72	58	
68	6	2	65	18.5	0.02	0.3	7.2	42	42	
72	6	2	52	18.3	0.03	0.1	8.8	30	12	
75	6	2	39	35.0	0.02	0.4	15.1	42	44	
79	6	2	67	32.8	0.03	0.3	15.3	82	66	
86	6	2	98	29.3	0.04	0.3	16.9	68	58	
89	6	2	111	24.0	0.02	0.3	5.8	90	78	
92	6	2	85	30.0	0.04	0.3	17.9	30	28	
95	6	2	118	31.3	0.02	0.3	14.3	98	78	
100	6	2	82	30.8	0.03	0.3	17.6	88	68	
103	6	2	95	37.5	0.03	0.3	19.7	84	64	
106	6	2	103	12.8	0.01	0.3	15.6	50	40	
109	6	2	65	36.3	0.02	0.3	13.4	30	26	
113	6	2	64	29.8	0.03	0.3	16.0	74	64	
117	6	2	72	30.5	0.03	0.3	13.2	98	70	
121	6	2	65	30.5	0.03	0.5	19.0	78	72	
124	6	2	52	31.5	0.02	0.3	17.4	102	70	
127	6	2	55	32.5	0.03	0.3	20.2	96	68	
135	6	2	48	31.5	0.03	0.4	19.2	96	68	

APPENDIX A4

TABULATED DATA FOR INFLUENT VALUE AT EACH PHASE DURING FORMATION OF AGS NAMELY AS BATCH3

Period	HRT	Phase	CODs	NH ₄ ⁺	NO ₂ ⁻	NO ₃ ⁻	P	SS	VSS
(d)	(h)								
1	8	1	133	48.80	0.01	0.1	-	60	66
5	8	1	195	36.30	0.01	0.1	-	32	26
8	8	1	231	47.50	0.01	0.2	-	70	70
13	8	1	93	47.70	0.01	0.1	-	36	44
18	8	1	116	45.70	0.01	0.1	-	46	54
22	8	1	141	37.80	0.01	0.1	-	112	88
27	8	1	161	41.20	0.01	0.2	-	60	62
32	8	1	86	42.50	0.01	0.1	15.2	40	44
36	6	2	167	40.70	0.02	0.1	14.0	32	46
41	6	2	146	44.30	0.01	0.1	18.9	100	98
46	6	2	126	44.30	0.07	0.2	15.8	110	122
50	6	2	166	39.70	0.01	0.1	19.0	62	78
57	6	2	203	52.50	0.01	0.1	19.5	136	118
62	6	2	120	22.30	0.01	0.1	13.3	110	96
67	6	2	139	48.20	0.01	0.1	15.3	124	106
71	6	2	168	45.20	0.01	0.1	18.3	100	102
77	6	2	140	30.30	0.01	0.1	14.6	100	94
83	6	2	151	37.50	0.01	0.1	11.4	100	96
91	6	2	171	31.70	0.01	0.1	15.8	78	56
97	6	2	140	35.20	0.01	0.1	17.0	114	112
105	6	2	157	35.70	0.01	0.1	7.2	115	110

APPENDIX A5

TABULATED DATA FOR INFLUENT VALUE AT EACH PHASE DURING FORMATION OF AGS NAMELY AS BATCH4

Period	HRT	Phase	CODs	NH ₄ ⁺	NO ₂ ⁻	NO ₃ ⁻	P	SS	VSS
(d)	(h)								
1	8	1	133	48.80	0.01	0.1	-	60	66
5	8	1	195	36.30	0.01	0.1	-	32	26
8	8	1	231	47.50	0.01	0.2	-	70	70
13	8	1	93	47.70	0.01	0.1	-	36	44
18	8	1	116	45.70	0.01	0.1	-	46	54
22	8	1	141	37.80	0.01	0.1	-	112	88
27	8	1	161	41.20	0.01	0.2	-	60	62
32	8	1	86	42.50	0.01	0.1	15.2	40	44
36	6	2	167	40.70	0.02	0.1	14.0	32	46
41	6	2	146	44.30	0.01	0.1	18.9	100	98
46	6	2	126	44.30	0.07	0.2	15.8	110	122
50	6	2	166	39.70	0.01	0.1	19.0	62	78
57	6	2	203	52.50	0.01	0.1	19.5	136	118
62	6	2	120	22.30	0.01	0.1	13.3	110	96
67	6	2	139	48.20	0.01	0.1	15.3	124	106
71	6	2	168	45.20	0.01	0.1	18.3	100	102
77	6	2	140	30.30	0.01	0.1	14.6	100	94
83	6	2	151	37.50	0.01	0.1	11.4	100	96
91	6	2	171	31.70	0.01	0.1	15.8	78	56
97	6	2	140	35.20	0.01	0.1	17.0	114	112
105	6	2	157	35.70	0.01	0.1	7.2	115	110